SIMULATION AND VALIDATION OF HYBRID GROUND SOURCE AND WATER-LOOP HEAT PUMP SYSTEMS

By

JASON EARL GENTRY

Bachelor of Science in Engineering

The University of Tennessee at Martin

Martin, Tennessee

2005

Submitted to the Faculty of the
Graduate College of the
Oklahoma State University
in partial fulfillment of
the requirements for
the Degree of
MASTER OF SCIENCE
May, 2007

SIMULATION AND VALIDATION OF HYBRID GROUND SOURCE AND WATER-LOOP HEAT PUMP SYSTEMS

Thesis Approved:

Dr. Jeffrey D. Spitler

Thesis Adviser

Dr. Daniel E. Fisher

Dr. A.J. Ghajar

Dr. A. Gordon Emslie

Dean of the Graduate College

ACKNOWLEDGEMENTS

This work is the culmination of the efforts of many people of whom, without their help, this would not have been possible. I would like to take this opportunity to thank them and recognize them for their efforts.

I would like to begin by thanking my advisor, Dr. Jeffrey Spitler, for giving me the opportunity to study under his direction. Dr. Spitler's knowledge and expertise in the field of thermal systems and HVAC are second to none, and I am grateful for the time I have had to study under him. I am very thankful for the energy he has expended and the endless hours he has spent on my account to make sure this work was the best it could be.

I would also like to thank Dr. Daniel Fisher for his continued guidance and support during this work. Dr. Fisher's optimism and smile were always refreshing when the work became overbearing.

I would like to thank Dr. A. J. Ghajar for his committed service and support as a member of my thesis committee.

There are many of my fellow students who willingly gave their support throughout the course of my work. I would like to thank Xiaowei Xu for his expert

knowledge in HVACSim+ and for the help he provided with the HGSHP validation. I would like to thank Sankaranarayanan K. Padhmanabban, a.k.a Sankar, for his expertise and help with EnergyPlus. I would like to thank Stephen Szczepanski for his help in maintaining the operation of the HGSHP research facility. I would like to thank Edwin Lee for his programming help. I would like to thank all them for the great times I had at Friday lunches and for the great stress reliever that was "office Olympics." I will definitely miss the cabinet Frisbee toss and the printer throwing competitions.

I would like to thank Dr. J. Douglas Sterrett for giving me the opportunity to work for the University of Tennessee at Martin Center for Energy Management, and for introducing me to the geothermal industry. I would also like to thank Linda Davis for all she did in helping me at UTM.

I would like to thank the Oklahoma Center for the Advancement of Science and Technology (OCAST) and ClimateMaster for funding this project. I would also like to thank Dan Ellis and Dr. Xiaobing Liu, of ClimateMaster, for their help and input during this work.

I would like to thank all of my family for their continued prayers and support over the last two years. I would especially like to thank my parents, Randy and Kathy Gentry, for raising me to be the man that I am today. I have always tried to make them proud in everything that I do. I am very thankful for their continued love and encouragement.

Finally, and most importantly I would like to thank my beautiful and very loving wife Clarissa. She has been the one true and constant beacon of light through the many hours of work and sleepless nights. She has sacrificed so much of herself in order to make this possible. She has stood by my side without waiver giving endless encouragement and undying love. I can't say enough about what she has done and how much her support has meant to me. I will always love her, and dedicate this thesis to her.

TABLE OF CONTENTS

Chapter Page

LIST OF TABLES

LIST OF FIGURES

1. INTRODUCTION

With today's world concern over energy, much research and development is being done around the world to improve the energy efficiency of everything from cars to household appliances to indoor lighting. Another area on which much emphasis has been placed is the heating, ventilating and air-conditioning (HVAC) systems that heat and cool us everyday. Although most people do not even think about an HVAC system until it breaks down, much is spent annually around the world for the comfort of an HVAC system.

Water-source heat pumps (WSHP) are an energy efficient technology for providing cooling. Two types of HVAC systems that utilize water-source heat pumps are hybrid ground source heat pump (HGSHP) systems and water-loop heat pump (WLHP) systems. This work will focus on modeling and validation of models for both HGSHP systems and WLHP systems. For WLHP systems, control strategies that further improve energy efficiency will be investigated.

1.1. Overview of Hybrid Ground Source Heat Pump Systems

Ground source heat pump (GSHP) systems, also known as geothermal heat pump (GHP) systems, are an energy efficient alternative for the heating and cooling of residential, commercial and institutional applications. The more moderate and constant temperatures of the earth used by the GSHP system as a heat sink/source are advantageous when compared to the outdoor air used by air-source heat pump systems.

A GSHP system usually consists of a ground loop heat exchanger (GLHE) through which water or an antifreeze solution is circulated and one or more water-source heat pumps. The GLHE usually consists of high-density polyethylene (HDPE) pipe buried in a horizontal trench or inserted in vertical boreholes. Depending on the season (heating or cooling), the system transfers thermal energy to or from the earth via the GLHE. A typical GSHP system can be seen below in Figure 1.1.

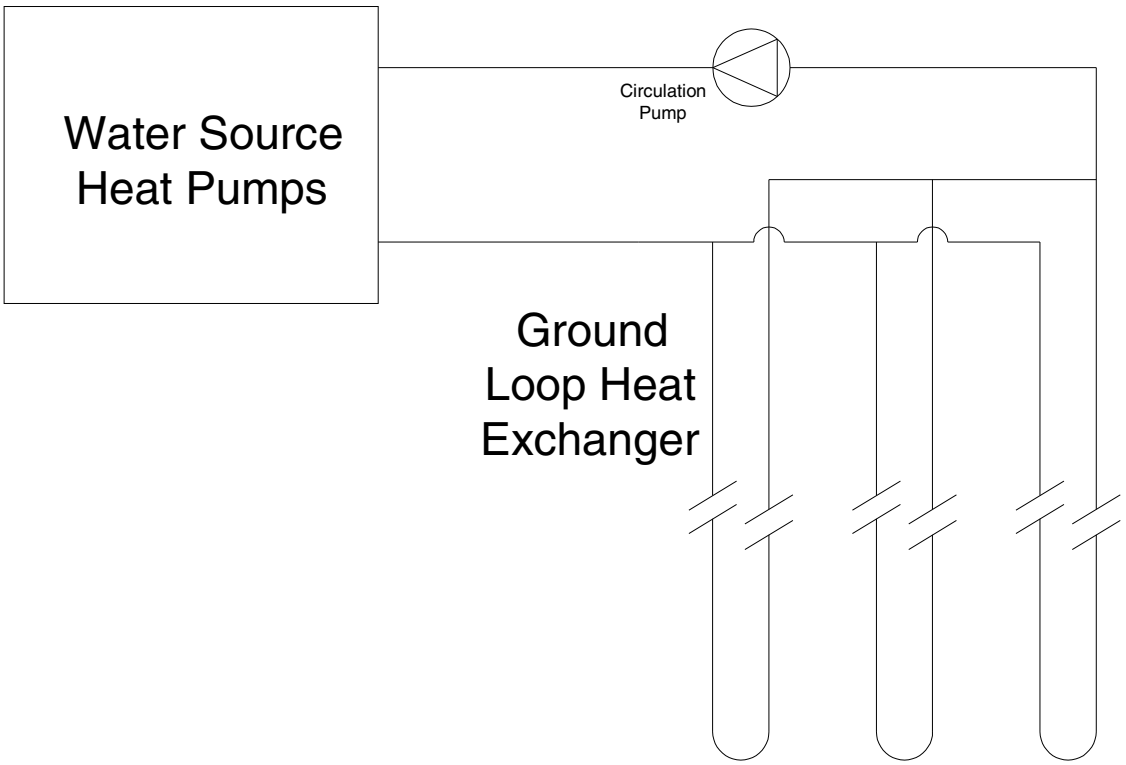

Figure 1.1 *Schematic of a typical GSHP system.*

Some of the advantages of using a GSHP system are their higher energy efficiency over conventional systems, lower CO_2 emissions and lower maintenance costs. While these are great, GSHP system market penetration has been limited because of its higher first costs (ASHRAE 1999).

Kavanaugh and Raffertey (1997) suggest the initial costs for installing a GSHP system could be as much as double that of a standard central heating and air-conditioning system for residential applications and for commercial applications anywhere from 20% to 40% higher than a unitary rooftop system.

HGSHP systems make the GSHP system more appealing for commercial and institutional applications by reducing the first cost of the system. The United States Department of Energy (2001) showed savings of more than 50% on first cost by using a hybrid system as opposed to a full GSHP system. Hybrid systems obtain these savings by using supplemental heat rejection devices such as a cooling tower, fluid cooler, cooling pond, or pavement heating system to reduce the GLHE size. One problem in many buildings is an annual imbalance between the amount of heat rejected to or extracted from the ground. More times than not commercial and institutional buildings have very large internal heat gains and are therefore generally cooling-dominated, causing more heat rejection through the GLHE than heat extraction on an annual basis. This causes a problem with heat build up in the ground which over time will cause loop temperatures to rise and decrease the efficiency of the heat pumps. One solution to the problem is to increase the size of the GLHE, increasing the first costs. A more reasonable and cost effective option can be to reduce the size of the GLHE and install one of the supplemental heat rejecters mentioned above.

Figure 1.2 shows a typical HGSHP system. The system shown uses a cooling tower as its supplemental heat rejecter. For this system, the tower is isolated from the ground loop heat exchanger via a plate heat exchanger.

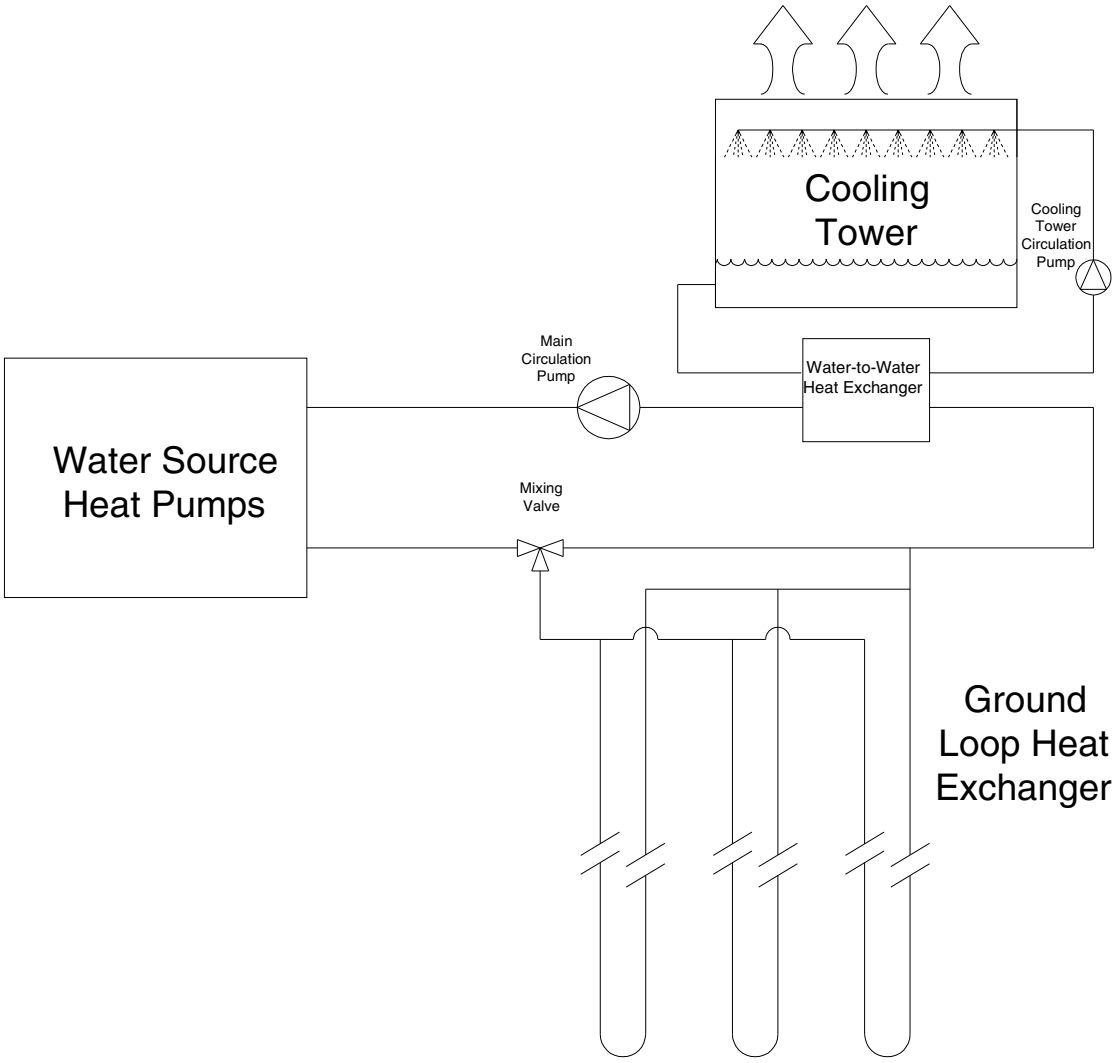

Figure 1.2 *Schematic of a typical HGSHP system.*

1.1.1. Design and Modeling of Hybrid Ground Source Heat Pump Systems

When designing a GSHP or HGSHP system, one of the most important aspects of the design is the sizing of the GLHE. Likewise, when modeling a GSHP system or a HGSHP system for energy analysis, an important component to consider is the GLHE. The model's ability to predict short-term and long-term temperature response of the

ground loop is important to predictions of heat pump energy consumption. Several design methods have been presented in the literature for the design of HGSHP systems. The first discussion of design of HGSHP systems for new construction appeared in ASHRAE (1995). Since that time other design methods have been presented and will be discussed in Section 2.1.1.

For the work done in this study, the HGSHP system is modeled and simulated using component models developed at Oklahoma State University (OSU) in the HVACSim+ modeling environment (Clark 1985). The computer model is validated against an experimental HGSHP system that is located on the campus of OSU in Stillwater, Oklahoma. The experimental facility will be discussed in detail in Section 3.1. The system model is comprised of four main component models which include a heat pump, cooling tower, plate frame heat exchanger and a GLHE. The system model and component models will be discussed in greater detail in Chapter 2.

1.1.2. Simulation and Validation of Hybrid Ground Source Heat Pump Systems

GSHP systems and ground loop heat exchangers are commonly designed with simulation-based procedures because the long time constant of the ground makes it necessary to ensure that the loop temperatures will not exceed the heat pump limits over the life of the system. Because of the interaction between loop temperatures, GLHE performance, heat pump performance and supplemental heat rejecter performance, simulation is even more necessary for the design of HGSHP systems.

Nevertheless, while some validations of GLHE and other HGSHP system components have been reported, no validations of the entire HGSHP system have been reported. Nor, for that matter, have any validations of an entire GSHP system been reported. Several authors have presented validations of ground heat exchanger models – McLain and Martin (1999) and Yavuzturk and Spitler (2001). Thornton, et al. (1997) report on an extensive calibration process which allows a GSHP system simulation to give a good prediction of maximum entering water temperature and heat pump energy consumption compared to the experimental measurements.

While it might be hoped that if each component model of the simulation were validated the entire simulation as a whole would be sufficiently accurate, this is not necessarily the case. In a GSHP or HGSHP system simulation, there is the potential for small errors to accumulate over time. Furthermore, because of the difficulty in characterizing the ground thermal properties, it seems inevitable that, at the least, small errors will always be present. From a designer's perspective, limited information on cooling tower performance, limited accuracy of manufacturer's heat pump data, etc. lead to additional small errors that also may be cumulative. The degree to which this is a problem is unknown, and suggests the need for experimental validation of the entire system simulation. It also suggests the need for experimental validation with and without individual model calibration.

This study presents an experimental validation of the entire system simulation, using an HGSHP system located at Oklahoma State University. Seven months (March to

September 2005) of five-minutely experimental data from an HGSHP system were used for validation purposes.

1.1.3. Control of Hybrid Ground Source Heat Pump Systems

Limited work has been done on developing control strategies for the operation of the supplemental heat rejecter in HGSHP systems. Yavuzturk and Spitler (2000) used a system simulation approach to compare the advantages and disadvantages of different methods of operating and controlling a cooling tower within a HGSHP system. The authors compared 5 cases which are listed below.

1. A GSHP system with no supplemental heat rejecters; correctly-sized GLHE.
2. A GSHP system with no supplemental heat rejecter, but GLHE sized as if there were a supplemental heat rejecter. The undersized GLHE leads to heat buildup over time.
3. The use of a cooling tower in the simulation being turned on when the entering or exiting temperature of the heat pump exceeds a fixed setpoint.
4. The cooling tower turned on when the difference in the entering or exiting heat pump temperature and the ambient wet-bulb temperature exceeds a setpoint.
5. A combination of a set point control and cool storage strategy by running the cooling tower 6 hours at night and whenever the entering heat pump temperature exceeds a fixed setpoint.

The authors showed that the most beneficial strategy was to operate the cooling tower based on the differential controller that took the difference between the entering or exiting heat pump temperature and the ambient wet-bulb temperature. The authors also noted that the use of the short time step GLHE model proved very beneficial in assessing the behavior of HGSHP systems. It should be noted that the simulations assumed perfect measurement of the wet-bulb temperature; this is unlikely to be achieved in practice.

1.2. Overview of Water Loop Heat Pump Systems

WLHP systems are heating and cooling systems that are used in commercial and institutional applications to provide space heating and cooling to multiple zones. Typically a heat pump is placed in each building zone to provide the proper amount of heating and cooling to that zone. Water is pumped through each heat pump via a piping system (loop). Heat pumps running in heating mode remove heat from the loop, while heat pumps running in cooling mode reject heat to the loop. The water is maintained within a desired range of temperatures with the assistance of a heat rejecter, e.g. cooling tower or fluid cooler and a heat source, e.g. a boiler. When the system is running with some heat pumps in heating and some in cooling, heat that may be removed from one zone can be added to another, saving energy. Figure 1.3 shows a typical WLHP system with a water-to-water heat exchanger. At the current time, a large emphasis is put on energy conservation and lower initial cost; two reasons why WLHP systems have become increasingly popular.

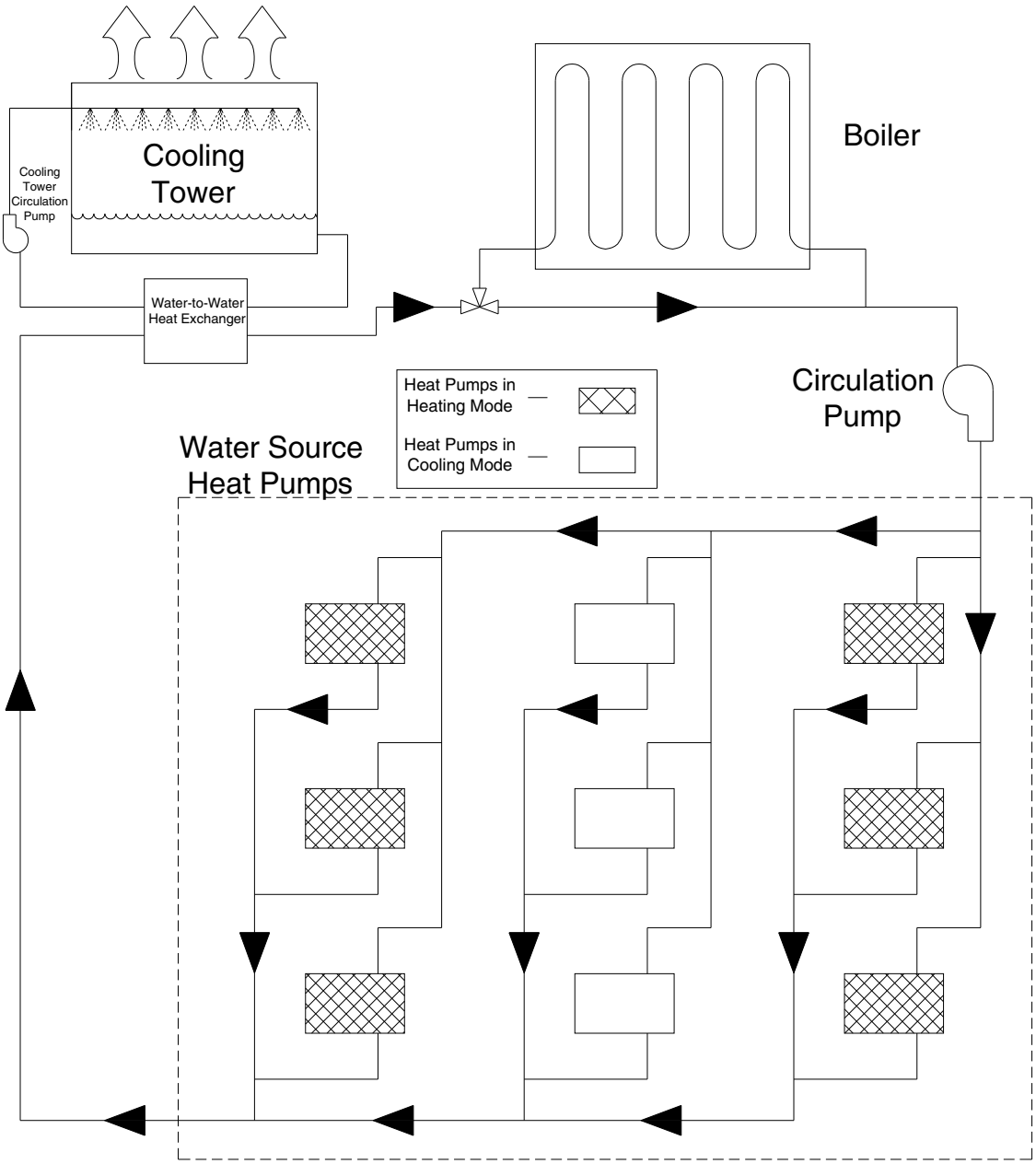

Figure 1.3 *Schematic of a WLHP system with water-to-water HX.*

1.2.1. Modeling of Water-Loop Heat Pump Systems

A WLHP system may be thought of as an HGSHP system with a boiler but without the GLHE and it can be modeled accordingly. In this study, the WLHP being analyzed is equivalent to the HGSHP system discussed above with the GLHE replaced with a boiler.

For the work done in this study, the WLHP system is modeled and simulated with both HVACSim+ (Clark 1985) and EnergyPlus (Crawley et al. 2002). Modeling the system in two distinctly different programs allows for cross-checking of results. Both the HVACSim+ system model and the EnergyPlus model are comprised of five main component models which include a heat pump, cooling tower, boiler, plate frame heat exchanger and a circulation pump. The system models and component models will be discussed in greater detail in Chapter 4. Both models require the input of building loads in kW. These loads were calculated using DesignBuilder (DesignBuilder Software Ltd, 2006) which uses EnergyPlus as its "computational engine".

1.2.2. Simulation and Validation of Water-Loop Heat Pump Systems

Howell and Zaidi (1991) developed several figures-of-merit (annual heat recovery, savings in cooling energy and annual savings in heating and cooling energy) to indicate the energy performance of WLHP systems. These parameters were developed by simulating a WLHP system using a commercially available energy analysis program

based on the following parameters; building shape, building core to perimeter ratio and geographic location. Their methodology is described in Section 4.1.1. They concluded that the WLHP system as an HVAC system has great potential for energy savings through heat recovery. Over a wide range of variables studied they reported heat recovery savings between 0.1 to 2.8 kWh/ft^2. They also concluded that the most heat recovery comes from buildings with large internal loads, large core to perimeter ratio, milder climates, and is related to the heat pumps' heating COP.

Cane et al. (1993) validated three models of WLHP systems in commercially available energy analysis programs against actual building data. They compared the models' predicted hourly energy consumption of the HVAC system to that of measured data. They concluded that the three models predict total building energy use within 1% to 15% of measured data. Although they agree this is very good, they state that the results hide "the wide variations observed at the HVAC system and component levels" (Cane et al. 1993). Two of the problems with the models that are noted by the authors are their inability to model variable-capacity pumping or thermal storage within the system.

This thesis presents an experimental validation of the entire system simulation, operating in cooling only mode, using the HGSHP research facility located at OSU. For the purposes of validating the WLHP system model, the GLHE was valved out of the system, leaving a typical WLHP system without the boiler to be used for validation purposes. The experimental WLHP system is much smaller than a typical commercial system.

1.2.3. Control of Water-Loop Heat Pump Systems

In control of WLHP systems, the conventional practice is to run the WLHP system between 60°F and 90°F (Howell 1988; Hughes 1990; Pietsch 1990; Howell and Zaidi 1990; Pietsch 1991; Howell and Zaidi 1991). The boiler is operated to maintain a minimum setpoint of 60°F entering the heat pumps and the cooling tower is operated to prevent the entering fluid temperature from exceeding 90°F. Other setpoints have been presented. Hughes (1990), when surveying current system configurations in practice, determined that typical WLHP setpoints for all of the United States to be 65°F for heating and 85°F for cooling. In trying to optimize WLHP design and performance, Kush and Brunner (1991), determined that in order to reduce the boiler use and increase performance, the minimum loop temperature should be held to 65°F or "slightly less." Kush and Brunner also suggested that it is beneficial to hold the maximum loop temperature to 85°F or "slightly below" in order to increase the cooling performance. Regardless of the setpoints, all past published recommendations, with the exception of Pietsch (1991), have been to hold the set points constant.

Pietsch (1991) suggested that there could be savings potential operating in mixed heating and cooling mode at an optimum temperature or at a fixed, constant temperature. Pietsch suggested a single optimum set point that was based on the ratio of heating load to cooling load. The boiler would run if below this optimum loop temperature and the cooling tower would run if above it. He determined that the optimum operating temperature would vary based on the heating-to-cooling load ratios with the lower ratios

requiring lower loop temperatures. Pietsch concluded that, although determining the ratio would perhaps be feasible, determining the precise heating-to-cooling load ratio to vary the loop temperature would be extremely difficult. Therefore, he examined setting the loop temperature to a constant 45°F and 60°F. He determined that the average power inputs for the two fixed cases and the optimum temperature case are essentially the same. His conclusion is, "operating at a loop temperature level that is consistent with the lowest feasible heat pump operating temperature would provide near-optimum heat pump operation" (Pietsch 1991). However, this analysis was made on a quasi-steady-state basis and did not mention the use of a dead band control and therefore did not consider the transient effects of switching between cooling tower and boiler operation.

While some (Hughes 1990; Pietsch 1990; Pietsch 1991) claimed that simultaneous heating and cooling is an important factor in energy conservation, only Pietsch (1990) looked at the effects of a small shift in the number of units operating in either mode. This shift can result in a switching between heating dominated operation (boiler in use) and cooling dominated operation (cooling tower in use) and during the shoulder seasons could typically occur over the course of a day. Therefore the use of thermal storage in a WLHP system may be an important part to the energy efficiency of a WLHP system and will be discussed in Chapter 4.

1.3. Thesis Objectives and Scope

This study can be divided into two main sections; work on HGSHP systems and work on WLHP systems. In dealing with HGSHP systems, this study presents an experimental validation of the entire system simulation using an HGSHP system located at Oklahoma State University. The system size is similar to residential systems, i.e. smaller than a typical HGSHP system. However, it contains all of the components of a typical HGSHP system – a heat pump, three boreholes, and a small direct contact evaporative cooling tower connected via a plate frame heat exchanger. Furthermore, it is carefully instrumented and monitored, so that the resulting data set is free from significant periods of missing or corrupted data that tend to plague data sets collected with building energy management systems. With this in mind, the three main objectives of this part of the study are:

- Develop a model of an HGSHP system in HVACSim+
- Simulate the model in HVACSim+
- Validate the model using experimental data

In dealing with the WLHP system, the main objective was to develop an optimized control strategy for operating WLHP systems. Within the scope of the main objective, the following objectives are also desired.

- Develop a model of a WLHP system in HVACSim+ and EnergyPlus
- Simulate the model in HVACSim+ and EnergyPlus

- Validate the model using a small experimental data set
- Investigate dynamic effects in WLHP system performance

2. SIMULATION OF HYBRID GROUND SOURCE HEAT PUMP SYSTEMS

Hybrid ground source heat pump systems incorporate both ground loop heat exchangers and auxiliary heat rejecters, such as cooling towers, fluid coolers, cooling ponds, or pavement heating systems. The design of the hybrid ground source heat pump system involves many degrees of freedom; e.g. the size of the cooling tower interacts with the control strategy, the ground loop heat exchanger design, and other parameters. This chapter presents a simulation of such a system using a direct contact evaporative cooling tower as the supplemental heat rejecter. The simulation is performed in a component-based modeling environment using component models of a vertical ground loop heat exchanger, plate frame heat exchanger, cooling tower, circulating pumps, and heat pumps. Specific adaptations to the models for purposes of experimental validation are also discussed.

2.1. Introduction

GSHP systems have become increasingly common in residential, commercial, and institutional buildings. In cases where there is significant imbalance between the annual heat rejection to the ground and annual heat extraction from the ground the loop fluid temperature tends to rise (or fall) from year to year. This effect can be moderated by

increasing the ground loop heat exchanger size. However, the capital cost requirements can be excessive and an alternative is to add an additional heat sink (or an additional heat source). Systems with additional heat sinks or sources are generally referred to as hybrid GSHP or HGSHP systems.

The most common heat sink device is a cooling tower, but other heat sinks include domestic water heating systems, closed-circuit fluid coolers, ponds, and pavement heating systems. Auxiliary heat sources include solar collectors or boilers.

2.1.1. Background/Literature Review

HGSHP systems seem to have arisen as a practical solution for fixing undersized GSHP systems that have begun to operate too hot (or too cold). Previously published literature on HGSHP systems has been scarce with essentially no discussion of validated HGSHP system models. The first discussion of design of HGSHP systems for new construction appeared in ASHRAE (1995). For cooling dominated systems, it was suggested that the supplemental heat rejecter could be sized to reject half of the average difference between the heat rejected by the system and the heat to be rejected to the ground for the peak cooling month. The basis for this recommendation is not clear.

Kavanaugh and Rafferty (1997) revised the design procedure by suggesting that the supplemental heat rejecter be sized to meet peak block load at the design conditions. Similar to ASHRAE (1995), the authors suggested calculating the nominal size of the

supplemental heat rejecter by taking the difference between the GLHE lengths that would be required to meet the cooling load and heating load. The text further discussed possible ways of integrating the supplemental heat rejecter with the GSHP system, recommending a parallel piping scheme.

Kavanaugh (1998) gives a modified procedure that iteratively approximates the annual heat rejection of the cooling tower or fluid cooler and then recomputes the loop length. The annual heat rejection is estimated using a heuristic expression that gives the equivalent full load run hours for the cooling tower or fluid cooler as a function of the equivalent full load run hours for cooling and the ratio of flow rates between the heat rejecter and the system. An alternative approach is also given which assumes that the heat rejecter can balance the annual heat rejection and heat extraction and then the required run hours for the heat rejecter can be estimated with a heuristic expression.

Several studies have looked at the performance of existing HGSHP systems. One such study by Phetteplace and Sullivan (1998) discussed a project undertaken to monitor a 2,230 m^2 (24,000 ft^2) administration building that was renovated in 1993 in Fort Polk, Louisiana. Performance data were presented for almost 22 months, including two heating and two cooling seasons. The hybrid system consisted of 70 vertical closed-loop boreholes approximately 61 meters (200 feet) deep with 3.3 meter (10.8 foot) spacing between them and a 275 kW (78 ton) cooling tower as the supplemental heat rejecter. The system is controlled using a differential control scheme that activates the cooling tower once the heat pump exiting fluid temperature (ExFT) reaches 36.1ºC (88.88ºF) and

deactivates once it gets below 35ºC (95ºF). After post processing the performance data obtained, the authors had concerns about the amount of possible heat buildup in the ground due to relatively high loop temperature of around 41ºC (105.8ºF). The report showed that over the monitoring period, 43 times more heat was rejected than extracted. To solve the problem, they suggested reducing the differential control setpoint and, from a design standpoint, suggested increasing the spacing between boreholes.

Another such study by Singh and Foster (1998) was conducted on a hybrid system being used in the 7,436 m^2 (80,000 ft^2) Paragon Center, in Allentown, Pennsylvania. The system consisted of 88 boreholes approximately 38 meters (125 feet) deep and a 422 kW (120 ton) closed-circuit fluid cooler. The hybrid system was designed for the GLHE to handle all of the heating demand and 80% of the cooling demand, allowing the fluid cooler to pick up the other 20% of the cooling demand. The study also looked at a 5,586 m^2 (60,127 ft^2) elementary school building in West Atlantic City, New Jersey. The school used a 411 kW (117 ton) closed-circuit fluid cooler which allowed the number of boreholes needed in the GLHE to be reduced by more than 25%. The authors concluded that both hybrid systems showed considerable savings on initial costs.

Work has also been done on comparing different control strategies for the operation of the supplemental heat rejecter in HGSHP systems. Yavuzturk and Spitler (2000) used a system simulation approach to compare the advantages and disadvantages of different methods of operating and controlling a cooling tower within a HGSHP system. The simulations were developed in the TRNSYS environment, using standard

TRNSYS types for the cooling tower, circulating pumps, and controls. The GLHE model (Yavuzturk and Spitler 1999) was based on an extension of past work by Eskilson (1987) to treat short time response. The authors showed that the most beneficial strategy was to operate the cooling tower based on the differential controller that took the difference between the entering or exiting heat pump temperature and the ambient wet-bulb temperature. The authors also concluded that the use of the short time step GLHE model proved very beneficial in assessing the behavior of HGSHP systems.

Simulation-based studies of HGSHP systems with alternative supplemental heat rejecters, such as cooling ponds (Ramamoorthy et al. 2001) and pavement heating systems (Khan et al. 2003) have been presented in the literature. Ramamoorthy, et al. (2001), using the control strategy suggested by Yavuzturk and Spitler (2000), operated the pond loop when the difference between the heat pump exiting fluid temperature and the average pond temperature exceeded a set value. The paper shows the optimization of the size of the HGSHP system through adjusting the borehole depth and pond loop heat exchanger lengths until a minimum life-cycle cost was found. A sensitivity analysis done on the differential controller showed that the choice of the dead band range had no significant impact on the economics of the system.

Khan et al. (2003) described a simulation study of an HGSHP system that utilized a pavement heating system as the supplemental heat rejecter. They concluded from their study that the HGSHP system has significantly lower first costs and lower annual

operating costs. The approach was similar to the HGSHP studies described by Ramamoorthy et al., but was performed within the HVACSIM+ environment.

Chiasson and Yavuzturk (2003) discuss the viability of using solar thermal collectors, as a supplemental heat source for an HGSHP system. The study uses loads obtained by simulation of a heating-dominated 4,924 m^2 (53,000 ft^2) school building in six U.S. cities in cold climates. They conclude that solar thermal collectors are economically viable for this application in cold climates, depending on drilling costs. The seasonal thermal solar energy storage in the ground was found to be enough to offset a larger ground storage volume that would be required with a conventional GSHP system.

GSHP systems and GLHE are commonly designed with simulation-based procedures because the long time constant of the ground makes it necessary to ensure that the loop temperatures will not exceed the heat pump limits over the life of the system. Because of the interaction between loop temperatures, GLHE performance, heat pump performance and supplemental heat rejecter performance, simulation is even more needed for design of HGSHP systems.

Never the less, while some validations of GLHE and other HGSHP system components have been reported, no validations of the entire HGSHP system have been reported. Nor, for that matter, have any validations of an entire GSHP system been reported. Several authors have presented validations of ground heat exchanger models – McLain and Martin (1999) and Yavuzturk and Spitler (2001). Thornton, et al. (1997)

report on an extensive calibration process which allows a GSHP system simulation to give a good prediction of maximum entering water temperature and heat pump energy consumption compared to the experimental measurements.

While it might be hoped that if each component model of the simulation were validated the entire simulation as a whole would be sufficiently accurate, this is not necessarily the case. In a GSHP or HGSHP system simulation, there is the potential for small errors to accumulate over time. Furthermore, because of the difficulty in characterizing the ground thermal properties, it seems inevitable that, at the least, small errors will always be present. Furthermore, from a designer's perspective, limited information on cooling tower performance, limited accuracy of manufacturer's heat pump data, etc. lead to additional small errors that also may be cumulative. The degree to which this is a problem is unknown, and suggests the need for experimental validation of the entire system simulation. It also suggests the need for experimental validation with and without individual model calibration.

2.1.2. Objectives

This thesis, in Chapter 3, presents an experimental validation of the entire system simulation, using an HGSHP system located at OSU. The system size is similar to residential systems, i.e. smaller than a typical HGSHP system. However, it contains all of the components of a typical HGSHP system – a heat pump, three boreholes, and a small direct contact evaporative cooling tower connected via a plate frame heat

exchanger. Furthermore, it is carefully instrumented and monitored, so that the resulting data set is free from significant periods of missing or corrupted data that tend to plague data sets collected with building energy management systems.

This chapter is organized by first describing the individual component models followed by the overall system simulation approach. Then, in Chapter 3, the experimental facility is described in detail, followed by a comparison between the experimental results and the system simulation results and a discussion of the calibration process which was used to obtain the best match. Finally, the system simulation is reconsidered from the designer's perspective, i.e. if calibration of individual models is impossible, how good are the simulation results that are of primary interest to the designer – energy consumption, cooling tower run time, and peak entering fluid temperature? The accuracy of these results without calibration and with varying degrees of calibration is examined.

2.2. Component Model Design and Simulation

2.2.1. Heat Pump Model

The heat pump model is a simple water-to-water equation-fit model developed by Tang (2005) and modified to account for multiple heat pumps within the model. If more than one heat pump is being utilized the total load seen by the heat pump during any given time step will be divided among the heat pumps. The model equations fit power,

source side heat transfer rate, and load side heat transfer rate to normalized entering fluid temperatures and normalized flow rates. The heat pump's source side heat transfer rates are then calculated using the fitted equations. The coefficients of the performance equations are evaluated according to catalog data provided by the heat pump manufacturer. This will be discussed in more detail in Chapter 3. Coefficients are read as parameters of the model. The computed load side heat transfer rate and the input load side heat transfer rate are compared and the ratio is used to determine a run time fraction for the time step. The heat pump model, TYPE 563, diagram can be seen below in Figure 2.1, showing all inputs, outputs, and parameters needed to run the model.

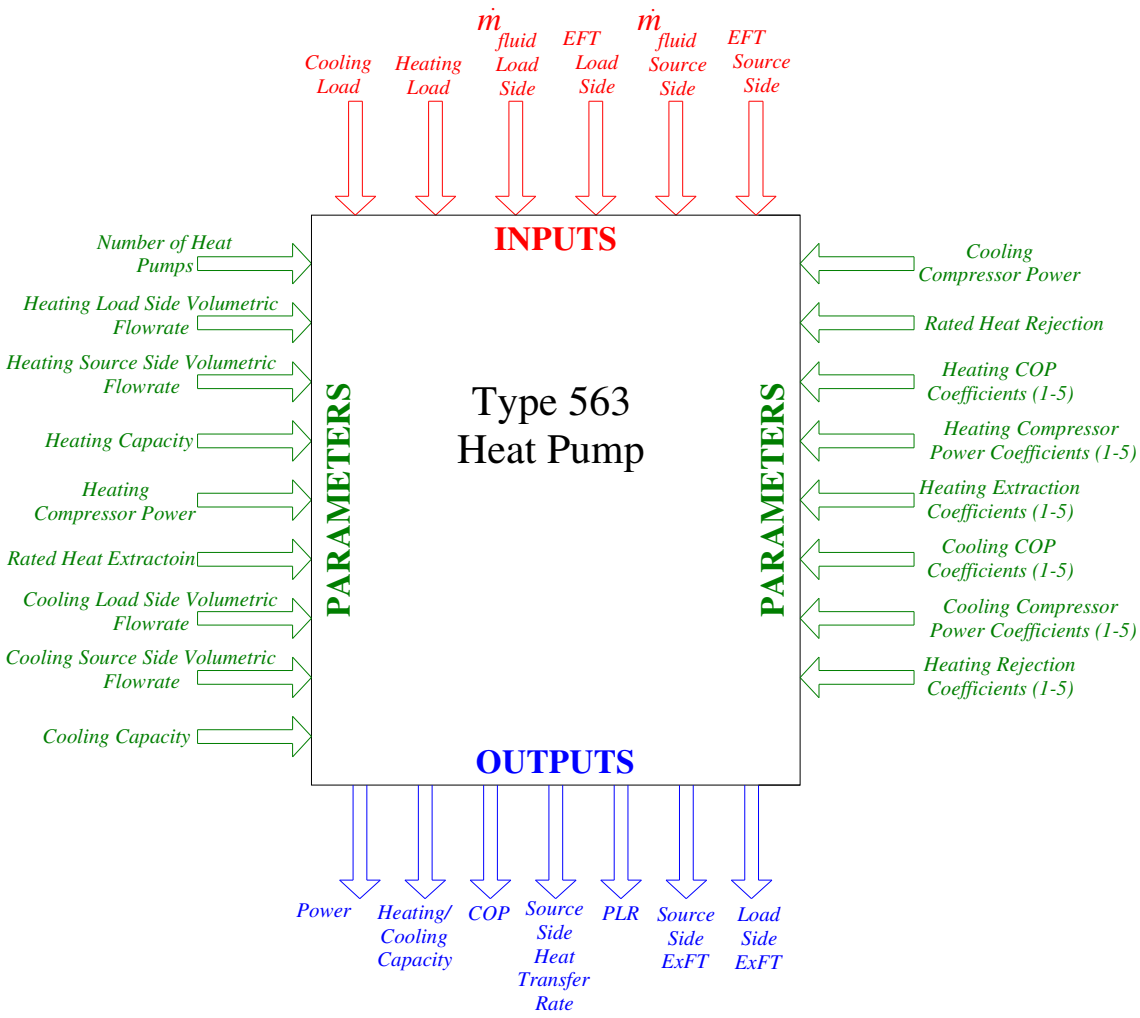

Figure 2.1 *Heat pump HVACSim+ model diagram.*

An equation-fit model was initially chosen over a parameter estimation-based model for the relative convenience of determining the inputs and fast execution speed. As was found in the validation, this convenience comes at the cost of poor model performance when one of the input variables falls outside the range of data used to fit the equations.

2.2.2. Ground-Loop Heat Exchanger Model

The GLHE model used for this work was developed by Xu and Spitler (2006) and is based on the long-time g-function model which was developed by Eskilson (Eskilson 1987). Xu and Spitler integrated a one-dimensional numerical model into the GLHE model which was used to determine the short time response of the boreholes. Eskilson's method for determining the temperature response of the ground heat exchanger is aimed at using pre-computed response factors to allow a computationally efficient simulation.

Eskilson started with looking at a single borehole, finding the temperature field through a set of finite-difference equations set up on a radial axial coordinate system in a homogenous ground. Next he superimposed the temperature field from the single borehole is space to obtain the temperature response of the entire bore field to a heat pulse. This response was non-dimensionalized to give a g-function or set of non-dimensional response factors. The procedure for obtaining the g-functions is quite computationally intensive. However, after obtaining the g-functions the temperature response at the wall of the borehole for a time-varying heat transfer rate can be quickly determined. Because the finite-difference model treated the borehole as a finite length line-source, its accuracy was poor for short, e.g. hourly, time steps.

Eskilson's model was extended by Yavuzturk, et al. (1999) to short time steps by developing short time step g-functions. The short time step g-functions were developed using a two-dimensional (radial-angular) finite volume method. The original method

utilized a fixed convective resistance. This was later modified (Yavuzturk and Spitler 2001) to account for variable convective resistances, but the thermal mass of grout and fluid were neglected.

Later investigation (Young 2004) showed that the thermal mass within the borehole was quite important for some scenarios. Xu and Spitler (2006) developed a one-dimensional (radial) model to compute the short time step response integrated with Eskilson's long time step model. By carefully precomputing borehole thermal resistance with a 2-D model Xu and Spitler were able to get short term response that matched a detailed 2-D finite volume model at a fraction of the computation time. This is the model used for this work.

The model parameters include the number of boreholes, borehole depth and radius, U-tube configurations, the U-tube, the grout and the ground thermal properties, fluid type, short-time step and the long time step g-functions. The model is formulated to take inlet temperature and mass flow rate as inputs, and give the outlet temperature as an output. Further details are given by Xu and Spitler (2006). The GLHE model, TYPE 620, diagram can be seen below in Figure 2.2, showing all inputs, outputs, and parameters needed to run the model.

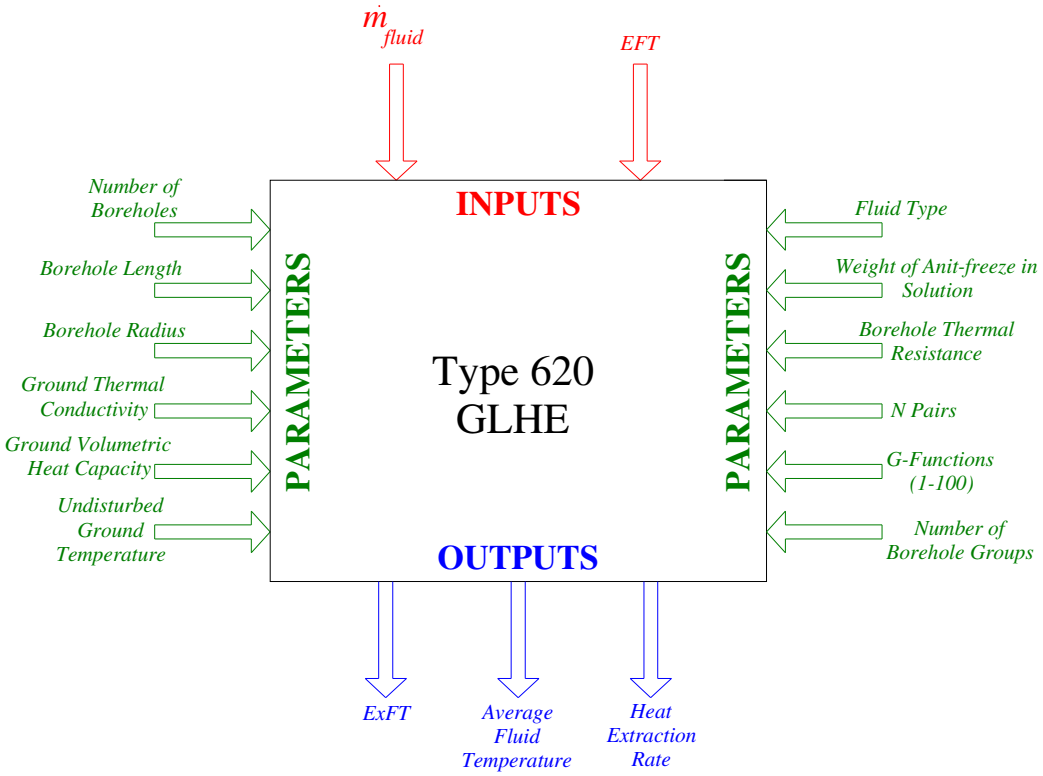

Figure 2.2 *GLHE HVACSim+ model diagram.*

2.2.3. Cooling Tower Model

Two versions of a cooling tower model were used in this work. First, the fixed-*UA* cooling tower model developed by Khan (2004), determines the exiting water temperature, as well as the exiting air wet-bulb temperature based on five inputs; water mass flow rate, air mass flow rate, entering water temperature, entering air wet-bulb temperature, and a cooling tower on/off control signal. The model also requires one parameter, the overall heat transfer coefficient which is estimated from the manufacturer's data and set as constant. From this parameter, an effective UA value, UA_e, is calculated according to the following equation.

$$UA_e = UA\frac{C_{pe}}{C_{p,moistair}} \tag{2.1}$$

Where C_{pe} is the effective specific heat (J/kg-K), $C_{p,moistair}$ is the moist air specific heat (J/kg-K).

The fixed-*UA* model seemed most appropriate at the beginning of the work. For the small cooling tower used with the system, only a single operating point was available from the manufacturer. If more data were available from the manufacturer, a more detailed model would be appropriate. For the validation, one of the improvements was to utilize the parameter-estimated-*UA* model proposed by Lebrun and Silva (2002):

$$UA_e = \left[k\dot{m}_w^x \dot{m}_a^y\right]\frac{C_{pe}}{C_{p,moistair}} \tag{2.2}$$

Where $\dot{m}_w$ is the entering water flow rate in [kg/s], $\dot{m}_a$ is the entering air flow rate in [kg/s], and *k*, *x*, and *y* are model parameters.

The Lebrun and Silva model allows the UA value to change as the water flow rate and air flow rate change. The model parameters include *k*, *m*, and *n* as shown above in Equation 2.2. As can be seen below from Figure 2.3, the model is formulated to take inlet water temperature, inlet air wet-bulb temperature, water mass flow rate, air mass flow rate, and a control signal as inputs, and give the outlet water temperature, outlet air wet-bulb temperature, and the overall heat transfer coefficient, UA, as outputs.

For experimental validation, the three parameters were estimated from experimental data because only one data point was available from the manufacturer. A simple univariate optimization procedure, applied iteratively, was used to estimate the three parameters from the experimental data. The procedure yielded estimates of the parameters as follows, k=764, n=1.11, and m=0.41. The cooling tower model, TYPE 768, diagram can be seen below in Figure 2.3, showing all inputs, outputs, and parameters needed to run the model.

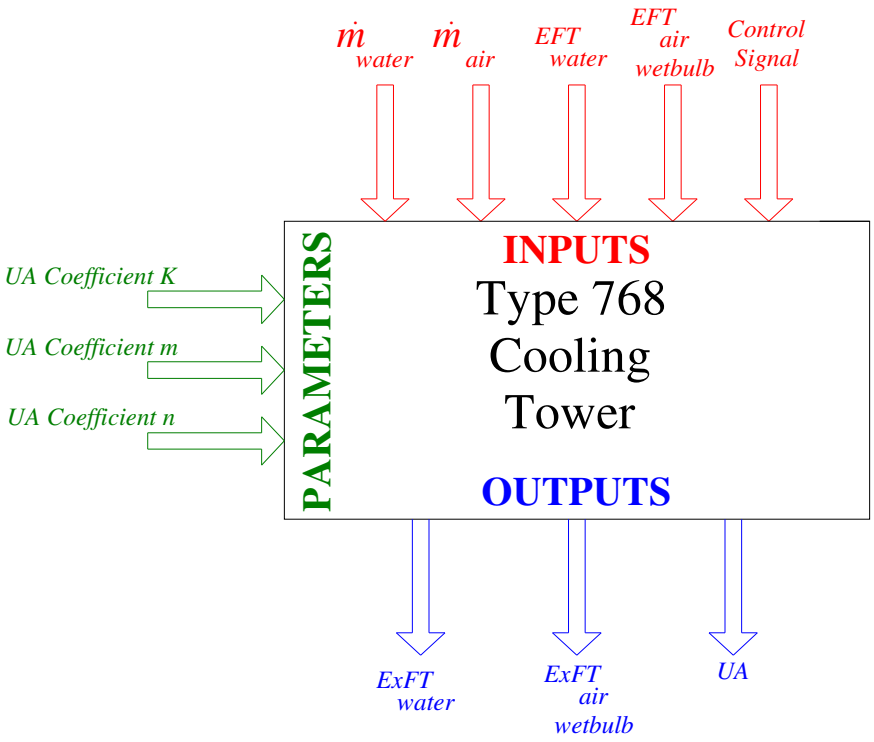

Figure 2.3 *Cooling tower HVACSim+ model diagram.*

2.2.5. Plate Frame Heat Exchanger Model

Hybrid ground source heat pump systems often use a liquid-to-liquid plate frame heat exchanger to isolate the cooling tower from the rest of the system. Initially, a parameter estimation-based model was developed, based on the general concept of Rabehl, et al. (1999). Rabehl, et al. developed a model of a fin-tube heat exchanger based on assumed correlations which were reduced to equations with a few unspecified parameters. These parameters were then fitted using catalog data. In this model, the plate frame heat exchanger is assumed to behave approximately as a series of flat plates with unknown critical local Reynolds numbers. Incropera and DeWitt (2002) give a general form as:

$$Nu_L = (0.037\, Re_L^{4/5} - A) Pr^{1/3} \tag{2.3}$$

Here, A is a variable that depends on the critical Reynolds number, but it may be grouped into another fitted parameter. The ultimate goal is to find UA of the heat exchanger, which will be approximated as the inverse sum of the two convective resistances. First hA on both sides of the heat exchanger must be found, and both sides are assumed to have the same general form of the correlation. Assuming the length L, heat exchanger area A, cross-sectional area A_c are unknown, the equation for hA can be reduced to:

$$hA = \left(c_1 \frac{Q^{4/5}}{\nu^{4/5}} - c_2 \right) \mathrm{Pr}^{1/3}\, k_{fluid} \tag{2.4}$$

Where Q is the volumetric flow rate (m^3/s), ν is the viscosity (m^2/s), Pr is Prandtl number (-), k_{fluid} is the thermal conductivity of the fluid, c_1 and are c_2 constants to be fitted.

Fluid properties are determined at the film temperature on each side of the heat exchanger, and separate coefficients are fitted for each side of the heat exchanger, using manufacturer's catalog data. Furthermore, it was initially assumed that the UA may be simply determined as the inverse of the sum of the two convective resistances. The validity of this assumption will be discussed in the Section 3.2.4. The plate heat exchanger model, TYPE 664, can be seen below in Figure 2.4, showing all inputs, outputs, and parameters needed to run the model.

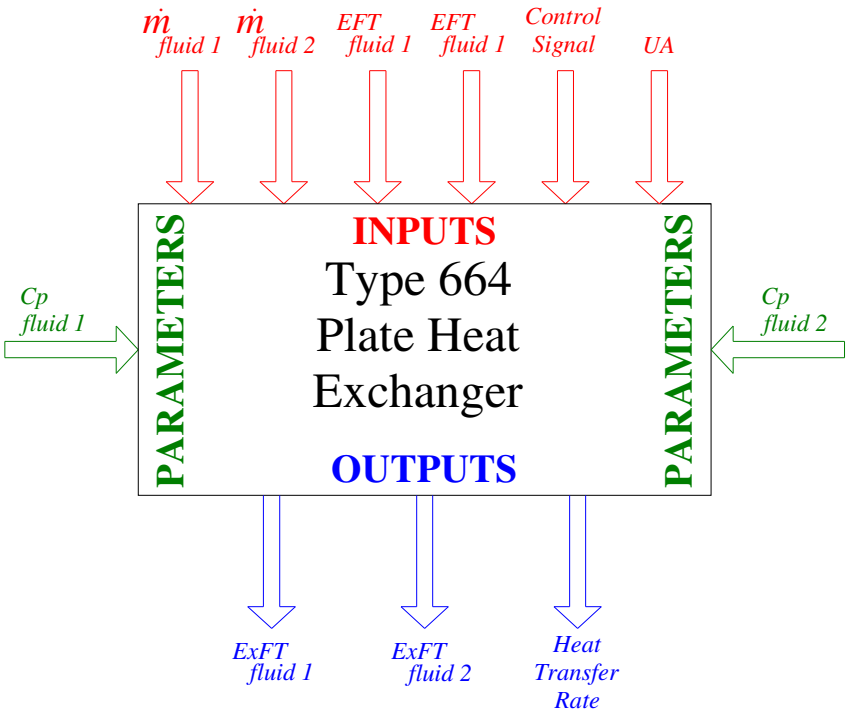

Figure 2.4 *Plate heat exchanger HVACSim+ model diagram.*

2.2.5. Cooling Tower Controller Model

For purposes of experimental validation two approaches to modeling the cooling tower control have been taken. For the first set of simulations, cooling tower on/off operation is simply set as a boundary condition. For the second set of simulations, a simple model of the cooling tower controller takes the difference between the outdoor ambient wet-bulb temperature, provided as a boundary condition, and the simulated exiting heat pump fluid temperature. When the difference exceeds a specified value, e.g. 4ºC (7.2ºF), the cooling tower is switched on. When the difference falls below another specified value, e.g. 2ºC (3.4ºF), the cooling tower is switched off. This approach mimics the actual control strategy that was used in the experiments. The two approaches are discussed further in Sections 3.2 and 3.3 below.

2.2.6. Empirical Pipe Heat Loss/Gain Model

Uninsulated piping in the experimental facility, either exposed to the environment or buried in the ground, has some not insignificant heat losses or gains. These heat transfers vary significantly over time. For example, the heat loss from the buried pipe leading to the cooling tower will be high (say 650 watts on average for the first 10 minutes) when the cooling tower is first switched on. After, say, an hour of cooling tower run time, the heat loss may drop to 350 watts.

As buried horizontal piping is a common feature of ground source heat pump systems, it would be useful to develop a component model that predicts the heat losses or gains. However, at present, no such model is available, and another approach was taken. A simple component model was developed that took the measured heat gain or loss as an input provided as a boundary condition, and computed the outlet temperature as:

$$T_{out} = T_{in} + \frac{Q_s}{\dot{m} C_p} \tag{2.5}$$

Where T_{out} is the temperature of the water leaving the pipe (^{o}C), T_{in} is the temperature of the water entering the run of pipe (^{o}C), and Q_s is the measured heat transfer rate (W).

This approach worked satisfactorily when the cooling tower control was treated as a boundary condition so that the simulated cooling tower on/off operation matched the experiment well. For cases where the cooling tower control was simulated, the short time variations in the empirical pipe heat losses or gains for the piping running to and from the cooling tower are no longer meaningful. Instead, a new boundary condition was developed that used the average heat gain/loss during cooling tower runtime for each component for each day. This was set as the boundary condition for every time step of the day, and maintained the heat loss or gain approximately correctly to the extent that the simulated daily cooling tower runtime matched the actual daily runtime.

2.3. System Model Design and Simulation

As mentioned previously, the system simulation was developed within the HVACSim+ environment (Clark 1985), aided by a graphical user interface (Varanasi

2002). The simulation was developed within a single superblock and five-minute time steps were used. All simulations used the following boundary conditions, measured on site, except where noted:

- Outside air wet-bulb temperature, determined from an aspirated dry bulb temperature measurement (on site) and a relative humidity measured at local weather station, about 1 km (0.6 miles) from the site.
- Heat pump source side load, measured on site. This forces the heat pump operation in the simulation to be the same as the experiment.
- Flow rates of water through the heat pump, GLHE and cooling tower.
- Heat transfer rates for the empirical pipe heat loss/gain model, described above.
- The plate frame heat exchanger UA was treated as a boundary condition; a separate model was used to determine the time-varying UA based on fluid flow rates and time, when fouling was included in the UA.

Besides the variations in component models and parameters that are described in the following sections, two variations of the system simulation approach were utilized:

1. For most of the simulations presented here, the cooling tower control was modeled as a boundary condition taken from the experiment. In this case, all control interactions are, in effect, treated as boundary conditions, and the primary question of interest is the degree to which heat pump entering fluid temperatures can be correctly predicted. Secondary comparisons of interest include heat transfer rates of the various components. This type of simulation was particularly useful when "debugging" the validation, as fluid temperatures at any point in the

loop could be compared directly against the experimental measurements at any time.

2. For the other simulations, the cooling tower control was modeled with a controller that mimicked the actual controller. Ultimately, this is the simulation that is of interest for validation from a designer's perspective. In this case, the questions to be asked include the degree to which the energy consumption can be predicted, the cooling tower run time, and the maximum entering fluid temperature. It is expected that, at best, the cooling tower run time fraction might be reasonably well predicted over a day. It is not expected that the cooling tower start/stop times can be accurately predicted.

For the second simulation approach, one additional boundary condition is an on/off signal that indicates whether or not the cooling tower may be operated. This prevented the simulation from running the cooling tower during the heating season or during several maintenance periods when it was turned off.

The validation simulations were performed in the order given above. The work started with the models and parameters that would be feasible for a designer to obtain in advance of constructing and operating the system. While keeping the cooling tower control fixed as a boundary condition, discrepancies in temperatures were addressed by improving the individual models or their parameters. Then, the simulations with the cooling tower controller explicitly modeled were performed. Starting with the final improved simulation, one could then work backwards to find the initial designer-feasible

models and parameters, and compare the heat pump energy consumption, cooling tower run time, and maximum entering fluid temperature. The HVACSim+ visual tool schematic of the HGSHP system can be seen below in Figures 2.5 and 2.6. Figure 2.5 shows the full schematic with all system connections shown. Each of the system components are identified. Blocks labeled "HEATER" are the empirical heat gain/loss component model. Figure 2.6 shows the flow from component to component.

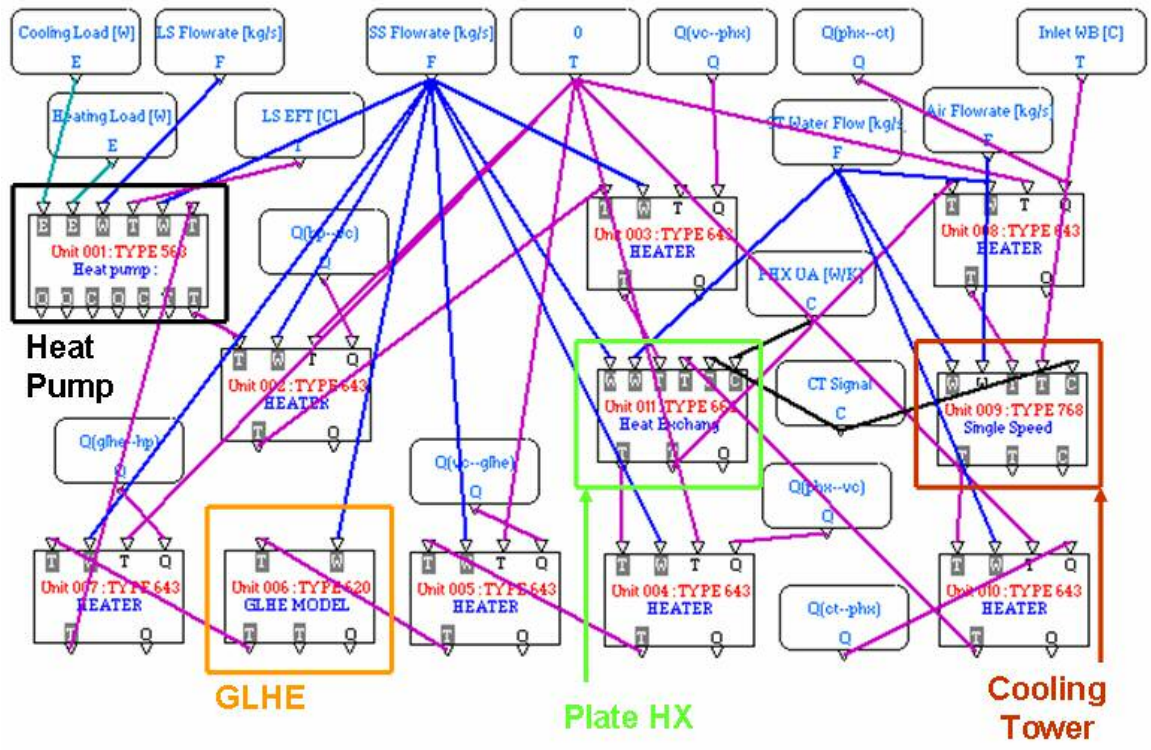

Figure 2.5 *HVACSim+ visual tool model showing system connections.*

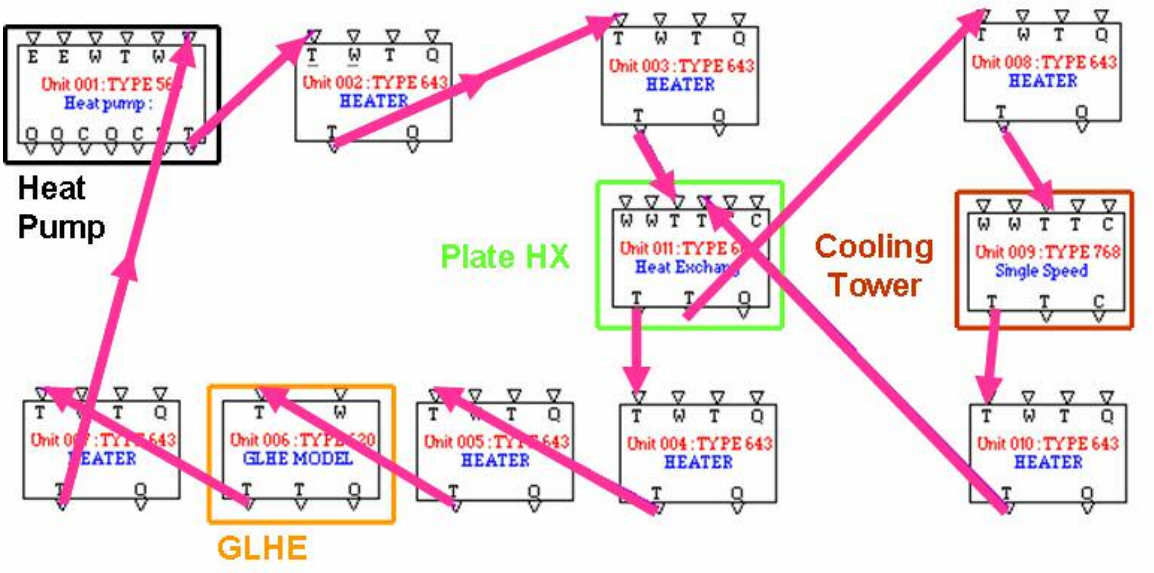

Figure 2.6 *HVACSim+ visual tool model showing flow direction.*

3. EXPERIMENTAL VALIDATION OF HYBRID GROUND SOURCE HEAT PUMP SYSTEMS

Seven months (March to September 2005) of five-minutely experimental data from an HGSHP system were used for validation purposes. The source side of the system consists of two packaged water-to-water heat pumps, a three-borehole ground loop heat exchanger, and a direct contact evaporative cooling tower, isolated by a plate frame heat exchanger. The load side serves two small buildings with hydronic heating and cooling. Experimental validations of each component simulation and the entire system simulation are presented below.

3.1. Experimental Facility

The data used to validate the component and system simulations were collected from the HGSHP research facility (Hern 2004) located on the campus of Oklahoma State University. Chilled water and hot water generated with the plant serve two small buildings. Below is a description of the experimental facility; a more detailed description of the facility is given by Hern (2004). Below, Figure 3.1 shows the HGSHP configuration and Figure 3.2 shows a picture showing the experimental facility.

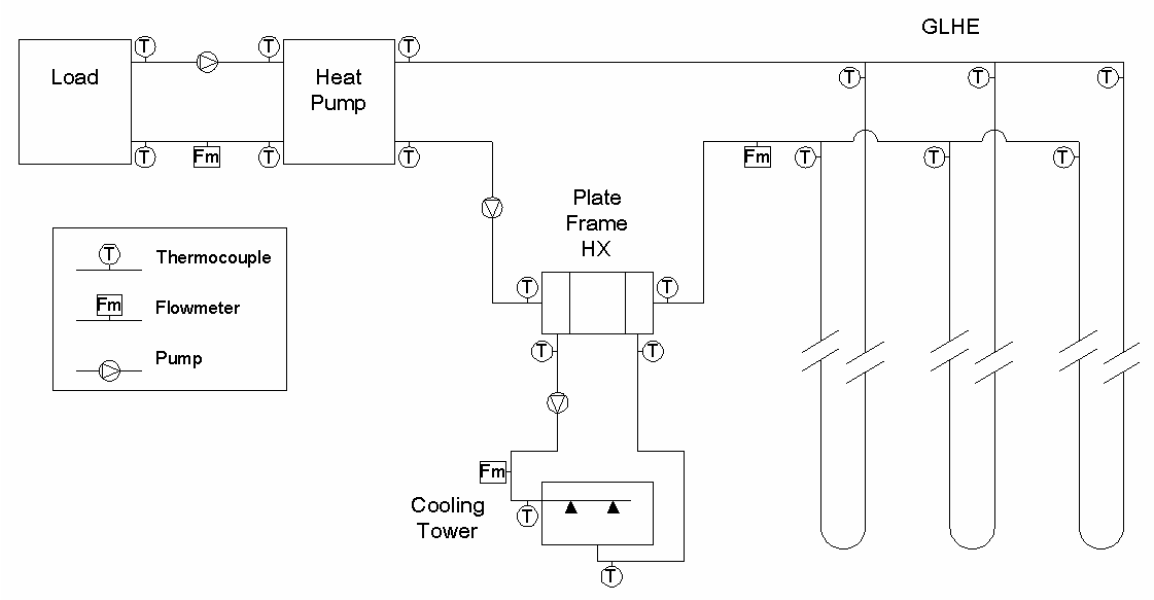

Figure 3.1 *HGSHP configuration for validation.*

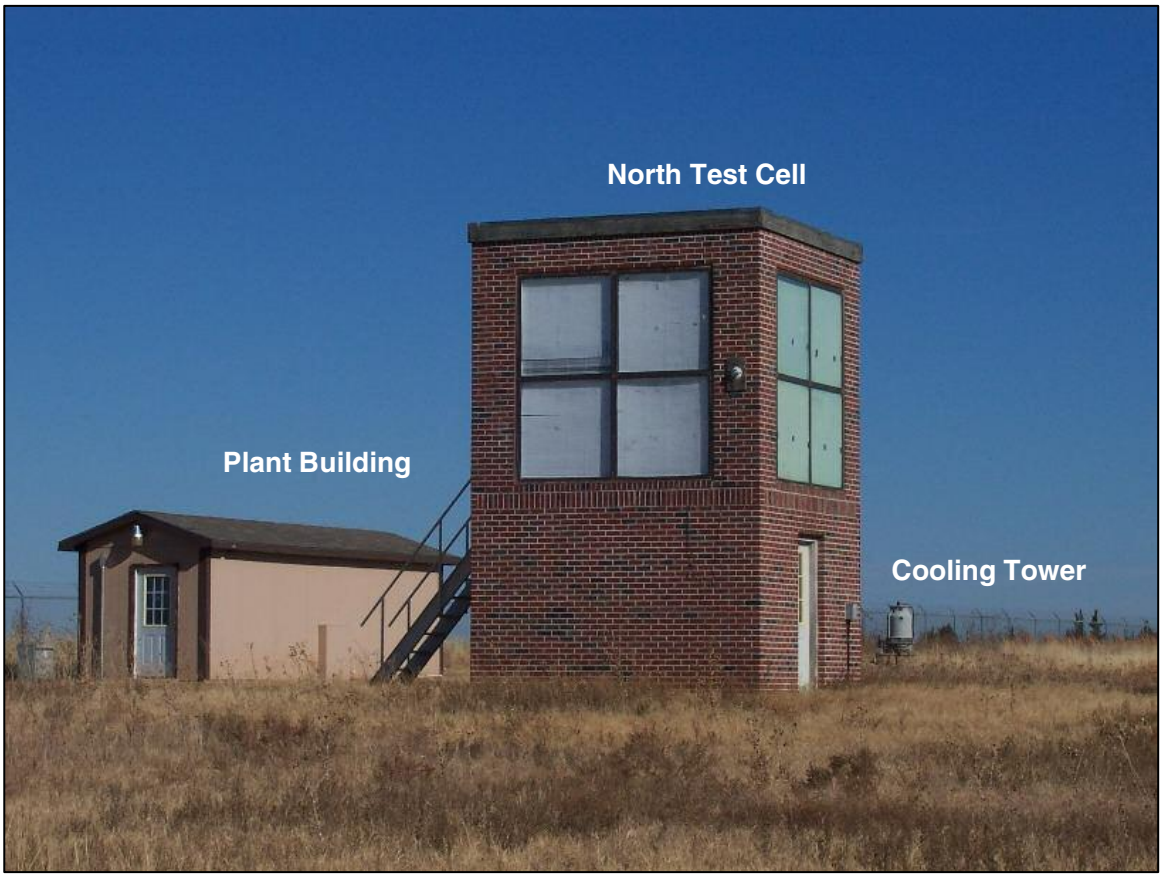

Figure 3.2 *OSU's HGSHP research facility.*

3.1.1. Heat Pumps

Two identical water-to-water heat pumps (Florida Heat Pump WP036–1CSC–FXX), of nominal capacity 10.6 kW (3 ton) are used to provide the chilled water and hot water. For the time period of interest in this simulation, only one heat pump is used at a time. Heating was provided between March 1 and March 29; after which cooling was provided. As the system simulation took the load imposed on the heat pump as a boundary condition, it was possible to model the system with a single heat pump. Catalog data – 35 points in cooling and 25 points in heating mode – at a range of flow rates and entering water temperatures on both the source side and load side obtained from the manufacturer are shown below in Table 3.1. Figure 3.3, below, shows the heat pumps inside the plant building.

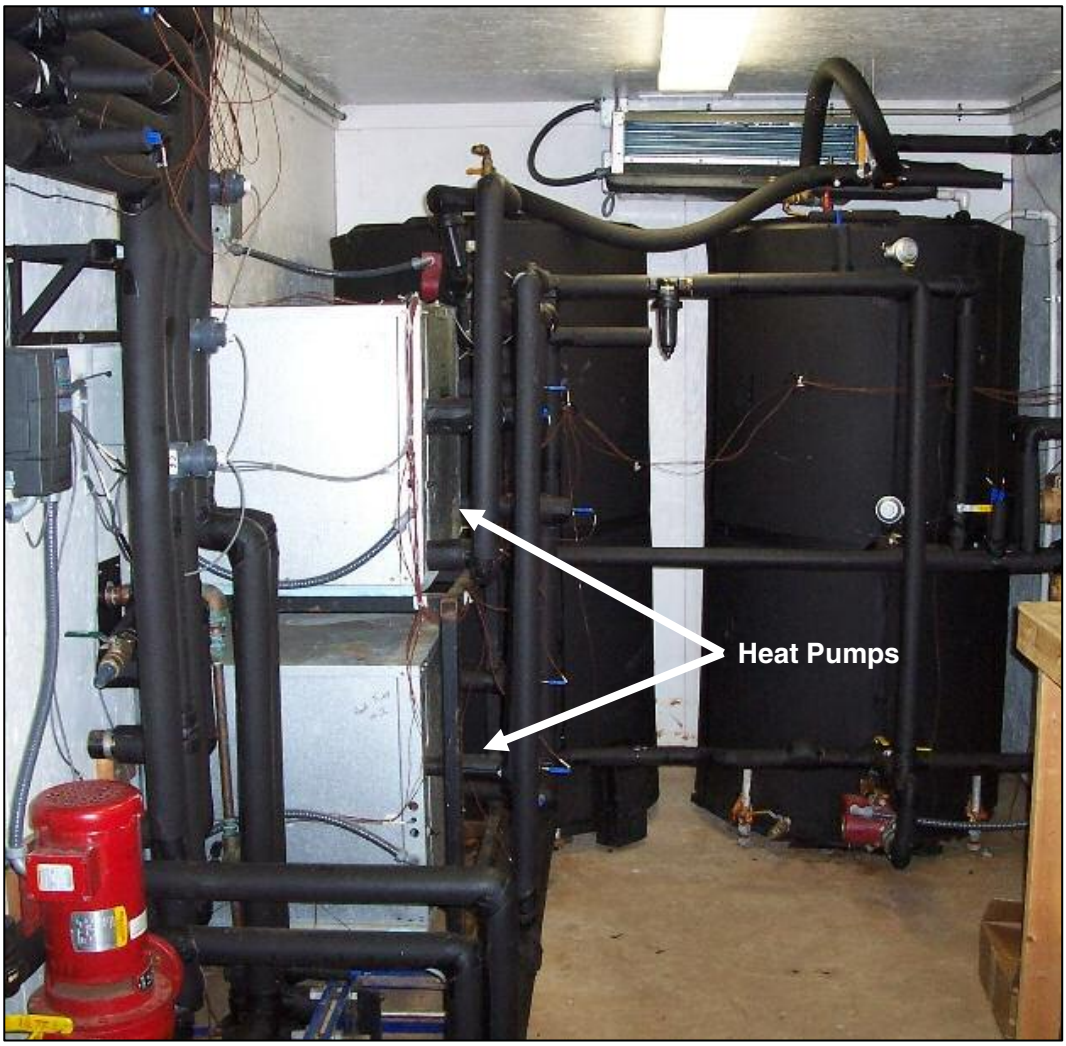

Figure 3.3 *Heat pumps inside the plant building.*

Table 3.1 *Heat pump catalog data. (Florida Heat Pump 2005).*

Cooling Performance Data							**Heating Performance Data**					
Based on 7 GPM chilled fluid and 10°F condenser fluid temp rise.							Based on 7 GPM source side flow and 10oF load temp rise.					
Leaving Chilled Fluid (°F)	Entering Cond. Fluid (°F)	Total Cap. (Tons)	Total Cap. (BtuH)	Power Input (Watts)	EER	Heat Rejection (BtuH)	Leaving Load Fluid (°F)	Entering Source Fluid (°F)	Heating Cap. (BtuH)	Power Input (Watts)	COP	Heat of Absorb. (BtuH)
40°	75°	2.66	31,965	2,251	14.2	39,645	100°	35°	29,085	2,219	3.8	21,513
	80°	2.56	30,717	2,330	13.2	38,667		40°	31,872	2,321	4	23,953
	85°	2.45	29,456	2,403	12.3	37,654		50°	37,802	2,502	4.4	29,266
	90°	2.35	28,184	2,469	11.4	36,609		60°	44,205	2,651	4.9	35,158
	95°	2.24	26,906	2,529	10.6	35,536		70°	51,090	2,767	5.4	41,649
42°	75°	2.78	33,410	2,277	14.7	41,177	110°	35°	27,432	2,296	3.5	19,599
	80°	2.68	32,120	2,360	13.6	40,174		40°	30,205	2,417	3.7	21,958
	85°	2.57	30,817	2,438	12.6	39,135		50°	36,035	2,640	4	27,027
	90°	2.46	29,505	2,509	11.8	38,066		60°	42,308	2,831	4.4	32,649
	95°	2.35	28,187	2,574	11	36,969		70°	49,024	2,988	4.8	38,829
44°	75°	2.91	34,899	2,300	15.2	42,749	120°	35°	25,686	2,350	3.2	17,667
	80°	2.8	33,565	2,389	14.1	41,717		40°	28,418	2,494	3.3	19,910
	85°	2.68	32,219	2,471	13	40,651		50°	34,177	2,759	3.6	24,765
	90°	2.57	30,864	2,548	12.1	39,556		60°	40,311	2,993	3.9	30,098
	95°	2.46	29,504	2,617	11.3	38,434		70°	46,859	3,193	4.3	35,963
45°	75°	2.97	35,669	2,311	15.4	43,555	125°	35°	24,772	2,370	3.1	16,685
	80°	2.86	34,312	2,402	14.3	42,509		40°	27,508	2,524	3.2	18,897
	85°	2.75	32,943	2,487	13.3	41,429		50°	33,210	2,811	3.5	23,618
	90°	2.63	31,566	2,566	12.3	40,320		60°	39,282	3,068	3.8	28,813
	95°	2.51	30,167	2,639	11.4	39,171		70°	45,747	3,291	4.1	34,519
46°	75°	3.04	36,450	2,322	15.7	44,371	130°	35°	23,839	2,385	2.9	15,703
	80°	2.92	35,054	2,416	14.5	43,298		40°	26,565	2,549	3.1	17,866
	85°	2.81	33,662	2,503	13.5	42,203		50°	32,227	2,860	3.3	22,470
	90°	2.69	32,262	2,584	12.5	41,080		60°	38,236	3,139	3.6	27,526
	95°	2.57	30,858	2,659	11.6	39,931		70°	44,606	3,385	3.9	33,056
48°	75°	3.17	38,032	2,342	16.2	46,023						
	80°	3.05	36,603	2,440	15	44,930						
	85°	2.93	35,148	2,533	13.9	43,792						
	90°	2.81	33,701	2,619	12.9	42,638						
	95°	2.69	32,250	2,699	12	41,460						
50°	75°	3.31	39,663	2,361	16.8	47,717						
	80°	3.18	38,183	2,464	15.5	46,589						
	85°	3.06	36,693	2,561	14.3	45,431						
	90°	2.93	35,181	2,653	13.3	44,232						
	95°	2.81	33,682	2,738	12.3	43,022						

The facility allows the source side of the heat pumps to be connected to a ground loop heat exchanger, an evaporative cooling tower, and/or a pond loop heat exchanger. These can be connected in any combination, but for the duration of these experiments, they were configured as a typical HGSHP system, with a GLHE, and a cooling tower.

The isolation heat exchanger was connected in series with the GLHE, and the cooling tower was switched on and off based on the difference in the exiting heat pump fluid temperature and the outdoor ambient wet-bulb temperature.

3.1.2. GLHE

The GLHE has, in total, 4 vertical boreholes and one horizontal loop. For these experiments, only 3 vertical boreholes are connected, as shown in Figure 3.1. The vertical boreholes are each approximately 75 meters (246 ft) deep, 114 mm (4.5 in.) in diameter and consist of a single HDPE U-tube of nominal diameter 19.05 mm (0.75 in.), backfilled with bentonite grout. In situ measurements of undisturbed ground temperature and thermal conductivity made by Hern (2004) are discussed in Section 3.2.2.

3.1.3. Cooling Tower

A direct-contact evaporative cooling tower, shown in Figure 3.4, (Amcot ST-5) with nominal capacity of 17.6 kW (5 ton) (defined at a water flow rate of 0.63 L/s (10 GPM) being cooled from 35ºC (95ºF) to 29.4ºC (85ºF) with an outdoor wet-bulb temperature of 25.6ºC (78ºF)) is connected to the source-side of the heat pumps via an isolation heat exchanger. No other performance data are available from the manufacturer. From the performance data given the overall heat transfer coefficient (UA) was calculated to be approximately 800 W/K. Performance data obtained from the manufacturer is shown below in Table 3.2.

Table 3.2 *Cooling tower manufacturer's data. (Amcot 2005).*

Model	Dimesnsions (inch)		Pipe Connections (inch)						Fan Motor (HP)	Fan Diameter (inch)	Air Volume (CFM)	Nominal Water Flow (GPM)	Pump Head (FT.)
	height	diameter	in	out	O	Dr	FLO	Q					
5	52	34	1.5	1.5	1	0.75	0.5		0.167	19.5	2,100	10	5

Figure 3.4 *Amcot cooling tower.*

3.1.4. Plate Heat Exchanger

The plate frame heat exchanger, shown in Figure 3.5, (Paul Mueller PHE AT4C-20) has a nominal capacity of 9.3 kW (2.6 ton) with flow rates of 0.5 L/s (8 GPM) on both sides of the heat exchanger and a temperature difference of 19.4ºC (35ºF) between the inlet temperatures. The manufacturer gave an additional 15 data points at various flow rates and temperatures as shown below in Table 3.3.

Figure 3.5 *Plate heat exchanger.*

Table 3.3 *Plate heat exchanger manufacturer's data. (Data obtained by manufacturer via e-mail).*

Loop Side (Hot)		CT Side (Cold)					
EFT (^oF)	Flow rate (GPM)	EFT (^oF)	Flow rate (GPM)	HTR (Btu/hr)	LMTD (^oF)	U (Btu/ft^2-hr-^oF)	Heat Transfer Area (ft^2)
100	6	75	6	21,448	17.8	405	3
120	6	85	6	23,737	27.0	296	3
140	6	95	6	35,467	33.0	361	3
100	8	75	8	28,597	17.8	540	3
120	8	85	8	31,650	27.0	394	3
140	8	95	8	47,289	33.0	482	3
100	12	75	12	41,703	18.0	779	3
120	12	85	12	47,474	27.0	591	3
140	12	95	12	70,934	33.0	723	3
100	14	75	14	47,262	18.2	874	3
120	14	85	14	55,387	27.0	690	3
140	14	95	14	82,756	33.0	843	3
140	6	95	10	56,200	29.7	638	3
140	12	95	8	70,934	30.0	797	3
140	14	95	6	62,046	29.7	704	3
120	10	85	14	59,368	24.7	809	3
120	6	85	14	44,540	24.0	624	3
120	8	85	12	51,457	24.1	718	3

3.1.5. Piping

In addition to the components that are shown explicitly in Figure 3.1, there is buried piping that connects the GLHE to the plant building (approximately 30 m (98 ft) in each direction), buried piping that connects the cooling tower to the plant building (approximately 31 m (102 ft) in each direction), and exposed (to the plant room environment) piping that connects the components inside the building. Under many conditions, e.g. when the piping is insulated, heat losses and gains to/from the piping may be negligible. However, buried, uninsulated piping, as used to connect the cooling tower and GLHE has a not-insignificant amount of heat transfer.

3.1.6. Experimental Measurement Uncertainty

A detailed uncertainty analysis was performed by Hern (2004). As can be seen from Figure 3.1, thermocouples, with an uncertainty of approximately ±0.11ºC (±0.2ºF), were placed on the inlets and outlets of all components. Vortex and paddle wheel flow meters were utilized to measure flow through the heat pump – GLHE loop and through the cooling tower loop; expressions for their uncertainty were given by Hern (2004).

Heat transfer rates are determined as the product of the mass flow rate, specific heat, and ΔT. Given the uncertainty in temperature measurement, the fractional uncertainty in the temperature difference measurement is:

$$e_{\Delta t} = \frac{\pm 0.16^{\circ} C}{\Delta T} \tag{3.1}$$

Then, the fractional uncertainty of the heat transfer rate may be given as:

$$e_{HTR} = \pm\sqrt{e_{\Delta t}^2 + e_{flow}^2} \tag{3.2}$$

where e_{flow} = fractional error in the flow rate.

Actual uncertainties vary with time and are shown with the results.

3.2. Component and System Model Validation-Cooling Tower Operation Set with Boundary Condition

In this section, validations of each component model, individually and within the system simulation, are presented. "Individually" means validation of the component

model by itself where the input temperatures are taken from experimental data. "Within the system simulation" means validation of the component model where the input temperatures are computed by the system simulation, when all fluid temperatures are being solved simultaneously. In addition, the model parameters determined from manufacturer's data and improvements based on calibration are discussed.

3.2.1. Heat Pump Model

The coefficients of the heat pump used for the model described in Section 2.2.1 were developed in Excel using a Visual Basic for Applications (VBA) program written by Tang (2005). The coefficient "calculator" takes the manufacturer's data, and fits equation coefficients utilizing the generalized least squares method. The coefficients are listed below in Table 3.4.

Table 3.4 *Heat pump coefficients.*

Coefficient Name	Coefficients obtained through Manufacturer's Data	Coefficients obtained through Experimental Data
1st COP Coefficient in Heating Capacity	1.41266	-5.61874
2nd COP Coefficient in Heating Capacity	-4.04836	-0.04688
3rd COP Coefficient in Heating Capacity	0.14638	5.84694
4th COP Coefficient in Heating Capacity	1.98893	0.99705
5th COP Coefficient in Heating Capacity	1.70755	-0.25909
1st COP Coefficient in Heating Compressor Power	-5.72324	-6.86601
2nd COP Coefficient in Heating Compressor Power	19.86488	7.04857
3rd COP Coefficient in Heating Compressor Power	-0.70239	0.11919
4th COP Coefficient in Heating Compressor Power	-10.32428	0.02566
5th COP Coefficient in Heating Compressor Power	-2.47377	0.03218
1st COP Coefficient in Heating Extraction	0.00551	-7.83259
2nd COP Coefficient in Heating Extraction	-0.00004	-2.82569
3rd COP Coefficient in Heating Extraction	0.00001	10.98915
4th COP Coefficient in Heating Extraction	0.27928	0.10341
5th COP Coefficient in Heating Extraction	1.00001	0.67269
1st COP Coefficient in Cooling Capacity	1.41266	-4.13867
2nd COP Coefficient in Cooling Capacity	-4.04836	5.67839
3rd COP Coefficient in Cooling Capacity	0.14638	-1.47811
4th COP Coefficient in Cooling Capacity	1.98893	0.67561
5th COP Coefficient in Cooling Capacity	1.70755	0.01583
1st COP Coefficient in Cooling Compressor Power	-5.72324	-5.80673
2nd COP Coefficient in Cooling Compressor Power	19.86488	0.39063
3rd COP Coefficient in Cooling Compressor Power	-0.70239	6.22099
4th COP Coefficient in Cooling Compressor Power	-10.32428	-0.01139
5th COP Coefficient in Cooling Compressor Power	-2.47377	-0.09678
1st COP Coefficient in Heating Rejection	0.00551	-6.24958
2nd COP Coefficient in Heating Rejection	-0.00004	6.29918
3rd COP Coefficient in Heating Rejection	0.00001	0.54542
4th COP Coefficient in Heating Rejection	0.27928	0.15376
5th COP Coefficient in Heating Rejection	1.00001	0.05115

The model using these coefficients is labeled as "uncalibrated" in Figures 3.6-3.8. The model gave poor results in heating mode due to the fact that the actual flow rates on both sides of the heat pump were larger than catalog data. This may be unavoidable in equation-fit models and could perhaps be addressed by specifying flow rate and temperature limits in the component model. However, it was addressed in our case by

using thousands of experimentally-measured data points in the data set and recalculating the model coefficients. Table 3.5 and Figures 3.6 and 3.7 show substantial improvements when this calibration is done. Or, it could be addressed by using a parameter-estimation based model (Jin and Spitler 2003). However, a recommendation for system designers is still needed and is a subject of future work.

Table 3.5 *Summary of uncertainties in HP model.*

Model	Source Side HTR RMSE (W)	Source Side HTR Mean Bias Error (W)	Load Side HTR RMSE (W)	Load Side HTR Mean Bias Error (W)	Power RMSE (W)	Power Mean Bias Error (W)	Source Side HTR Typical Uncertainty	Load Side HTR Typical Uncertainty	Power Typical Uncertainty
Simulated (calibrated system simulation)	451	-141	171	-33	77	-32	450 W	500 W	4.5 W
Simulated (calibrated component simulation)	457	-179	72	12	27	5			
Simulated (uncalibrated component simulation)	1823	1113	751	-333	414	-81			

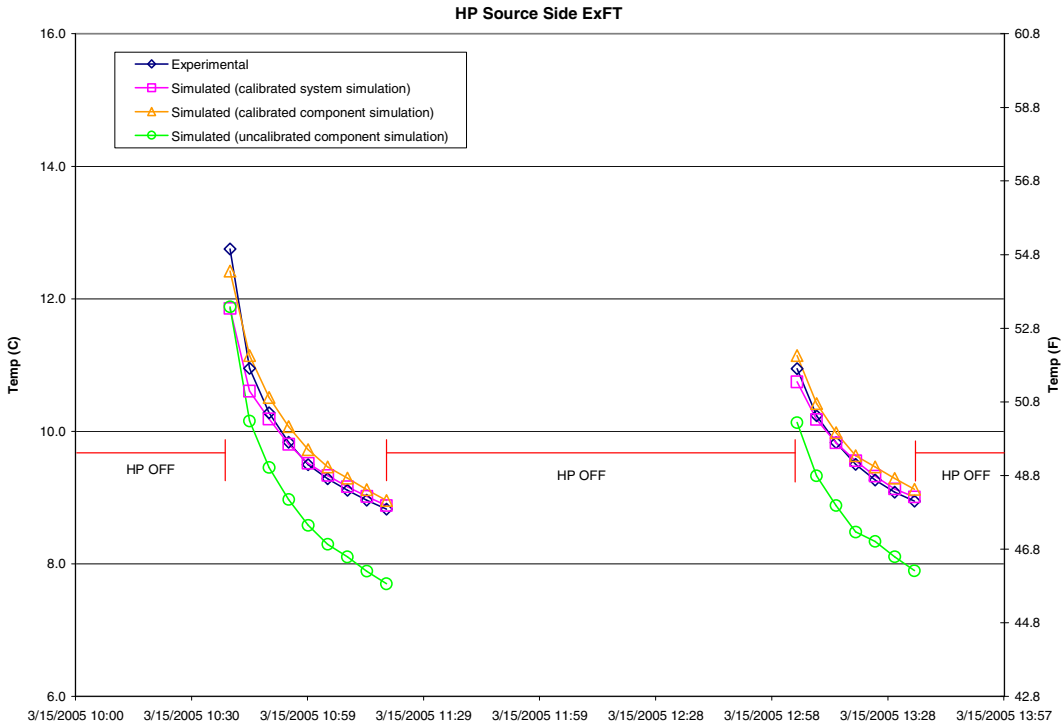

Figure 3.6 *HP source side ExFT for a typical heating day.*

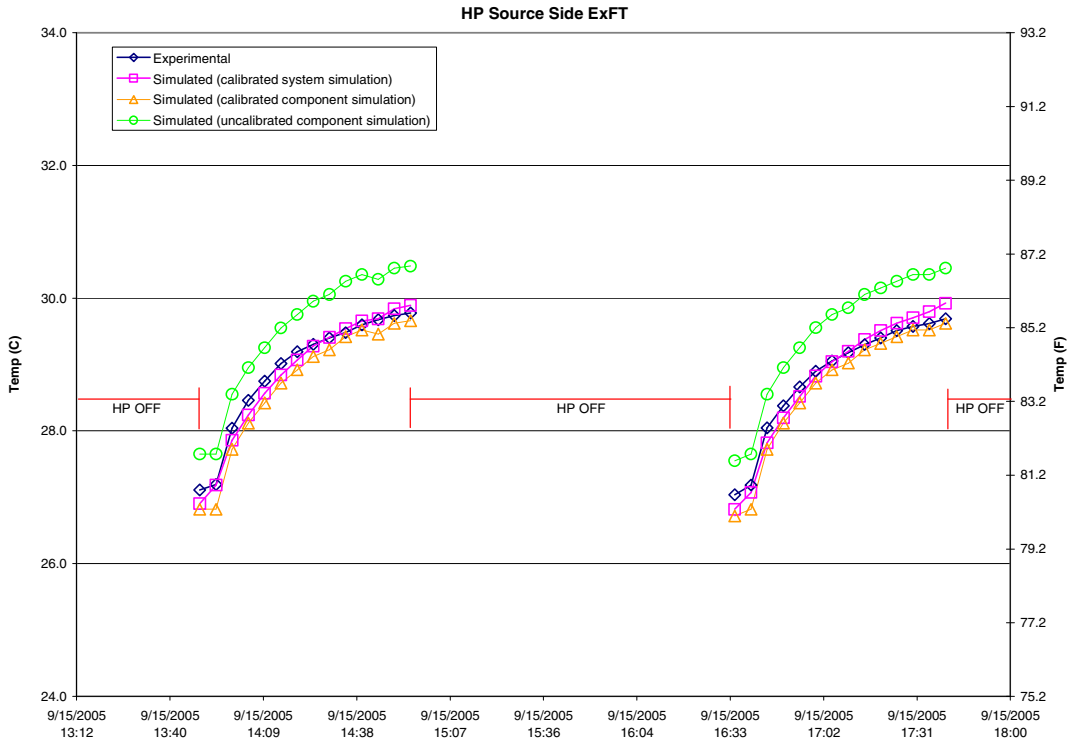

Figure 3.7 *HP source side ExFT for a typical cooling day.*

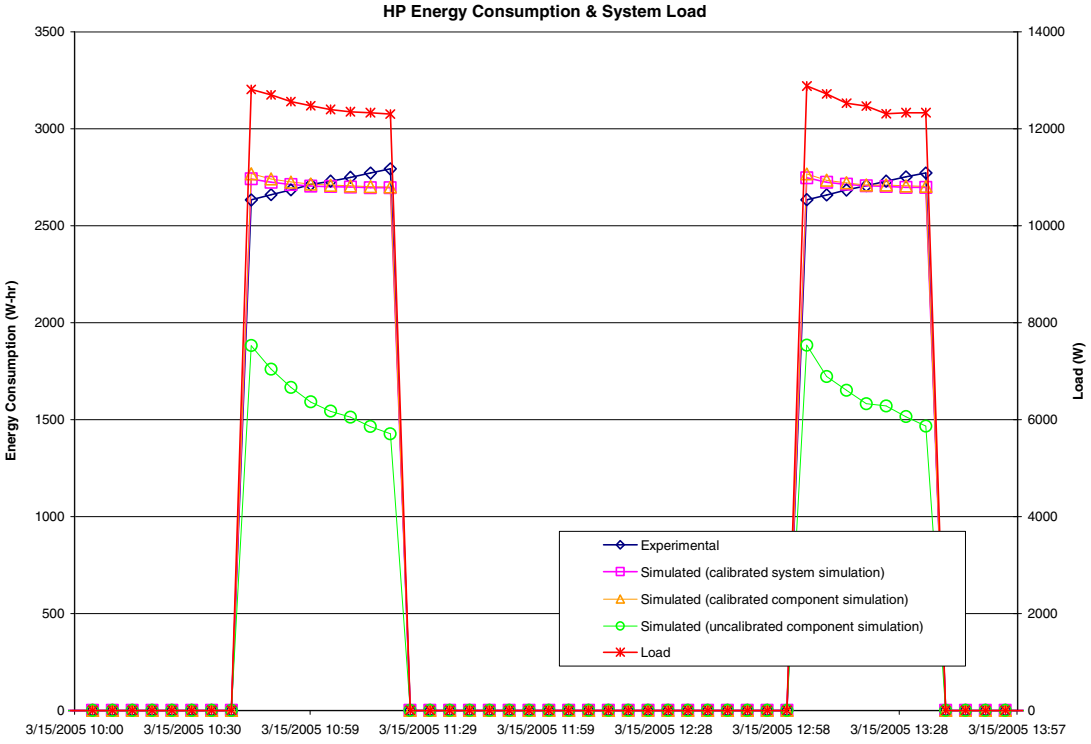

Figure 3.8 *HP energy consumption and load for a typical heating day.*

3.2.2. Ground-Loop Heat Exchanger Model

The GLHE model requires specification of a number of parameters related to the geometry and thermal properties of the fluid, grout, and surrounding ground. While there are many parameters, the results are moderately sensitive to three parameters that are challenging to estimate precisely: the undisturbed ground temperature, the effective grout thermal conductivity, and the effective ground thermal conductivity.

For larger commercial systems, these parameters are typically estimated as part of an in situ thermal conductivity test, which would be performed for one or a few test boreholes. (Austin et al. 2000, Shonder and Beck 2000, Gehlin and Nordell 2003, Sanner et al. 2005). Additional uncertainty, beyond sensor errors, is introduced because of the nonhomogeneous nature of the ground; the time-varying nature of the undisturbed ground temperature, which is affected by seasonal changes near the surface; and downhole variations in the U-tube location and borehole diameter. Hern (2004) measured all three boreholes; the range of values and mean value are summarized in Table 3.6. The calibrated values, presented in the table, are found by minimizing the sum-of-the-squares-of-the-error of the GLHE exiting fluid temperature for the seven-month period evaluated here. The minimization was done with a univariate process applied iteratively. Because the parameters are interrelated, the calibration may find best-fit values that are outside the estimated uncertainty range of the experimental measurements, as found for the effective grout thermal conductivity.

Table 3.6 *GLHE Parameters.*

Parameter	Range measured by Hern (2004)	Mean measured by Hern (2004)	Estimated Uncertainty	Calibrated Value
Undisturbed ground temperature (°C)	17.1-17.4	17.25	± 1.0 º C	18
Undisturbed ground temperature (°F)	*62.78-63.32*	*63.05*	*± 1.8 º F*	*64.4*
Effective grout thermal conductivity (W/m-K)	1.07-1.19	1.11	± 15%	1.56
Effective grout thermal conductivity (Btu/hr-ft-°F)	*0.62-0.69*	*0.64*	*± 15%*	*0.90*
Effective ground thermal conductivity (W/m-K)	2.37-2.68	2.54	± 15%	2.25
Effective ground thermal conductivity (Btu/hr-ft-°F)	*1.37-1.55*	*1.47*	*± 15%*	*1.30*

Figure 3.9 compares experimental and simulated outlet temperatures resulting from the component GLHE simulation (calibrated and uncalibrated) as well as the system simulation (calibrated only) for five hours of a typical cooling day. Figure 3.10 gives the heat transfer rates for the same time period. During these five hours, the heat pump went through two on/off cycles. During the off portion of the cycle, it may be noted that there is a small negative heat transfer rate. The circulation pump was operated continuously. Also, during this time period, the cooling tower was operated continuously, and heat was exchanged between the ground and the horizontal piping that runs between the plant and the cooling tower. The net effect is the small negative heat transfer rate; i.e. heat is being extracted from the ground, and is "pre-cooling" the ground during the heat pump off cycle.

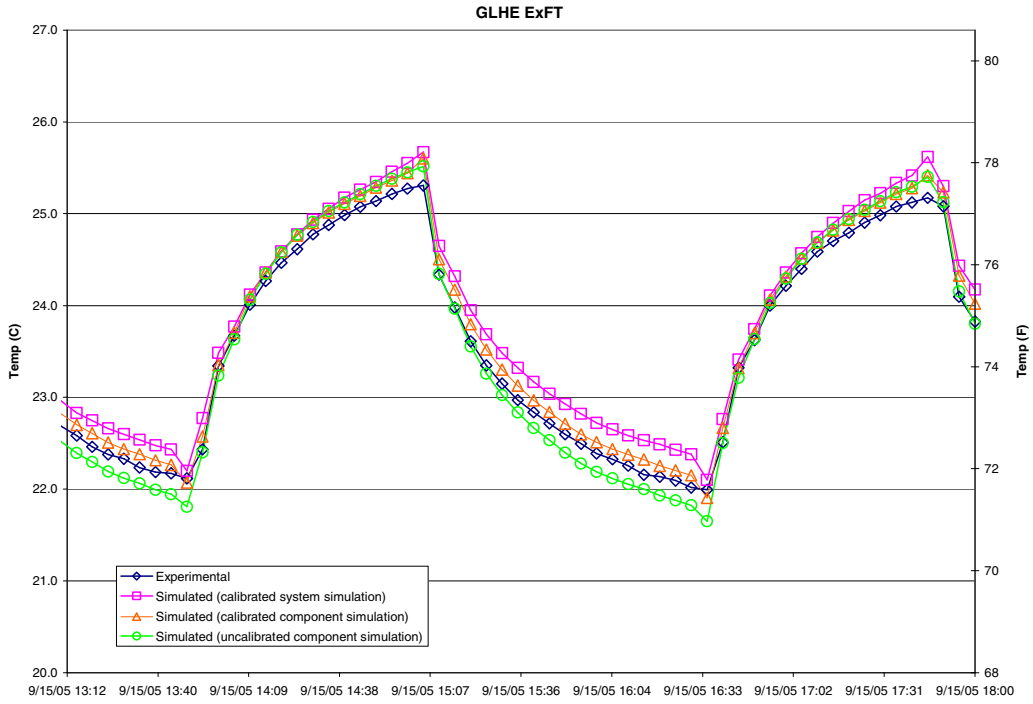

Figure 3.9 *GLHE ExFTs for five hours of a typical cooling day.*

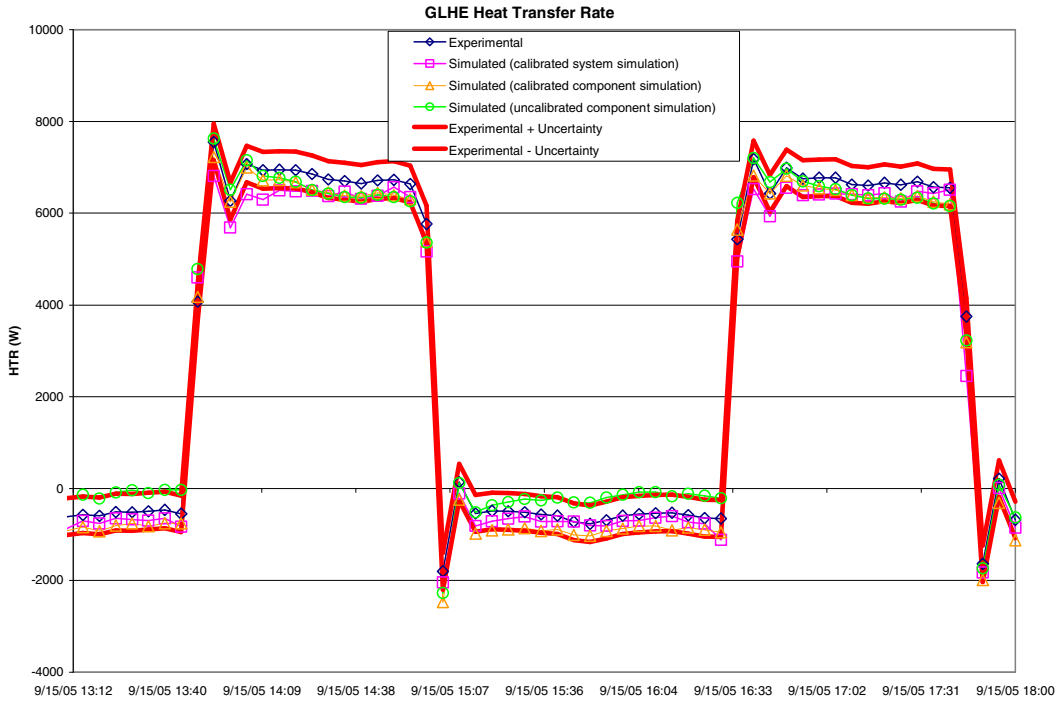

Figure 3.10 *GLHE heat transfer (rejection) rates for five hours of a typical cooling day.*

For the component simulations, the experimental inlet temperature was used to drive the model. As expected, the calibrated component model simulation with the correct inlet temperature gives the best results. It represents a small improvement over the uncalibrated component model simulation. It may be inferred from this that the thermal properties measured with the in situ test give adequate accuracy. The system simulation, which uses the inlet temperature calculated by the simulation, shows an increased amount of error.

For the uncalibrated component model simulation, the RMSE of the heat transfer rate over the seven month evaluation period is 463 W; the mean bias error (MBE) is 10 W; the simulation predicted, on average, 10 W more heat rejection than was experimentally measured. The calibrated component model simulation has a lower RMSE of 377 W, but an MBE of 320 W. This suggests that the calibration procedure might be rethought – perhaps the sum of the squares of the error criterion is not the best. Finally, when the calibrated model is run as part of the system simulation, the RMSE increases to 652 W, but the MBE drops to 62 W.

These errors should be compared to the experimental uncertainty of the heat transfer measurement. The uncertainty varies with flow rate and ΔT, but a typical value when the heat pump is operating is ±400 W. Figure 3.10 shows the upper and lower bounds on the experimental uncertainty. As shown, the system simulation produces some results that are just outside the bounds of experimental uncertainty.

3.2.3. Cooling Tower Model

As the cooling tower manufacturer gave only a single operating point as catalog data, the first cooling tower model utilized a fixed UA value of 800 W/K. For larger cooling towers, additional manufacturer's data should be available to support a variable-UA model. For our experiment, the variable UA model was developed based on measured data, resulting in:

$$UA_e = \left[764\dot{m}_w^{1.11}\dot{m}_a^{0.41}\right]\frac{C_{pe}}{C_{p,moistair}} \tag{3.3}$$

Figures 3.11 and 3.12 show results for a portion of a typical cooling day, with several cooling tower on/off cycles. Here, the uncalibrated component simulation represents the results from the fixed UA model; while the calibrated simulations represent results with the variable-UA model. The model improvements do not result in obviously significant improvements in the model predictions. The RMSE in the heat transfer rate is 862 W for the uncalibrated component simulation. Going to the calibrated variable UA model only reduces the RMSE to 762 W. However, the MBE goes from 329 W to 71 W of overprediction by the simulation. When the calibrated model is simulated as part of the system, the RMSE is 359 W and the MBE is 16 W of underprediction by the simulation.

The lower and upper bounds of the experimental uncertainty in the cooling tower heat transfer rate measurement are shown in Figure 3.12. In addition, the simulation has an experimental uncertainty component – the wet-bulb temperature (an input) has a

typical uncertainty of ± 0.5ºC – and this results in an uncertainty in the simulation results. Error bars are shown for two sample points in Figure 3.12. The uncertainty caused by the uncertainty in the wet-bulb temperature appears to be the limiting factor in the simulation. This also suggests that, in practice, caution is warranted in using a control based on wet-bulb temperature.

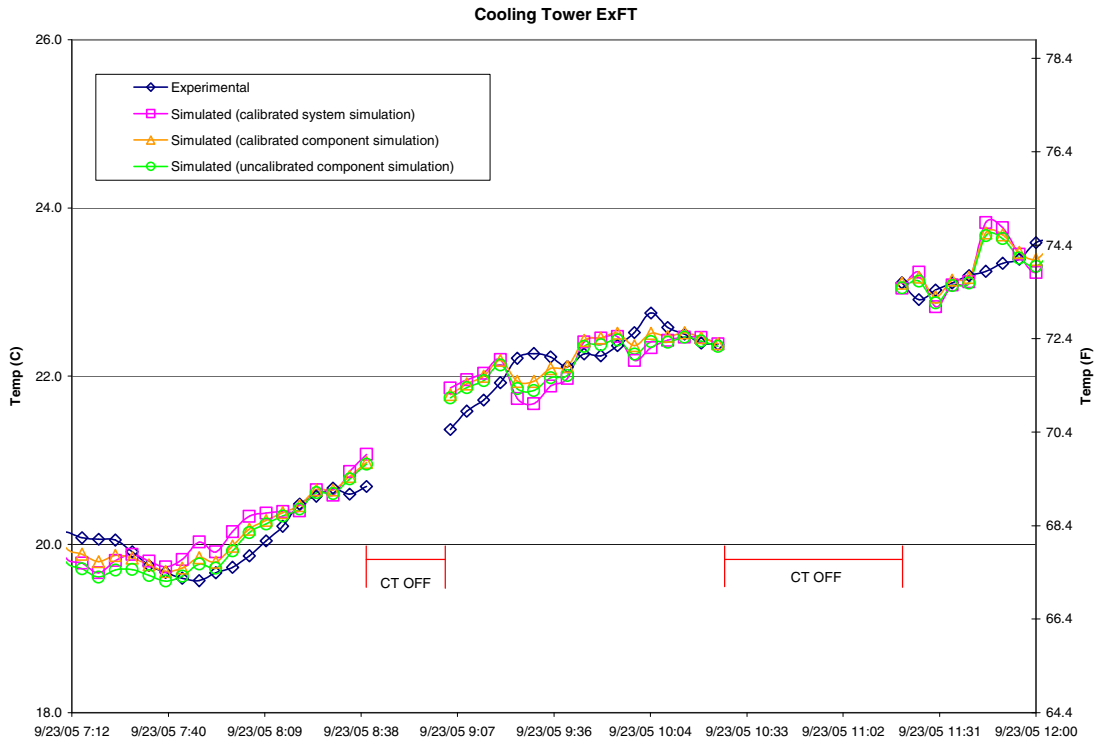

Figure 3.11 *Cooling tower ExFTs for a typical cooling day.*

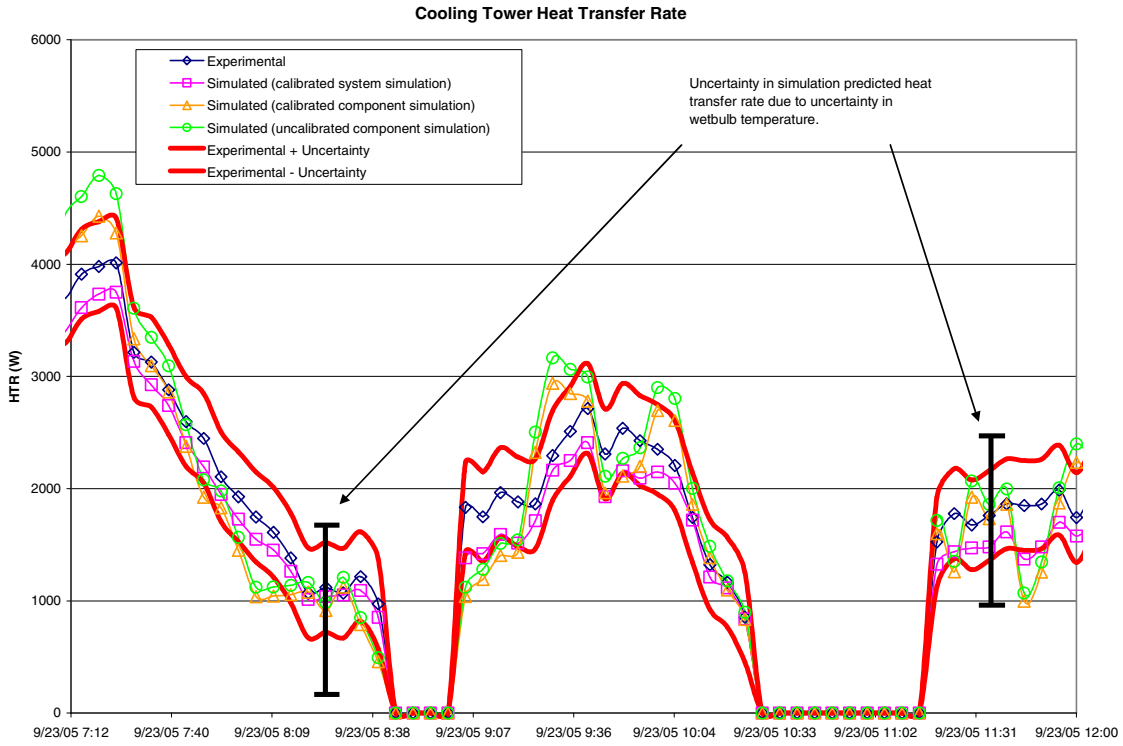

Figure 3.12 *Cooling tower heat transfer rates for a typical cooling day.*

3.2.4. Plate Frame Heat Exchanger Model

Sixteen data points were available from the manufacturer of the plate frame heat exchanger model. Initially, a fixed UA model was utilized for the heat exchanger with a value of 800 W/K, given by the manufacturer's data. However, calculation of the UA value at every time step based on experimental measurements revealed two interesting phenomena:

1. First, the UA varied moderately as fluid flow rates and temperatures changed. This phenomenon was addressed by developing the parameter estimation-based model, based on the general concept of Rabehl, et al. (1999), as described above.

2. More significantly, the UA decreased substantially over the seven month period of experimentation. Significant fouling was observed on the cooling tower supply side of the loop, and a chemical treatment regime introduced belatedly did not reverse the UA degradation. Prediction of fouling does not seem to be feasible, so a heuristic approach was taken by adding a fouling factor that increased linearly with time.

Figure 3.13 shows a comparison of the various simulations with the experimental results. Clearly, the original approach, without the fouling adjustment, yields large errors. With the fouling adjustment the system simulations give heat transfer rates that are substantially improved. However, the model results are better for the typical cooling day than other days. The RMSE of the heat transfer rate prediction is 1839 W for the uncalibrated model; 854 W for the calibrated model; and 968 W for the calibrated model in the system simulation. The MBE is 1380 W of overprediction for the uncalibrated model; 311 W of overprediction for the calibrated model; and 3 W of underprediction for the calibrated model in the system simulation. So, while the calibration process helps significantly, the inherently unpredictable nature of fouling leaves a difficulty for the system designer.

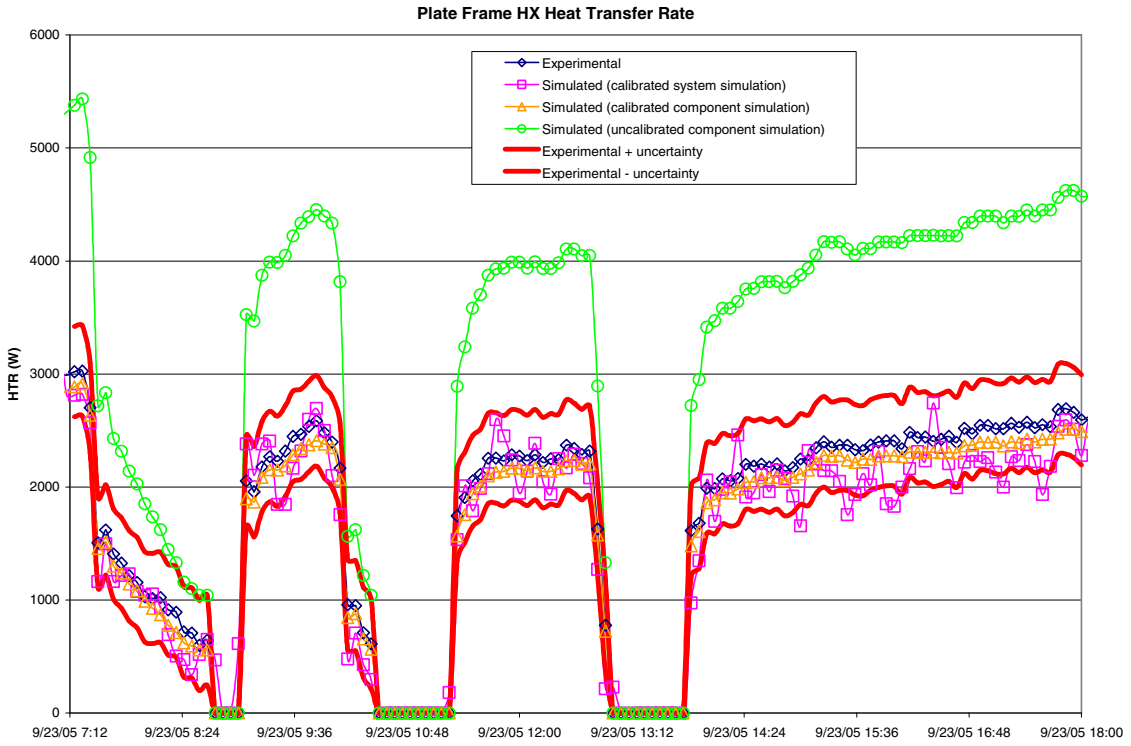

Figure 3.13 *Plate frame HX heat transfer rate for a typical cooling day.*

3.3. System Model Validation-Cooling Tower Control Simulated

After adjusting component models and their parameters while setting the cooling tower operation to exactly match the experimental data, attention may be turned to the broader question of how the model performs with the cooling tower control explicitly modeled. Again, this is the simulation that is of interest for validation from a designer's perspective. The starting case (uncalibrated system simulation) will be compared to the improved heat pump model case, the final case (calibrated system simulation), and experimental results. Three results are of primary interest: system energy consumption, cooling tower run time, and maximum entering fluid temperature to the heat pump.

Starting with the system energy consumption, Figure 3.14 shows the component-by-component energy consumption over the period of April to September of the uncalibrated system simulation, the improved heat pump model, the final calibrated system simulation, and the experimental results. It should be noted that the heat pump model, with the flow rate outside the manufacturer's data used to generate the polynomial coefficients gave negative power values for heat pump operation during the month of March (heating season) and therefore March is not included in the figure. During this six month period the uncalibrated system simulation overpredicts the energy consumption by more than 8%, and if the month of March were included the deviation would be even greater. As is shown by calibrating just the heat pump model improves the prediction to where the simulation underpredicts experimentally measured energy consumption by 6.1%. The final calibrated system simulation improves the accuracy of the energy consumption prediction to within 5%. As was previously shown, the calibration improved the fidelity of the model with respect to fluid temperatures and heat transfer rates and as can be seen from Figure 3.14 this translated into improvements in energy consumption prediction. The inaccuracy of the uncalibrated system simulation was primarily due to problems with the heat pump operating outside catalog data. With the calibrated heat pump model the results provide hope that, for the designer, reasonable accuracy in predicting energy consumption can be had with information available at the time of the design. This presumes that the heat pump is operated within the manufacturer's data or that a model with better performance, such as a parameter-estimation-based model, is used.

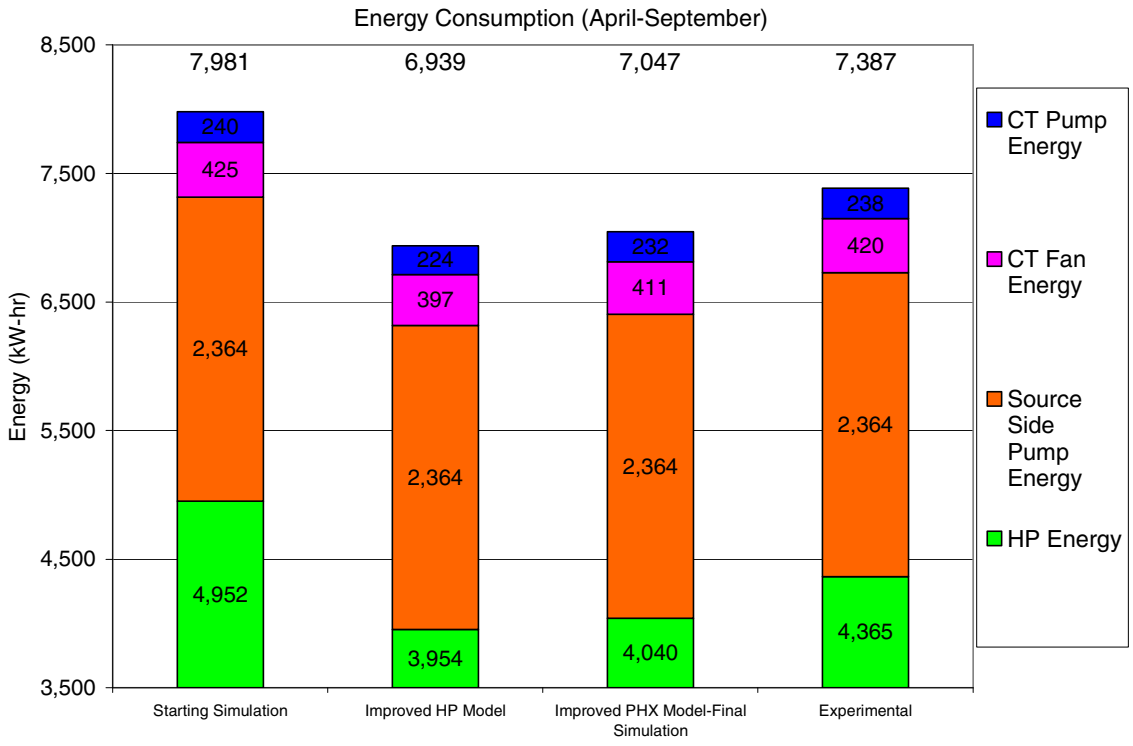

Figure 3.14 *System energy consumption, April-September. Note: Y-axis begins at 3,500 kW-hr.*

The monthly energy consumption for the uncalibrated simulation, final calibrated simulation, and the experimental results are shown in Figure 3.15. Most months show significant improvement when the heat pump model is calibrated and further improvement with all of the other components calibrated.

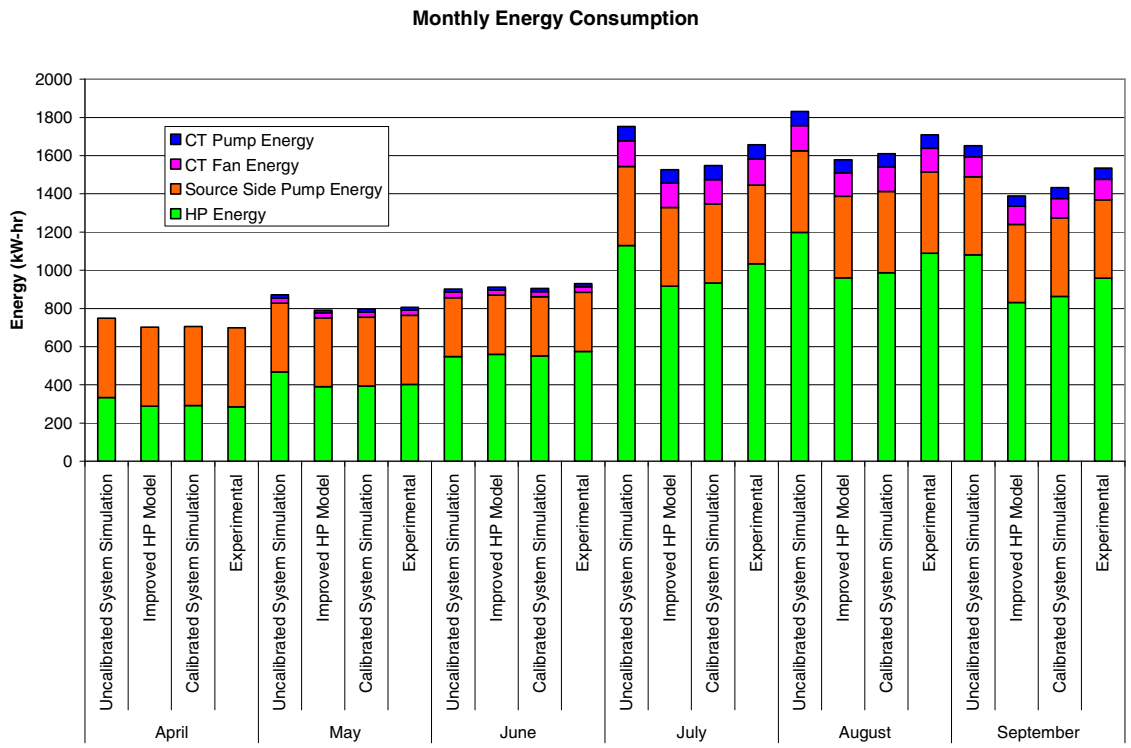

Figure 3.15 *Experimental vs. simulated (calibrated and uncalibrated) monthly energy consumption.*

The cooling tower run times predicted by each model variation and the experiment are summarized in Table 3.7. Again, all variations of the model fall within a few percent of the experimental results, and this accuracy should be quite adequate for any design simulation.

Table 3.7 *Cooling tower run times.*

	Uncalibrated System Simulation	Improved HP Model	Calibrated System Simulation	Experimental
Cooling Tower Run Time (Hours)	1,805	1,686	1,745	1,786

A final parameter of interest is the predicted maximum entering fluid temperature. Ground loop heat exchangers serving cooling-dominated buildings are generally sized to not exceed a maximum entering fluid temperature, so this parameter is of particular interest. As shown in Table 3.8, all of the simulations overpredict the maximum entering fluid temperature, although the model improvements generally increase the accuracy.

Table 3.8 *Maximum heat pump entering fluid temperatures.*

	Uncalibrated System Simulation	Improved HP Model	Calibrated System Simulation	Experimental
Max HP EFT (°C)	32.7	30.3	30.5	29. 9

3.4. Conclusions/Recommendations

This section described a validation of a hybrid ground source heat pump system simulation, previously unreported in the literature. The validation was considered from two perspectives. First, it was considered from the researcher's perspective, where calibration of individual model components can be used to improve the match between simulation and experiment and provide insight into the nature of the model performance. From this perspective, the simulation is able to provide an acceptable match to the experimental results. In particular, calibration of the heat pump model gives a significant improvement in the results. Calibration of the cooling tower model and plate frame heat exchanger model give significant improvements, but limitations in the accuracy of the wet-bulb temperature measurement and knowledge of fouling are obstacles to achieving further improvements.

Second, the validation was considered from the designer's or simulation user's perspective, where calibration of models based on operating data is impossible since the simulation is informing the design. From this perspective, the performance of the system simulation with all models relying only on manufacturers' data was good. The problem with the starting case was principally due to operating the heat pumps outside the range of catalog data provided by the manufacturer. Caution is warranted in applying equation-fit models outside the range of data used to fit the data.

Recommendations for further research and development include the following:

1. As horizontally-buried piping is a common feature of GSHP systems, it would be useful to have a component model that covers this feature.
2. The equation-fit-based heat pump model used here performed poorly with catalog data. A parameter-estimation-based model and/or some checks on the input data to the model combined with some more intelligent extrapolation should be investigated.
3. The sensitivity of the cooling tower results to the uncertainty in wet-bulb temperature suggests caution by practitioners when using control based on the wet-bulb temperature. Further research into control strategies that either do not depend on the wet-bulb temperature or that only partly depend on the wet-bulb temperature is warranted.
4. While it is almost certainly impossible to predict fouling in an accurate manner, research that investigates fouling scenarios and approximate approaches may make it possible to develop recommendations for designers. Also, fouling factors

for the system with cooling towers should be investigated and tabulated for designers' use.

4. WATER-LOOP HEAT PUMP SYSTEM MODELING IN ENERGYPLUS AND HVACSIM+

4.1. Introduction

As has been previously discussed WLHP systems are heating and cooling systems that are used in commercial and institutional applications to provide space heating and cooling to multiple zones. Water is pumped through each heat pump via a piping system (loop). Heat pumps running in heating mode remove heat from the loop, while heat pumps running in cooling mode reject heat to the loop. The water is maintained within a desired range of temperatures with the assistance of a heat rejecter, e.g. cooling tower or fluid cooler and a heat source, e.g. a boiler. When the system is running with some heat pumps in heating and some in cooling, heat that may be removed from one zone can be added to another, saving energy.

This chapter, along with Chapters 5 and 6, is aimed at better understanding the impact of the loop temperature control and development of optimized control strategies. Two simulation environments will be used to model the WLHP system in order to allow intermodel validation. Chapter 5 will present experimental validation of the model and

Chapter 6 will present the use of the model to investigate the optimization of control strategies.

4.1.1. Background/Literature Review

WLHP systems, in commercial heating, ventilating, and air-conditioning (HVAC) applications, date back as far as 1962 (Howell and Zaidi 1991). Interest in WLHP systems, due to their energy saving capabilities, has grown a great deal, particularly since the mid 1980's (Howell and Zaidi 1990, Pietsch 1990).

A WLHP system consists of a set of water-source heat pumps (WSHP), typically water-to-air heat pumps connected to a two-pipe system, a supply loop of pipes and return loop of pipes connecting the water side of all of the heat pumps, a main circulating pump, a heat rejection device (e.g. evaporative cooling tower), and a heat addition device (e.g. boiler). The WLHP system is ideal for applications where different parts of the building may be calling for cooling and heating simultaneously. In a WLHP system, the loop acts as a heat source or heat sink, depending upon operating mode. One benefit of the WLHP system is its heat recovery ability. If there is a situation where heat pumps in the core of a building are in cooling mode, the heat that is rejected to the loop can be used by other heat pumps that are in heating mode, such as perimeter heat. Although they can be used in other applications, WLHP systems are typically going to be found in commercial and institutional applications where at least 100 tons of capacity is needed (Hughes 1990).

In controlling WLHP systems the conventional practice most commonly described (Howell 1988; Hughes 1990; Pietsch 1990; Howell and Zaidi 1990; Pietsch 1991; Howell and Zaidi 1991) is to run the WLHP system between 15.6ºC (60ºF) and 32.2ºC (90ºF). Other set points have been presented. Hughes (1990), when surveying current system configuration in practice, determined that typical application temperature extremes for all of the United States to be 18.3ºC (65ºF) and 29.4ºC (85ºF). Kush and Brunner (1991), in trying to optimize WLHP design and performance, determined that in order to reduce the boiler use and increase performance the minimum loop temperature should be to held to 18.3ºC (65ºF) or "slightly less". Kush and Brunner also determined that in order to increase the cooling performance it is beneficial to hold the maximum loop temperature to 29.4ºC (85ºF) or "slightly below."

Pietsch (1991), in an effort to optimize the loop temperatures of WLHP systems, suggested that there could be savings potential operating in mixed heating and cooling mode at an optimum temperature or at a fixed, constant temperature. He determined that the optimum operating temperature will vary based on the heating-to-cooling load ratios according to the following equation.

$$T_{L(opt)} = \frac{2.02\left(\frac{1}{3}\times\frac{1}{3.412}\times\frac{EER_{ARI}}{COP-H_{ARI}}\times\frac{Q_h}{Q_c}\right)0.5-0.72}{0.012\left(\frac{1}{3}\times\frac{1}{3.412}\times\frac{EER_{ARI}}{COP-H_{ARI}}\times\frac{Q_h}{Q_c}\right)0.5+0.004} \qquad (4.1)$$

where

EER_{ARI} = energy efficiency ratio (EER) at Air-Conditioning and Refrigeration Institute (ARI) rating conditions, dimensionless

$COP-H_{ARI}$ = heating coefficient of performance at ARI rating conditions, dimensionless

Q_h = perimeter heating load, Btu/h (W)

Q_c = core cooling load, Btu/h (W)

Pietsch concluded that, although feasible, determining the precise heating-to-cooling load ratio to vary the loop temperature would be extremely difficult. Therefore he examined setting the loop to temperature to a constant 7.2ºC (45ºF) and 15.6º (60ºF). He determined that the average power inputs for the two fixed cases and the optimum temperature case are essentially the same. His conclusion is "operating at a loop temperature level that is consistent with the lowest feasible heat pump operating temperature would provide near-optimum heat pump operation" (Pietsch 1991). A problem that could arise with such a control scheme (operating the loop at a single setpoint) is the effect of cycling the cooling tower and boiler at a fast rate.

In an effort to validate existing WLHP models, Cane et al. (1993) reviewed three models of WLHP systems in commercially available energy analysis programs. The review included a validation of the models' predicted energy consumption of the HVAC system against measured building energy consumption. With each model (models A, B, and C) all heat pumps that were located within a thermal zone were simulated as one large heat pump. With models A and B, minimum and maximum temperature limits are set and an energy balance is performed on the water loop. If the calculated loop temperature rises above the maximum temperature limit the cooling tower is activated,

and if the calculated loop temperature falls below the minimum temperature limit the boiler is activated. Model C uses the ASHRAE modified monthly bin method and therefore cannot perform an energy balance on the water loop. As a result the model sets the loop temperature to either the minimum set point or the maximum set point, depending on the cooling load to heating load ratio. Cane et al. conclude that the three models predict total building energy use within 1% to 15% of measured data. Although they agree this is very good, they state that the models hide "the wide variations observed at the HVAC system and component levels" (Cane et al. 1993). Several problems that are noted with the models are their inability to model variable-capacity pumping, their inefficiency to model thermal storage simply by increasing water volume, and their inability to handle ground-coupling.

Howell and Zaidi (1991) developed several parameters (annual heat recovery, savings in cooling energy, and annual savings in heating and cooling energy) to indicate the energy performance of WLHP systems. These parameters were developed by simulating a WLHP system using a commercially available energy analysis program based on the following parameters; building shape, building core to perimeter ratio, and geographic location. Their methodology was as follows. The annual heat recovery (*HR*) on a percent basis is given by the following equation.

$$HR = \frac{QH - (PH + BH)}{QH} \times 100 \tag{4.2}$$

where

QH = annual building heating requirement, kW-hr

$PH =$ annual energy required by heat pumps for heating, kW-hr

$BH =$ annual energy required by boiler for heating, kW-hr

The savings in cooling energy (*CS*) on a percent basis is given by the following equation.

$$CS = \frac{QREJ - CT}{PC + QREJ} \times 100 \tag{4.3}$$

where

$QREJ =$ $(QC + PC)3412/100{,}000 \times 0.3$, kW-hr

$QC =$ annual building cooling requirement, kW-hr

$PC =$ annual energy required by heat pumps for cooling, kW-hr

$0.3 =$ cooling tower power use factor, kW/100,000 Btuh

$100{,}000 =$ Btu/h factor

$CT =$ annual cooling tower energy required, kW-hr

The annual savings in heating and cooling energy (*CHS*) on a percent basis is given by the following equation.

$$CHS = \frac{(QREJ - CT) + [QH - (PH + BH)]}{QH + PC + QREJ + PUMP} \times 100 \tag{4.4}$$

where

$PUMP =$ annual energy required by water circulating pumps, kW-hr.

Hughes (1990) asserts that, generally speaking, in order to obtain high heat recovery rates the core of a building must have a significant cooling load all year and a perimeter-heating load during part of the year. They concluded that the use of a WLHP could save

up to 20% on annual heating and cooling energy, although it is not clear what the savings are compared to.

More recently Palahanska-Mavrov, et al. (2006) developed the following theoretical models applied with a bin method to determine the optimum loop temperature. The assumption is made that the building consists of two-zones: a perimeter zone and a core zone. All heat pumps found within a thermal zone are treated as one heat pump. When the perimeter zone is in cooling mode (k>0) and

$$Q_c = \alpha \times Q_{sys,d} + k \times (1-\alpha) \times Q_{sys,d} \tag{4.5}$$

$$Q_h = 0 \tag{4.6}$$

where

Q_c = building cooling load, Btu/h (W)

Q_h = building heating load, Btu/h (W)

$Q_{sys,d}$ = system design capacity, Btu/h (W)

α = core zone load ratio (interior zone cooling load as a fraction of the system design capacity), dimensionless

k = perimeter zone partial load ratio(ratio of perimeter zone heating/cooling load and the perimeter zone cooling design load), dimensionless

If the perimeter zone is in heating mode (k<0) then

$$Q_c = \alpha \times Q_{sys,d} \tag{4.7}$$

$$Q_h = k \times (1-\alpha) \times Q_{sys,d} \tag{4.8}$$

The compressor electricity consumption can then be calculated based on the following equations.

$$W_c = \frac{Q_c}{COP_c} \tag{4.9}$$

$$W_h = \frac{Q_h}{COP_h} \tag{4.10}$$

The rejected and extracted heat to and from the loop is then expressed with the following equations.

$$Q_{in} = Q_c \times \left(1 + {}^{1}\!/_{COP_c}\right) \tag{4.11}$$

$$Q_{out} = Q_h \times \left(1 + {}^{1}\!/_{COP_h}\right) \tag{4.12}$$

Using the building heating and cooling load the water loop temperature change can then be found with the following equation.

$$\Delta T = \frac{Q_h - Q_c}{\dot{m} C_p} - \frac{\frac{Q_h}{COP_h} + \frac{Q_c}{COP_c}}{\dot{m} C_p} \tag{4.13}$$

The amount of heat added by the boiler or removed by the cooling tower can be calculated from the equation below.

$$Q_{loop} = \dot{m} C_p \Delta T \tag{4.14}$$

If heat is being added, Q_{loop} is negative, the boiler gas energy consumption can be calculated as follows.

$$G_{boiler} = -\frac{Q_{loop}}{\eta_b} \tag{4.15}$$

where

$\eta_b =$ boiler efficiency

The overall cost can then be calculated according to the following equation.

$$COST = P_{elec} \times (W_c + W_h) + P_{gas} \times G_{boiler} \tag{4.16}$$

where

$P_{elec} =$ electricity costs, \$/kW-hr.

$P_{gas} =$ gas costs, \$/MMBtu

In their methodology Palahanska-Mavrov, et al. do not consider the costs associated with circulating pumps, cooling tower, and fans. Palahanska-Mavrov, et al. concluded that the optimal supply water temperature can be determined by minimizing the operating energy costs recognizing that at full load conditions the supply water temperature is recommended to be 3.3ºC (6ºF) higher than the outdoor air wet-bulb temperature. They conclude that the optimal temperature schedule is strongly dependent on α and k. They find one could reduce compressor and boiler operating costs by 24%, although they do not state what they savings are based on or compared to.

Other performance enhancing measures that were considered in the literature were optimizing loop water flow rates (Pietsch 1990; Kush and Brunner 1991) and optimizing thermal storage (Howell 1988; Pietsch 1990). Typical WLHP systems operate at approximately 3GPM/ton (Pietsch 1990; Howell and Zaidi 1990; Kush and Brunner 1991). Pietsch (1990) found that for running a constant speed pump 24 hours a day, 365 days a year, flow rates from 1 to 2 GPM/ton yielded the optimum annual performance. Pietsch found that this approach would save anywhere from 10% to 30% compared to running the system at higher flow rates e.g. 3GPM/ton. Another approach, presented by Pietsch, is to replace the constant speed pump with a variable speed pump and valve off heat pumps that are not operating. It should be noted that this is now the standard required by ASHRAE Standard 90.1-2004 (ASHRAE 2004) and California Title 24 (California Energy Commission 2005). The optimum flow found using the variable speed pump was approximately 3 GPM/ton and could save an estimated 20% to 40% over classical systems running at constant speed through all heat pumps. The variable speed option would then save an additional 10% to the "reduced flow" method. Likewise Kush and Brunner (1991) suggest a variable speed pumping system, showing energy savings of up to 75% with perimeter pumping and approximately 35% with core pumping compared to constant speed systems.

WLHP systems, without additional thermal storage, have little thermal storage capabilities (Pietsch 1990). With a typical 15.6ºC – 32.2ºC (60ºF – 90ºF) system there is typically 12 gallons or 100 lb of water per ton of cooling capacity (Pietsch 1990). Pietsch suggests that most of the time the loop temperature is moving rapidly towards either the

maximum or minimum set point. He also suggests that with no additional thermal storage the rate of temperature change is approximately ¼ to ½ºF per minute, meaning that the temperature could go from one extreme to the other within one to two hours. Pietsch suggests savings of 25% to 35% during unoccupied periods, with adequate thermal storage (50 to 100 gal/ton (50 to 100 L/kW)); although he also notes the cost of adding extra thermal storage should be considered to determine the cost effectiveness of adding thermal storage. Howell (1988) suggests savings of up to 12% annually on HVAC energy consumption on a 54,000 ft^2 (5,016m^2) building by adding up to 16,000 gallons (61m^3) of water storage compared to no storage.

4.1.2. Objectives

The main objective of this chapter is to develop a WLHP system model within HVACSim+ and EnergyPlus. Within the scope of the main objective the following are also desired:

- Develop a controller model that can be optimized to obtain the most energy efficient settings.
- Test the HVACSim+ and EnergyPlus models using simulated building loads.
- Compare the results against each other.
- Validate the HVACSim+ model with experimental data obtained at OSU (see Chapter 5).

- Make recommendations as to the optimal control of WLHP systems (see Chapter 6).

4.2. Methodology – HVACSim+

Before developing the computer model of the WLHP system, typical system designs were researched. ASHRAE Standard 90.1-2004 (ASHRAE 2004) and California Title 24 (California Energy Commission 2005) were reviewed to make sure the simulated system met current accepted standards. After reviewing the standards the system shown below in Figure 4.1 was chosen as the standard configuration for the WLHP system computer model.

The system has the following features

- N heat pumps plumbed in parallel, where N is set by the user.
- Each heat pump is equipped with a 2-way valve on the source water supply that opens only when the heat pump is on.
- A variable speed pump with minimum flow 30% of full flow capacity. The pump speed is controlled by the pressure difference across the inlet and outlet of the heat pumps.
- A bypass opens when less than 30% of full flow is required with the heat pumps on. This is necessary for system operation with a single variable speed circulating pump with a 30% minimum flow requirement.

- A counter flow plate heat exchanger.
- A cooling tower with its own constant speed pump.
- A boiler with its own constant speed pump coupled to the heat pump loop via a common pipe allowing the two sides of the loop (heat pump and boiler) to operate at different flow conditions with no interaction between the variable speed pump and the boilers constant speed pump. For this system simulation the common pipe is a "unidirectional flow" common pipe in that the flow through the heat pump side of the loop will always be greater than the flow through the boiler side of the loop and therefore the flow always flows in one direction.

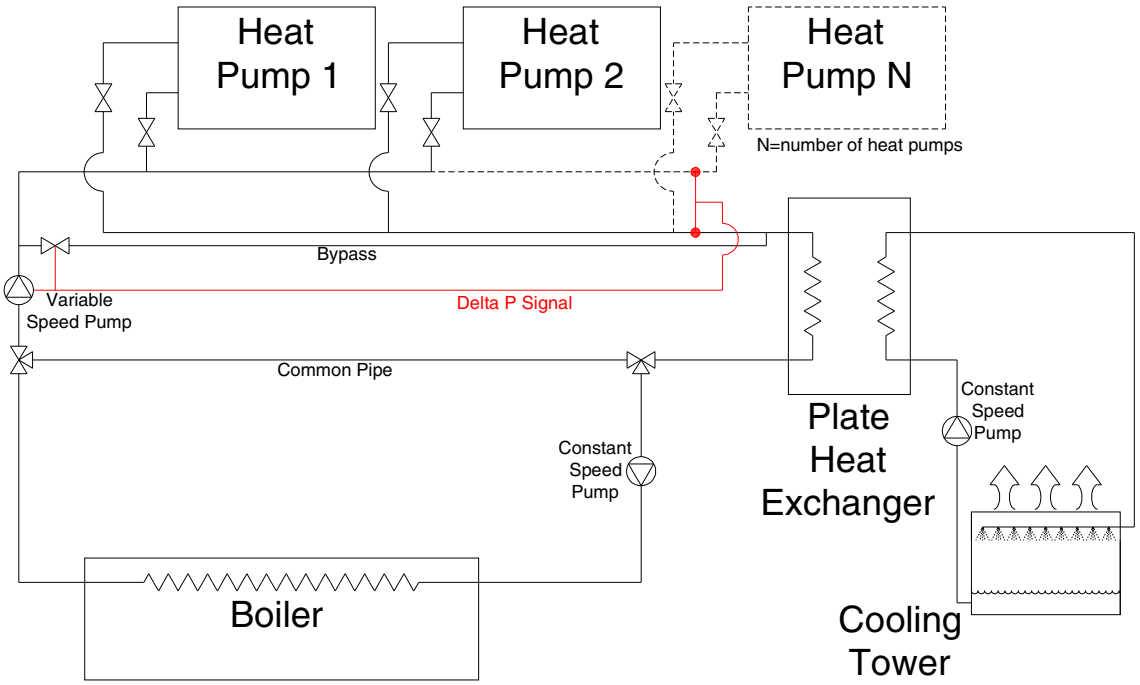

Figure 4.1 *WLHP design schematic.*

In developing an HVACSim+ WLHP system model, existing component models for heat pumps, cooling towers, boilers, plate heat exchangers and pumps were analyzed to determine the best model for use within a WLHP system simulation. The selection and discussion of each component selected or developed is given below. In an effort to simplify the system simulation it was decided to embed the WLHP controls within the component models. The controls needed for the cooling tower were embedded inside the cooling tower model and likewise the controls needed for the boiler were embedded inside the boiler model. The simulation models flow by:

1. assuming the variable speed pump is controlled to maintain constant pressure difference across the heat pumps.
2. therefore the flow rate is proportional to the number of heat pumps operating at any give time step.
3. assuming the variable speed can not give less that 30% of the max flow capacity.
4. with flow rate determined, the pump power is estimated with an equation fit described in Section 4.2.4.1.

4.2.1. Heat Pump Model

The selected heat pump model is a simple water-to-water equation-fit model with flow control developed by Xu (2006). The model is sometimes referred to as the "gang of heat pumps" model and is designed to represent multiple heat pumps without the need to have separate models for each individual heat pump. Per ASHRAE Standard 90.1 the

heat pumps are assumed to be equipped with two-way valves. The total load seen by the building during any given time step will be divided among the heat pumps. The model is assumed to always meet the load.

The first step of the model is to determine the flow rate required to serve the heat pumps that are on at any given time step. This is done by calculating the number of heat pumps, in heating and cooling, that are needed to meet the required load, heating and cooling, at any given time step. Once the number of heat pumps needed to meet the load is determined the flow rate needed to operate these heat pumps is calculated. The required flow for that time step is then sent to the variable speed pumping model, discussed in Section 4.2.4.1., where the power required to operate the pump is calculated.

The heating and cooling COPs are computed based on heating and cooling COP coefficients, the heat pump entering fluid temperature and the required flow rate for a single heat pump. The COP fitted equations for both heating and cooling are shown below in Equations 4.17 and 4.18 respectively.

$$COP_{heating} = C_1 + C_2 \cdot EFT + C_3 \cdot EFT^2 + C_4 \cdot \dot{m}_s + C_5 \cdot \dot{m}^2{}_s + C_6 \cdot EFT \cdot \dot{m}_s \quad (4.17)$$

$$COP_{cooling} = C_7 + C_8 \cdot EFT + C_9 \cdot EFT^2 + C_{10} \cdot \dot{m}_s + C_{11} \cdot \dot{m}^2{}_s + C_{12} \cdot EFT \cdot \dot{m}_s \quad (4.18)$$

where

$COP_{heating}$ = heat pump coefficient of performance during heating mode, dimensionless

$COP_{cooling}$ = heat pump coefficient of performance during cooling mode, dimensionless

EFT = heat pump entering fluid temperature, ºC

$\dot{m}_s$ = mass flow rate of a single heat pump, kg/s

C_{1-6} = fitted coefficients for heating mode, dimensionless

C_{7-12} = fitted coefficients for cooling mode, dimensionless

For the experimental work described in Chapter 4, the calculated COP coefficients are given in Section 3.1.1. For the study described in Chapter 6, the calculated COP coefficients can be found in Appendix B. After calculating the COPs the power required to operate the heat pumps is calculated by dividing the load, heating or cooling, by the COP. Knowing the load, flow rate and entering fluid temperature the exiting fluid temperature is calculated by taking an energy balance of the fluid.

The heat pump model, TYPE 559, diagram can be seen below in Figure 4.2, showing all inputs, outputs, and parameters needed to run the model.

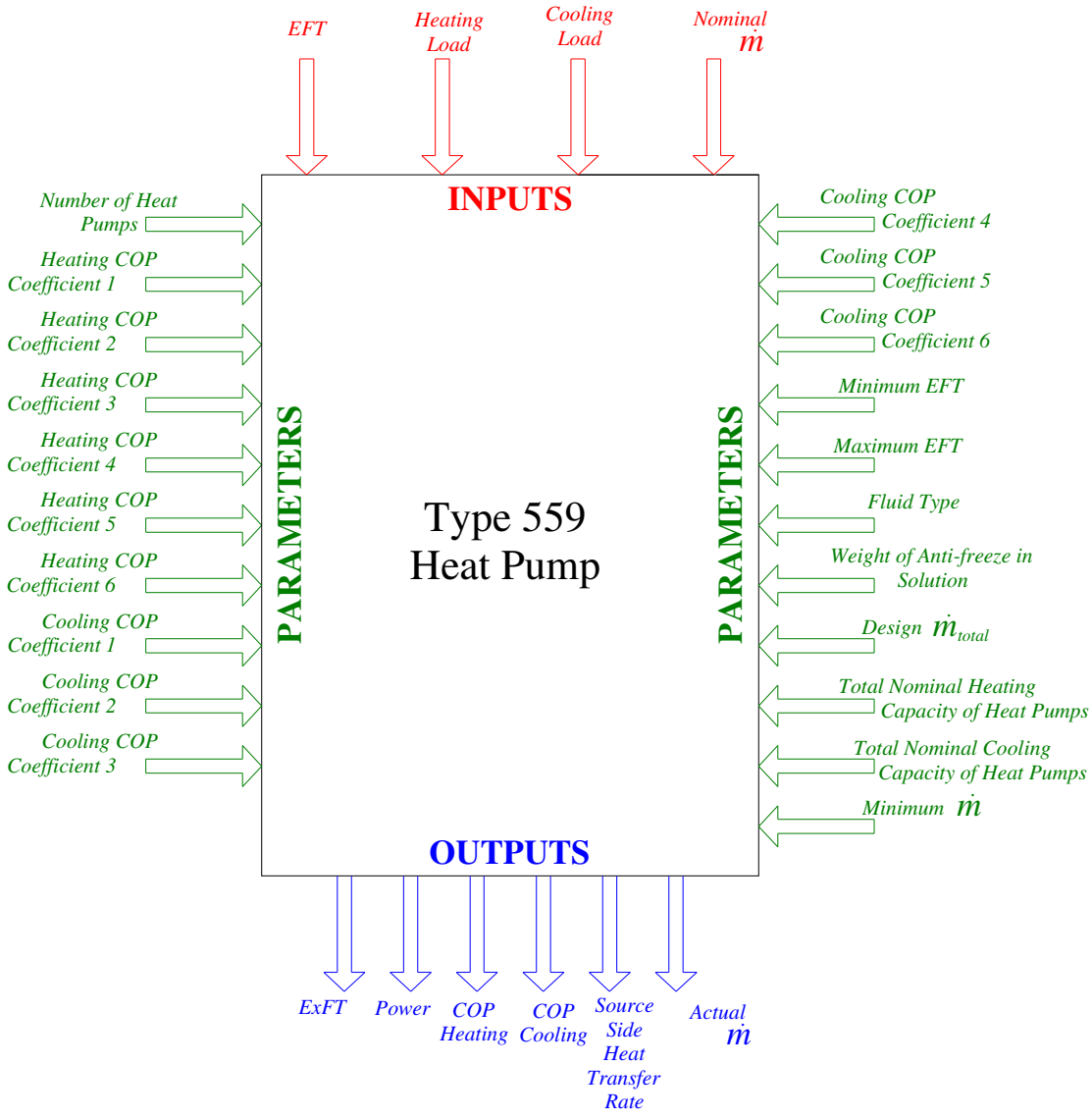

Figure 4.2 *TYPE 559 heat pump HVACSim+ model diagram.*

4.2.2. Cooling Tower & Cooling Tower Controller Model

The selected cooling tower model, TYPE 771, is based on a model developed by Khan (2004), which determines the leaving water temperature and the leaving air wet-bulb temperature based on the entering water mass flow rate in kg/s, the entering air mass flow rate in kg/s, the entering water temperature in ºC, the entering air wet-bulb temperature in ºC, and the overall heat transfer coefficient in W/K.

The cooling tower model is based on Merkel's theory and enthalpy potential with embedded controls used to operate the cooling tower. Also, the model has an output signal that allows the cooling tower to control its circulation pump; only allowing the pump to operate if the cooling tower was in operation.

The cooling tower is controlled in on-off operation with a setpoint and a dead band. The setpoint may be fixed or may be reset based on the temperature difference across the heat pumps or with other strategies to be investigated in Chapter 6.

The use of the dead band control is necessary in order to prevent the unwanted cycling of the cooling tower fan and pump. ASHRAE (2000) suggests that some problems can occur that include motor burnout from repeatedly cycling the tower on and off too often. The Marley Cooling Tower Company in their Cooling Tower Fundamentals book by Hensley (1983) suggest that for the cooling tower fan, 30 seconds of acceleration time should not be exceeded within one hour. For instance if a fan

requires 10 seconds to reach full speed, then no more than 3 start-ups should occur within one hour. Once the cooling tower is in operation the dead band will allow the cooling tower to run until the loop temperature has dropped low enough below the setpoint as to not automatically begin operation again after operation has stopped.

The cooling tower model, TYPE 771, diagram can be seen below in Figure 4.3, showing all inputs, outputs, and parameters needed to run the model. The parameters will change depending on which of the control strategies, discussed in Chapter 6, is being used.

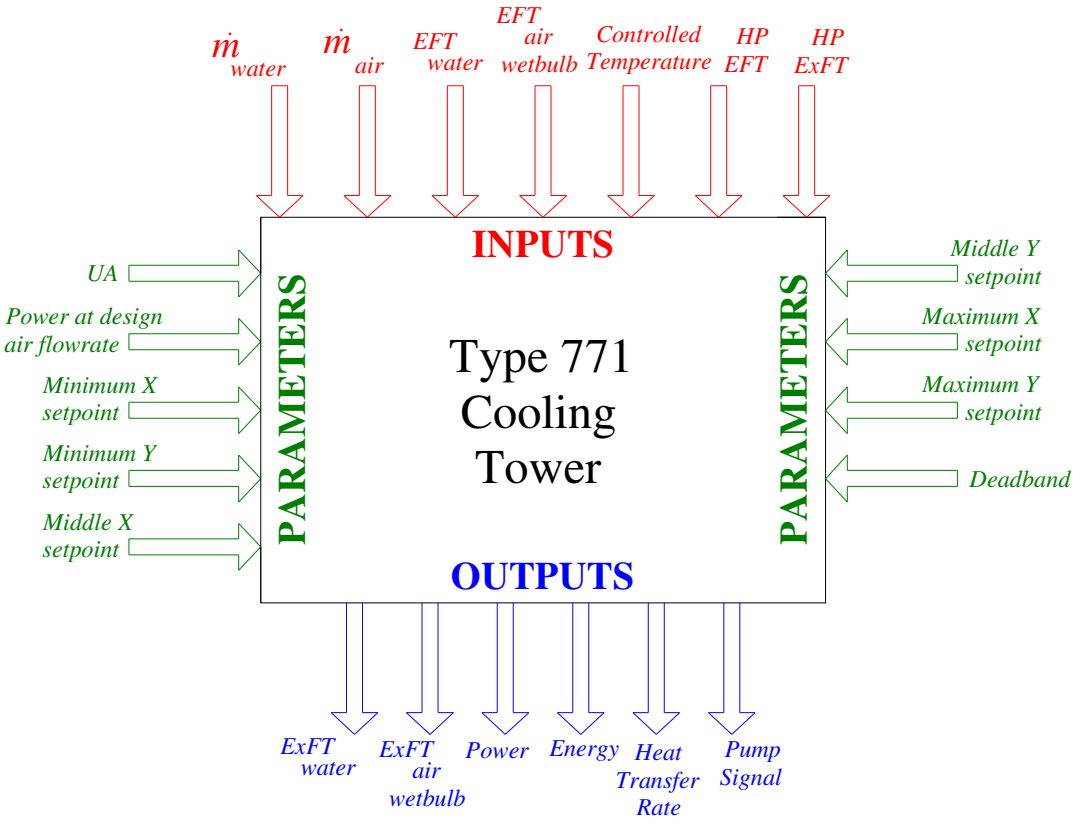

Figure 4.3 *TYPE 771 cooling tower HVACSim+ model diagram.*

4.2.3. Plate Heat Exchanger

The selected plate heat exchanger model is TYPE 663, which determines the leaving water temperature for both streams of the heat exchanger in ºC and the corresponding heat transfer rate in kW. The outputs are calculated based on the entering fluid temperature of each stream in ºC, entering mass flow rate of each stream in kg/s, specific heat of each fluid stream in kJ/kg-K and the effectiveness of the heat exchanger.

The heat exchanger model is intended for use in a large parametric study, where it is highly desirable to avoid having to select a specific heat exchanger from a manufacturer's catalog, fit coefficients, etc. Instead, a simpler approach was taken that involves assuming that the heat exchanger would be sized to meet a specific effectiveness at full flow conditions, and that the effectiveness at part-flow conditions on one side of heat exchanger could be modeled as a function of the flow rate. Manufacturers' data was used to develop an equation for effectiveness as a function of the fraction of full flow:

$$\varepsilon = C_0 + C_1 \cdot FFF + C_2 \cdot FFF^2 + C_3 \cdot FFF^3 \qquad (4.19)$$

The effectiveness of the heat exchanger was taken from a manufacturer's catalog at different flow rates and different temperatures. The effectiveness was then plotted vs. fraction of full flow as shown in Figure 4.4. The slightly different curves represent different temperatures. As can be seen, the effect of the flow rate on effectiveness is far more important, and a generic polynomial equation is fitted to all of the data points. This generic equation gives an effectiveness between 0.51 and 0.78 as a function of flow rate

on the water loop side of the heat exchanger. Variations in effectiveness due to temperature variations are neglected in the model.

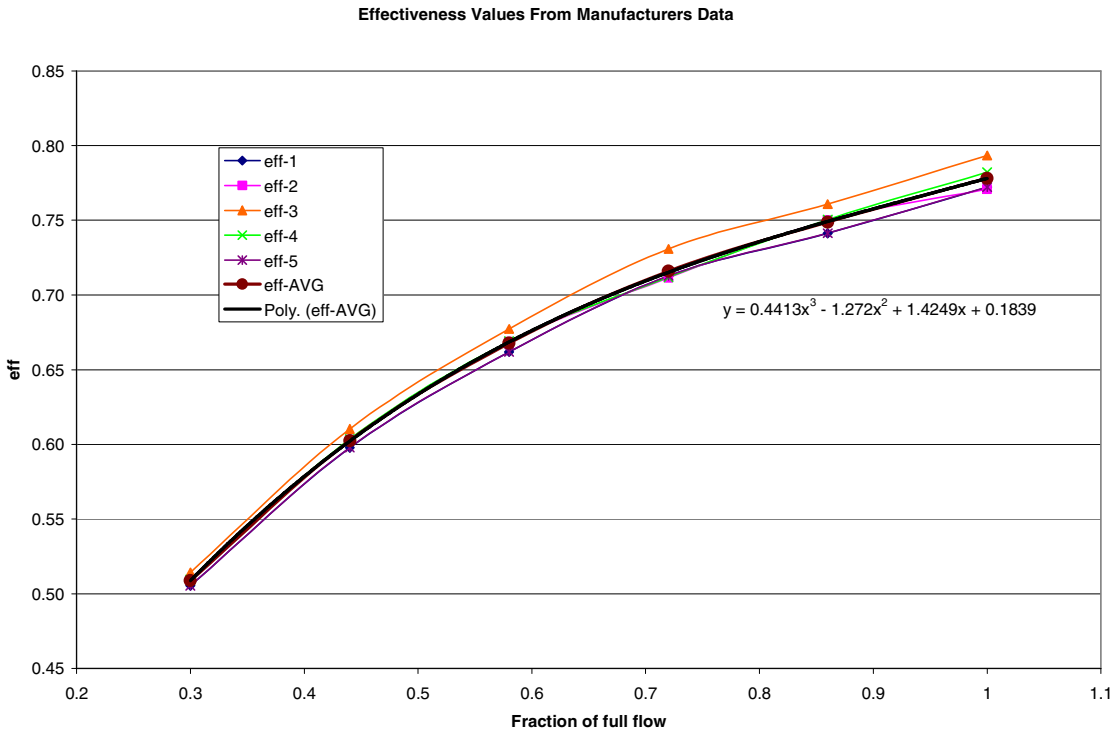

Figure 4.4 *Plot of effectiveness vs. fraction of full flow.*

The plate heat exchanger model, TYPE 663, diagram can be seen below in Figure 4.5, showing all inputs, outputs, and parameters needed to run the model. It should be noted that the model is always connected such that "Fluid 1" refers to the "hot side" or heat pump side of the plate heat exchanger and "Fluid 2" refers to the "cold side" or cooling tower side of the plate heat exchanger. It should also be noted that the polynomial equation is hard coded into the model with the fraction of full flow rate being determined by dividing the mass flow rate of "Fluid 1" (an input variable) by the full mass flow rate specified as a parameter.

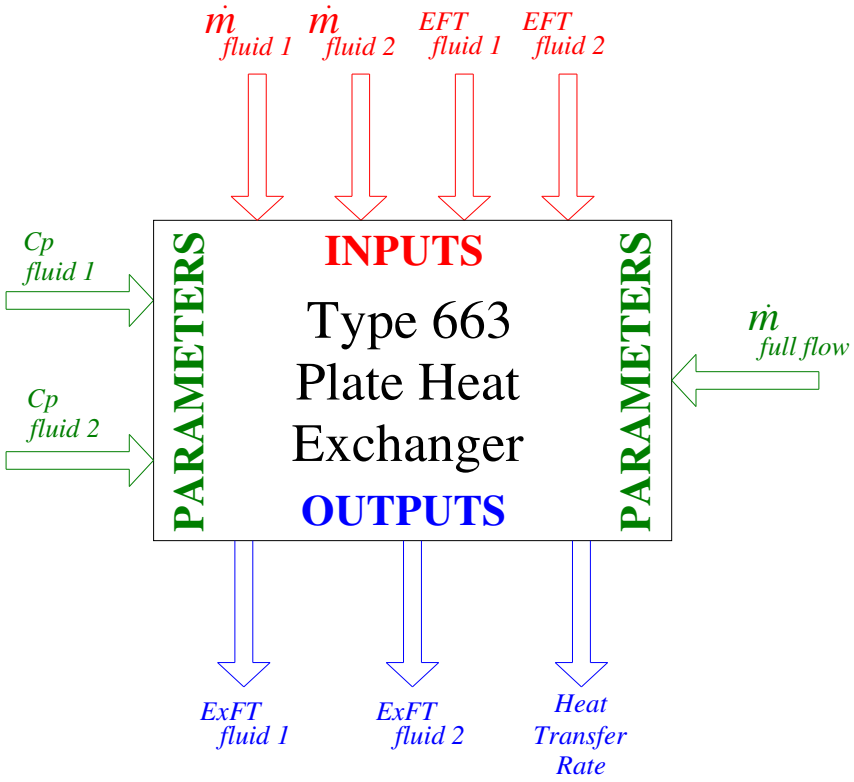

Figure 4.5 *TYPE 663 plate heat exchanger HVACSim+ model diagram.*

4.2.4. Pump Models

Two pump models are used within the system simulation; a variable speed pump model for the main loop and a constant speed pump model for the cooling tower and boiler. As discussed earlier, the pump models serve to account for the pumping power and temperature rise, but are not used to determine flow rates.

4.2.4.1. Variable Speed Pump

The selected variable speed circulating pump model is TYPE 591. The model relies on the fraction of full power (FFP) having been fitted to the fraction of full flow (FFF). The pump model also relies on the heat pump model, TYPE 559, to send the flow rate required to operate the heat pumps. The variable speed pump model then calculates the power that is required to operate at the flow rate set by the heat pump model. This is done by first calculating the FFF which is based on the ratio of actual flow rate to the design flow rate.

$$FFF = \frac{\dot{m}_{actual}}{\dot{m}_{design}} \tag{4.20}$$

where

FFF = fraction of full flow

$\dot{m}_{actual}$ = Mass flow rate required by the heat pump model

$\dot{m}_{design}$ = Mass flow rate of a system if all heat pumps are in operation

Next, the FFP is computed using a polynomial with fitted coefficients.

$$FFP = C_0 + C_1 \cdot FFF + C_2 \cdot FFF^2 + C_3 \cdot FFF^3 \tag{4.21}$$

where

FFP = fraction of full power

C_0 = 1st FFP coefficient

C_1 = 2nd FFP coefficient

C_2 = 3rd FFP coefficient

C_3 = 4th FFP coefficient

To determine the coefficients needed for Equation 4.21 above, the total pressure drop is calculated for the system. Knowing the design flow rate and the pressure drop a pump is chosen to meet the requirements. Using data from the selected pump non-dimensional equations of head vs. flow and efficiency vs. flow are obtained. An analysis is performed in a spreadsheet to determine pumping power over the full range of possible number of heat pumps on. This, in turn, is used to fit a polynomial to represent fraction of full power as a function of fraction of full flow. The coefficients used for the motel and office system simulations can be seen below in Table 4.1. Figures showing FFF vs. FFP for both buildings can be found in Appendix B. It should be noted that the power calculated is based on the efficiency of the pump, but does not account for motor or drive losses. It should also be noted that the curve of fraction of full flow vs. fraction of full power is generic in that it is assumed to apply to different size pumps.

Table 4.1 *Variable speed pump coefficients.*

Motel Coefficients

C_0 =	-0.0006175
C_1 =	0.0043769
C_2 =	-0.0012741
C_3 =	0.9982553

Office Coefficients

C_0 =	0.0051313
C_1 =	0.0723504
C_2 =	0.0229433
C_3 =	0.9003347

Finally, the power required to operate the pump can be calculated according the following equation.

$$Power = FFP \cdot Power_{design} \tag{4.22}$$

where

$Power_{design}$ = power required by the pump at full flow

The model outputs the temperature exiting the pump, the power consumption of the pump, the operating flow rate, and the amount of heat that is added to loop by its operation. The exiting fluid temperature is calculated according to the following equation.

$$T_{outlet} = T_{inlet} + \frac{Power}{\dot{m} c_p} \tag{4.23}$$

The flow rate used above is the maximum of the flow rate required by the heat pumps or the minimum flow rate given as a parameter. The variable speed pump model, TYPE 591, diagram can be seen below in Figure 4.6, showing all inputs, outputs, and parameters needed to run the model.

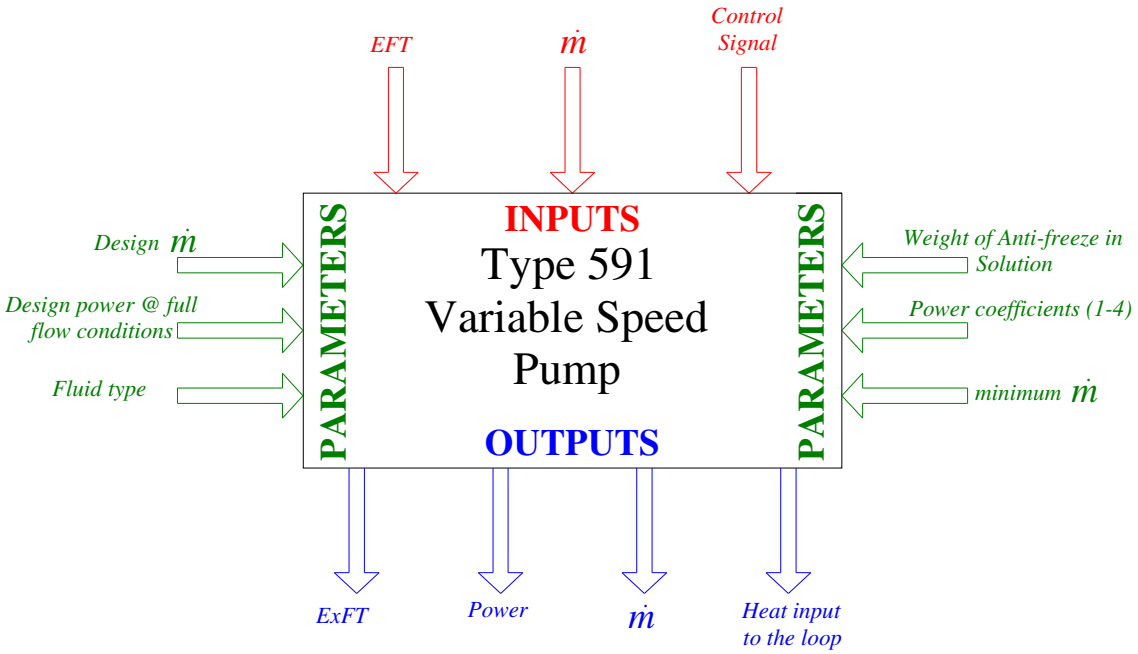

Figure 4.6 *TYPE 591 variable speed pump HVACSim+ model diagram.*

4.2.4.2. Constant Speed Pump

The selected constant speed circulating pump is TYPE 590. This is a simple pump model which calculates temperature rise and power consumption of the pump with given efficiency, mass flow rate and the pressure rise across the pump. The efficiency is obtained from manufacturer's data. The temperature rise across the pump is determined with Equation. 4.23, above. The constant speed pump model, TYPE 590, diagram can be seen below in Figure 4.7, showing all inputs, outputs, and parameters needed to run the model.

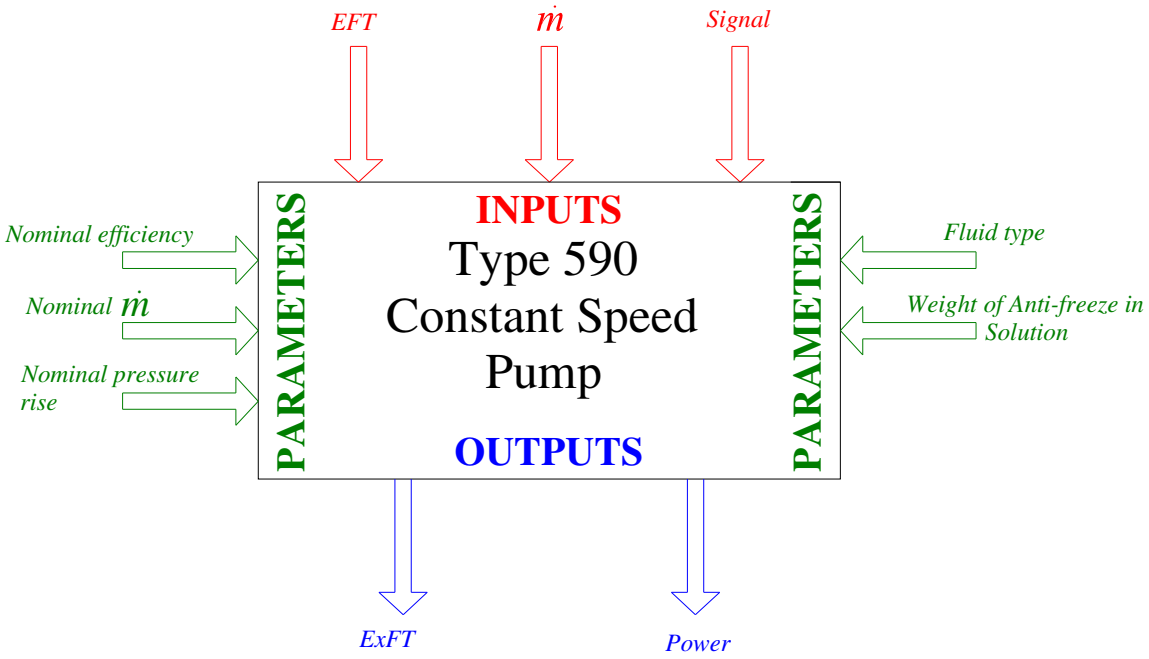

Figure 4.7 *TYPE 590 constant speed pump HVACSim+ model diagram.*

4.2.5. Boiler & Boiler Controller Model

In examining the boiler models currently in HVACSim+ it was determined that none were suitable for the WLHP system model. Therefore it was determined that a new boiler model needed to be developed. This model is based on an EnergyPlus (Crawley et al. 2002) boiler model.

As with the cooling tower model it was also decided to incorporate the operating controls of the boiler inside the boiler model. The boiler model is designed in such a way as to operate at a desired outlet temperature when in operation. The boiler is modeled as an electric boiler that is always able to output a “desired outlet temperature” that is set by

the user as a parameter. From the "desired outlet temperature" the boiler model can then determine the load that is required to meet that temperature according to

$$Q_{boiler} = \dot{m}_{boiler} C_P (T_{set} - T_{in}) \tag{4.24}$$

where

Q_{boiler} = boiler heat transfer required to meet the desired outlet temperature

$\dot{m}_{boiler}$ = mass flow rate required to operate the boiler

T_{set} = "desired outlet temperature", set by user

T_{in} = Boiler entering fluid temperature

The boiler is switched on and off based on a setpoint and dead band. The setpoint may be fixed or may be reset based on algorithms that will be investigated in Chapter 6.

It should also be noted the boiler outputs a pump signal that activates the boiler circulation pump only when the boiler is in operation. The component configuration for the new boiler model is shown in Figure 4.8. The parameters vary with the control strategy; one permutation is shown in Figure 4.8. As discussed above the model was taken from an existing EnergyPlus model, which allowed for part load effects, parasitic power, and various fuels to be used. For application in this investigation, a 100% efficient electric boiler was used, and hence many of the parameters shown in Figure 4.8 are neither needed nor used in this investigation.

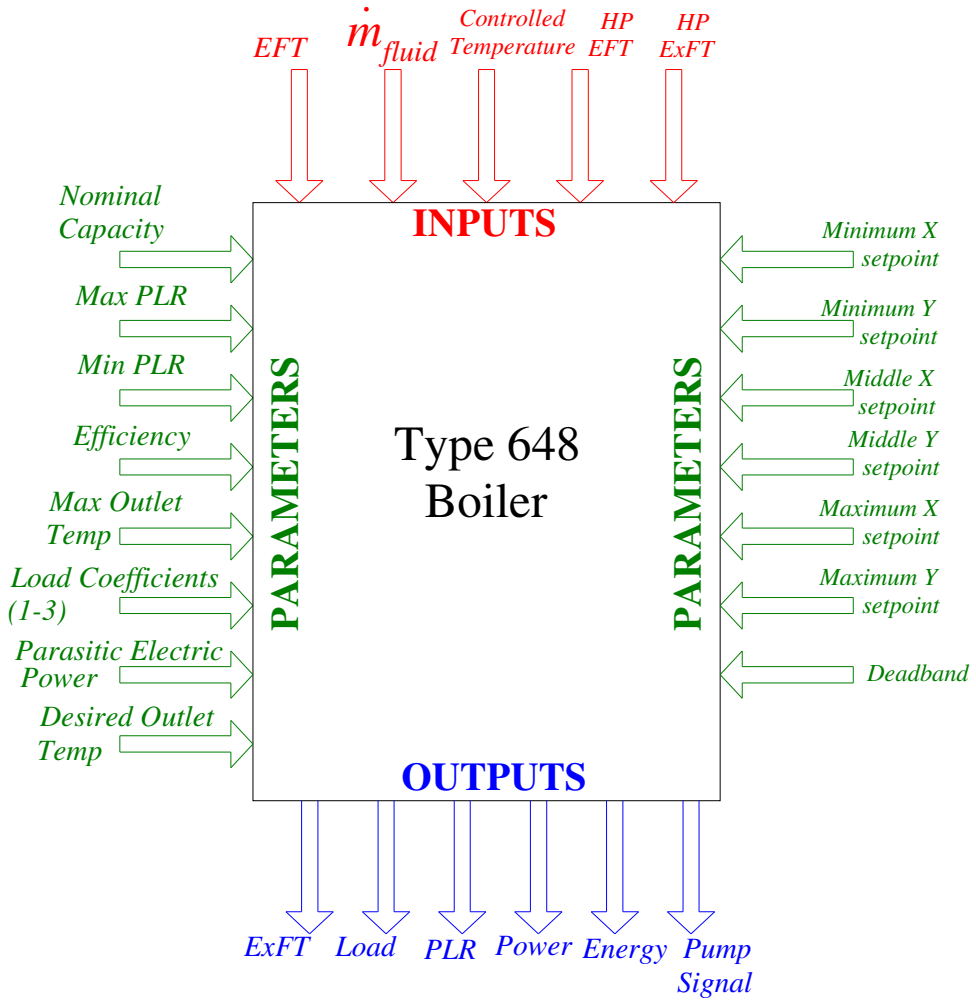

Figure 4.8 *TYPE 648 boiler HVACSim+ model diagram.*

4.2.6. Unidirectional Flow Common Pipe Model

A common pipe model was developed for situations where the boiler requires a constant flow, but the system flow rate may be varied depending upon heat pump operation. In applications such as these a common pipe, shown in Figure 4.9 between *a* and *b*, is an alternative to placing a bypass and three-way valve in the system (McQuiston et al. 2005). The common pipe allows the two sides of the system, operating at different

flow conditions, to operate with essentially no interaction between the source side and load side pumps.

In general simulation applications where the flow quantities are not known in advance careful consideration would have to be given to reversing flow through the common pipe. With the systems used in this investigation, the flow through the variable speed side of the system (heat pump) is always greater than the flow through the constant speed side of the system (boiler) and therefore a simple model was developed that does not handle reversing flow.

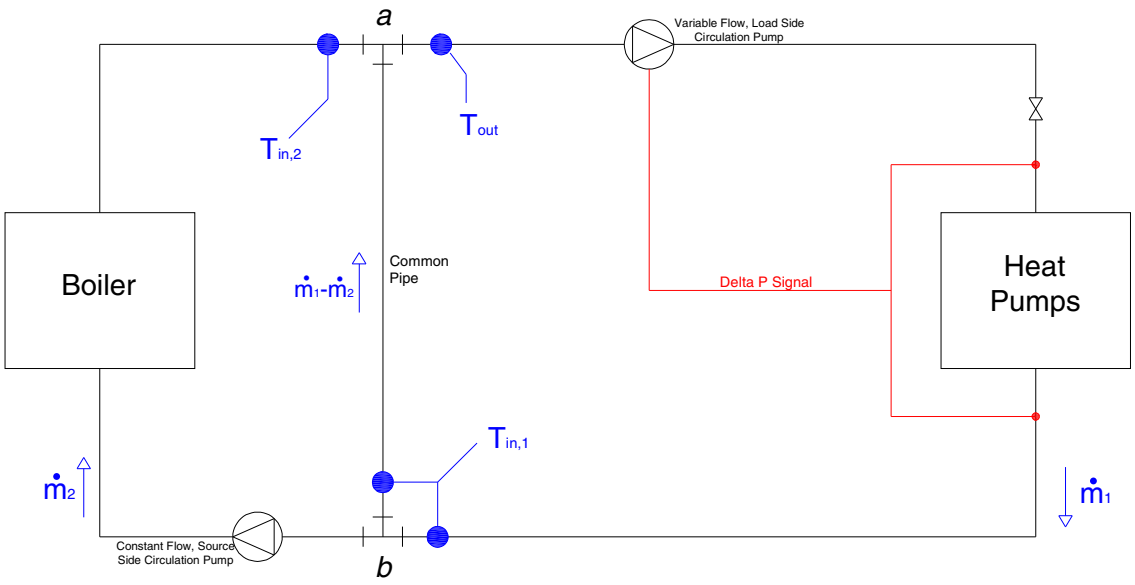

Figure 4.9 *Unidirectional flow common pipe application schematic.*

The exiting fluid temperature of the model is computed based on a fraction of the two fluid stream flow rates and entering fluid temperatures according to the following equation.

$$T_{out} = \frac{(\dot{m}_2 \cdot T_{in,2} + (\dot{m}_1 - \dot{m}_2) \cdot T_{in,1})}{\dot{m}_1} \tag{4.25}$$

In cases where the boiler is not in operation the outlet temperature would be equal to $T_{in,1}$.

The common pipe model, TYPE 592, diagram can be seen below in Figure 4.10, showing all inputs, outputs, and parameters needed to run the model. It should be noted that HVACSim+ requires at least one parameter; the "DUMMY" parameter shown in the figure does not get used by the model.

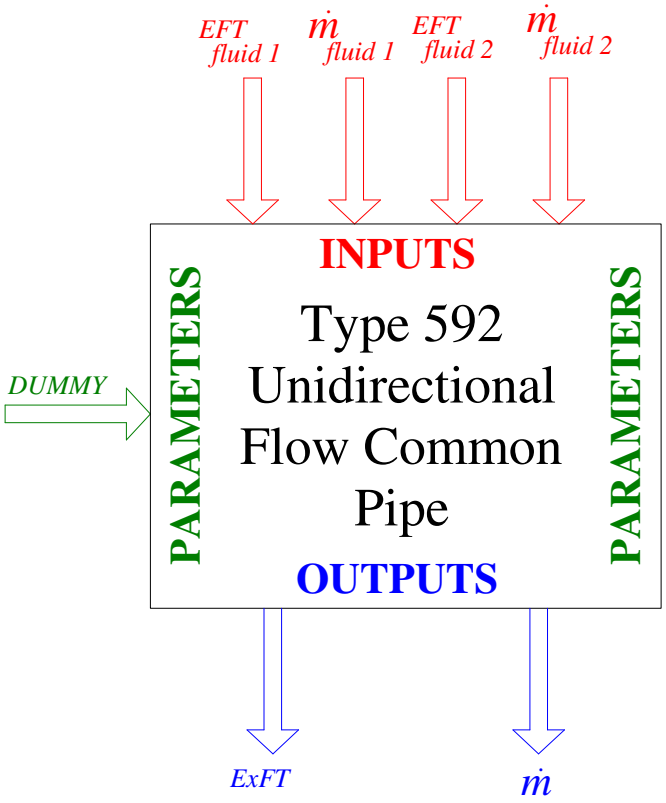

Figure 4.10 *TYPE 592 common pipe HVACSim+ model diagram.*

4.3. HVACSim+ Model Implementation

The components described above were connected as shown in Figure 4.11 and 4.12. The HVACSim+ interface model of the system is shown below with the main equipment of the system spelled out for clarity. Figure 4.11 shows the full schematic with all system connections shown and superblocks listed. Each of the system components is identified. Figure 4.12 shows the flow from component to component.

It should be noted that multiple superblocks were needed to better handle the discontinuity caused by the controllers of both the cooling tower and the boiler. The sudden transients due to the controllers switching between on and off caused problems with the convergence of the entire system when trying to solve both control signals and temperatures used to drive the control signals, all within the same time step. Adding a superblock gives, in effect, a transit delay to the system and allows the control signal to be based on the previous time step's temperature values. Adding a superblock has an effect equivalent to adding a plug flow thermal mass to the loop. In Chapter 6, the equivalence between the superblock and added thermal mass will be discussed further.

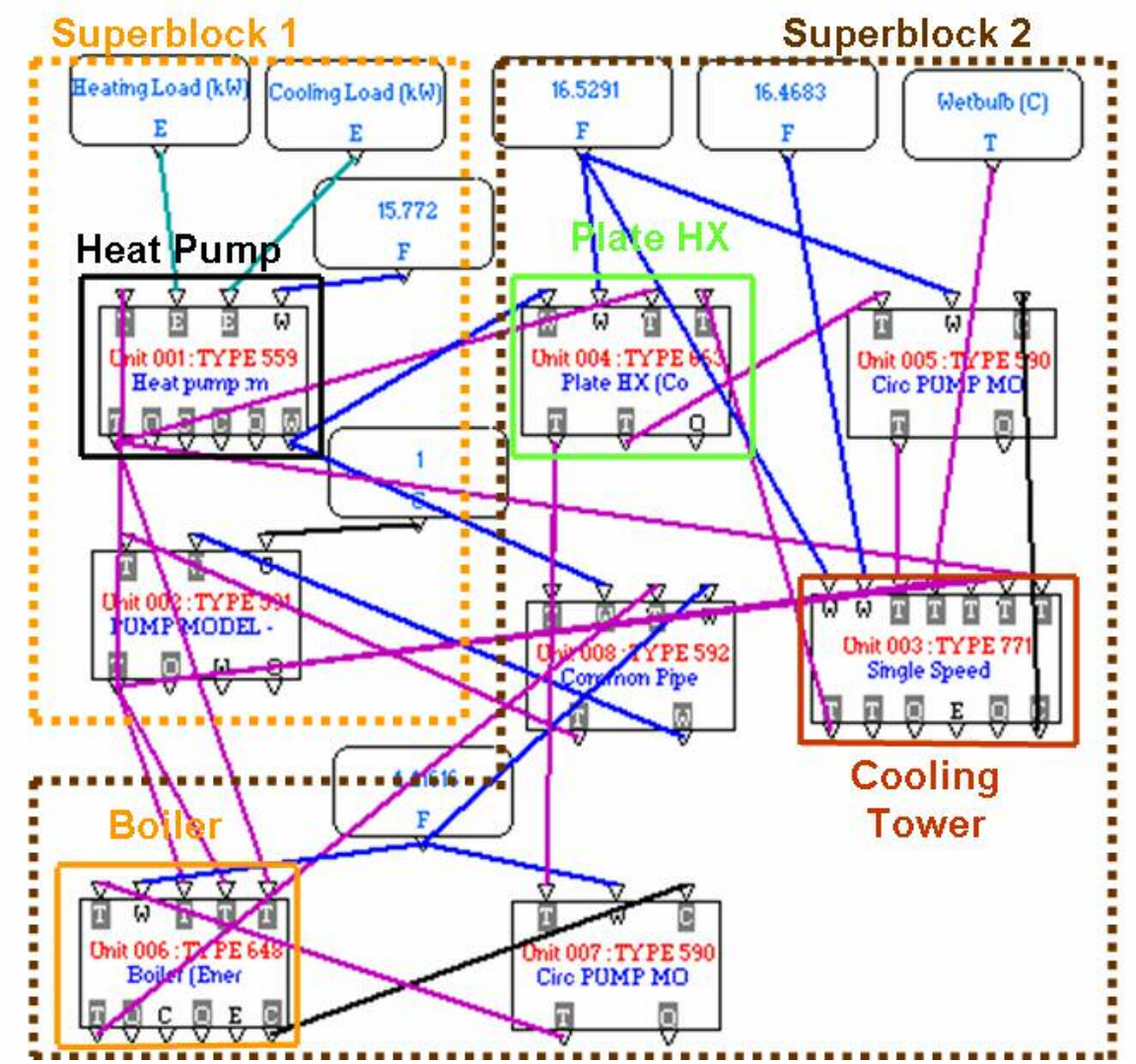

Figure 4.11 *HVACSim+ visual tool model showing system connections.*

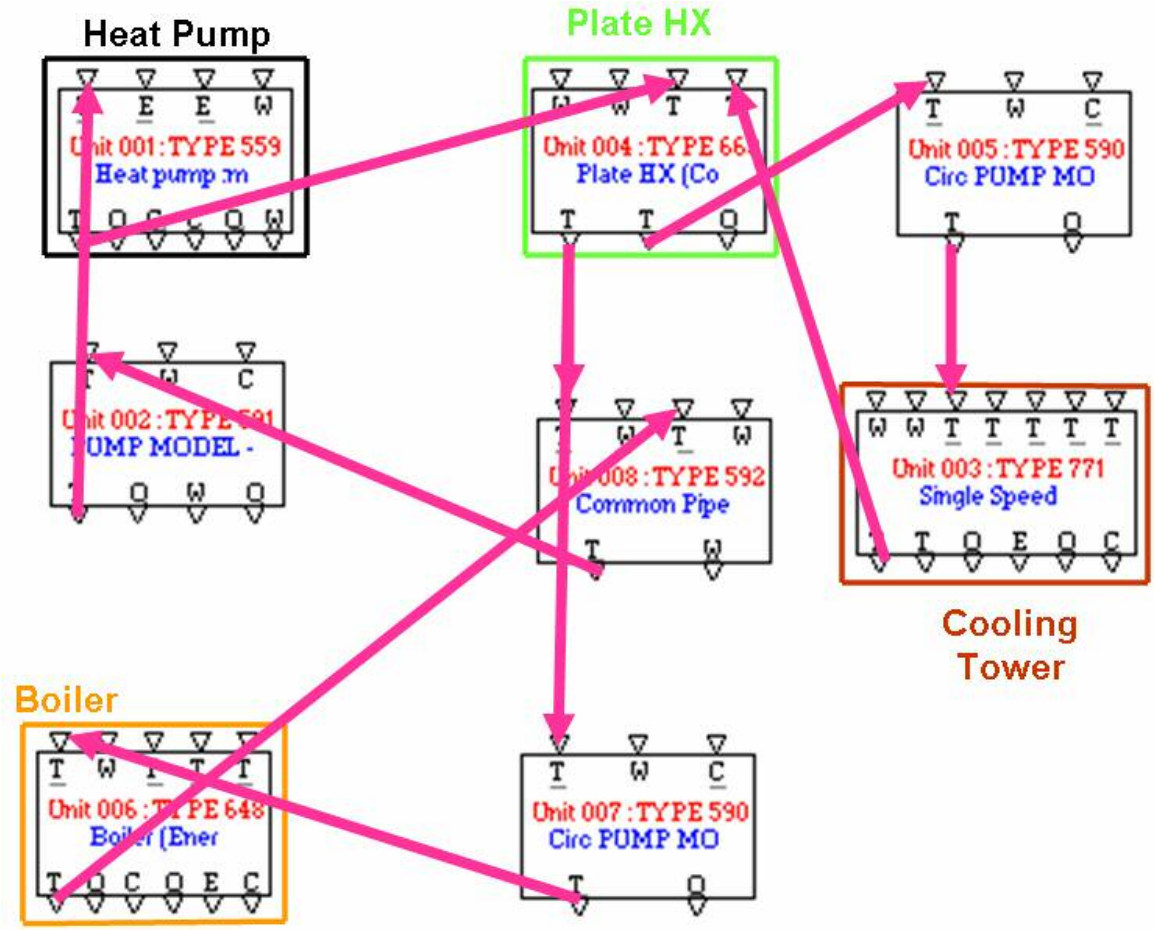

Figure 4.12 *HVACSim+ visual tool model showing flow direction.*

4.4. Methodology – EnergyPlus

In developing a WLHP system model within EnergyPlus the models listed below were used with the first two developed for this work; the remaining models were already incorporated into EnergyPlus.

- Heat Pump Model (discussed in Section 4.4.1)
- WLHP Controller Model, boiler and cooling tower controls (discussed in Section 4.4.2)

- Boiler Model
- Cooling Tower Model
- Plate Heat Exchanger Model
- Constant Speed Pump Model

A schematic of the system is shown below in Figure 4.13.

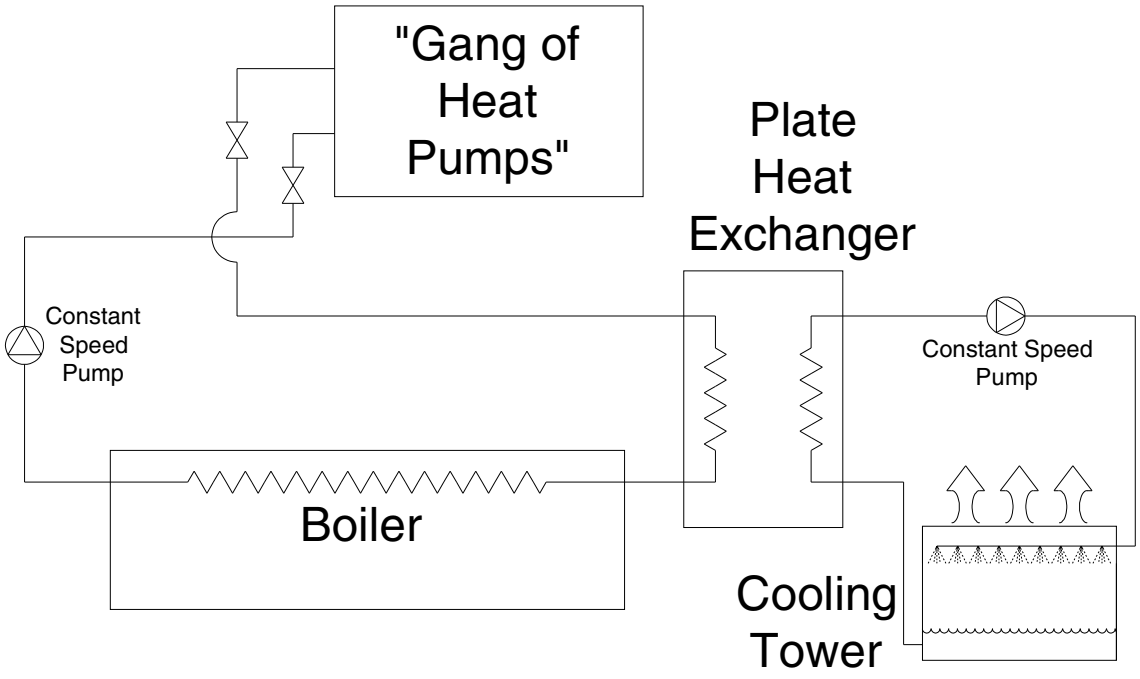

Figure 4.13 *Schematic of WLHP system modeled in EnergyPlus.*

It should be noted that the heat pump model and controller model that were developed in EnergyPlus were very similar to those developed by HVACSim+. An explanation will be given as to what changes had to be made with each model below.

4.4.1. Heat Pump Model

The first attempt at developing a WLHP system model in EnergyPlus involved placing two of the existing heat pumps in each zone, one for cooling and one for heating. For a 3-story, 10 zone per story building used in this work, 60 heat pumps would be needed. Consequently much time was spent in developing the input data file (IDF) for this model. Once the IDF was developed the average runtime of a simulation was over an hour. In order to improve execution time a new "gang of heat pumps" model was developed based on the for HVACSim+ model described in Section 4.2.1. The heat pump model is based on the COP of the heat pump both in heating and cooling according to Equations 4.17 and 4.18. The input data dictionary (IDD) for the "gang of heat pumps" model can be found in Appendix A.

4.4.2. WLHP Controller Model

In developing the EnergyPlus controller model to control the loop temperature to within a desired range, the dual setpoint point controls already incorporated in EnergyPlus were used as a starting point. The modified control model varies the loop setpoints depending upon the temperature difference across the heat pumps. This is analogous to the controls developed for HVACSim+. The controller controls the loop temperature by operating the boiler or cooling tower to maintain the temperature between two setpoints. These setpoints can be reset according to a piecewise linear function of the

temperature difference across the heat pumps. The IDD for the WLHP controller model can be found in Appendix A.

4.5. Building Models & Test Cities

Building loads were created with the EnergyPlus program. This section describes the methodology used to determine the loads with EnergyPlus and DesignBuilder.

4.5.1. EnergyPlus/DesignBuilder Background

EnergyPlus is a building energy simulation program for modeling building heating, cooling, lighting, ventilating, and other energy flows. It is based on the most popular features and capabilities of BLAST (Building Loads Analysis and System Thermodynamics) and DOE-2. They were born out of concerns driven by the energy crisis of the early 70s, realizing that building energy is a major component of America's energy usage. Both were developed in the late 1970s and early 1980s to help design engineers and architects to size HVAC equipment, study retrofits, optimize energy performance, etc. EnergyPlus came out with its first Alpha version on December 4, 1998, and its Version 1 on April 12, 2001. EnergyPlus was designed with new capabilities such as being able to handle time steps of less than an hour, handle thermal comfort models based on activity, inside DB, humidity, etc. Also it is able to link to other simulation environments (i.e. WINDOW5) to allow for more detailed analysis of

building components. The problem has been that it is a stand-alone simulation program without a user-friendly graphical interface.

DesignBuilder is an interface that uses EnergyPlus as its "computational engine". The way that DesignBuilder and EnergyPlus interact with one another is shown below in a block diagram of the process.

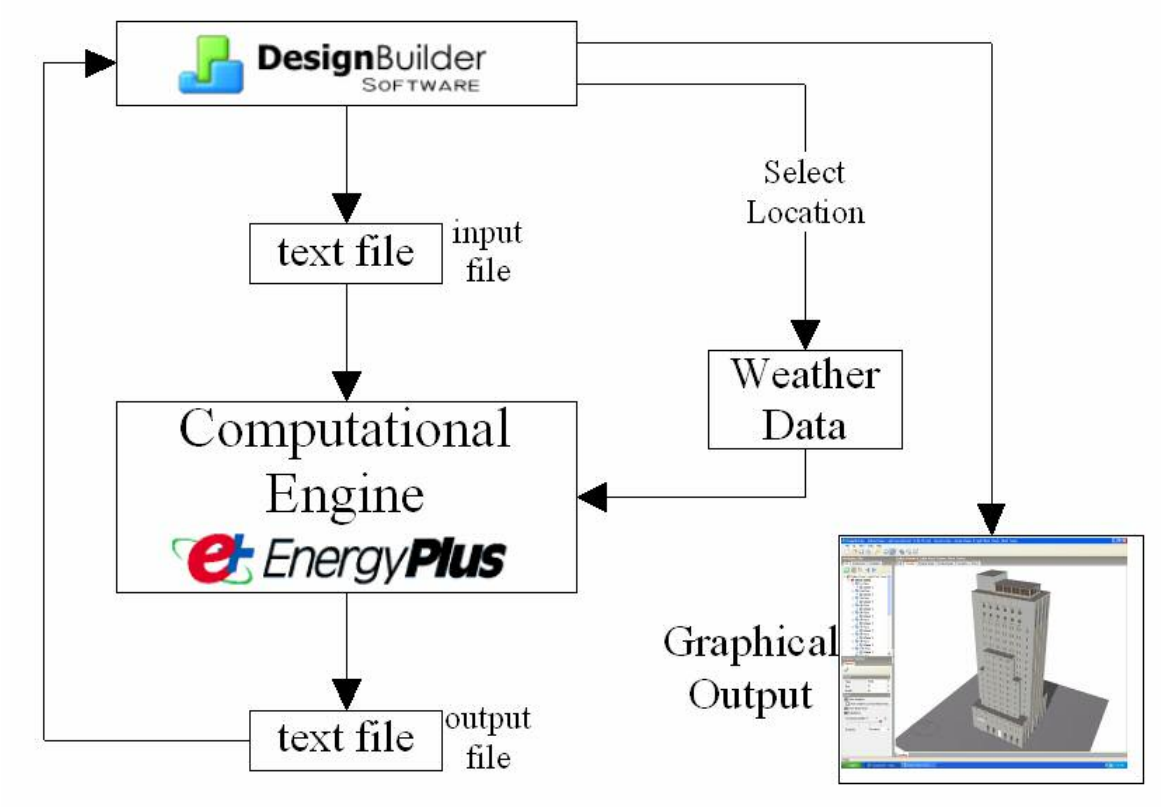

Figure 4.14 *Flow diagram of how DesignBuilder works with EnergyPlus.*

DesignBuilder is an easy-to-use OpenGL solid modeler that allows building models to be assembled by positioning 'blocks' in 3-D space. There are no limitations on surface shape; surfaces having more than 4 vertices are broken up into triangles to ensure compatibility with the EnergyPlus simulator. Data templates allow you to load a wide

variety of input data such as building constructions, activities, HVAC & lighting systems, thermal comfort setting, etc. If you can't find what you're looking for, DesignBuilder also allows you to add your own templates. You can also control the level of detail in each building model allowing the tool to be used effectively at any stage of the design or evaluation process. Once the model is competed the user can run the 'Visualization' feature, which provides realistic 3D rendered visualization and solar shadow modeling. The visualization capabilities can be seen from the model shown in Figure 4.15 below.

Figure 4.15 *DesignBuilder visualization of the Dallas Power & Light Building.*

The user can also run the 'Simulation' feature that directly works with EnergyPlus in calculating such things as heating and cooling equipment sizes.

4.5.2. Test Buildings & Cities

In order to study the performance of various WLHP systems, two prototypical buildings were modeled in thirteen U.S. locations. DesgnBuilder was used to determine annual heating and cooling loads for the two buildings and thirteen locations. In an effort to look at control strategies for very different building types with different occupancy levels and internal heat gains a high occupancy office building and a low occupancy motel were used for this work. The buildings are described below.

4.5.2.1. Office Building (high occupancy)

The first prototypical building was based on a typical floor plan from the Bank of Oklahoma (BOK) Tower shown below in Figure 4.16. The BOK building is a 52-story, of which only three stories are modeled for this work, multipurpose building that is approximately 48.8 meters by 48.8 meters (160 feet by 160 feet). The BOK building is located in downtown Tulsa, and as of 1999 was the tallest building in the State of Oklahoma. The building glazing area is 60-70% of the exterior envelope.

Figure 4.16 *BOK building.*

(Picture provided by Dr. Jeffrey Spitler (2006))

The BOK building was chosen because information regarding the building was readily available in Feng's (1999) M.S. thesis for Oklahoma State University. Since a building with a range from 100 to 500 tons was desired, the typical office building was modeled as an office building having three floors with the same floor plan as that of the BOK building. Each of the three floors had ten zones, 6 perimeter zones and 4 core zones. The building was modeled and simulated using DesignBuilder according to the following conditions. It should be noted that the building was intentionally modeled with a high occupancy level and large setback.

1. Office occupancy of 1 person per 5 m^2 (54 ft^2).
2. Equipment heat gains of 10 W/m^2 (0.9 W/ft^2).
3. Lighting heat gains of 13.13 W/m^2 (1.18 W/ft^2).
4. Minimum fresh air per person of 9.4 L/s-person (20 ft^3/min-person).
5. Infiltration of 0.5 ach.

6. Day time (7am-6pm, Monday-Friday), night time and weekend thermostat settings are specified for each zone. During the day, the temperature set point is 20.0ºC (68.0ºF) for heating and 24ºC (75.2ºF) for cooling. A night and weekend setback has been set for 5ºC (41ºF) for heating and 30ºC (86ºF) for cooling.

The following schedule, shown in Figure 4.17, was used for the office building Monday thru Friday. The building is unoccupied during the weekend and the thermostat is setback to 5ºC (41ºF) for heating and 30ºC (86ºF) for cooling.

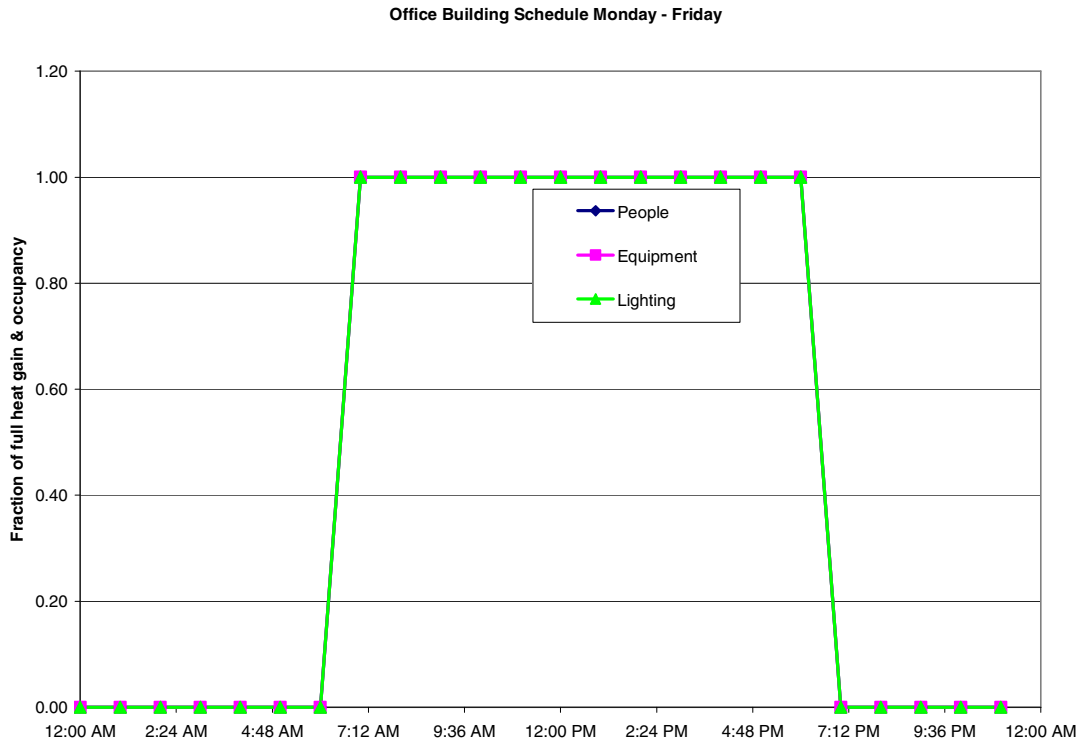

Figure 4.17 *Office building schedules.*

A rendering of the model can be seen below in Figure 4.18. Figure 4.19 shows the ground floor of the building with the core and perimeter zones partitioned.

Figure 4.18 *DesignBuilder rendering of office building.*

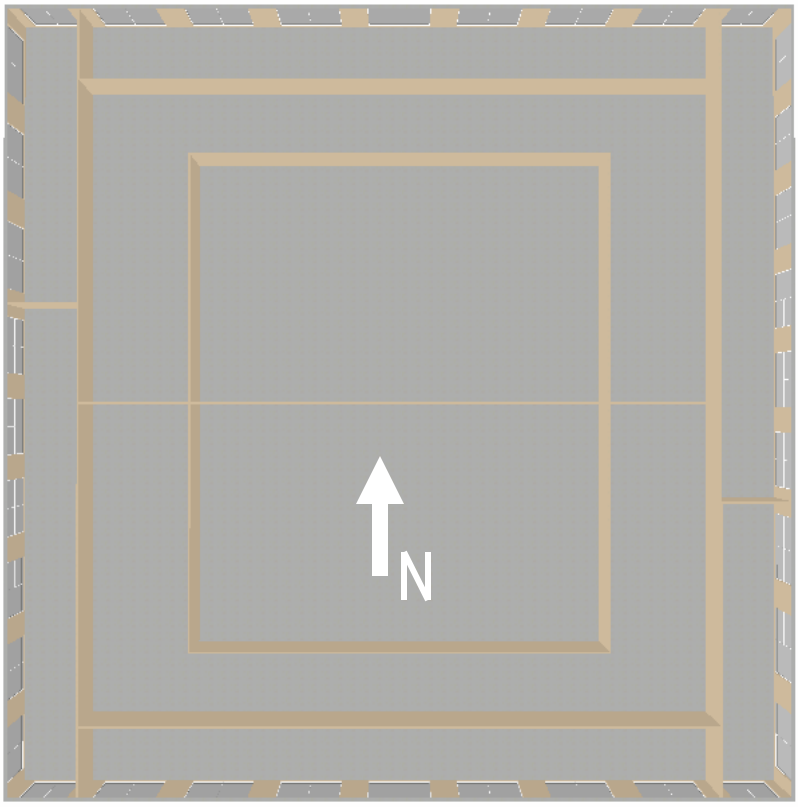

Figure 4.19 *DesignBuilder rendering of BOK building ground floor.*

Calculated loads can be seen below for Chicago, Figure 4.20, and Houston, Figure 4.21. Detailed information regarding equipment used to run the WLHP system simulation for the office building can be found in Appendix B.

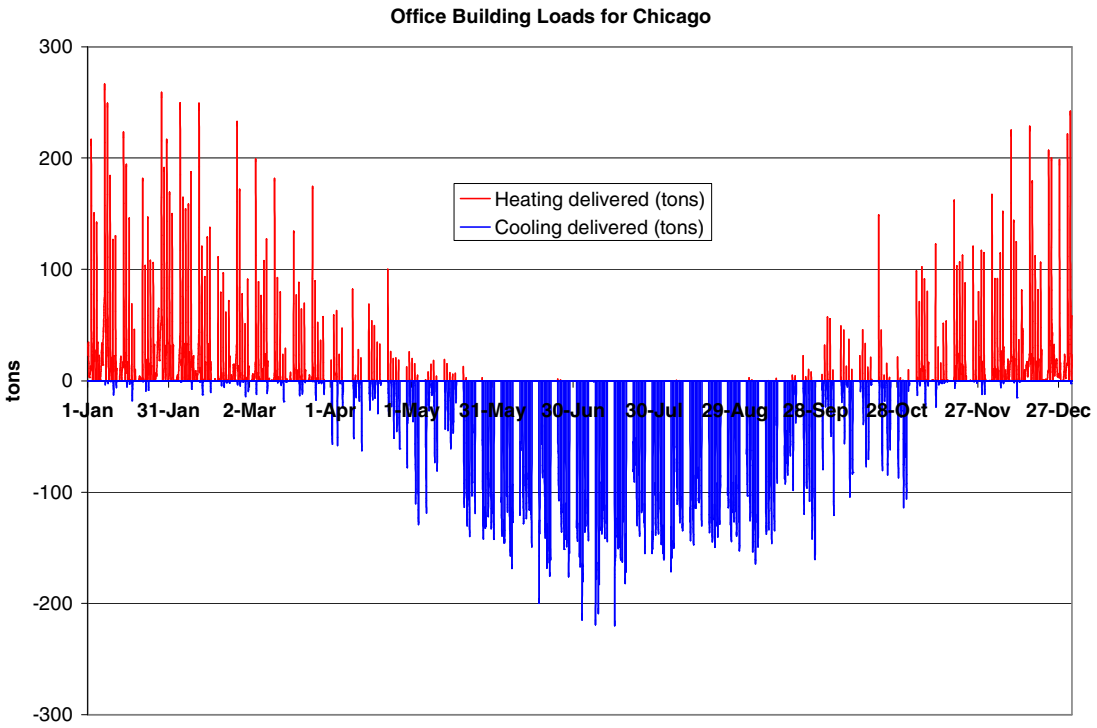

Figure 4.20 *Office building loads for Chicago.*

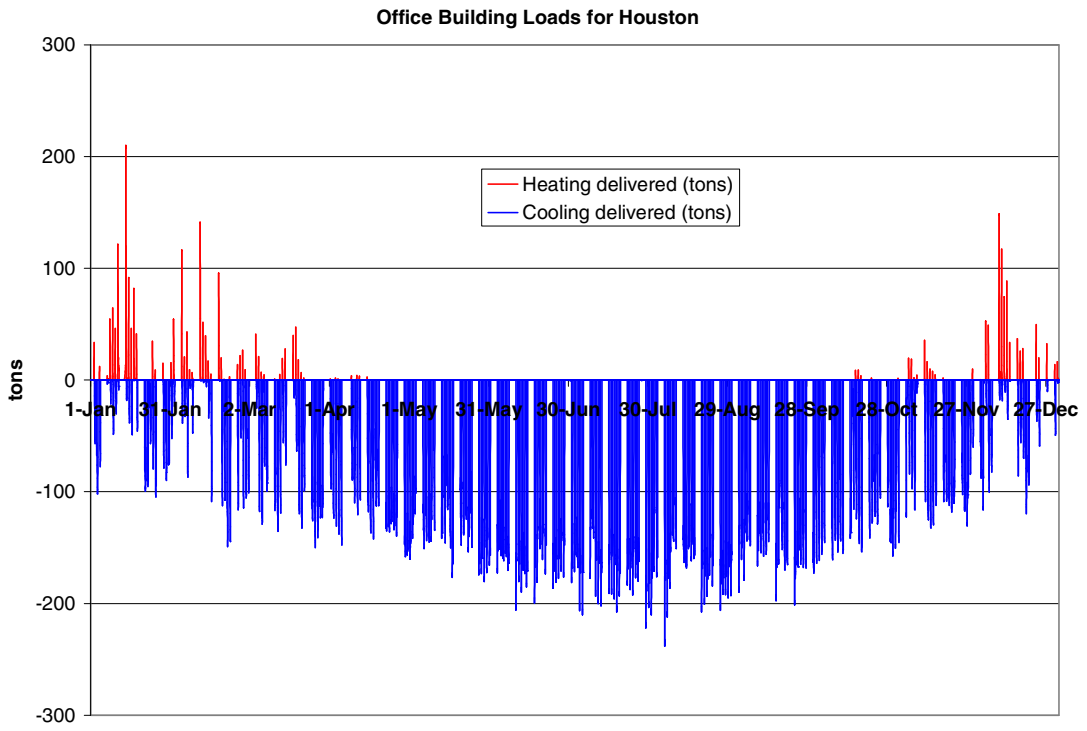

Figure 4.21 *Office building loads for Houston.*

4.5.2.2. Motel

The second prototypical building used to test the WLHP system model is based on an actual motel in Tulsa, Oklahoma as described by Chen (1996). The motel building is a 2-story building that is approximately 61 meters by 17 meters (200 feet by 56 feet). Since a building with a load ranging from 100 to 500-tons was desired, the motel building was modeled as three identical buildings having ten floors with the same floor plan minus the indoor swimming pool. The building was modeled and simulated using DesignBuilder according to following conditions. All heat gains and occupancy levels given are peak values; a detailed schedule can be seen in Figure 4.22.

1. Motel occupancy of 1 person per 36.23 m^2 (390 ft^2).
2. Equipment heat gains of 3.33 W/m^2 (0.30 W/ft^2).
3. Lighting heat gains of 7.76 W/m^2 (0.70 W/ft^2).
4. Minimum fresh air per person of 7 L/s-person (15 ft^3/min-person).
5. Infiltration of 0.2 ach.
6. Thermostat settings are specified for each zone. The temperature setpoints are 20.0ºC (68.0ºF) for heating and 24ºC (75.2ºF) for cooling. There is no setback.

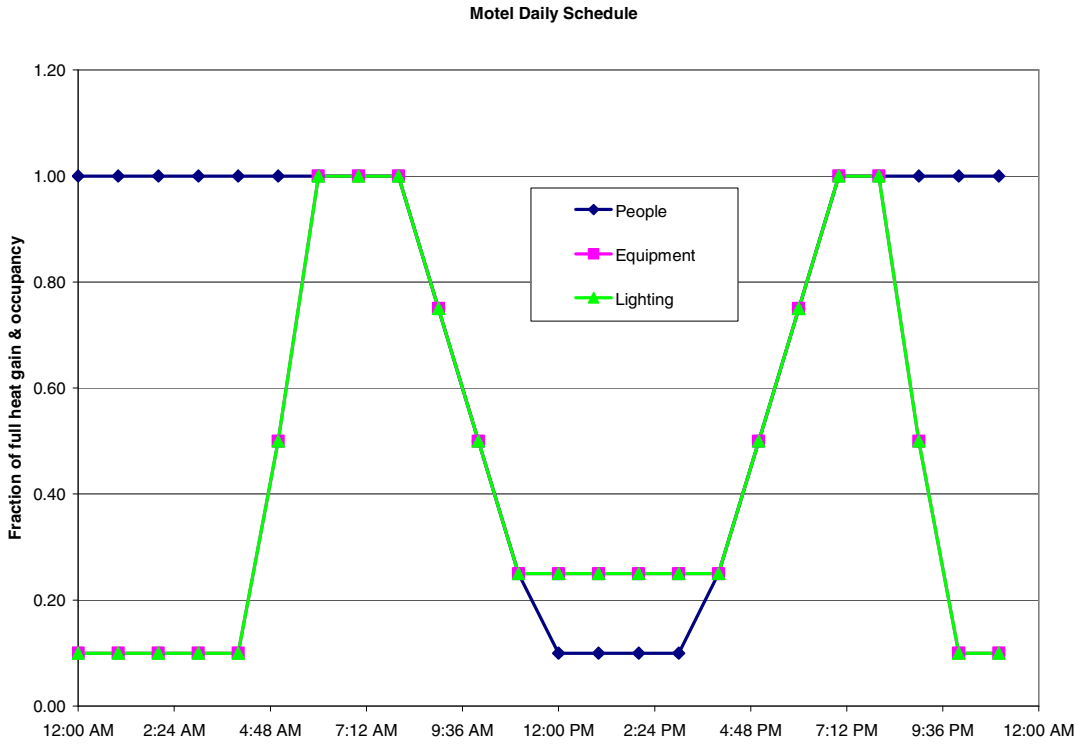

Figure 4.22 *Motel schedules.*

The first floor as shown below in Figure 4.23 has 20 guest rooms, a lobby and a hallway.

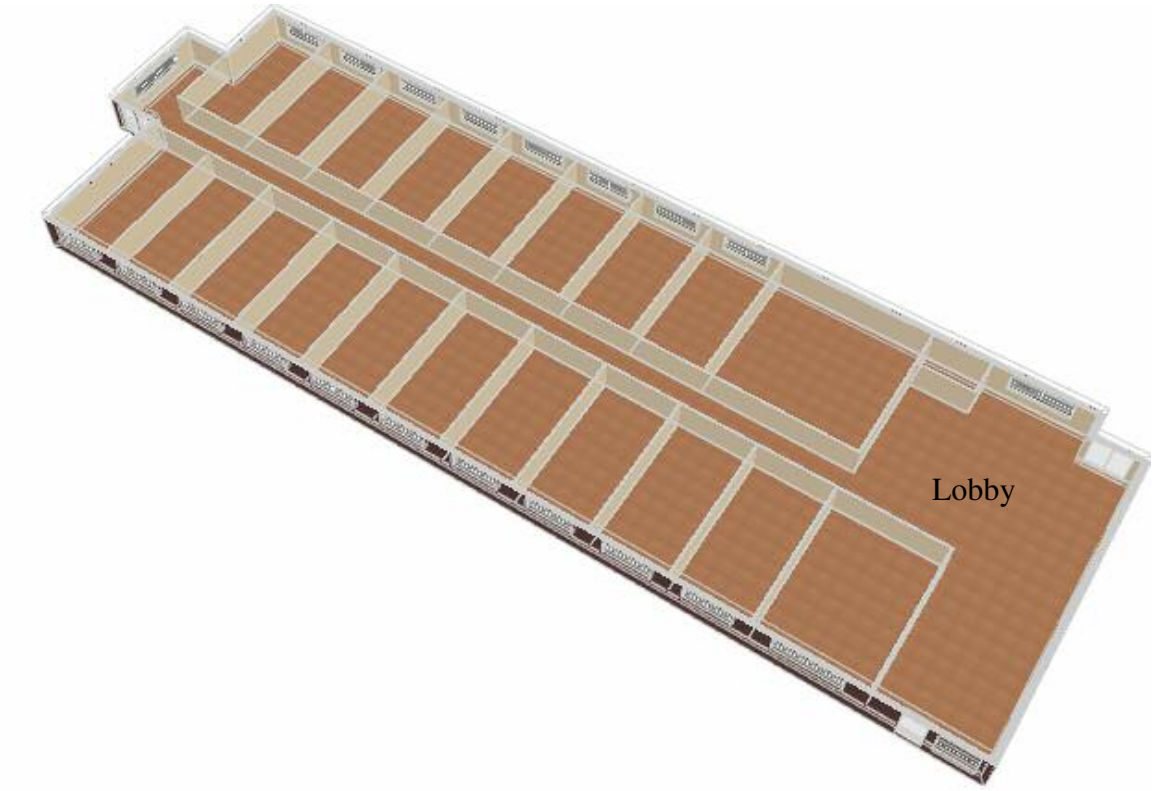

Figure 4.23 *1st Floor layout of the motel.*

Floors two through ten each has 22 guest rooms and a hallway, as shown below in Figure 4.24.

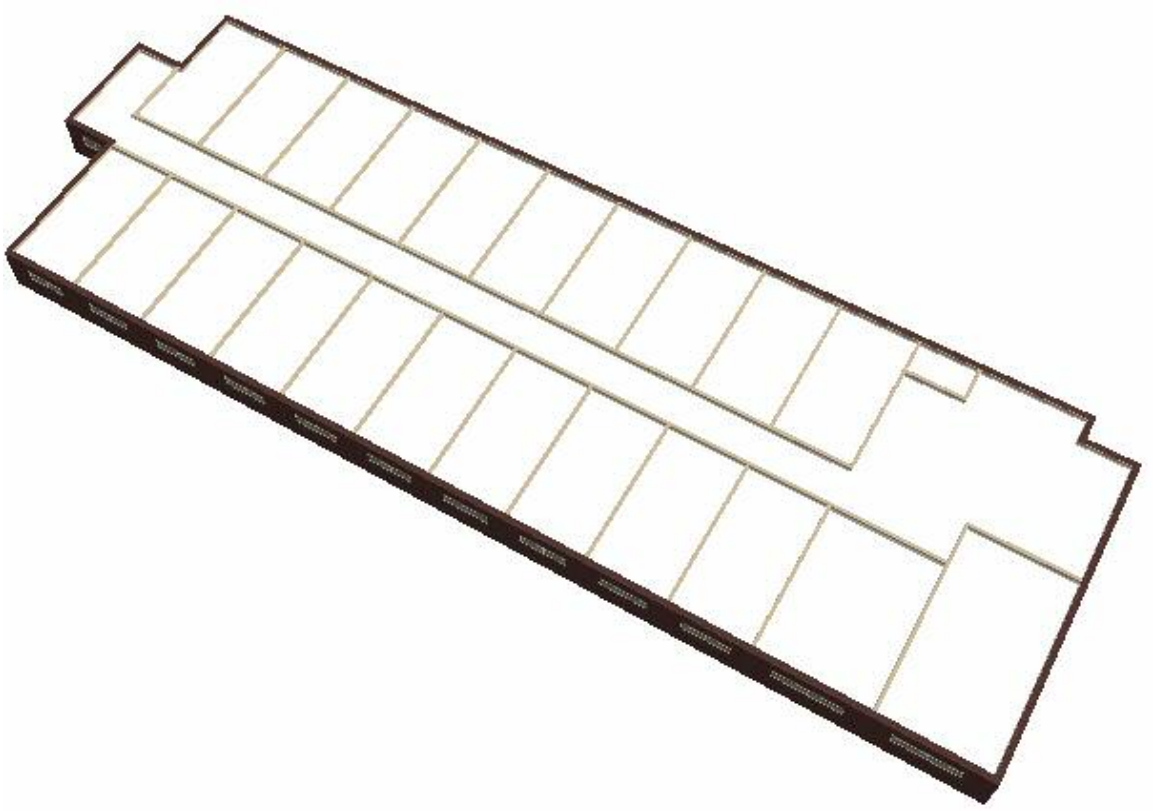

Figure 4.24 *Floors 3-10 layout of the motel.*

The building was modeled and simulated using DesignBuilder. A rendering of the model can be seen below in Figure 4.25.

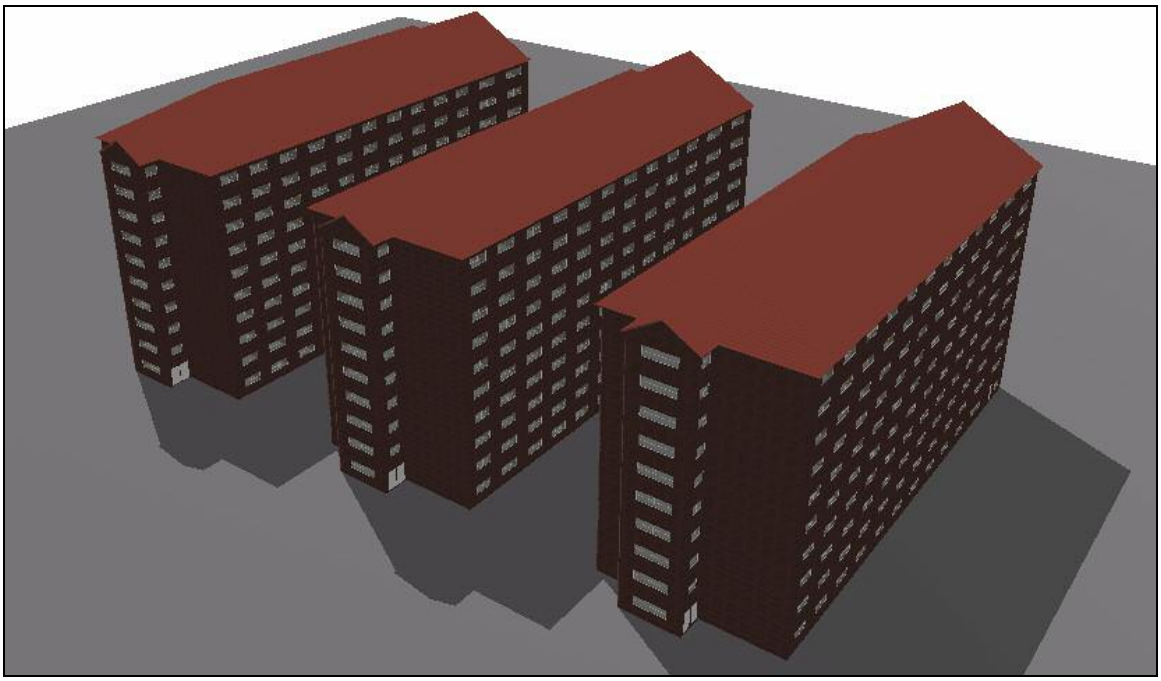

Figure 4.25 *DesignBuilder rendering of the motel.*

Calculated loads are shown for Chicago in Figure 4.26, and for Houston in Figure 4.27. Detailed information regarding equipment used to run the WLHP system simulation for the motel can be found in Appendix B.

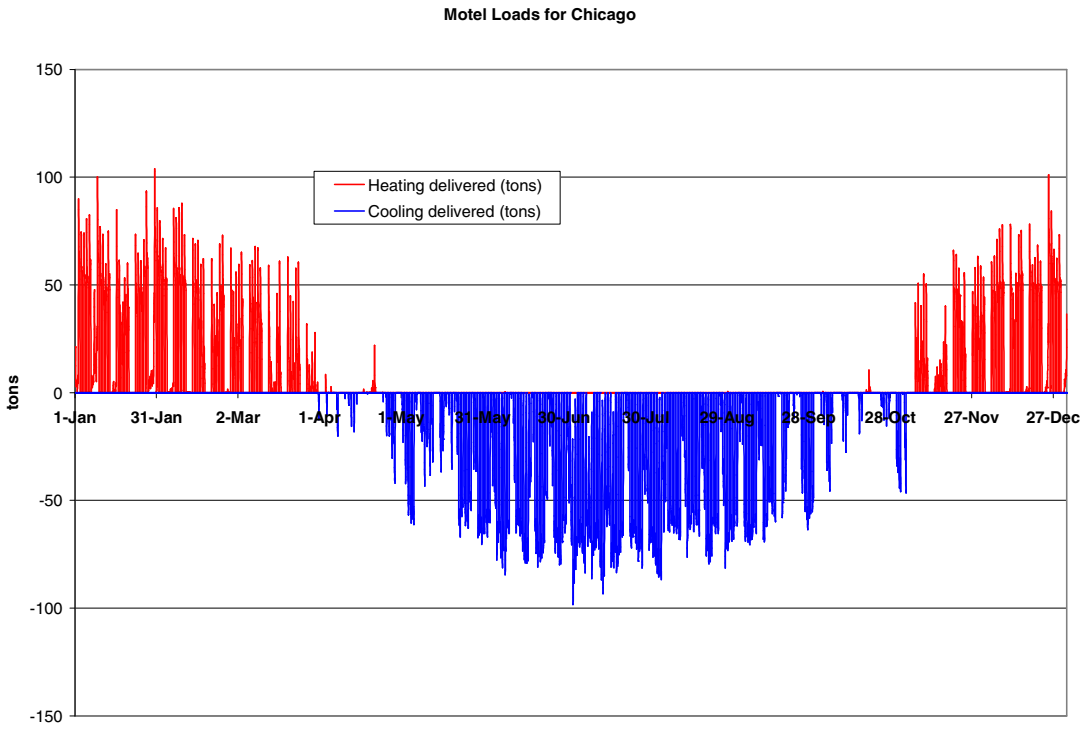

Figure 4.26 *Motel building loads for Chicago.*

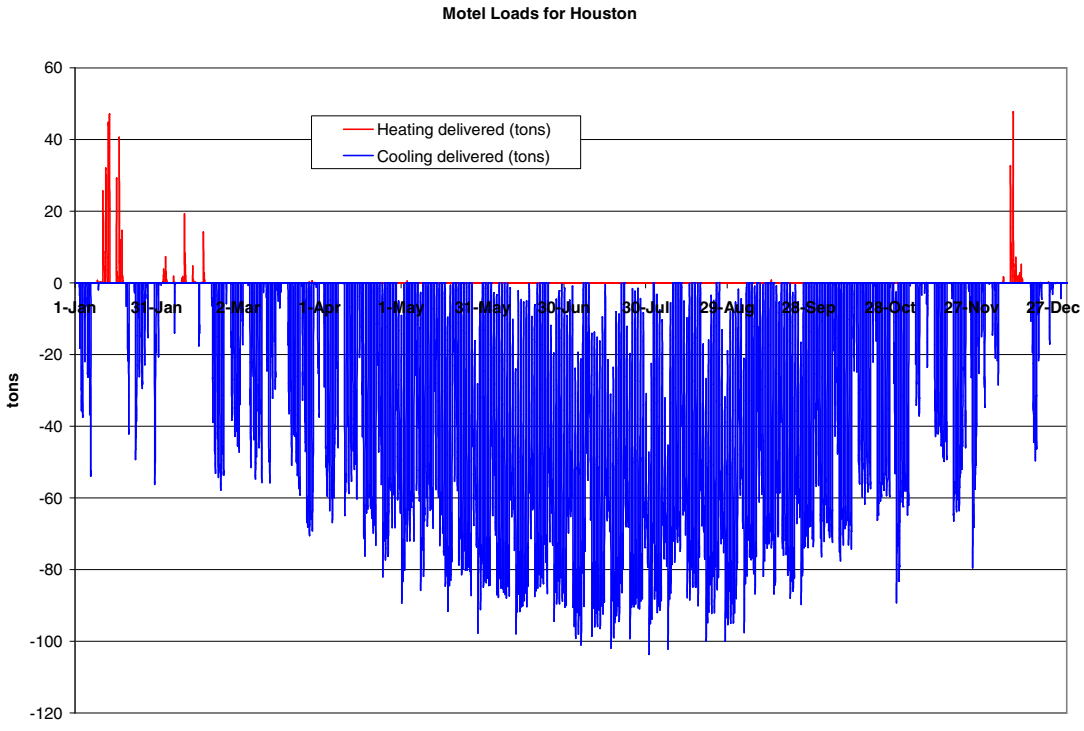

Figure 4.27 *Motel building loads for Houston.*

4.5.3. Test Cities

The two building models listed above were placed in 13 different cities and building loads were obtained that were used as boundary conditions for the WLHP system model. The 13 cities were chose somewhat heuristically based on a list seen at a class presentation. It was later discovered that they corresponded to a new proposed Department of Energy (DOE) classification (Briggs et al., 2002) which gives climate zones on the basis of heating degree days, cooling degree days, and humidity. Figure 4.28 shows a map of the zones and Table 4.2 gives their description. Of the 17 climate zones, representative cities are given for those 15 zones that exist within the U.S. Of those 15 representative cities, the list heuristically chosen for this work covers 12 cities, plus one additional city (Tulsa, Oklahoma). Three climate zones that exist within the U.S. (3C, 4C, and 6B) are missed in the list chosen. The 13 cities utilized and their climate zones are listed below. It is recommended for any future work that the missing 3 climate zones be added.

- Albuquerque, New Mexico – Mixed-Dry
- Baltimore, Maryland – Mixed-Humid
- Boise, Idaho – Cool-Dry
- Burlington, Vermont – Cold-Humid
- Chicago, Illinois – Cool-Humid
- Duluth, Minnesota – Very Cold
- El Paso, Texas – Warm-Dry
- Fairbanks, Alaska – Subarctic

- Houston, Texas – Hot-Humid
- Memphis, Tennessee – Warm-Humid
- Miami, Florida – Very Hot-Humid
- Phoenix, Arizona – Hot-Dry
- Tulsa, Oklahoma – Warm-Humid

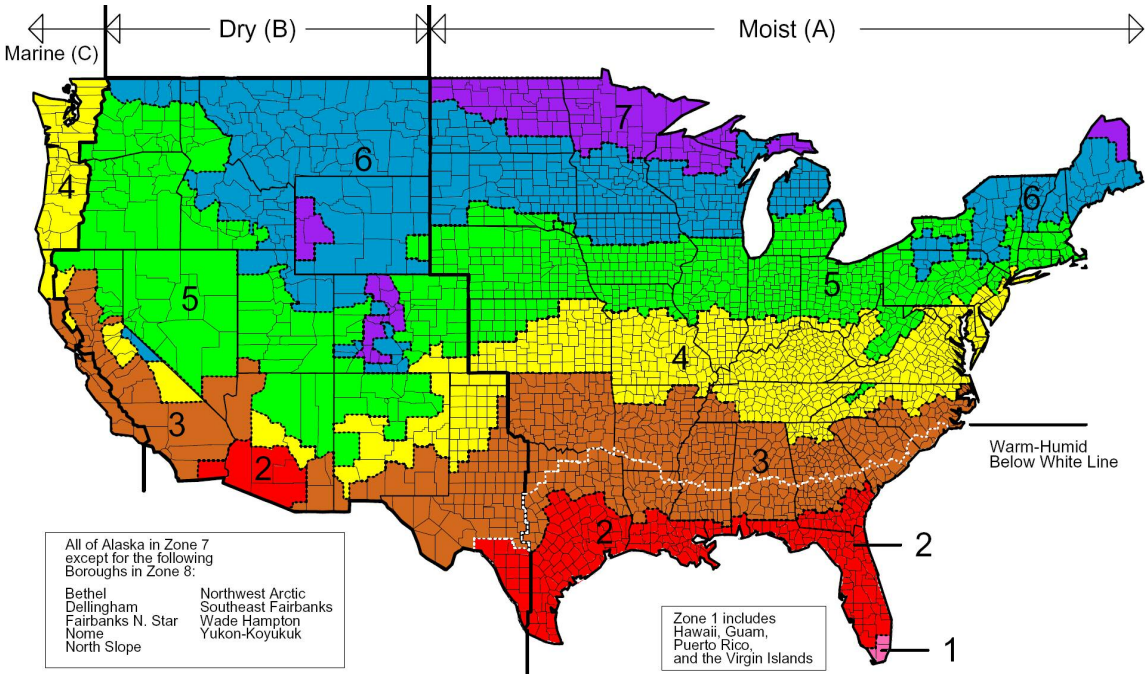

Figure 4.28 *Map of DOE's proposed climate zones (Department of Energy 2003).*

Table 4.2 *Description of climate zones (Briggs et al. 2002).*

Zone No.	Climate Zone Name and Type	Representative U.S. City
1A	Very Hot-Humid	Miami, Fl
1B	Very Hot-Dry	- - -
2A	Hot-Humid	Houston, TX
2B	Hot-Dry	Phoenix, AZ
3A	Warm-Humid	Memphis, TN
3B	Warm-Dry	El Paso, TX
3C	Warm-Marine	San Francisco, CA
4A	Mixed-Humid	Baltimore, MD
4B	Mixed-Dry	Albuquerque, NM
4C	Mixed-Marine	Salem, OR
5A	Cool-Humid	Chicago, IL
5B	Cool-Dry	Boise, ID
5C	Cool-Marine	- - -
6A	Cold-Humid	Burlington, VT
6B	Cold-Dry	Helena, MT
7	Very Cold	Duluth, MN
8	Subarctic	Fairbanks, AK

5. VALIDATION OF THE WATER-LOOP HEAT PUMP SYSTEM MODEL

In an effort to validate the HVACSim+ WLHP model the experimental facility described in Chapter 3 was switched from running the GLHE and the HGSHP system to running, effectively, a WLHP system. This was done as an afterthought and the limited time available allowed for only a limited validation. Four days (September 22, 2006 to September 25, 2006) of five-minutely experimental data from the WLHP system were used for validation purposes. As was mentioned in Chapter 3 the source side of the system consists of two packaged water-to-water heat pumps (of which only one was used for purposes of the WLHP validation), a three-borehole ground loop heat exchanger (which was valved off for purposes of simulating a WLHP system), and a direct contact evaporative cooling tower, isolated by a plate frame heat exchanger. The load side serves two small buildings with hydronic heating and cooling. The experimental data was taken during a time period when there were no heating loads, as the research facility does not have a boiler in the system. Ergo, the validation of the model is only for the cooling season. The experimental facility is described below in Section 5.1. Descriptions of the models are given in Section 5.2. Experimental validations of each component simulation and the entire system simulation are presented below in Section 5.3. In addition, an intermodel validation was done with EnergyPlus and will be discussed in Section 5.4 below.

5.1. Experimental Facility

The data used to validate the component and system simulations were collected from the OSU HGSHP research facility described in Chapter 3 and by Hern (2004). Chilled water and hot water generated with the plant serve two small buildings. Figure 5.1 below shows the system as configured for WLHP experimental validation.

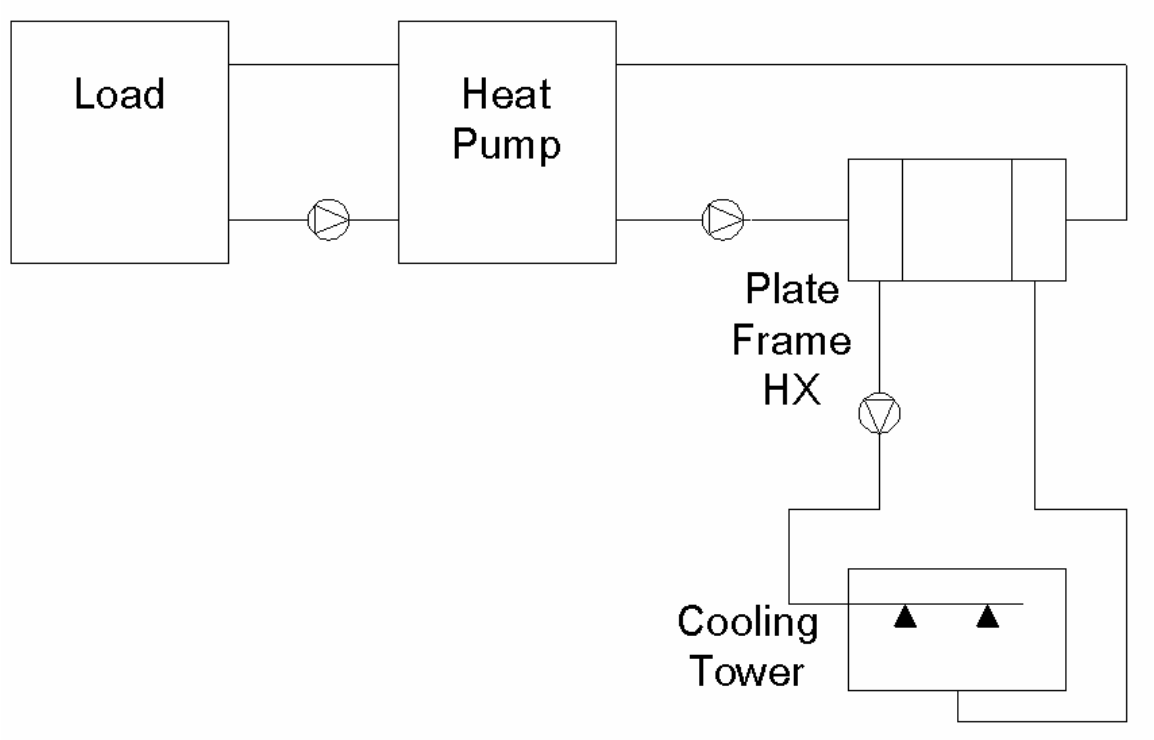

Figure 5.1 *Schematic of WLHP system used for experimental validation.*

The only changes necessary to run the system as a WLHP system were to remove the GLHE from the system by valving it off and to change the control of the cooling tower to the desired strategy. For validation purposes the cooling tower was controlled by the heat pump entering fluid temperature as is typically done in practice. The cooling

tower was switched on if the heat pump entering fluid temperature rose above 32.22°C (90°F). To protect the equipment from cycling on/off to frequently a dead band of 1°C (1.8°F) was placed on the controls. I.e. the cooling tower, once switched on, would not be switched off until the heat pump entering fluid temperature fell below 31.22°C (88.2°F).

A brief description of the equipment used in the experimental facility is given below. A more detailed description including manufacturers' data is given in Chapter 3. The same experimental measurement uncertainties described in Chapter 3 are present here.

5.1.1. Heat Pump

For the purposes of this validation only one heat pump (Florida Heat Pump WP036–1CSC–FXX), of nominal capacity 10.6 kW was utilized for purposes of providing chilled water to the system. A more detailed description of the heat pump can be found in Section 3.1.1.

5.1.2. Cooling Tower

A direct-contact evaporative cooling tower (Amcot ST-5) with nominal capacity of 17.6 kW (5-tons) (defined at a water flow rate of 0.63 L/s (10GPM) being cooled from 35ºC (95ºF) to 29.4 ºC (85ºF) with an outdoor wet-bulb temperature of 25.6 ºC (78ºF)) is

connected to the source-side of the heat pumps via an isolation heat exchanger. More information for the cooling tower can be found in Section 3.1.3.

5.1.3. Plate Heat Exchanger

The plate frame heat exchanger (Paul Mueller PHE AT4C-20) has a nominal capacity of 9.3 kW (2.65-tons) with flow rates of 0.5 L/s (GPM) on both sides of the heat exchanger and a temperature difference of 19.4^{o}C (35^{o}F) between the inlet temperatures. More information for the cooling tower can be found in Section 3.1.4.

5.1.4. Piping

Buried piping connects the cooling tower to the plant building (approximately 31m (100ft.) in each direction). Exposed (to the plant room environment) piping connects the components inside the building. Under many conditions, e.g. when the piping is insulated, heat losses and gains to/from the piping may be negligible. However, buried, uninsulated piping, as used to connect the cooling tower may have a not-insignificant amount of heat transfer and are therefore modeled as a separate component within the HVACSim+ model. This model is described in Section 2.2.6.

5.2. HVACSim+ Component and System Models used for Experimental Validation

The simulation was developed within two superblocks and utilized five minute time steps. The heat pump model used was TYPE 563 described in Section 2.2.1. The plate heat exchanger model used was TYPE 664 described above in Section 2.2.4. The cooling tower model used was TYPE 771, with slight modifications, and is described in detail in Section 4.2.2. TYPE 771 mentioned in Section 4.2.2. can only handle a constant UA, the modified TYPE 771 will allow for varying UA based on entering air flow rate and water flow rate similar to TYPE 768 described in Section 2.2.3. Finally the empirical heat loss/gain model, TYPE 643, is the same model discussed in Section 2.2.6. All simulations used the following boundary conditions, measured on site, except where noted:

- Outside air wet-bulb temperature, determined from an aspirated dry bulb temperature measurement (on site) and a relative humidity measured at local weather station, about 1 km (0.6 miles)from the site.
- Heat pump source side load, measured on site. This forces the heat pump operation in the simulation to be the same as the experiment.
- Flow rates of water through the heat pump and cooling tower.
- Heat transfer rates for the empirical pipe heat loss/gain model.
- With TYPE 664 the plate frame heat exchanger UA was treated as a boundary condition; a separate model was used to determine the time-varying UA based on the experimental data being used for the validation.

As with the HGSHP validation, the work on the WLHP system simulation started with the models and parameters that would be feasible for a designer to obtain in advance of constructing and operating the system. While keeping the cooling tower control fixed as a boundary condition, discrepancies in temperatures were addressed by improving the individual models or their parameters. Then, the simulations with the cooling tower controller explicitly modeled were performed. Starting with the final improved simulation, one could then work backwards to find the impact of using only designer-feasible models and parameters.

The HVACSim+ visual tool schematic of the experimental WLHP system can be seen below in Figures 5.2 and 5.3. Figure 5.2 shows the full schematic with all system connections shown and superblocks listed. Each of the system components is identified. Blocks labeled “HEATER” are the empirical heat gain/loss component model. Figure 5.2 shows the flow from component to component.

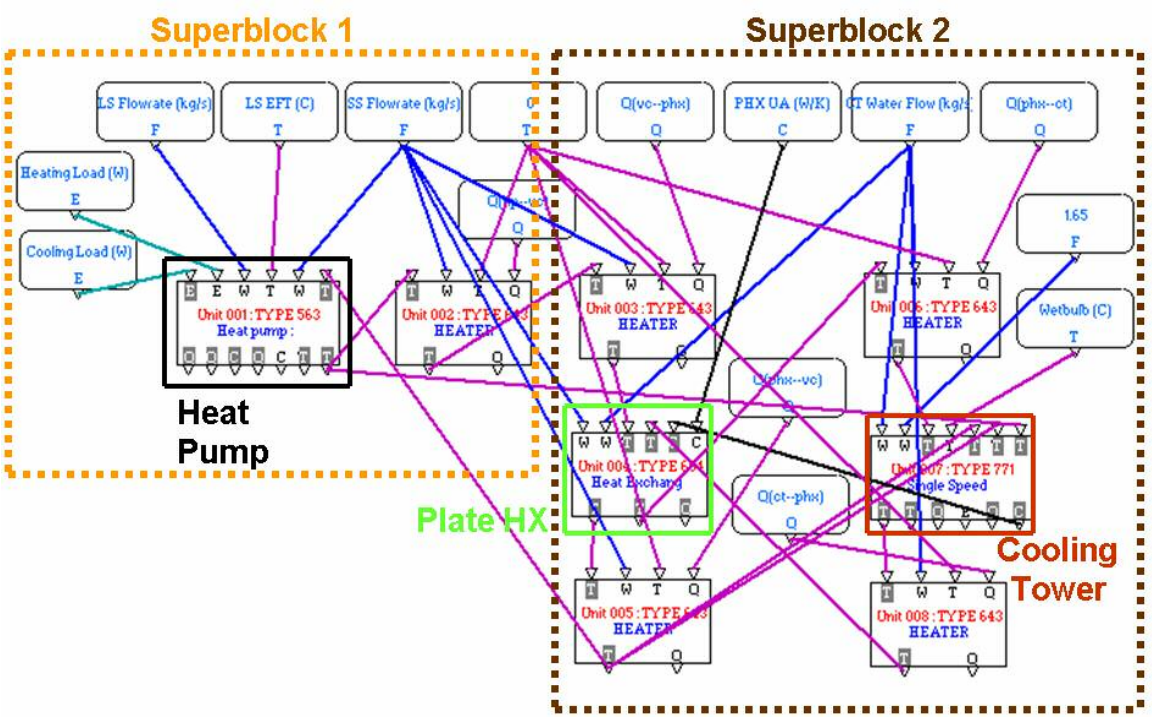

Figure 5.2 *HVACSim+ visual tool model showing system connections.*

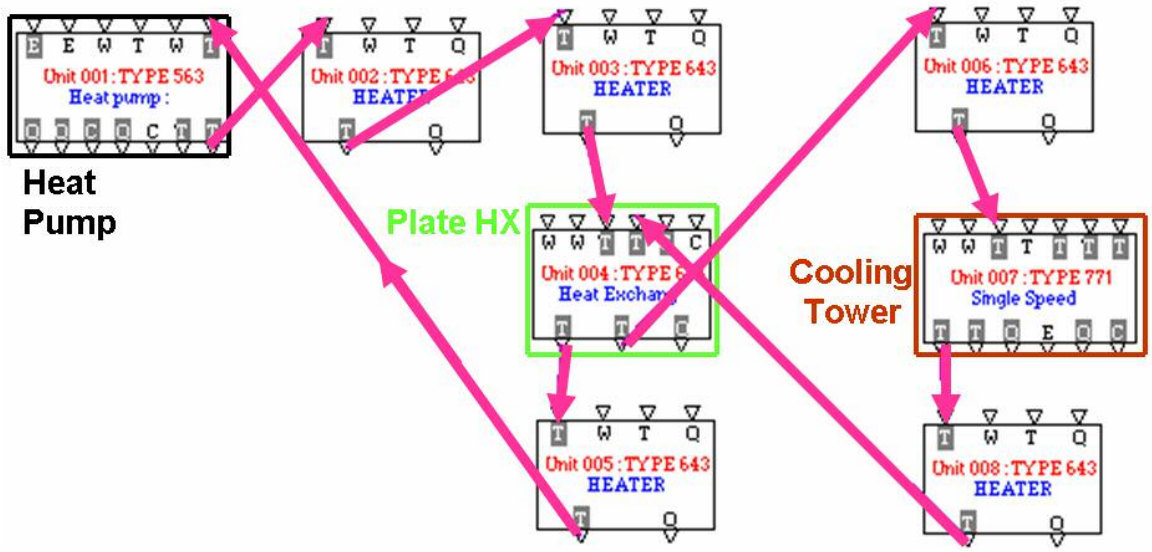

Figure 5.3 *HVACSim+ visual tool model showing flow direction.*

5.3. Experimental Validation

5.3.1. Heat Pump Model

The coefficients originally used for the heat pump model were generated with manufacturer's data and are given in Table 3.4. The resulting model is labeled as "uncalibrated" in Figures 5.4-5.6. The model gave poor results due to the fact that the actual flow rates on both sides of the heat pump were significantly larger than catalog data. The flow rates on the source side were even higher than those measured in Chapter 3; without the GLHE, there is less resistance to flow. Therefore the flow is higher and the model errors are greater. As with the HGSHP validation, this problem was addressed by using experimentally-measured data and recalculating the model coefficients. Because the source-side flow rates are significantly higher, the model coefficients were recalculated and are different than those in given in Table 3.4. Table 5.1 gives the new coefficients; Table 5.2 and Figures 5.4-5.6 show substantial improvements when this calibration is done.

Table 5.1 *Heat pump coefficients.*

Coefficient Name	Coefficients obtained through Experimental Data
1st COP Coefficient in Heating Capacity	-6.96830
2nd COP Coefficient in Heating Capacity	9.12295
3rd COP Coefficient in Heating Capacity	-2.32365
4th COP Coefficient in Heating Capacity	0.98262
5th COP Coefficient in Heating Capacity	0.30022
1st COP Coefficient in Heating Compressor Power	-5.20677
2nd COP Coefficient in Heating Compressor Power	-1.32697
3rd COP Coefficient in Heating Compressor Power	7.12769
4th COP Coefficient in Heating Compressor Power	-0.02709
5th COP Coefficient in Heating Compressor Power	-0.08953
1st COP Coefficient in Heating Extraction	-2.97521
2nd COP Coefficient in Heating Extraction	4.71950
3rd COP Coefficient in Heating Extraction	0.12436
4th COP Coefficient in Heating Extraction	-0.16872
5th COP Coefficient in Heating Extraction	-0.73435
1st COP Coefficient in Cooling Capacity	-6.96830
2nd COP Coefficient in Cooling Capacity	9.12295
3rd COP Coefficient in Cooling Capacity	-2.32365
4th COP Coefficient in Cooling Capacity	0.98262
5th COP Coefficient in Cooling Capacity	0.30022
1st COP Coefficient in Cooling Compressor Power	-5.20677
2nd COP Coefficient in Cooling Compressor Power	-1.32697
3rd COP Coefficient in Cooling Compressor Power	7.12769
4th COP Coefficient in Cooling Compressor Power	-0.02709
5th COP Coefficient in Cooling Compressor Power	-0.08953
1st COP Coefficient in Heating Rejection	-2.97521
2nd COP Coefficient in Heating Rejection	4.71950
3rd COP Coefficient in Heating Rejection	0.12436
4th COP Coefficient in Heating Rejection	-0.16872
5th COP Coefficient in Heating Rejection	-0.73435

Table 5.2 *Summary of uncertainties in HP model.*

Model	HP Source Side HTR RMSE (W)	% Error of Max HTR	HP Source Side HTR MBE (W)	HP Power RMSE (W)	% Error of Max Power	HP Power MBE (W)	HP Source Side HTR Typical Uncertainty
Simulated (calibrated system simulation)	354	2.61%	-31	55	2.20%	16	510 W
Simulated (calibrated component simulation)	355	2.62%	-33	20	0.80%	-1	
Simulated (uncalibrated component simulation)	1,519	11.21%	1,382	932	37.28%	-913	

As can be seen from Figure 5.4 the calibrated component simulation exiting fluid temperature (ExFT) matches the experimental results very well, while the system simulation ExFT does not appear to. This is caused by errors that have propagated through the component models. Although the ExFT trend does not match, as can be seen in Figure 5.5 the heat transfer rates match extremely well. This can also be seen in Figure 5.4 by the red lines labeled "HP ΔT". The heat pump entering and exiting fluid temperature are plotted for both the experimental results and the system simulation showing again that the temperature difference across the heat pump is the same even though the temperature values are not.

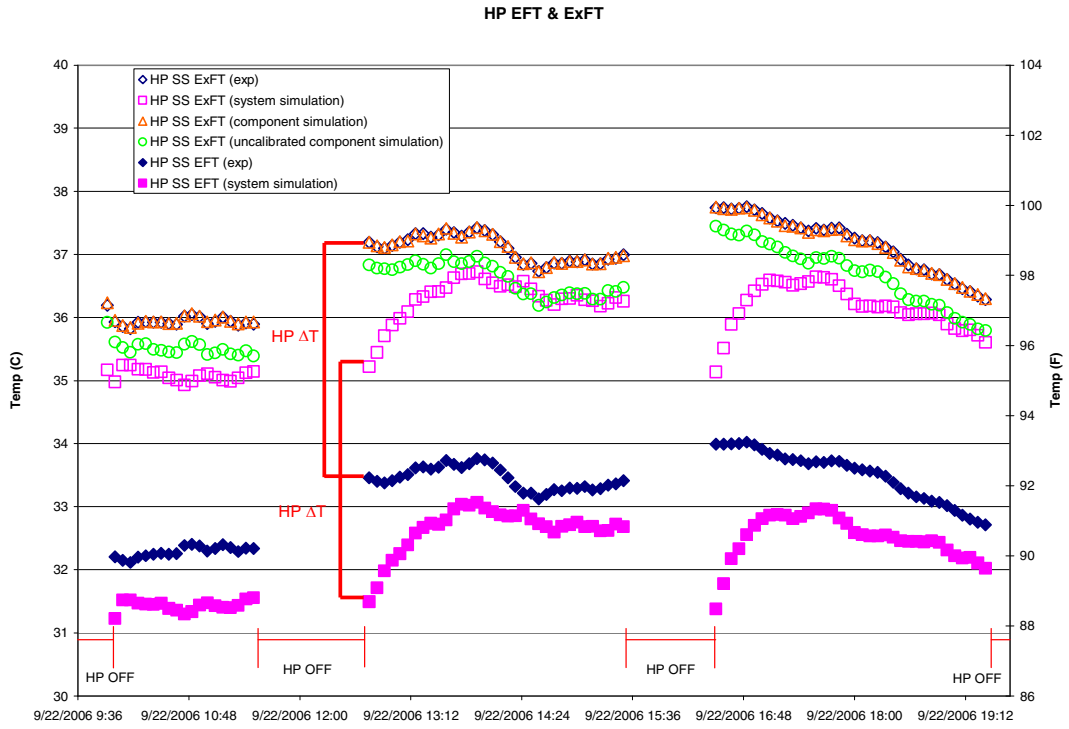

Figure 5.4 *HP source side ExFT for a typical cooling day.*

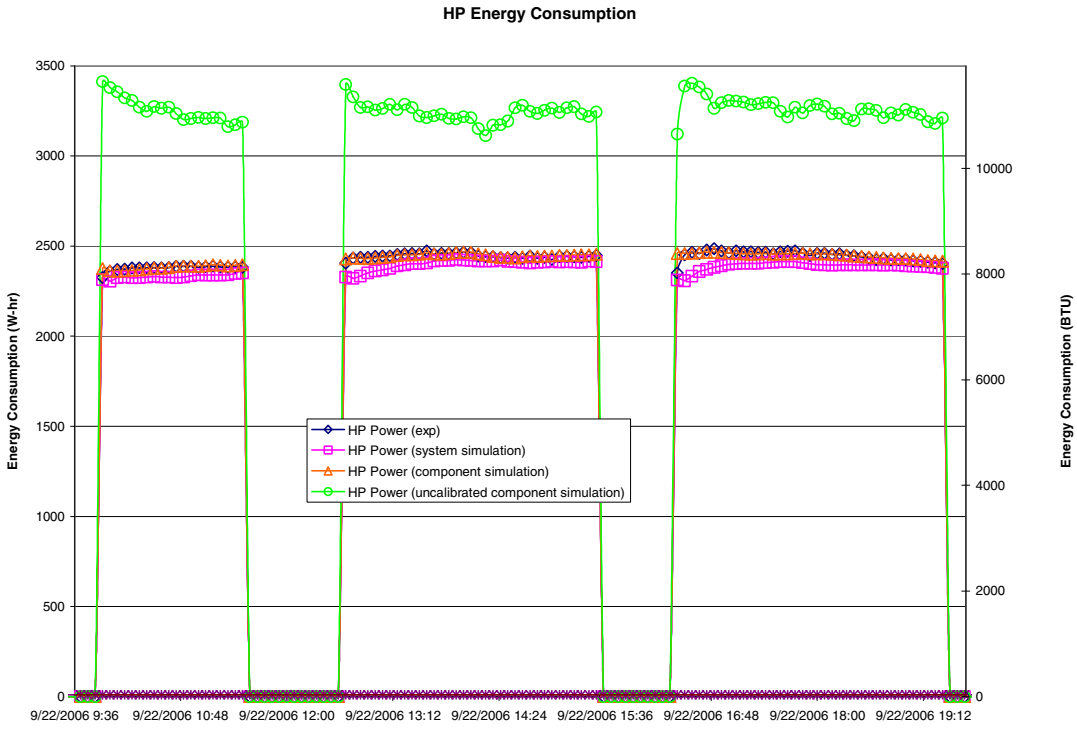

Figure 5.5 *HP energy consumption for a typical cooling day.*

Figure 5.6 *HP source side heat transfer rate for a typical cooling day.*

As another check, the models' ability to predict cumulative energy consumption was investigated. The total energy consumption was calculated for the four day period and the comparison is shown below in Figure 5.7 for the calibrated system, calibrated component, and uncalibrated component compared to experimental energy consumption. As can be seen the error found by running the system simulation is less than one percent that of the experimental values. Also shown is the large improvement that is gained by using experimental data to determine model coefficients, showing almost a 40% improvement from the uncalibrated component model to the calibrated component model. This suggests a parameter estimation-based model might be worth investigating.

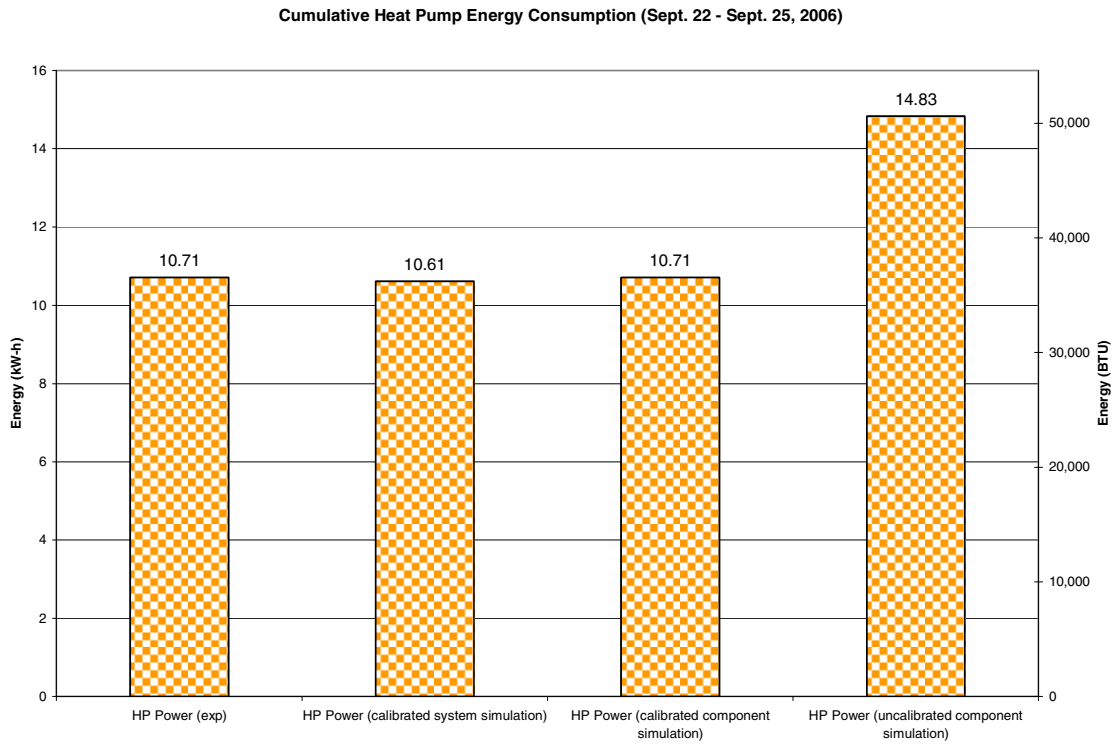

Figure 5.7 *Cumulative heat pump energy consumption (September 22 – 25, 2006).*

5.3.2. Cooling Tower Model

As discussed in Chapter 3 the cooling tower manufacturer gave only a single operating point as catalog data. Ergo, the first cooling tower model ("designer-feasible") utilized a fixed UA value of 800 W/K, labeled in the figures below as "uncalibrated". As an improvement, the variable UA model given in Equation 3.3 with coefficients calibrated to experimental data measured earlier was utilized. The cooling tower model was not recalibrated; the coefficients are given in Equation 3.3. Figures 5.8 and 5.9, shown below, show results for a portion of a typical cooling day, with several cooling tower on/off cycles. Here, the uncalibrated component simulation represents the results

from the fixed UA model as mentioned; while the calibrated simulations represent results with the variable-UA model. The model improvements result in not insignificant improvements in the model predictions. The RMSE in the heat transfer rate is 2,659 W or a little more that 16% of the maximum heat transfer rate for the uncalibrated component simulation. Going to the calibrated variable UA model reduces the RMSE to 815 W or just under 5% of the maximum heat transfer rate while the MBE goes from 2,411 W to 40 W of overprediction by the simulation. When the calibrated model is simulated as part of the system, the RMSE is 870 W or just over 5% of the maximum heat transfer rate and the MBE is 341 W of overprediction by the system simulation. These results are summarized below in Table 5.3.

Table 5.3 *Summary of uncertainties in CT model.*

Model	CT HTR RMSE (W)	% Error of Max HTR	CT HTR MBE (W)	CT HTR Typical Uncertainty
Simulated (calibrated system simulation)	870	5.30%	341	850 W
Simulated (calibrated component simulation)	815	4.97%	40	
Simulated (uncalibrated component simulation)	2,659	16.21%	2,411	

It should be noted that both the experimental measurements and simulation-predicted-values of cooling tower heat transfer rate have significant uncertainty. The lower and upper bounds of the experimental uncertainty in the cooling tower heat transfer rate measurement, caused by uncertainty in measurements of mass flow rate and temperature difference, are shown in Figure 5.9. In addition, the simulation has an experimental uncertainty component – the wet-bulb temperature (an input) has a typical

uncertainty of ± 0.5ºC (± 0.9ºF) – which results in an uncertainty in the simulation results. Error bars for the simulation results are shown for two sample points in Figure 5.9. The uncertainty caused by the uncertainty in the wet-bulb temperature appears to be the limiting factor in the simulation. This also suggests that, in practice, caution is warranted in using a control based on wet-bulb temperature.

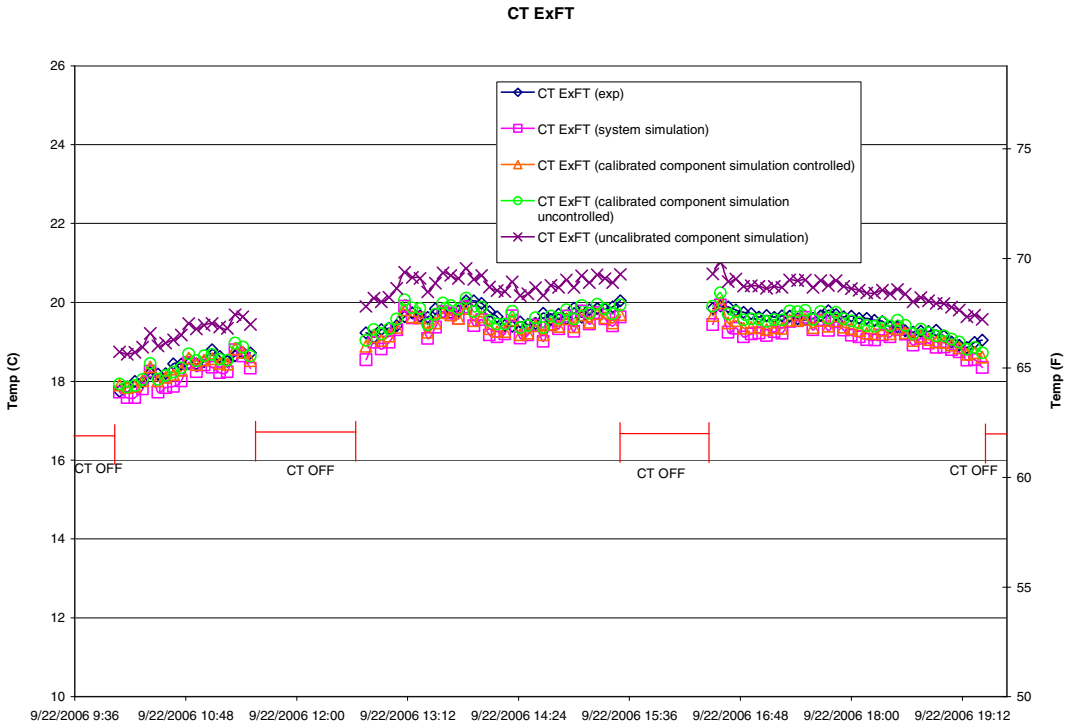

Figure 5.8 *Cooling tower ExFTs for a typical cooling day.*

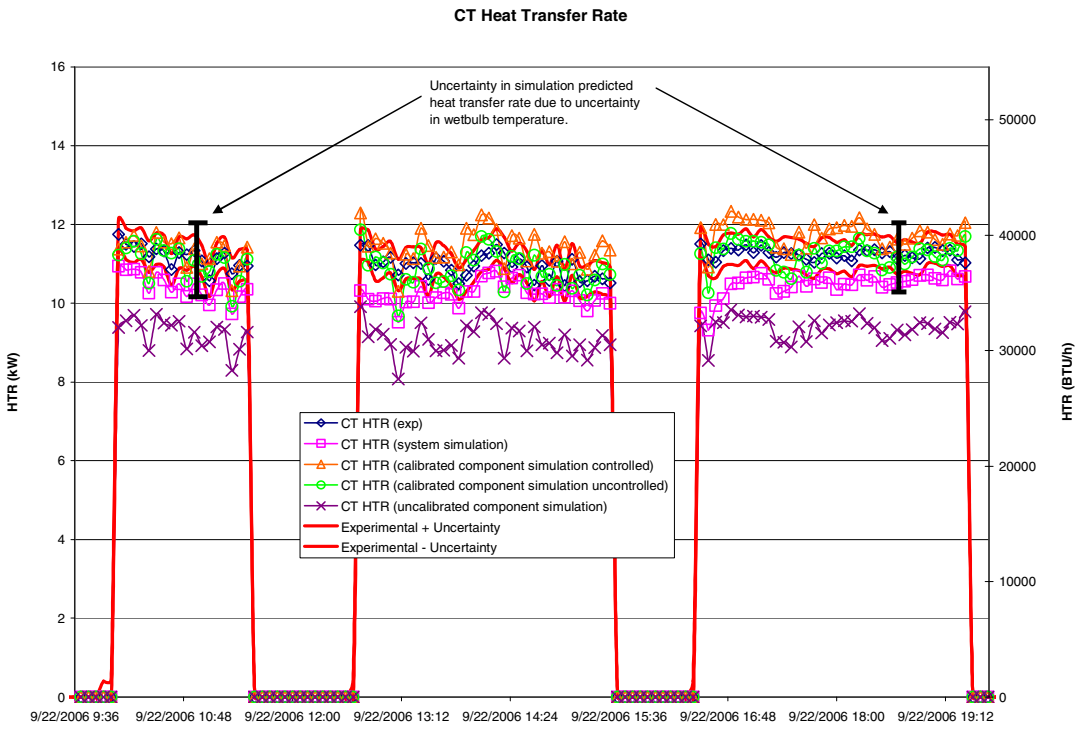

Figure 5.9 *Cooling tower heat transfer rates for a typical cooling day.*

5.3.3. Plate Frame Heat Exchanger Model

Three permutations of the plate heat exchanger model were utilized for simulation and validation purposes:

1. A fixed UA model, with UA estimated from manufacturer's data (uncalibrated component simulation – fixed UA). Sixteen data points were available from the manufacturer of the plate frame heat exchanger model. Initially, a fixed UA model was utilized for the heat exchanger with a value of 800 W/K.

2. A variable UA model with UA fitted as a function of mass flow rates and entering fluid temperatures to experimental data (calibrated component simulation – variable UA).
3. A fixed effectiveness model with effectiveness fitted to experimental data (calibrated component simulation – fixed eff.). The fixed effectiveness model was found to have a nominal effectiveness of 0.27.

Chapter 3 discusses the effects of fouling on the plate heat exchanger. While this was found to be a problem for modeling a seven-month period, as the fouling changed substantially over the seven month period, the effects were negligible over a four day validation.

For all results given, "Fluid 1" refers to the "hot side" or heat pump side of the plate heat exchanger and "Fluid 2" refers to the "cold side" or cooling tower side of the plate heat exchanger. Figures 5.10 and 5.11 show a comparison of the various simulations with the experimental results for the plate heat exchanger exiting fluid temperature and heat transfer rates respectively. Figure 5.10 shows only calibrated results while Figure 5.11 shows both calibrated and uncalibrated. Table 5.4 summarizes the error and uncertainty associated with the plate heat exchanger model.

Table 5.4 *Summary of Uncertainties in PHX model.*

Model	PHX HTR RMSE (W)	% Error of Max HTR	PHX HTR MBE (W)	PHX HTR Typical Uncertainty
Simulated (calibrated system simulation)	579	3.53%	64	510 W
Simulated (calibrated component simulation-variable UA)	3	0.02%	0	
Simulated (calibrated component simulation-fixed ε)	474	2.89%	58	
Simulated (uncalibrated component simulation-fixed UA)	519	3.16%	85	

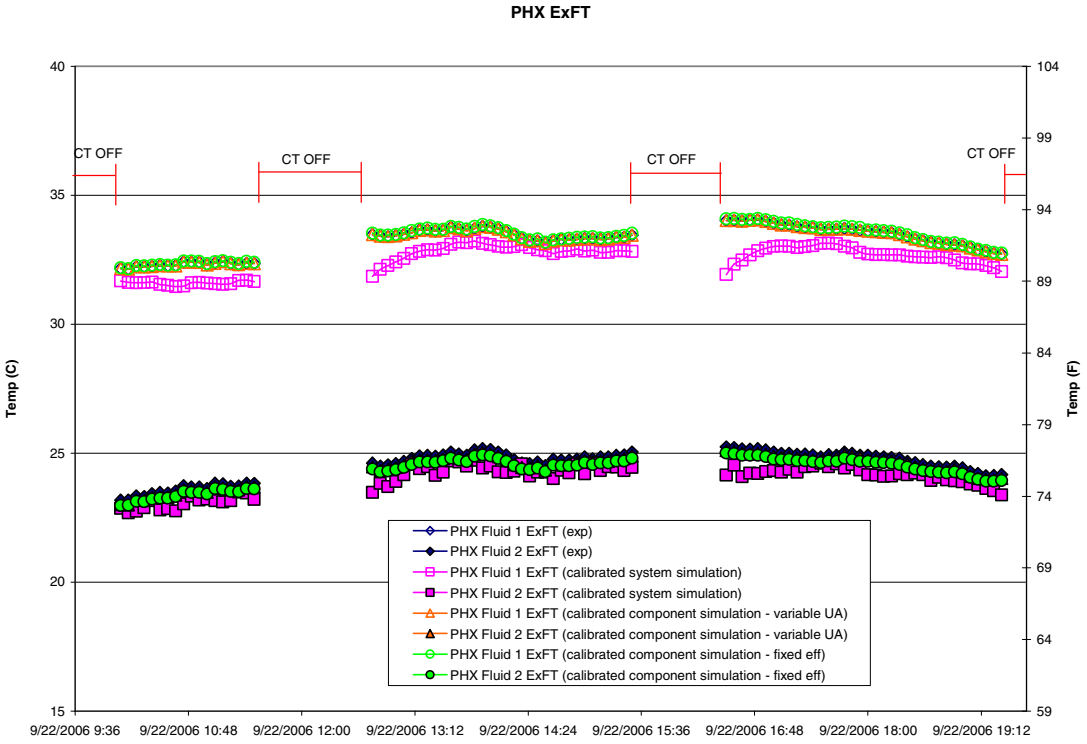

Figure 5.10 *Plate frame HX ExFTs for a typical cooling day.*

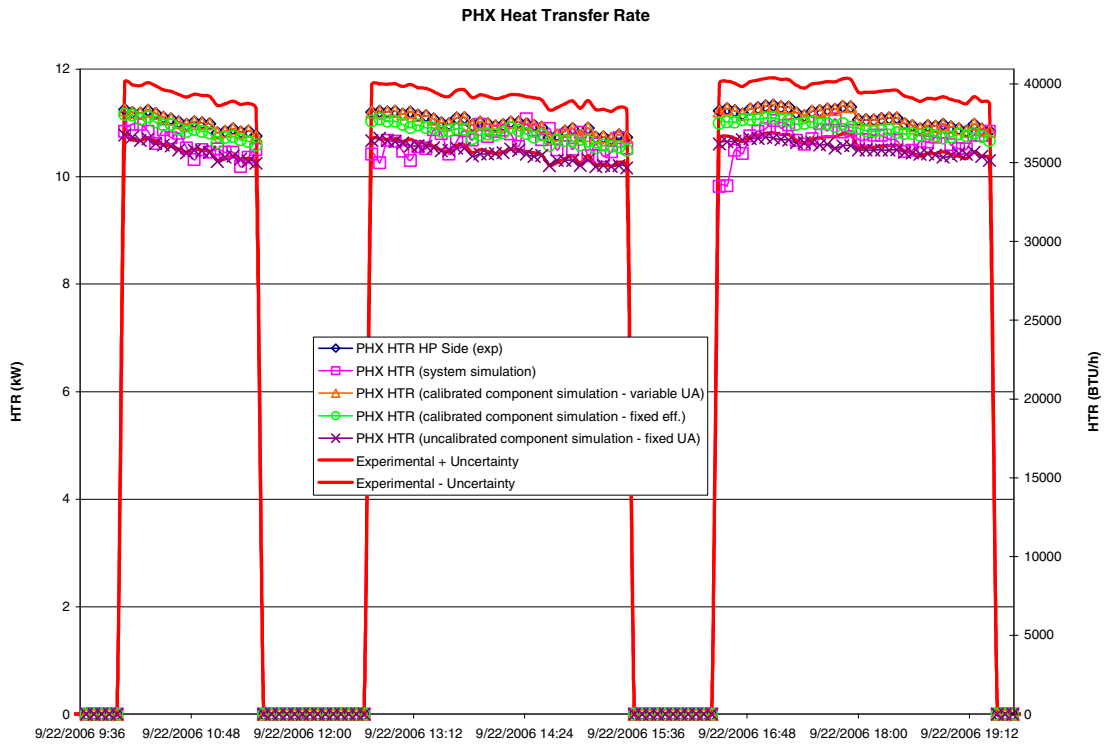

Figure 5.11 *Plate frame HX heat transfer rate for a typical cooling day.*

5.3.4. System Simulation with Heat Pump EFT Controlled

Upon reviewing the results it was found that the heat transfer rates matched extremely well as did the heat pump temperature difference comparison, but the temperature values showed errors on the order of 0.28-2.6ºC. It was hypothesized that the temperature value error is due to the nature of simulation which is controlled by load side heat transfer rates on the heat pump side and wet-bulb temperature on the cooling tower side allowing for temperature values to drift. The temperature drift is then propagated around the loop.

In order to confirm this hypothesis a system simulation was run with the heat pump entering fluid temperature controlled as a boundary condition. The idea was that this would effectively solve the temperature drift propagation by fixing a temperature within the loop. The heat pump results are essentially flawless since in the simulation the load side and source side of the system are defined by experimental data as inputs, therefore only plots of the cooling tower and plate heat exchanger exiting fluid temperatures are shown below in Figures 5.12 and 5.13. Figure 5.12 shows that the system simulation with the heat pump entering fluid temperature controlled matches more closely than that of the system simulation without the heat pump entering fluid temperature being controlled. Likewise, in Figure 5.13 the simulation with the heat pump entering fluid temperature controlled as a boundary condition significantly improves the prediction of the plate frame heat exchanger exiting fluid temperature. From these figures we can see that by setting a single temperature within the loop, the errors in temperature prediction are significantly reduced, strongly suggesting that the propagation of error around the loop results in predicted temperature drifting away from the experimental measurements.

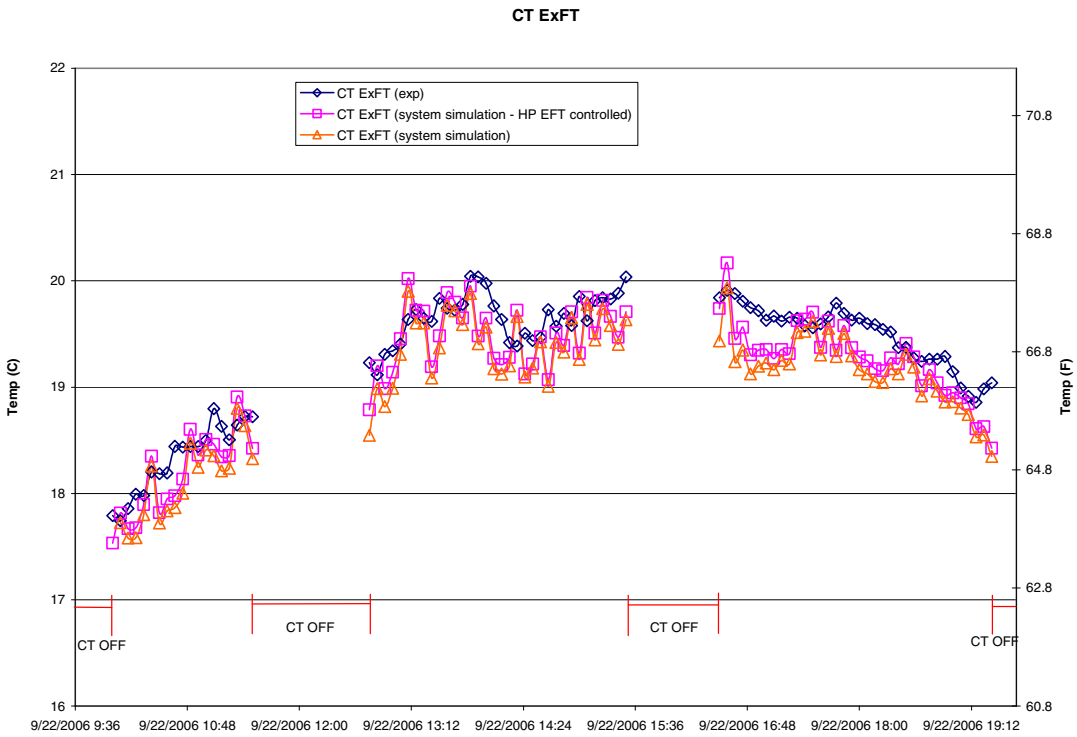

Figure 5.12 *Cooling tower ExFTs for a typical cooling day with and without HP EFT set by using experimental data.*

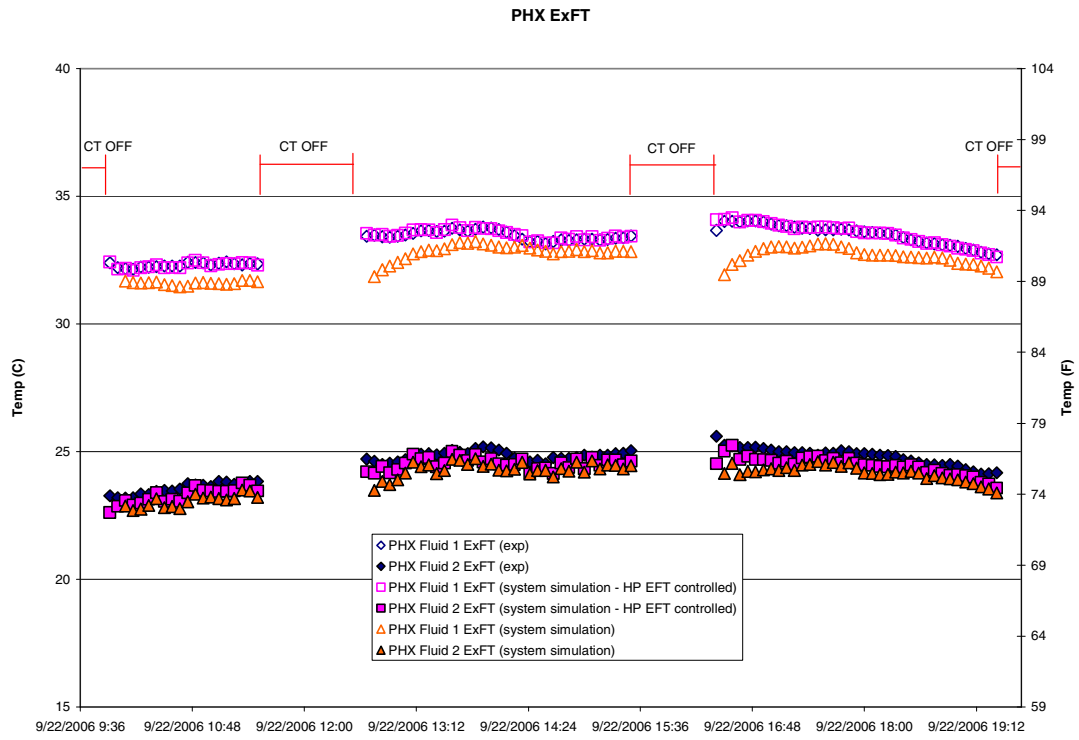

Figure 5.13 *Plate frame HX ExFTs for a typical cooling day with and without HP EFT set by using experimental data.*

5.4. Intermodel Validation

In order to further validate the HVACSim+ WLHP system model, it was compared to a WLHP system modeled in EnergyPlus. At the time the work was being done a common pipe model did not exist in EnergyPlus; therefore the system modeled in both programs utilized a constant speed pumping system. The system was modeled according to Figure 5.14, as shown below. While the cooling tower had its own pump the heat pumps and boiler shared a pump, as shown.

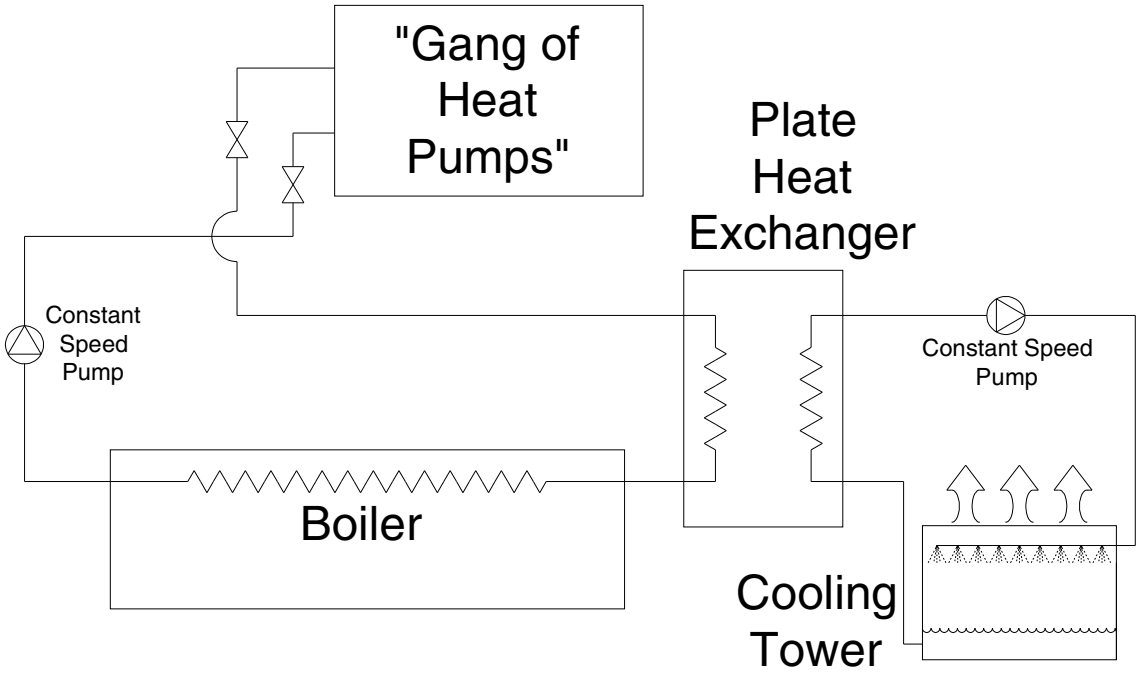

Figure 5.14 *WLHP system schematic used for intermodel validation.*

The EnergyPlus simulation was run with an input of 13.5m^3 of loop fluid volume which has both a transient delay effect and lumped capacitance effect on the system. The simulation, in both programs, was run at four-minute time steps with a constant flow rate of 45.74 kg/s. As discussed in Section 4.3 having multiple superblocks in HVACSim+ gives an approximate thermal mass that is equal to the product of the time step, in seconds, and the flow rate, in kg/s. Again this is an approximation of the superblock causing the system to lag one time step thereby causing the temperatures to lag by one time step effectively creating a thermal mass. With the time step and flow rate listed above the HVACSim+ simulation has an effective thermal mass of 11,000 kg of water in a plug flow scenario. This is calculated by multiplying the mass flow rate by the time step.

Figure 5.15 shows heat pump entering and exiting fluid temperatures for March 25, a typical shoulder season day. As can be seen, a somewhat large heating load is seen first thing in the morning and gradually decreases while as the afternoon approaches a cooling load begins to dominate. As is shown, the system goes from running the boiler in the morning to running the cooling tower in the afternoon with approximately 6 hours between the last time the boiler is operated to the first time the cooling tower it operated. The temperature response of the two simulations matches very well. Some difference can be seen when the boiler is being operated in the morning with the HVACSim+ results showing a saw-tooth on/off pattern. Both the EnergyPlus and HVACSim+ boiler models are designed to produce a desired outlet temperature when operating. The HVACSim+ model will then operate the boiler until the heat pump entering fluid temperature falls below the dead band. The saw-tooth temperature response during this period is due to the effects of having multiple superblocks. The boiler is switched on during one time step and reaches the desired outlet temperature, with the time step delay the very next time step the temperature has fallen back below the setpoint minus the dead band but the control signal for the boiler does not see this effect until the following time step causing the boiler to be switched on/off every other time step. Although this is not ideal it is difficult to overcome without running the simulation in one superblock.

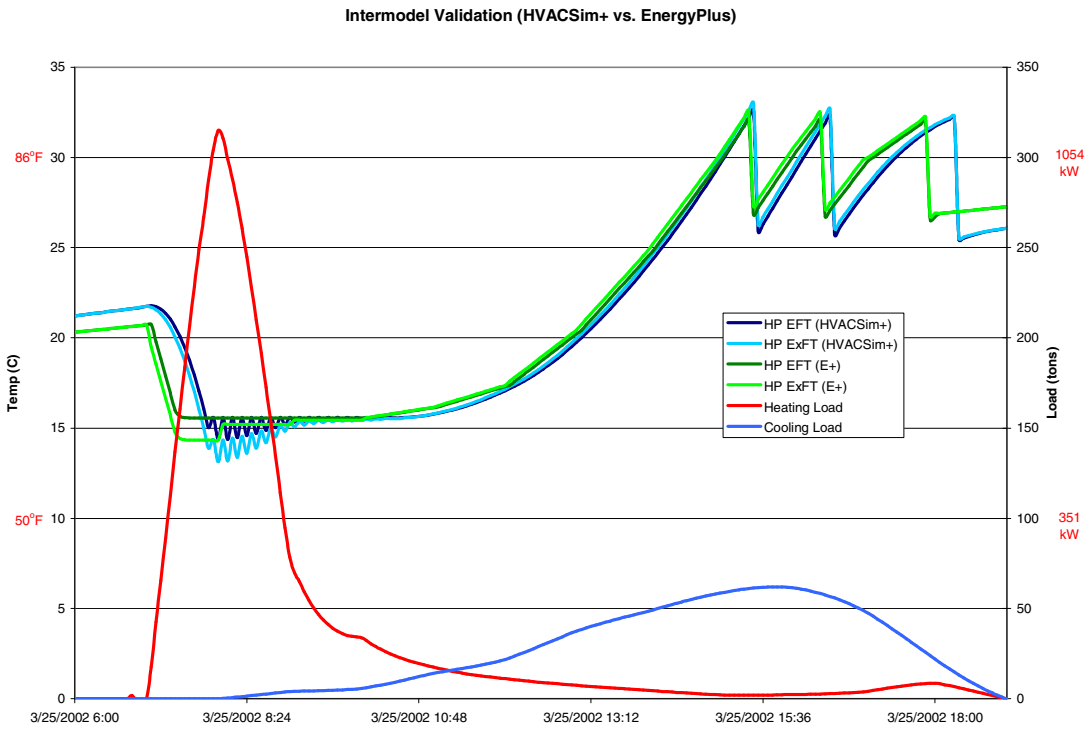

Figure 5.15 *Intermodel validation plot of typical shoulder season day.*

5.5. Conclusions/Recommendations

This chapter described a limited experimental validation of a water loop heat pump system simulation in HVACSim+ and an intermodel validation with EnergyPlus. The experimental validation was done using experimental data obtained from OSU's HGSHP research facility over a four day period. The results showed that while there were slight temperature errors that propagated through the system, the predicted energy consumption matched very well when all components were calibrated. Likewise, the intermodel validation showed a good match between the temperatures predicted by HVACSim+ and EnergyPlus. There were slight differences in the thermal mass causing the response of the cooling tower on/off cycles to vary slightly.

Recommendations for further research and development include the following:

1. The equation-fit-based heat pump model used here performed poorly with catalog data. A parameter-estimation-based model and/or some checks on the input data to the model combined with some more intelligent extrapolation should be investigated.
2. The sensitivity of the cooling tower results to the uncertainty in wet-bulb temperature suggests caution by practitioners when using control based on the wet-bulb temperature. Further research into control strategies that either do not depend on the wet-bulb temperature or that only partly depend on the wet-bulb temperature is warranted and will be discussed further in Chapter 6.
3. It would be beneficial to have more experimental data and have experimental data available for both heating and cooling seasons to use for a longer term validation.
4. Further work to help predict fouling of the plate heat exchanger would be useful.

6. OPTIMIZATION OF WATER-LOOP HEAT PUMP SYSTEM CONTROL STRATEGIES

6.1. Introduction

As discussed in Chapter 4, the most common control strategy for WLHP systems (Howell 1988; Hughes 1990; Pietsch 1990; Howell and Zaidi 1990; Pietsch 1991; Howell and Zaidi 1991) is to control the heat pump entering fluid temperature between 15.6ºC (60ºF) and 32.2ºC (90ºF). The boiler is operated as necessary to prevent the heat pump entering fluid temperature from falling below 15.6ºC (60ºF). The cooling tower is operated as necessary to prevent the heat pump entering fluid temperature from rising above 32.2ºC (90ºF).

The main focus of Chapter 4 was to develop a model of a WLHP system in HVACSim+ and EnergyPlus. The focus of Chapter 5 was to validate the HVACSim+ model through a small experimental data set obtained from OSU's HGSHP research facility and also validate the model through intermodel validation with EnergyPlus. The objective of Chapter 6 is to take the model developed in Chapter 4 and investigate new and improved control strategies that can be used to save on the WLHP system annual energy consumption. Specifically, control strategies that dynamically adjust loop

setpoints to reduce system energy consumption are of interest. Control strategies that will be inexpensive for manufacturers and designers to implement within new and existing WLHP systems are of the most interest.

6.2. General Overview of Control Strategies

In examining strategies to control the loop temperature within WLHP systems, one must consider the effects the loop temperature will have on energy consumption. This will depend upon the "mode" of operation, meaning the relative dominance of heat pumps providing heating vs. heat pumps providing cooling at any point in time. By lowering the loop entering fluid temperature, the cooling performance of the system will likely improve. But if any of the heat pumps are providing heating, the lower loop entering fluid temperature may result in higher energy consumption. Likewise, by raising the loop entering fluid temperature, the heating performance of the system will likely improve. But if any of the heat pumps are in cooling, the higher loop entering fluid temperature may result in higher energy consumption.

Another aspect of the system operation to consider is the effect of thermal mass in the system. This may be particularly important where the system mode of operation shifts between heating and cooling, as may occur during a shoulder season day. All systems have thermal mass, but augmenting the amount of thermal mass in a system by adding a water storage tank could also be considered (Pietsch 1991). With thermal storage, the current loop setpoint will also have an impact on the near-term future

operation of the system. During shoulder season days, the system could have a heating load during the morning hours and later in the day change to a rather large cooling load. In this case, it might be best to run at a low boiler setpoint and take advantage of the thermal storage in the system to allow for lower heat pump entering fluid temperatures later in the day.

Also, the tradeoff between heat pump energy consumption and cooling tower fan and pump energy consumption should be considered. Running the cooling tower more hours may save heat pump energy; this will be at the expense of energy used to run the cooling tower fan and pump. This may be helpful up to a certain point, at which a point of diminishing returns is reached and the cooling tower fan and pump energy consumption exceeds the heat pump energy savings.

This work first attempts to address the issue of how the mode of operation (relative dominance of heating vs. cooling) can feasibly be determined at any time. After this, control strategies that adjust the loop setpoints based on the mode of operation are investigated. Then, optimal setpoints are investigated. Finally, a preliminary investigation into forecasting control strategies for WLHP systems with augmented thermal mass is made in order to estimate the potential for additional savings. This is discussed in Section 6.4.6.

6.2.1 Determining Mode of Operation

In determining the mode of operation, it would be useful to be able to distinguish between a range of operating conditions. There may be times when all of the heat pumps are operating in cooling, times when all of the heat pumps are operating in heating, and still other times when some of the heat pumps are operating in cooling and some are operating in heating. Presumably the best setpoint is going to be directly related to the mode of operation (Pietsch 1991). Determining the number of heat pumps operating in heating or cooling at any given time may not be convenient for a user to measure, especially if the user does not have a full building energy management system. Ergo, this work attempted to find a surrogate measure that would be relatively easy to make and that would not be susceptible to sensor drift and error. One can imagine several ways to do this:

- Measuring the flow rate and ΔT across the heat pumps could be used to determine the net heat rejection/extraction rate. This would likely serve as the best surrogate for mode of operation. However, flow meters are susceptible to drift over time and introduce an additional undesirable maintenance requirement.
- Measuring the ΔT across the heat pumps and the control signal to the variable speed drive (VSD) would be another possibility. Flow rate is proportional to the signal, though at minimum flow an unknown amount of flow might be bypassing the heat pumps.

- Measuring the ΔT across the heat pumps would be a good measure for constant flow systems, but is less meaningful for variable flow systems. However, this option has the advantage of being very simple.

In the event, the last option was chosen for investigation, and time precluded investigation of the other options. As can be seen in this chapter, the ΔT does appear to be adequate as a surrogate for mode of operation.

Figure 6.1 shows histograms of heat pump ΔT (heat pump inlet – heat pump outlet) for both buildings in all locations with a variable flow system (30% minimum flow). Positive ΔT indicates heating dominated operation and negative ΔT indicates cooling dominated operation. As can be seen from the figure, the heat pumps operate at a wide range of temperature differences annually. The figures show the number of hours each building is operating at each range of temperature differences and the number of hours that there are no heat pumps in operation. As can be seen, there are many hours the office building has no heat pumps in operation. This is due mainly to the relatively large night and weekend setback.

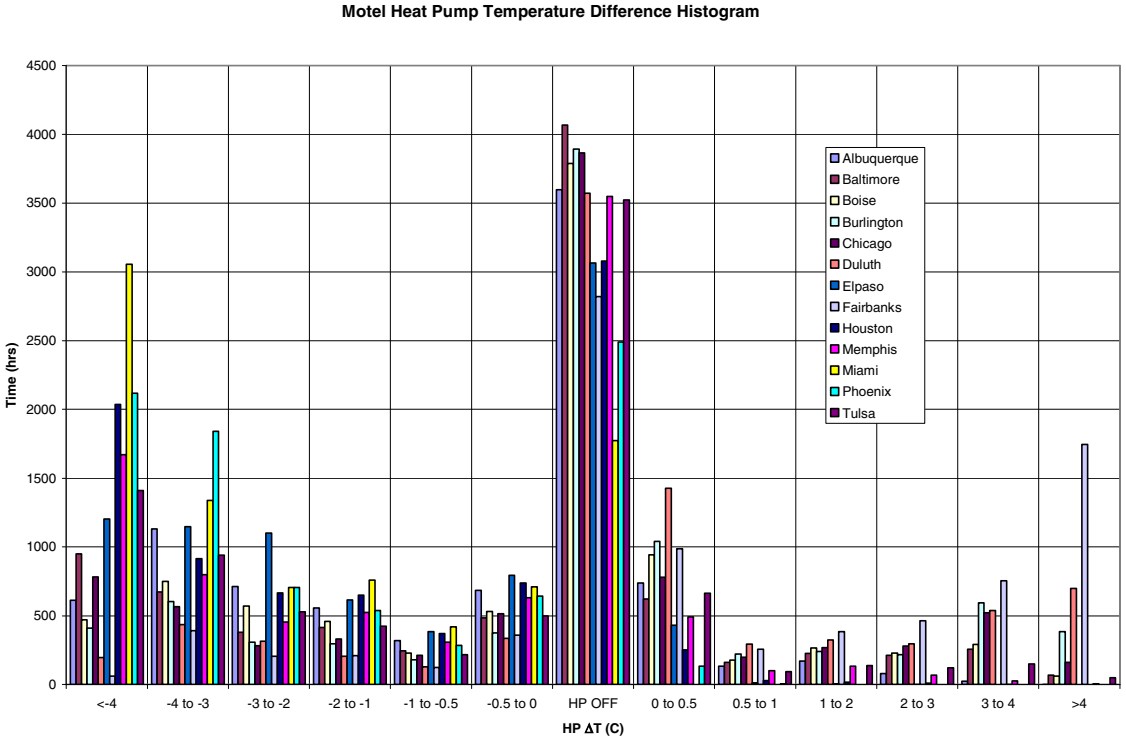

(a) *Motel.*

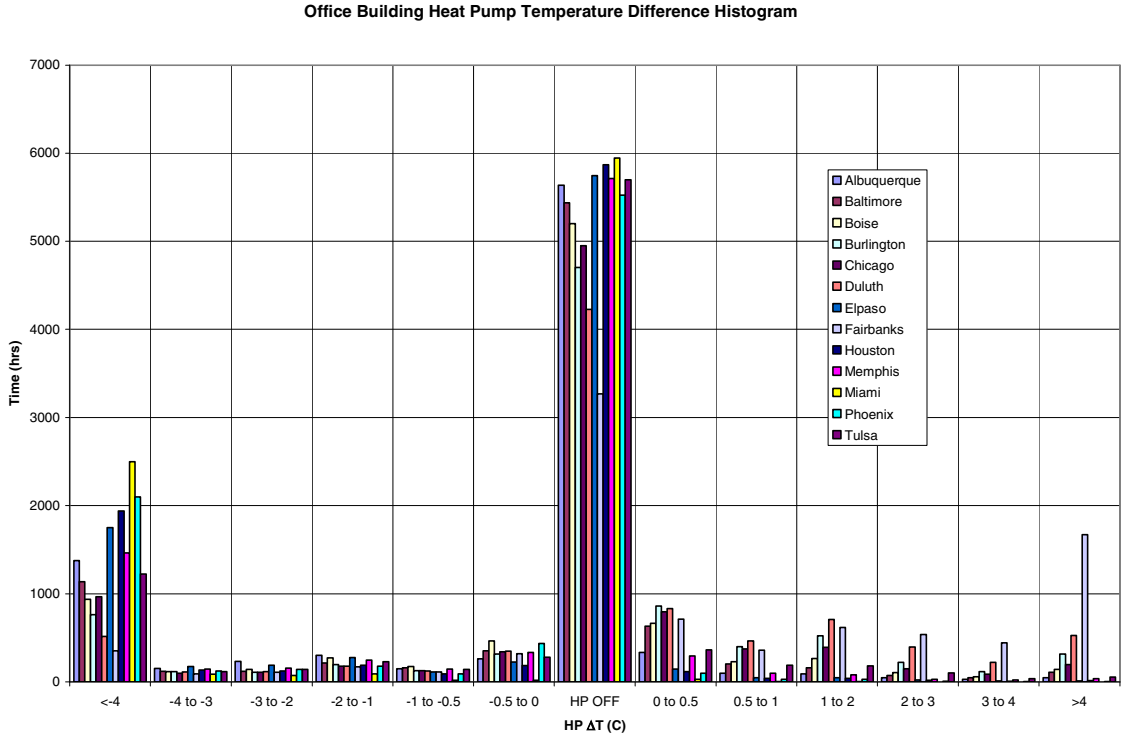

(b) *Office building.*

Figure 6.1 *Heat pump ΔT histograms.*

6.2.2 Example

Having selected heat pump ΔT as a surrogate measure of mode of operation, this section illustrates how it is used. Figure 6.2 (*b*) shows how a new control strategy might work sensing the heat pump temperature difference and setting the cooling tower setpoint based on the equation of the setpoint line (shown in blue). Once the heat pump entering fluid temperature exceeds that setpoint, the cooling tower begins operation and will continue operation until the heat pump entering fluid temperature falls below the dead band (shown in magenta).

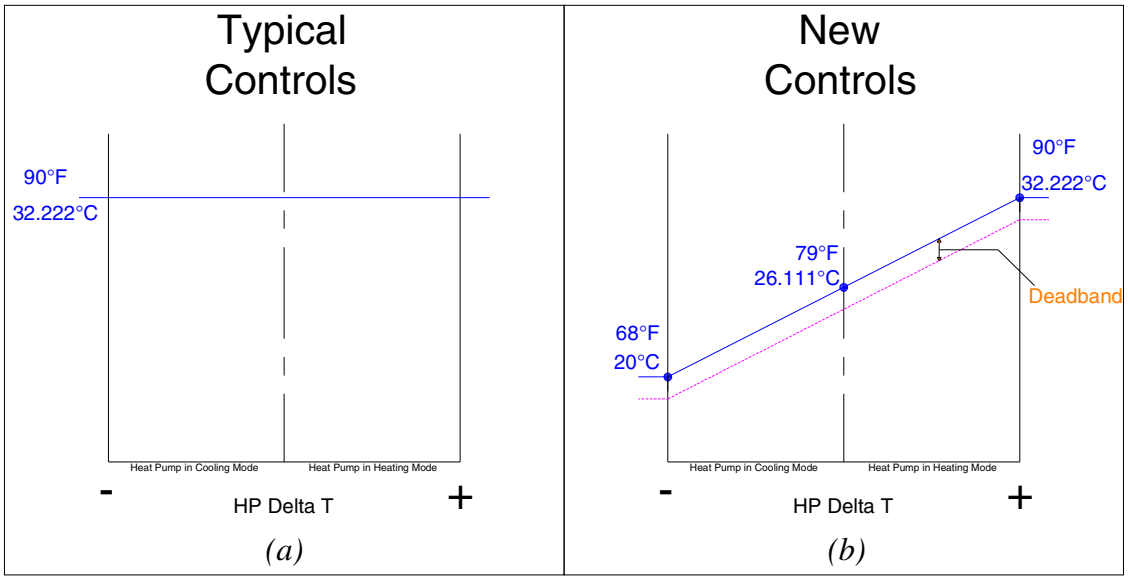

Figure 6.2 *Cooling tower controls schematic.*

In contrast, the typical controls shown in Figure 6.2 (*a*) are simple, single setpoint controls that remain constant with the temperature difference across the heat pump.

As an example of the resulting operation from such a control strategy, Figure 6.3 shows a plot of heating and cooling loads, the number of heat pumps in operation (both heating and cooling), the heat pump temperature difference, and the cooling tower setpoint for an office building in Albuquerque, NM, on February 12. As can be seen, the cooling tower setpoint is raised in the morning when there is a heating load and lowered in the afternoon as the cooling load increases. The energy impacts of such a control strategy will be discussed in more detail later in the chapter.

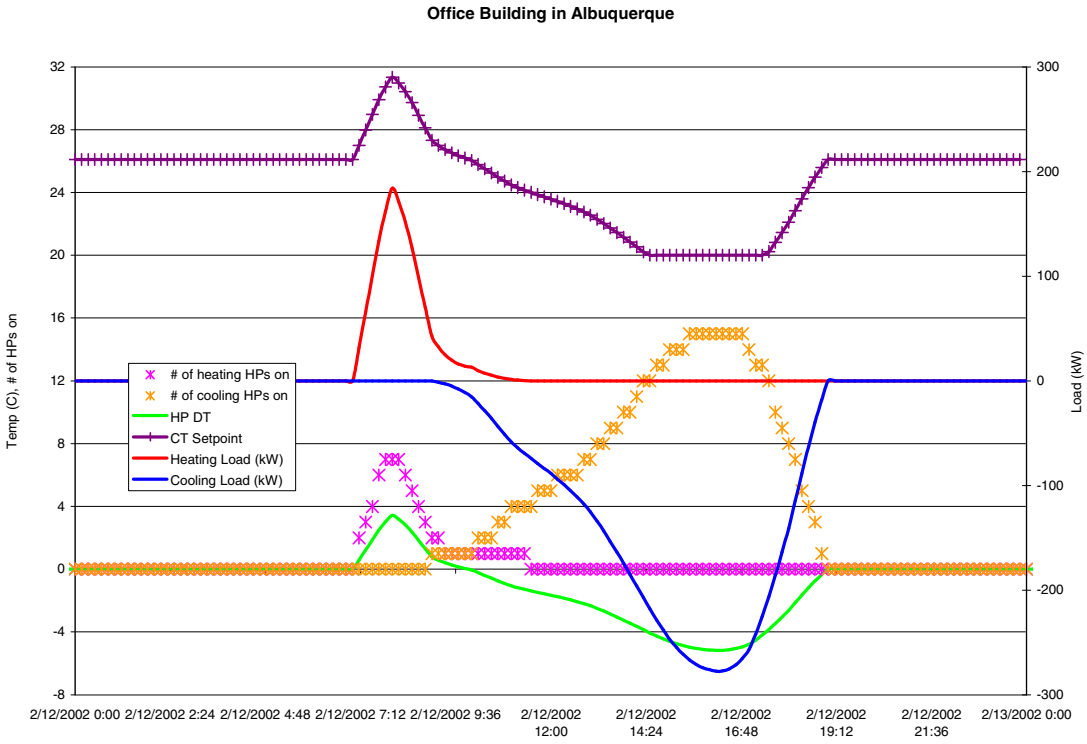

Figure 6.3 *Plot of loads, operating heat pumps, and cooling tower setpoint for an office building in Albuquerque, NM, on February 12.*

As can be seen below in Figure 6.4, the boiler controls are similar to those described earlier for the cooling tower operation. The boiler controls determine the temperature difference across the heat pumps and determine through the equation of the setpoint line (shown in red) what the operating setpoint is at that temperature difference. Once the heat pump entering fluid temperature falls below the setpoint, the boiler begins operation and will continue operation until the heat pump entering fluid temperature rises above the dead band (shown in green). As will be discussed below, the system energy consumption was not significantly improved by allowing the boiler setpoint to change dynamically, so a constant setpoint was used.

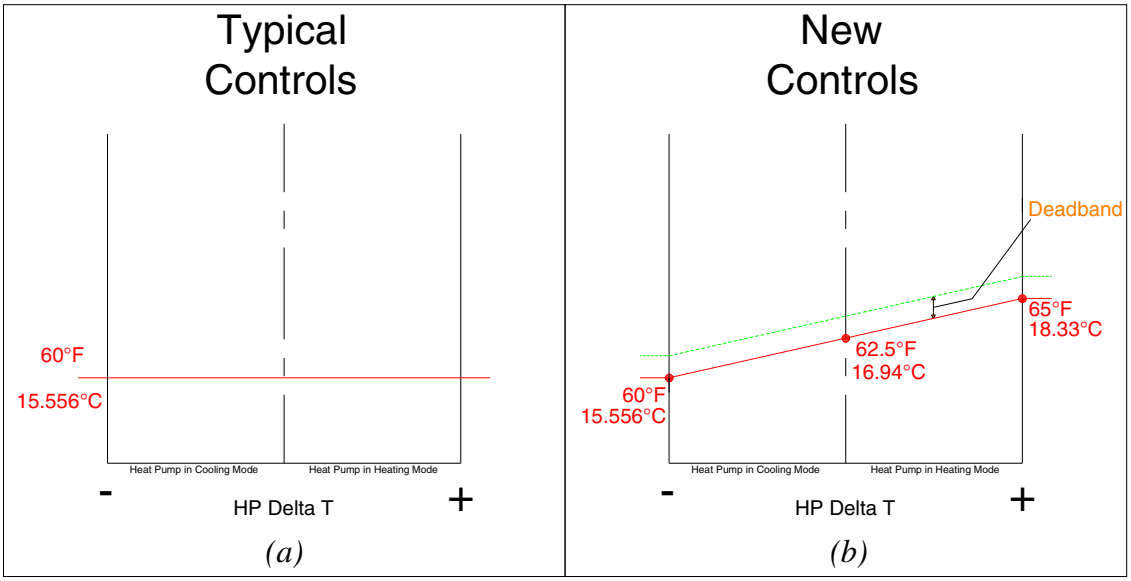

Figure 6.4 *Boiler controls schematic.*

6.3. Methodology

The approach taken in this investigation was to first formulate a new control strategy, then to optimize its setpoints for the two building types in 13 U.S. locations. This gives an indication of the potential energy savings of the strategy under the best-case scenario where setpoints were custom optimized. Finally, engineering judgment is used to determine a control strategy that can be used by various building types in different climate regions. This control strategy is dubbed the "common control".

The remainder of this section covers the methodology used to optimize the setpoints for a particular building type and location. There are four main components of the optimization methodology. The four main components are listed below.

1. HVACSim+
2. Buffer Program
3. GenOpt (Generic Optimization Program)
4. Batch File

The four work together as shown below in the flow diagram in Figure 6.5. Each of the four main optimization components will be discussed in more detail in the following sections.

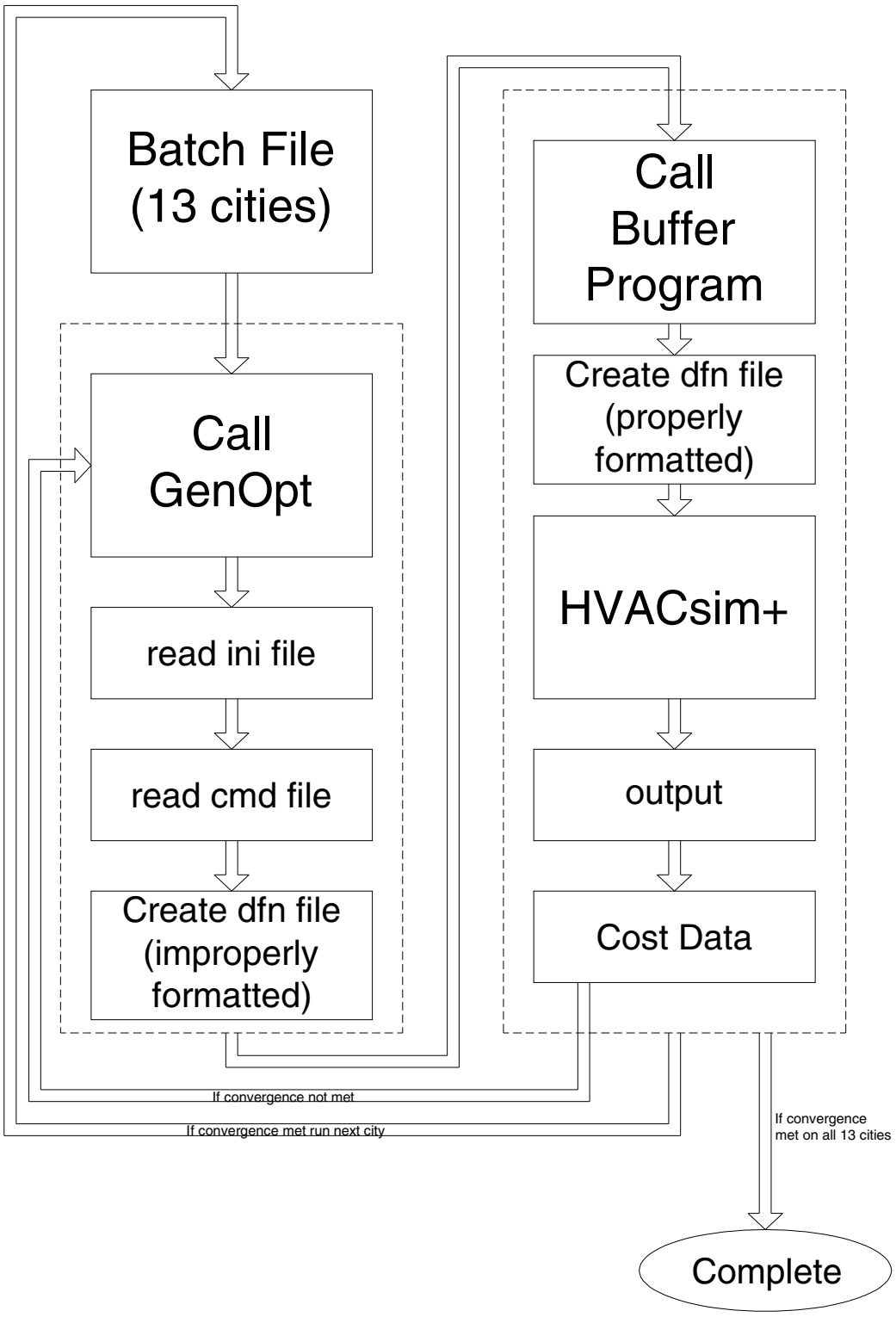

Figure 6.5 *Optimization methodology flow diagram.*

6.3.1. HVACSim+

The HVACSim+ WLHP system model is comprised of seven different component models that are connected together to form a WLHP system. The component models are listed below along with the section number where more detailed information can be found on each model.

1. Heat Pump Model – Section 4.2.1.
2. Cooling Tower & Cooling Tower Controller Model – Section 4.2.2.
3. Plate Heat Exchanger Model – Section 4.2.3.
4. Variable Speed Pump Model – Section 4.2.4.1.
5. Constant Speed Pump Model – Section 4.2.4.2.
6. Boiler & Boiler Controller Model – Section 4.2.5.
7. Common Pipe Model – Section 4.2.6.

The HVACSim+ model was formed from the WLHP schematic that is shown below in Figure 6.6, and is discussed in more detail in Chapter 4. For this study, all simulations were run on a four-minute time step. More detailed information regarding model parameters and equipment specifications used for the WLHP system simulation for the office building and motel can be found in Appendix B.

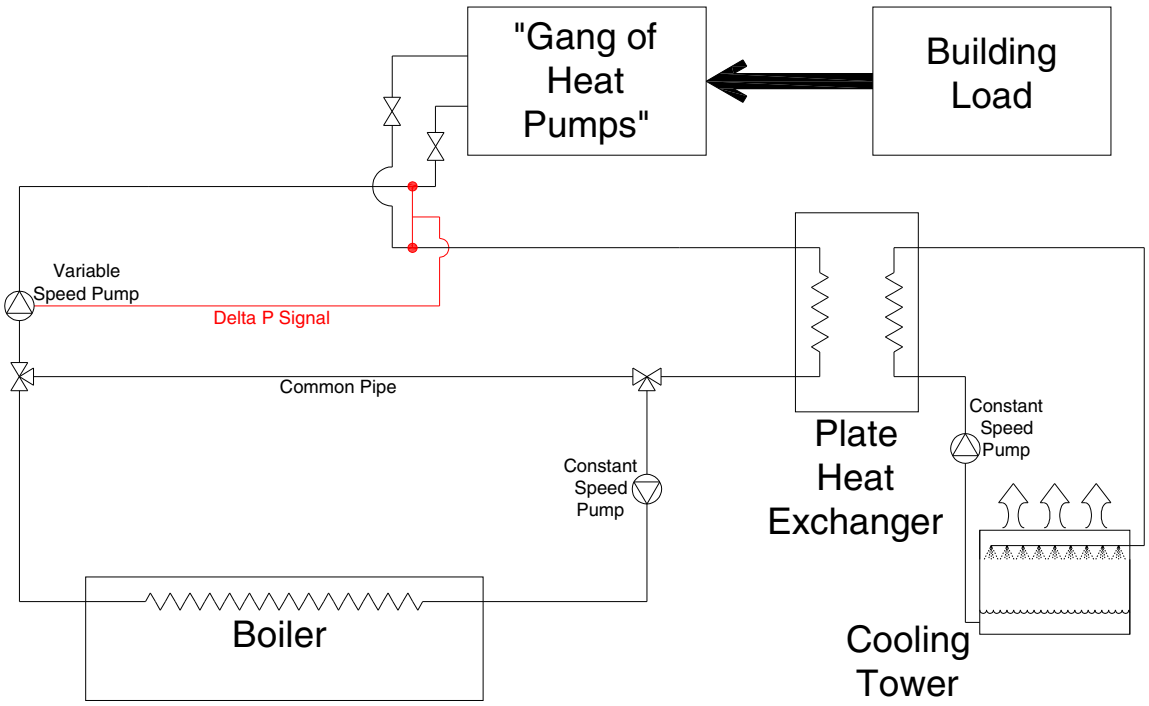

Figure 6.6 *WLHP system schematic.*

In order to perform a simulation for a specific building, location, and set of parameters (e.g. setpoints), HVACSim+ needs three files:

1. Input file, which specifies the names of the boundary file and definition file.
2. The boundary file, which contains site-specific weather data and building site-specific heating and cooling loads.
3. The definition file (dfn) which describes the system configuration and parameter site-specific parameter values.

The input file and boundary file are files created in advance for each building and location combination and need no changes during the optimization. The dfn file is provided by the buffer program discussed in the next section.

6.3.2. Buffer Program

The buffer program serves three purposes. First, it takes the dfn file created by GenOpt, which is not properly formatted and cannot be directly read by HVACSim+, and formats it to where it can be used by HVACSim+. Second, it executes HVACSim+. Finally, since the objective function is only concerned with annual energy costs and not energy costs on a time step basis, the buffer program also reads from the output file created by HVACSim+, computes the annual HVAC energy consumption (heat pump energy, variable speed pump energy, boiler energy, boiler pump energy, cooling tower, and cooling tower pump energy) and annual energy cost based on a given cost per unit of energy. For this study, a cost of $0.08/kW-hr was used. The annual energy cost is the objective function minimized by GenOpt. The buffer program takes this objective function value and writes it to a file which is then read by GenOpt in order to determine the next set of control parameters if the optimization has not converged.

6.3.3. GenOpt

GenOpt (Wetter 2000, Wetter 2004) was used to optimize the control strategy for each location and building type. GenOpt is a generic optimization program that minimizes an objective function by varying desired parameters. The number of parameters used for this study was dependent upon which control strategy was being optimized. In order to perform an optimization for a specific building, location, and set of parameters (e.g. setpoints), GenOpt needs the following files:

1. Initialization file with directory locations for the GenOpt program and files needed to run the simulation in HVACSim+.
2. Command file with parameters that are to be optimized, their initial values, upper and lower limits, and the optimization procedure that will be used for the optimization.
3. Configuration file containing specification for how the simulation program is started.
4. Simulation input template file (specifically for this work the dfn file which is used to create the actual input file used by the simulation program) with the location of the parameters that are to be optimized in the HVACSim+ dfn file.

GenOpt automatically writes an improperly formatted definition (dfn) file for HVACSim+ based on a template dfn file and initial settings. GenOpt then calls the buffer program, described above, which creates a properly formatted dfn file, runs HVACSim+, and writes the annual energy into a file that is read by GenOpt. GenOpt checks the value of the objective function being considered and writes a new input file based on new parameters determined by its optimization algorithm. This process is repeated until the minimum objective function is found.

Two optimization algorithms were used for this work with several re-starts. The optimizations were executed with both the Nelder Mead Simplex algorithm and particle swarm optimization. Optimizations were run with different initial settings in an effort to

find the global minimum. Once the minimum objective function was found with one set of initial settings, a re-start optimization was performed, using the optimized parameters from the last optimization as one of the new initial guesses. It should be noted that with the different algorithms used and the re-starts it is still possible that a local minimum was found instead of the global minimum and therefore, in some cases, actual energy savings might be higher than those presented below.

6.3.4. Batch File

As discussed in Chapter 4, DesignBuilder was used to calculate building loads for two prototypical buildings, an office and a motel, in 13 different cities. These were described in more detail in Sections 4.4.2.1. and 4.4.2.2. The 13 cities are listed in Section 4.4.3. along with a map (Figure 4.24) showing the location of each city.

With the need to test and optimize two buildings in 13 cities, it was beneficial to create a simple batch file that would allow the user to optimize multiple locations without the need to manually change locations after the completion of one. The batch file internally calls the input file for a particular building and location and renames it to a generic name (INPUTFILE.DAT) needed to run in GenOpt. It then internally copies the dfn file for that building and location and renames it to a generic name (JASON.dfn) needed to run in GenOpt. The batch file then executes GenOpt. Finally, the generic output files are renamed with building and location specific names. This is done for the two building types and the 13 cities.

6.4. Results

As the base case, the commonly accepted control strategy of operating the cooling tower and boiler to maintain heat pump entering fluid temperature between 60ºF and 90ºF (15.56 – 32.22ºC), shown in Figure 6.7 was used in determining annual energy consumption and cost for each of the 13 cities and both building types.

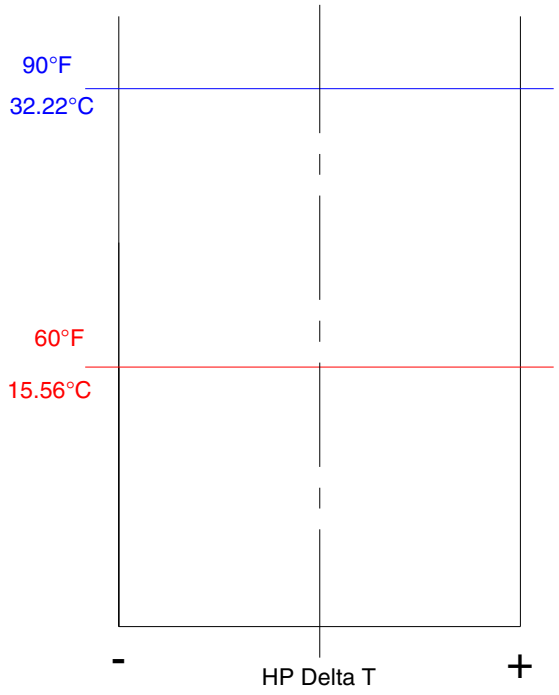

Figure 6.7 *Baseline control strategy.*

The results found using this control strategy will be used as the point of comparison for each of the new control strategies described below. It should be noted that all simulations were ran with different cooling tower and boiler sizes for each building and location. A table showing cooling tower and boiler sizes can be found in Appendix B.

6.4.1. 2-Parameter Case

The first control strategy optimized was the 2-parameter case. The control strategy used is the same strategy as the baseline case where the equipment is controlled on or off based on two setpoints regardless of the temperature difference across the heat pumps. With the initial points of the optimization set as the baseline case, each of the 13 cities with both building types were optimized using GenOpt to determine the optimum value of the two setpoints. The two setpoints were both allowed to be varied as shown in Figure 6.8 below. No restrictions were placed on the temperature difference between the two setpoints. However, a dead band of 1ºC was used with both setpoints. E.g. if the optimized value of the cooling tower setpoint is 32.2ºC (90ºF), the cooling tower will come on when the heat pump entering fluid temperature reaches 32.2ºC (90ºF) and go off at 31.2ºC (88.2ºF). If the optimized value of the boiler setpoint is 15.6ºC (60ºF), the boiler will come on at 15.6ºC (60ºF) and go off at 16.6ºC (61.9ºF).

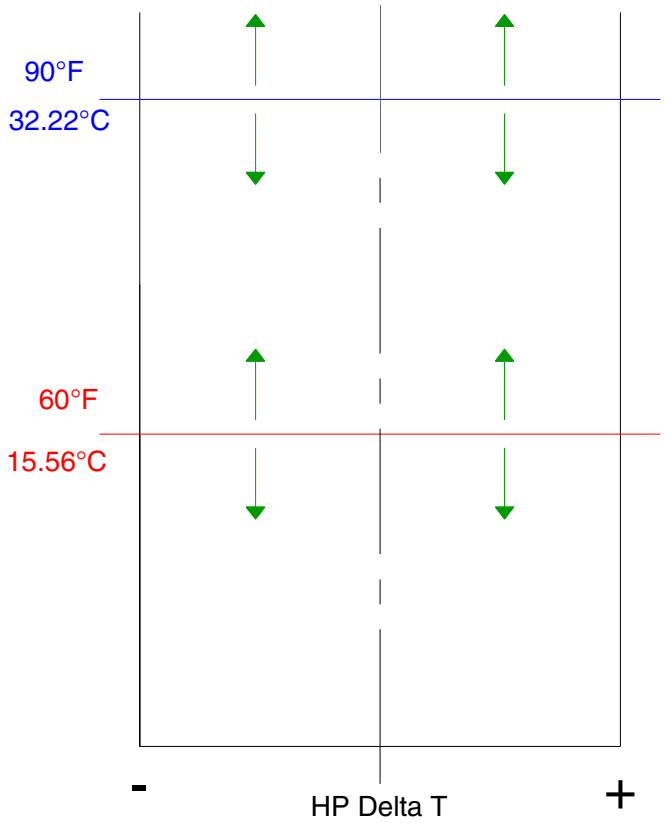

Figure 6.8 *2-parameter control strategy.*

The optimized 2-parameter setpoints and the annual HVAC energy savings over the base case are given below in Table 6.1.

Table 6.1 *2-parameter setpoints and HVAC energy savings.*

		Cooling Tower Setpoint (ºC)	Cooling Tower Setpoint (ºF)	Boiler Setpoint (ºC)	Boiler Setpoint (ºF)	Annual HVAC Energy Savings
Motel Setpoints	Albuquerque	18.2	64.8	2.0	35.6	16.7%
	Baltimore	21.7	71.0	5.1	41.2	7.5%
	Boise	17.9	64.2	5.3	41.5	10.6%
	Burlington	21.2	70.2	6.4	43.6	4.7%
	Chicago	22.2	71.9	5.1	41.2	5.4%
	Duluth	20.3	68.6	3.8	38.9	2.8%
	El Paso	18.0	64.4	8.6	47.4	18.0%
	Fairbanks	18.2	64.8	2.0	35.6	1.5%
	Houston	23.1	73.6	4.5	40.0	8.1%
	Memphis	22.7	72.9	5.2	41.4	9.0%
	Miami	24.0	75.3	4.3	39.7	7.9%
	Phoenix	17.5	63.5	3.0	37.4	18.2%
	Tulsa	21.5	70.7	5.8	42.4	8.2%
Office Setpoints	Albuquerque	20.5	69.0	2.3	36.1	11.9%
	Baltimore	25.4	77.8	2.0	35.6	5.0%
	Boise	20.9	69.7	2.0	35.6	8.4%
	Burlington	23.3	74.0	2.0	35.7	2.8%
	Chicago	24.0	75.1	2.2	36.0	4.2%
	Duluth	24.8	76.6	2.0	35.6	1.9%
	El Paso	21.5	70.7	16.8	62.2	12.4%
	Fairbanks	20.3	68.5	2.1	35.8	1.0%
	Houston	26.7	80.0	2.8	37.0	4.6%
	Memphis	25.7	78.3	2.0	35.7	4.9%
	Miami	26.6	79.9	6.3	43.3	4.2%
	Phoenix	23.0	73.4	2.7	36.8	11.4%
	Tulsa	26.4	79.5	2.7	36.8	4.0%

As can be seen by the savings for each building and location, the highest potential for savings comes in warm or hot, dry climate regions. Presumably, this is due to the combination of high cooling loads and low wet-bulb temperatures that allow lower heat pump entering fluid temperatures and better heat pump cooling performance. The 2-

parameter results also show very little potential in colder climates, especially in Fairbanks and Duluth.

The cooling tower setpoints range from 17.5ºC (63.5ºF) to 26.7ºC (80.0ºF) with the higher setpoints coming in warmer, humid regions. On average the cooling tower setpoints are higher for the office building and the potential savings are higher in the motel. As load profiles vary with every location, it is difficult to give a general reason for this trend. However, the office building generally has higher peak cooling loads relative to the average cooling loads, and hence, a relatively larger cooling tower if compared to the average cooling load. So it is possible that the extra energy required to run the cooling tower discourages additional usage of the tower. This is further complicated by the fact that the cooling tower does not always reach the setpoint, so at many hours two different setpoints might give the same heat pump entering fluid temperature.

The boiler setpoints range from 2.0ºC (35.6ºF) to 8.6ºC (47.4ºF) with many of the setpoints, especially for the office building, in the 2.0ºC (35.6ºF) range. On average the boiler setpoints are higher for the motel. The low boiler setpoints could be dangerously close to freezing and may need to be increased. This will be addressed below. It should also be noted that reduced heat pump entering fluid temperatures will have a direct impact on heat pump capacity. For this work the heat pump was designed to always meet the load. This was checked in cold climate regions and verified that the load was being met at low boiler setpoints.

6.4.2. 11-Parameter Case (10 CT Parameters, 1 Boiler Parameter)

The next control strategy optimized was the 11-parameter case. After some preliminary investigation into control strategies, it was found that most of the savings potential with a control strategy came from the cooling tower controls and not the boiler controls. Therefore, only a single boiler setpoint over all HP ΔT was optimized. A schematic of this control strategy can be seen below in Figure 6.9. As can be seen from the figure, five points were used to define the cooling tower setpoint profile, requiring ten parameters. The number of points could vary, but five were originally used to investigate whether the optimal setpoint profile would be curvilinear or linear. The left and right end points were optimized; beyond the end points, the cooling tower setpoint did not change.

It should be noted that, the more parameters, the more computer time is required to perform optimizations. For example with a 2.48GHz, dual core AMD processor the 2-parameter cases took an average of 33 minutes to optimize with the minimum taking 17 minutes and the maximum 70 minutes. The 11-parameter cases took an average of 230 minutes with a minimum time of 67 minutes and a maximum of 719 minutes. The 12-parameter cases (11-parameter with wet-bulb described in Section 6.4.5.) took an average of 235 minutes with a minimum time of 93 minutes and a maximum of 750 minutes.

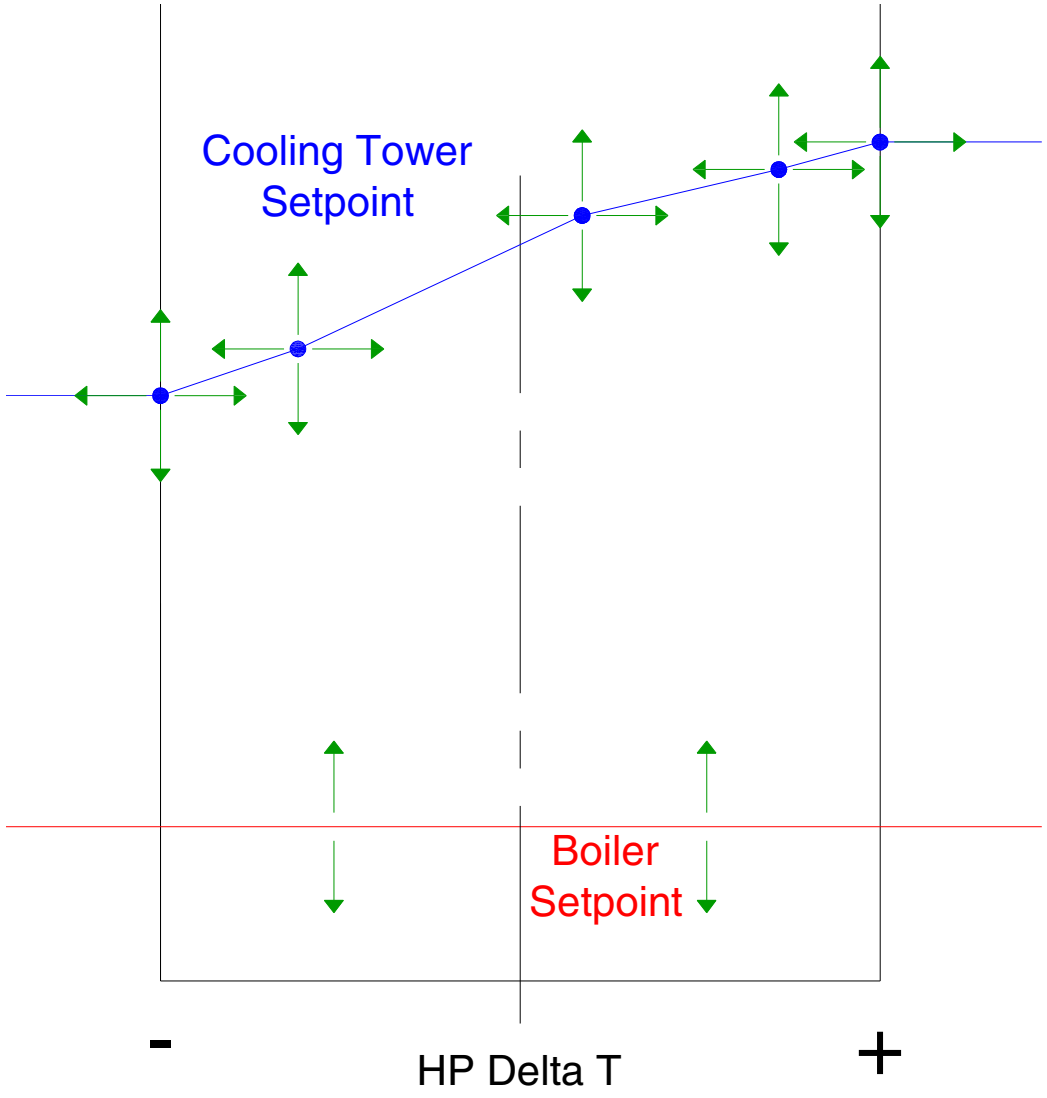

Figure 6.9 *11-parameter control strategy.*

The optimized cooling tower setpoints for the 11-parameter case can be seen below in Figure 6.10 ((*a*)-motel parameters, (*b*)-office building parameters). The optimized cooling tower setpoints for the 11-parameter case are given in tabular form in Appendix C.

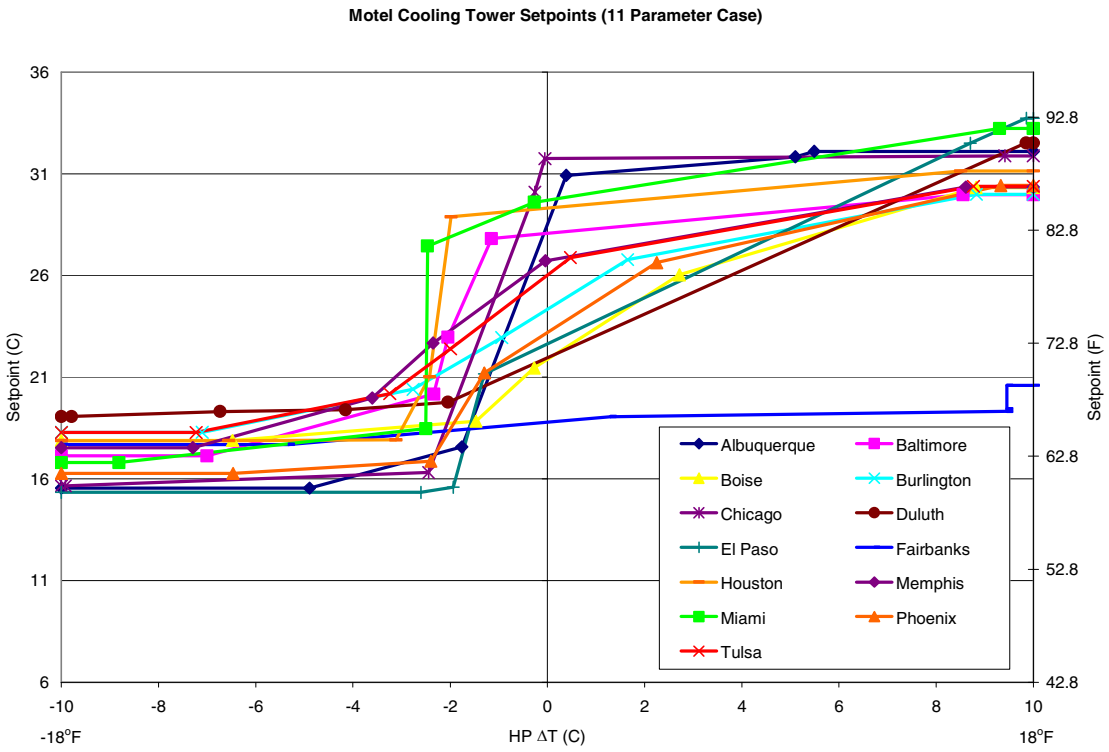

(a) Motel.

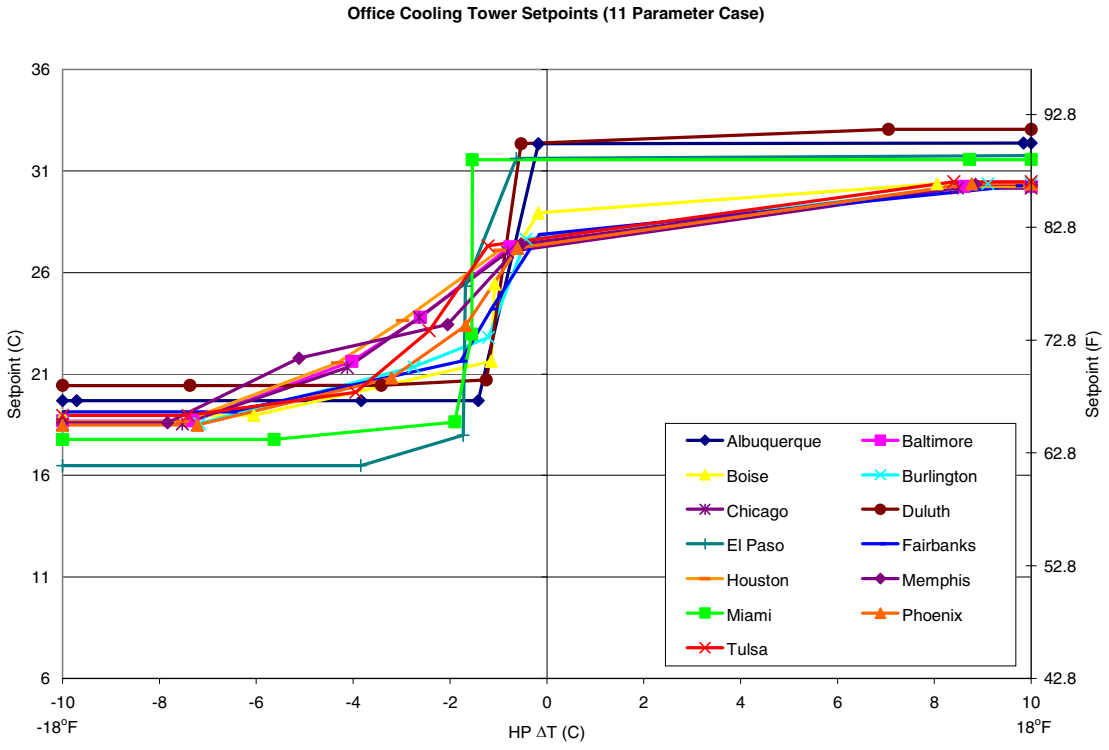

(b) Office building.

6.10 *Optimized 11-parameter cooling tower setpoint profiles.*

The annual HVAC savings are shown below in graphical form showing annual HVAC savings compared to the base case results. Figure 6.11 shows results for the motel (*a*) and office building (*b*) for Albuquerque, Baltimore, Boise, Burlington, Chicago, Duluth, and El Paso. Figure 6.12 shows results for the motel (*a*) and office building (*b*) for Fairbanks, Houston, Memphis, Miami, Phoenix, and Tulsa. The figures show percent savings of annual HVAC costs for the optimized 2-parameter case discussed above in Section 6.4.1 as well as the optimized 11-parameter case.

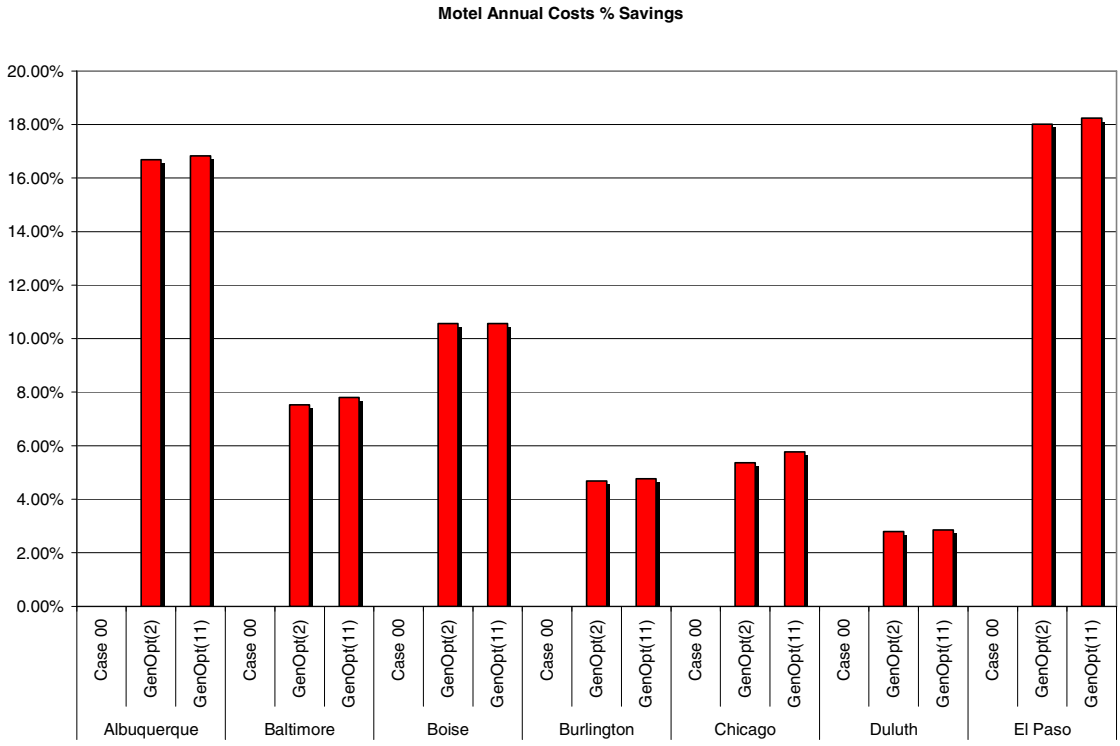

(a) *Motel.*

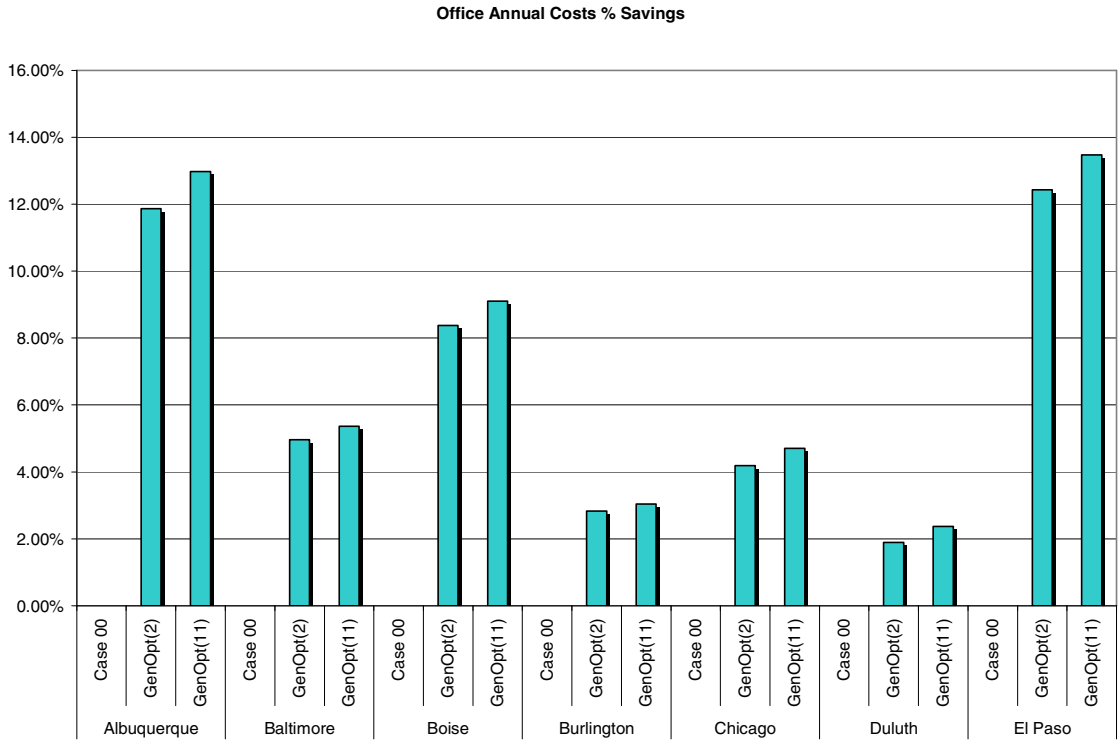

(b) *Office building.*

Figure 6.11 *Annual savings per control strategy (2-parameter and 11-parameter).*

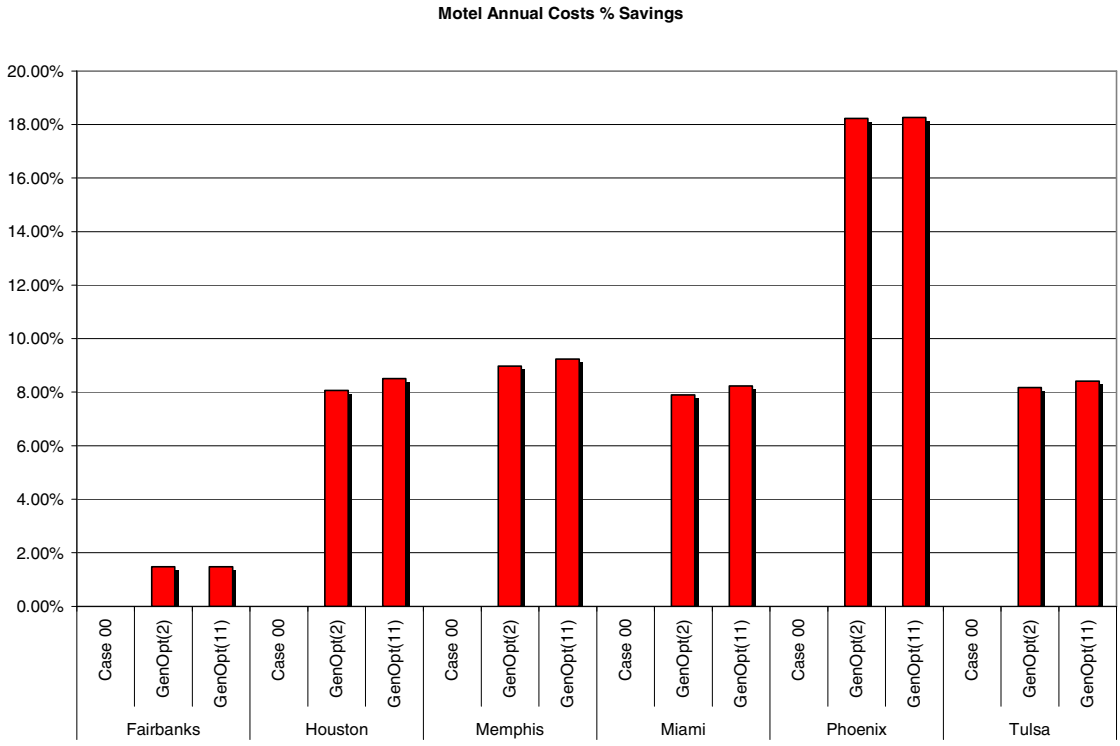

(a) *Motel.*

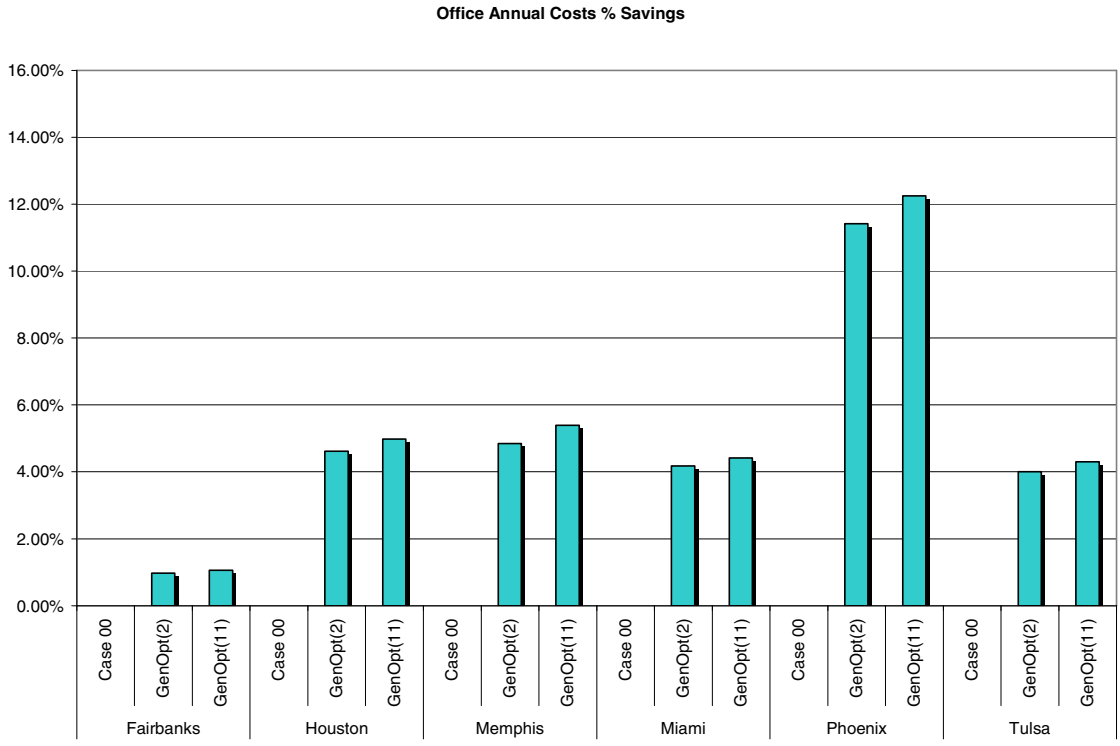

(b) *Office building.*

Figure 6.12 *Annual savings per control strategy (2-parameter and 11-parameter).*

As can be seen by the optimized 11-parameter savings for each building and location, there is not a large increase in savings compared to the optimized 2-parameter cases. The highest increase comes from the office building in Albuquerque with a 1.11% increase in savings potential. Most of the locations show less than 1% increase in savings potential over the optimized 2-parameter results. There are at least two explanations as to why the optimized 11-parameter control strategy only gives a small improvement over the optimized 2-parameter control strategy. First, as much of the cooling load occurs at relatively high heat pump ΔTs (see Figure 6.1) the far left hand portion of the cooling tower setpoint control profiles ($\Delta T < -4$ºC) shown in Figure 6.10 is the most important portion. With a few exceptions for more heating-dominated cases, the setpoint is constant or near-constant in this region. Comparing these values to the optimized 2-parameter setpoints, it can be seen that the 11-parameter setpoint is generally 1-5ºC lower than the 2-parameter setpoint. This difference is fairly small; near these setpoints, the heat pumps will experience about 0.1% power reduction per 1ºC of reduction in the entering fluid temperature. The resulting savings in this region of operation, plus savings in other regions might account for more than the savings realized. However, as will be shown later in the chapter, on high cooling load days, either setpoint may not be realized, in which case the cooling tower will run continuously, regardless of which control strategy is selected. This is a side effect of having sized the tower based on standard conditions of 35ºC (95ºF) cooling tower entering fluid temperature, 29.4ºC (85ºF) cooling tower exiting fluid temperature, and 23.9ºC (75ºF) outdoor wet-bulb temperature.

More detailed results of the savings for each case by city can be found in Appendix D. The table in Appendix D gives a breakdown of the HVAC energy consumption by component. It lists the total annual savings for each case, and the annual cost comparison for each case based on $0.08/kW-hr.

6.4.3. 2-Parameter Common Control

Each of the control strategies discussed above (2-parameter and 11-parameter) were specifically optimized for each building and location separately. This would be beneficial for that city and building type, but this does not necessarily give a good recommendation for other buildings in the same location or similar buildings in different locations. Therefore, in an effort to find a control strategy that could be used more widely, a "common" control strategy was investigated. This investigation was done heuristically, looking for setpoints that would work well for both building types and a range of locations.

In the first attempt at developing a 2-parameter common control the cooling tower setpoints were averaged for the 26 cases (2 building types and 13 locations) and the boiler setpoints were averaged for the 26 cases. The setpoints chosen for the 2-parameter common control are shown below in Table 6.2. Energy savings for these setpoints and other variations in this section are shown in Figures 6.13 and 6.14. Savings for this first attempt are labeled "common control (2)a."

Table 6.2 *2-parameter common control setpoints (a).*

Cooling Tower Setpoint (ºC)	Cooling Tower Setpoint (ºF)	Boiler Setpoint (ºC)	Boiler Setpoint (ºF)
22.1	71.9	4.2	39.6

It was found that this did not give good results for the warm and hot humid locations, especially with the office building. In Miami these setpoints result in higher energy consumption than the base case, and for the office building in Houston, Memphis, and Tulsa the savings are very small. This is most likely due to the lower cooling tower setpoint that is used by the common control vs. the optimized 2-parameter setpoint for each of the four cities listed above (e.g. for the office building in Houston, the optimum cooling tower setpoint is 26.7ºC (80ºF) while the common control cooling tower setpoint is 22.1ºC (71.8ºF)). The 2-parameter common control setpoint is so much lower for the humid locations that the cooling tower runs so much that the increased energy needed to run the cooling tower exceeds that energy saved by the heat pump. Therefore, the locations were divided into two groups as shown below in Table 6.3 and two new sets of 2-parameter common control setpoints were calculated and are shown in Table 6.4. The groups were subjectively divided based on the results obtained from the "common control (2)a" although they can be divided based on climate regions as shown in the table. The resulting energy savings are labeled "common control (2)b" in Figures 6.13 and 6.14.

Table 6.3 *Cities divided into two groups.*

Group A – Climate Zones 1-3 Humid	
• Houston, Texas • Memphis, Tennessee	• Miami, Florida • Tulsa, Oklahoma
Group B – Climate Zones 4-8 and 1-3 Dry	
• Albuquerque, New Mexico • Baltimore, Maryland • Boise, Idaho • Burlington, Vermont • Chicago, Illinois	• Duluth, Minnesota • El Paso, Texas • Fairbanks, Alaska • Phoenix, Arizona

Table 6.4 *2-parameter common control setpoints (b).*

Cooling Tower Setpoint (°C)	Cooling Tower Setpoint (°F)	Boiler Setpoint (°C)	Boiler Setpoint (°F)
Group A			
24.6	76.3	4.2	39.5
Group B			
21.1	69.9	3.4	38.1

There are some locations that perform worse than the common control (2)a results, but all locations now show positive savings, although some show very little, signifying that this is still not a good common control. Other climatic divisions might be investigated further, but time precluded this from being done. The common control (2)b was chosen as the best out of the two. Still there is the problem with the boiler setpoint being too close to freezing range. Therefore, another set of simulations were run with the

cooling tower setpoints from Table 6.4 being used with a boiler setpoint of 10ºC (50ºF). The resulting energy savings are labeled "common control (2)c" in Figures 6.13 and 6.14.

The results for all of these strategies are shown below in Figures 6.13 and 6.14. The figures show percent savings of annual HVAC costs for the 2-parameter case discussed above in Section 6.4.1, the 11-parameter case discussed in Section 6.4.2, the 2-parameter common control for both buildings and all locations (Common Control (2)a), the 2-parameter common controls for the two climate regions (Common Control (2)b), and the 2-parameter common controls for the two climate regions with a 10ºC (50ºF) boiler setpoint (Common Control (2)c).

As can be seen by the first set of common control strategy results (Common Control (2)a) there are cases where there are negative savings. This is due to the cooling tower setpoint being so low that the system exceeded the point of diminishing returns and ran the cooling tower more than the optimum amount. The results for the two sets of common controls (Common Control (2)b) show positive savings for each location, but they are sometimes minimal (e.g. the office building in Baltimore and Houston). The final attempt at a 2-parameter common control with the boiler setpoint set to 10ºC (50ºF) (Common Control (2)c) did not show much difference from the previous results (Common Control (2)b) except for the office building in Baltimore the savings go slightly negative. With many locations there was a slight increase in energy consumption.

The system, with an electric boiler, is configured such that the boiler setpoint does not affect the steady state heating performance of the system. All heating energy comes from electricity provided to the boiler or the heat pump compressors. Furthermore, even in steady state mixed operation, when heating dominates and the boiler is running, the system performance is constant, regardless of the boiler setpoint. Therefore, this slight increase in energy consumption with increased boiler setpoint must be due to transient operation. When the system moves from a large cooling load to a small heating load, the amount of heat rejected in cooling mode that can then be recovered in heating mode will decrease as the boiler setpoint is increased. Likewise, when the system transitions from heating mode to cooling mode, the loop will start at a higher temperature (with an increased boiler setpoint) and cooling COP will be adversely affected. The smaller the thermal mass in the system, the less effect the boiler setpoint temperature will have on system performance. With the relatively small amount of thermal mass present in this simulation, the boiler setpoint has a small effect.

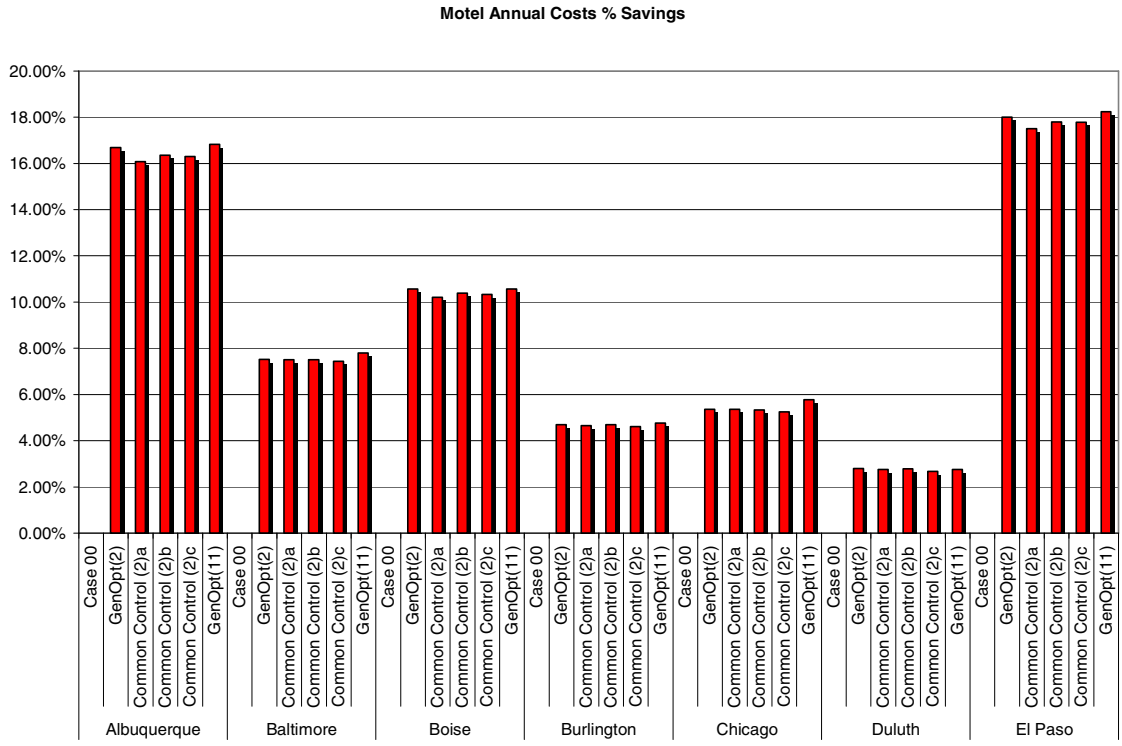

(a) *Motel.*

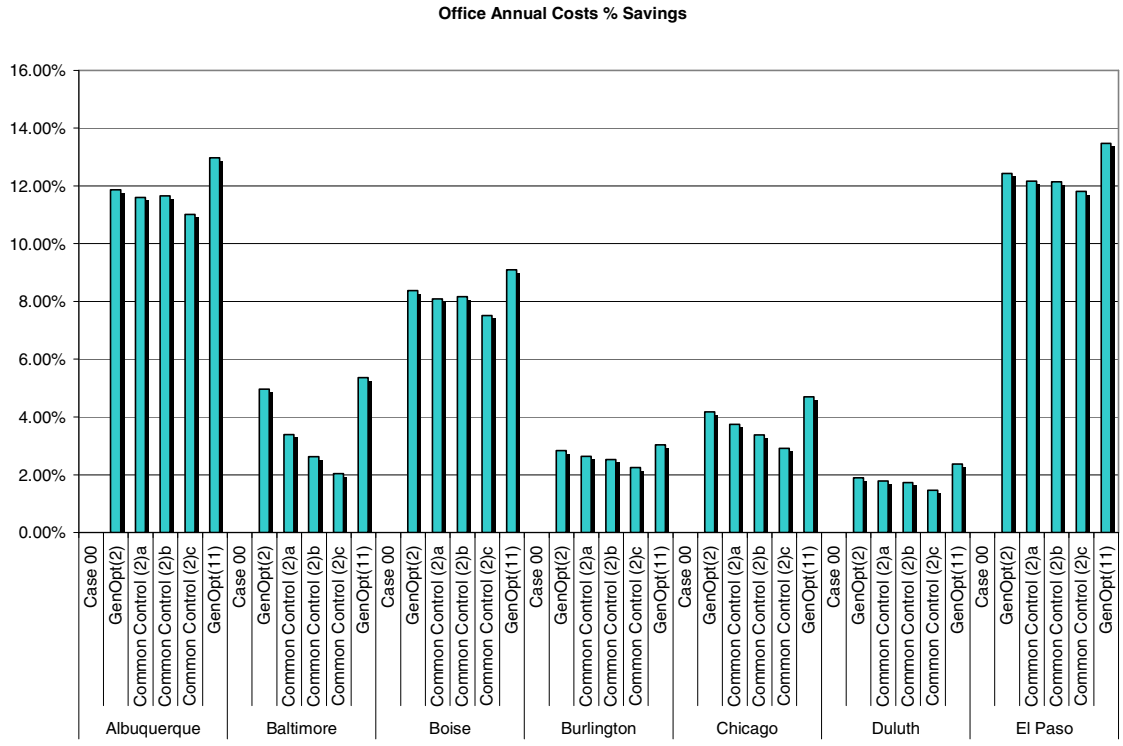

(b) *Office building.*

Figure 6.13 *Annual savings per control strategy (2-parameter common control).*

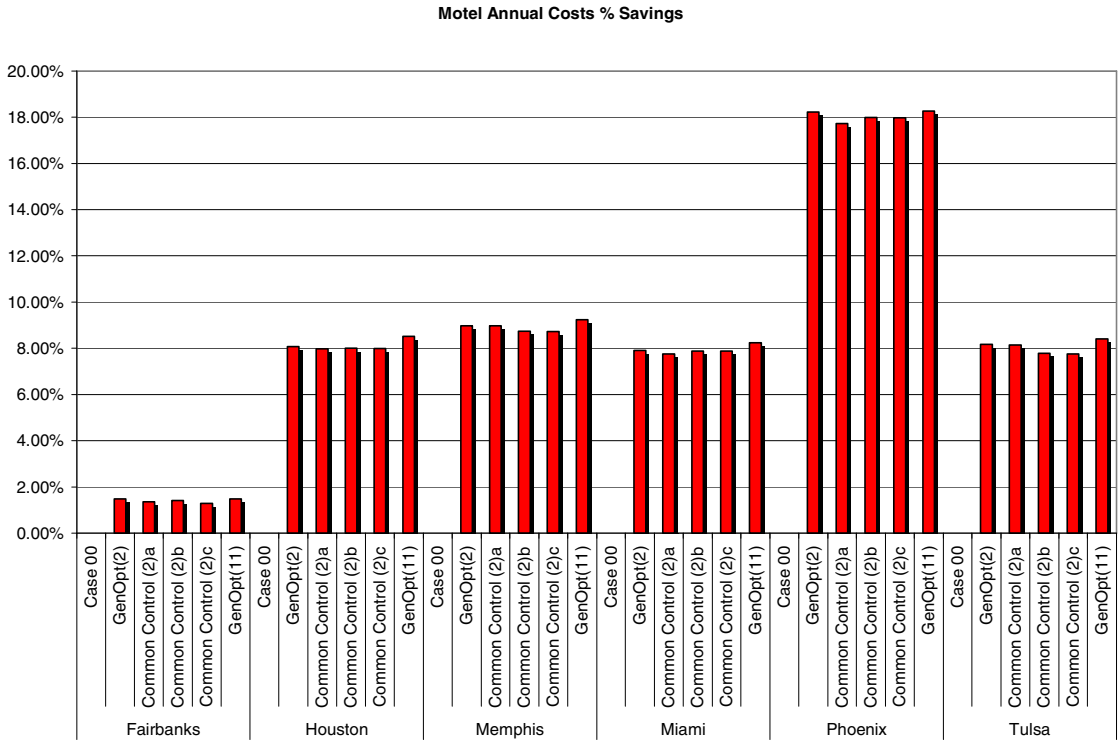

(a) *Motel.*

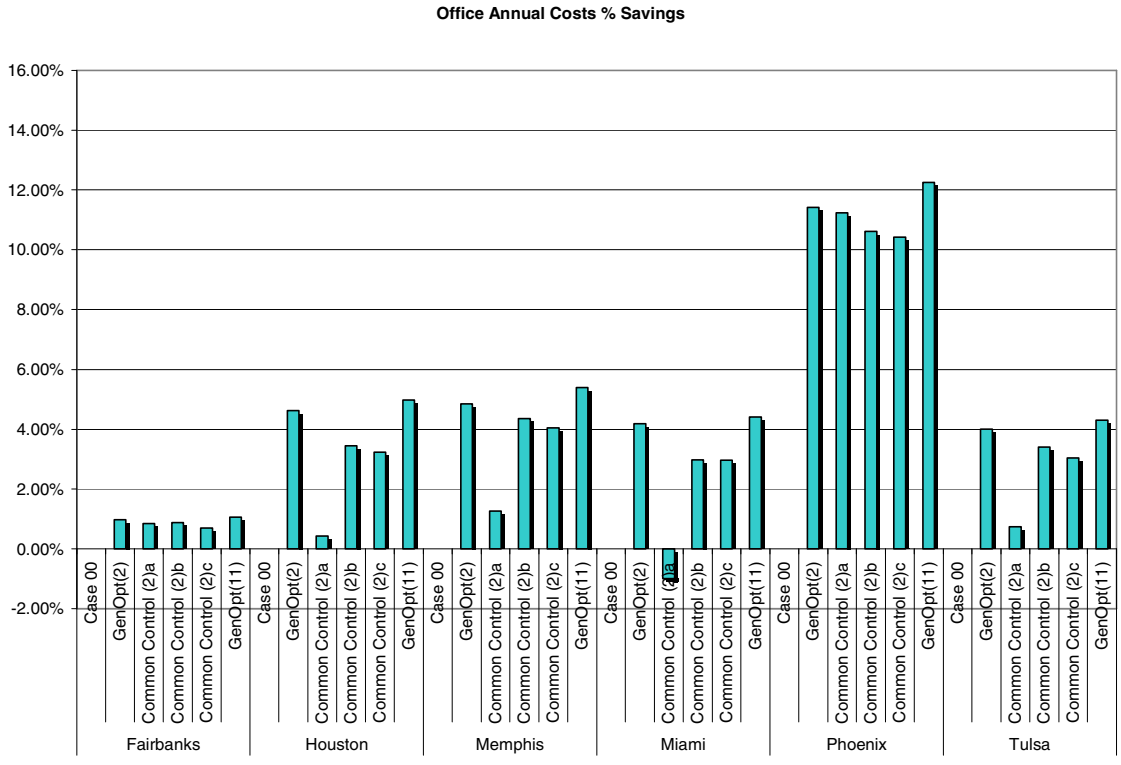

(b) *Office building.*

Figure 6.14 *Annual savings per control strategy (2-parameter common control).*

With the 2-parameter common control strategies completed there does not appear to be a good 2-parameter common control that can be used for multiple locations. It may be possible to achieve better results, on average, if the locations were divided into more regional climate zones. Time precluded the further investigation into more regional specific strategies.

More detailed results of the savings for each case by building type and city can be found in Appendix D.

6.4.4. 7-Parameter Common Control (6 CT Parameters, 1 Boiler Parameter)

As discussed above, a good 2-parameter common control was not found during the time of this work. Therefore, in an effort to find a dynamic control strategy that could be used by a larger area of the country, a dynamic common control strategy was developed based on the results from the 11-parameter optimized cases.

When investigating the 7-parameter common control strategy, two things were considered. First, the setpoint profiles for each building and location were reviewed to try and find similarities. Second, the heat pump ΔT histograms were reviewed for relative importance of heating vs. cooling. After examining the setpoint profiles and the ΔT histograms, there appeared to be some distinction between optimized setpoints for more temperate/warmer climate regions and colder climate regions, or locations that

required the most heating. Therefore, the thirteen cities were divided up into two groups as shown below in Table 6.5.

Although Boise, Idaho and Chicago, Illinois are both in climate zone 5, Boise is a dry climate and has significantly lower heating loads than Chicago. Presumably, with the dry climate, Boise has more sunshine during the winter and this results in lower heating loads. In any case, the climate regions are divided such that 5A (cold, moist) falls in with the colder climates and 5B (cold, dry) is grouped with the warmer climates.

Table 6.5 *Cities divided into climate regions.*

Climate Zones 1-4 and 5B	
• Albuquerque, New Mexico • Baltimore, Maryland • Boise, Idaho – 5B Cool-Dry • El Paso, Texas • Houston, Texas	• Memphis, Tennessee • Miami, Florida • Phoenix, Arizona • Tulsa, Oklahoma
Climate Zones 6-8 and 5A	
• Burlington, Vermont • Chicago, Illinois – 5A Cool-Humid	• Duluth, Minnesota • Fairbanks, Alaska

One setpoint profile was found for the heating dominated regions and one setpoint profile was found for the cooling dominated regions. For the first attempt at a common control strategy, the nine cooling dominated setpoints from both building types were

averaged to give one setpoint line with 10 parameters. Likewise, the four heating dominated setpoints from both building types were averaged to give one setpoint line with 10 parameters. Then, in an effort to make the setpoint profiles for each as simple as possible, engineering judgment was used to approximate the two profiles with six parameters instead of ten. It was found that as the heat pump temperature difference increases, the two control strategies, heating dominated and cooling dominated, were very similar. The largest difference was how low the setpoint would fall as the heat pump temperature difference became more negative. Therefore, to further simplify the control strategies they were made the same except for how low the setpoint would fall. The 7-parameter common control cooling tower setpoints can be seen below in Figure 6.15 and are shown in tabular form in Table 6.6.

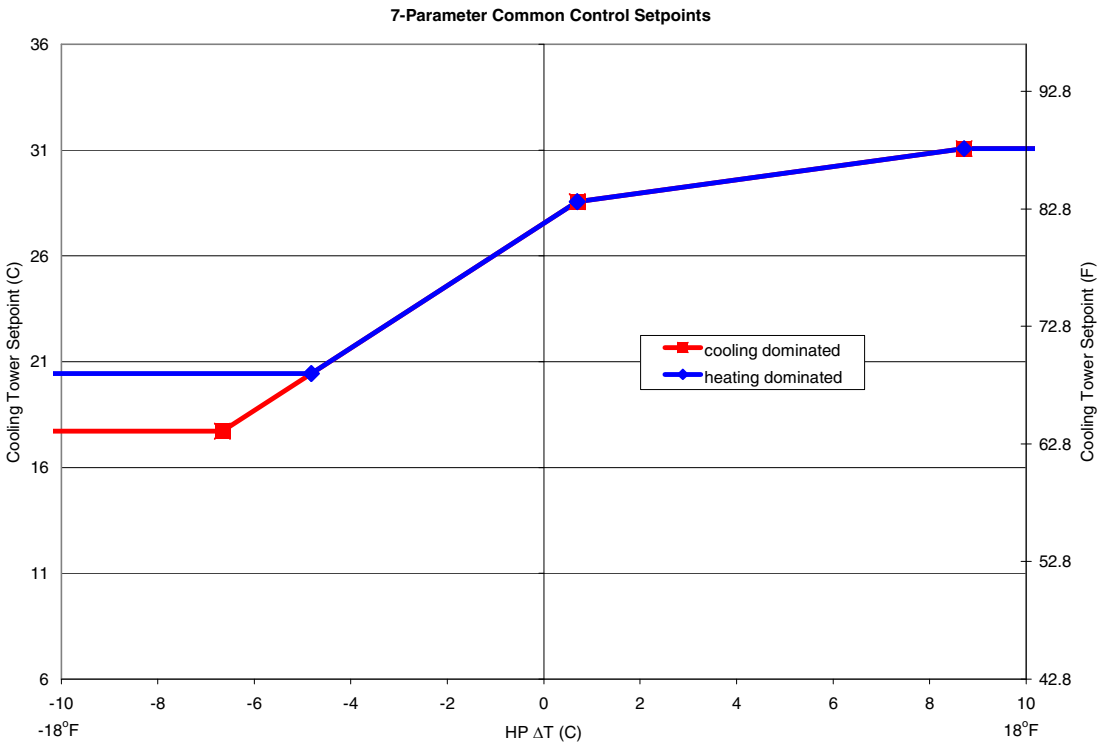

Figure 6.15 *7-parameter common control cooling tower setpoint profiles.*

Table 6.6 *7-parameter common control cooling tower parameters.*

	ΔT-1	Setpoint-1	ΔT-2	Setpoint-2	ΔT-3	Setpoint-3
Cooling Dominated Parameters (ºC)	-6.7	17.7	0.7	28.5	8.7	31.1
Heating Dominated Parameters (ºC)	-4.8	20.4	0.7	28.5	8.7	31.1

The boiler setpoint for the cooling dominated regions was found to be 6.8ºC (44.2ºF) and the boiler setpoint for the heating dominated regions was found to be 5.9ºC (42.6ºF). As with the 2-parameter common control there was some concern over the boiler setpoint being too close to freezing range. Therefore, the 7-parameter common control strategy was also run with a boiler setpoint of 10ºC (50ºF).

The annual HVAC savings for the 7-parameter common control strategies are shown below in graphical form in Figures 6.16 and 17. Figure 6.16 shows results for the motel (*a*) and office building (*b*) for Albuquerque, Baltimore, Boise, Burlington, Chicago, Duluth, and El Paso. Figure 6.17 shows results for the motel (*a*) and office building (*b*) for Fairbanks, Houston, Memphis, Miami, Phoenix, and Tulsa. The figures show percent savings of annual HVAC costs for the optimized 2-parameter case discussed above in Section 6.4.1, the optimized 11-parameter case discussed in Section 6.4.2., and the 7-parameter common control cases. The results for the 7-parameter common control strategy with the boiler setpoint set to averaged optimized values is labeled "Common Control (7)a" and the results for the 7-parameter common control strategy with the boiler setpoint set to 10ºC (50ºF) is labeled "Common Control (7)b".

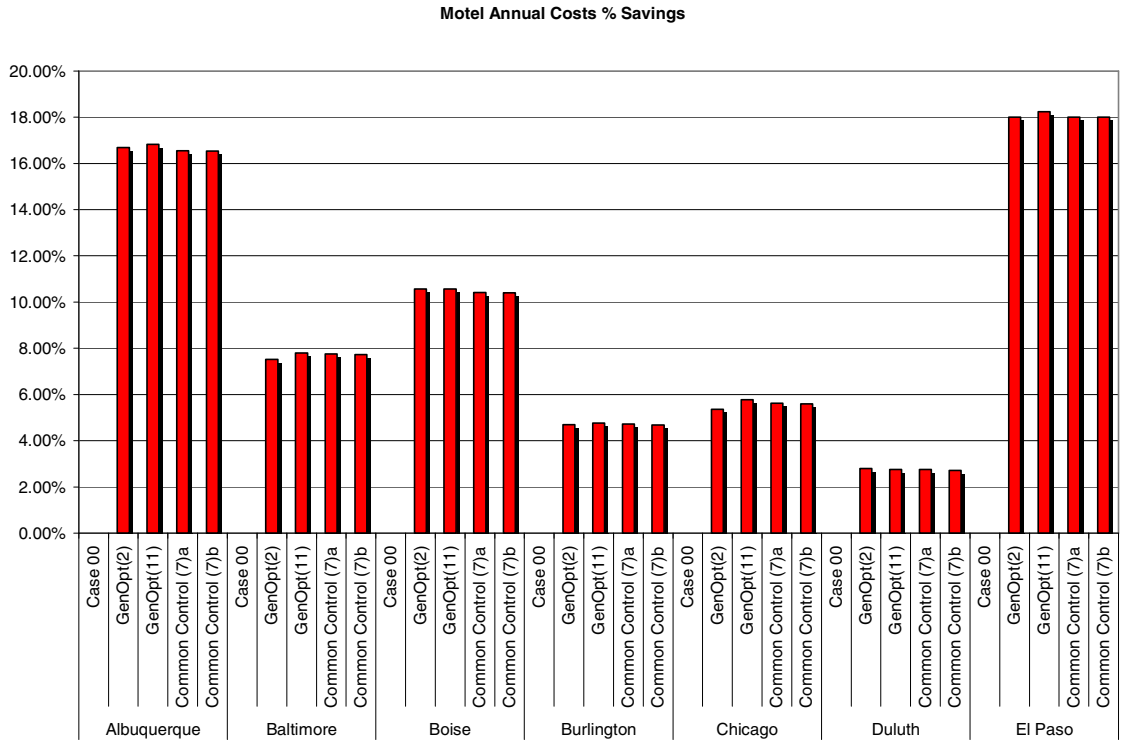

(a) *Motel.*

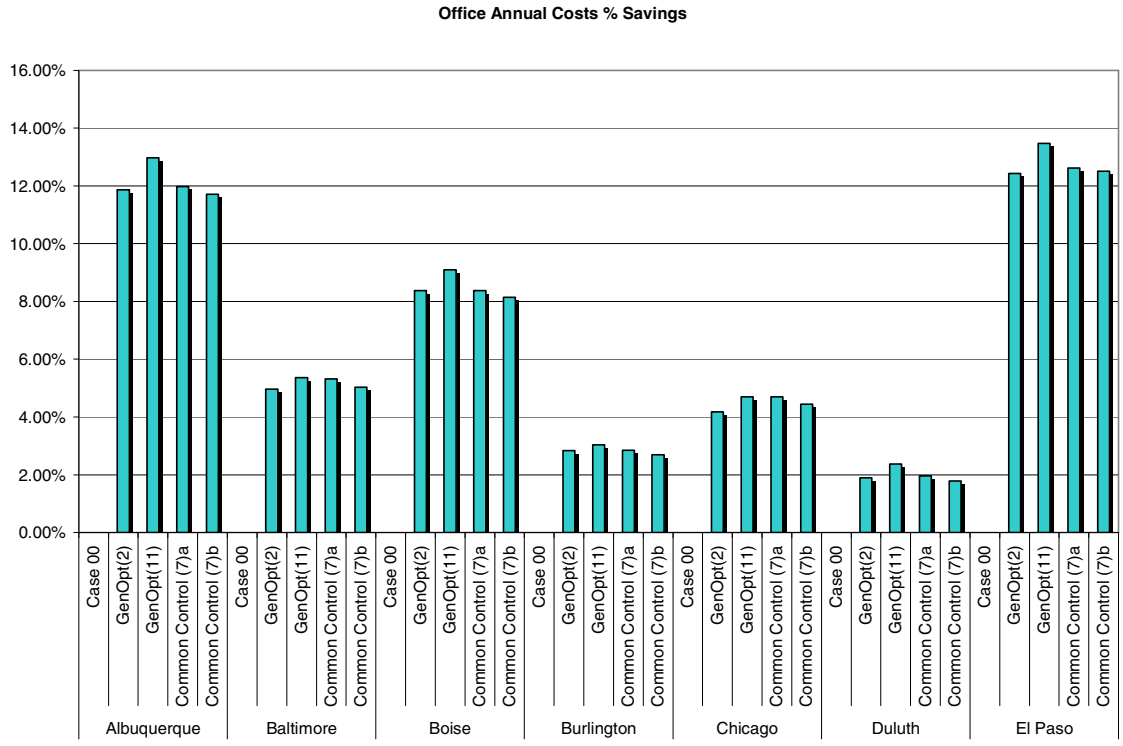

(b) *Office building.*

Figure 6.16 *Annual savings per control strategy (7-parameter common control).*

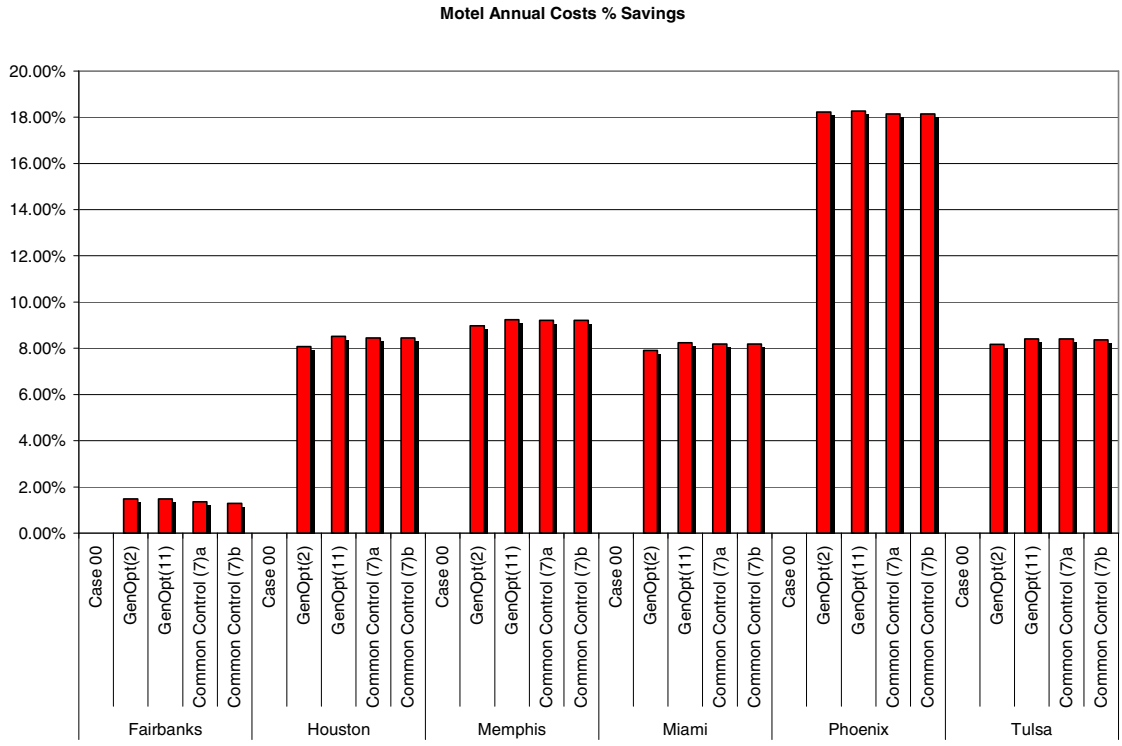

(a) *Motel.*

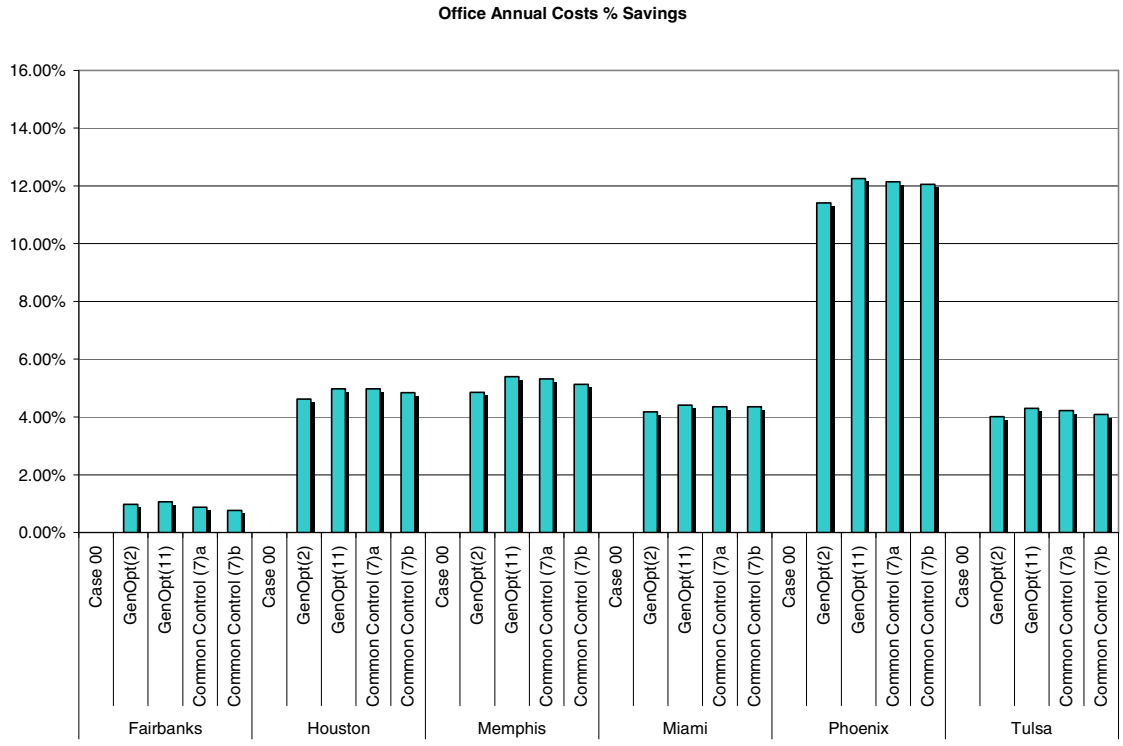

(b) *Office building.*

Figure 6.17 *Annual savings per control strategy (7-parameter common control).*

Unlike the 2-parameter common control strategies, the dynamic 7-parameter common control strategies give very good results for each building and location. There is only a slight drop off in savings for each location compared to the 11-parameter optimized savings, which is to be expected. There is also very little difference in the results with the boiler setpoint set to 10ºC (50ºF), showing again that the savings potential is almost all with how the cooling tower is controlled. As a whole the common control strategies for the two climate regions appear to perform very well.

6.4.5. 11-parameters with Wet-bulb Case

Besides the control strategies discussed above, there were two control strategies that were investigated on a smaller scale to determine if there would be any savings potential. In an effort to investigate different climate regions, the following four cities were chosen for investigation.

- Chicago, Illinois – Cool-Humid Region
- El Paso, Texas – Warm-Dry Region
- Houston, Texas – Hot-Humid Region
- Memphis, Tennessee – Warm-Humid Region

The first of these exploratory control strategies looked at the potential of utilizing the outdoor wet-bulb temperature as an additional means of controlling the cooling tower setpoint. There may be times that the cooling tower setpoint is lower than the wet-bulb, in which case the cooling tower would continue to run even though the

setpoint can never be achieved. In cases such as this, it may be beneficial to reset the setpoint to something slightly above the wet-bulb. Therefore, a wet-bulb temperature difference (ΔT) parameter was created and optimized along with the 10 other cooling tower parameters and the one boiler parameter. The control strategy first determines the cooling tower setpoint based on the 10 parameters as in the 11-parameter control strategy discussed in Section 6.4.2. It then looks at the outdoor wet-bulb temperature. If the cooling tower setpoint based on the heat pump ΔT is less than the wet-bulb temperature plus the wet-bulb ΔT parameter, it resets the setpoint to be equal to the wet-bulb plus the wet-bulb ΔT parameter. For example, if the original setpoint is 70ºF (21.11ºC) and the entering wet-bulb temperature is 75ºF (23.89ºC) then the setpoint used would be the 75ºF (23.89ºC) plus the optimized wet-bulb ΔT parameter.

It should be noted that this control strategy was investigated to determine what potential, if any, there would be by utilizing the outdoor air wet-bulb. It should also be noted that the overall performance of this control strategy would be dependent on an accurate and reliable measurement of the wet-bulb. If significant potential savings are found, the implementation of this control strategy by a building operator would still have to overcome the difficulty of obtaining reliable and accurate wet-bulb measurements.

The annual HVAC savings for the 11-parameter with wet-bulb with wet-bulb cases are compared below to the optimized 2-parameter case, the optimized 11-parameter case and the 7-parameter common control with the boiler setpoint set to 10ºC (50ºF). The results are shown in Figures 6.18. Figure 6.18 (*a*) shows results for the motel 6.18 (*b*)

shows the results for the office building. The wet-bulb ΔT parameter ranges between 0ºC and 4.5ºC; all control parameters for the 11-parameters with wet-bulb case are tabulated in Appendix E.

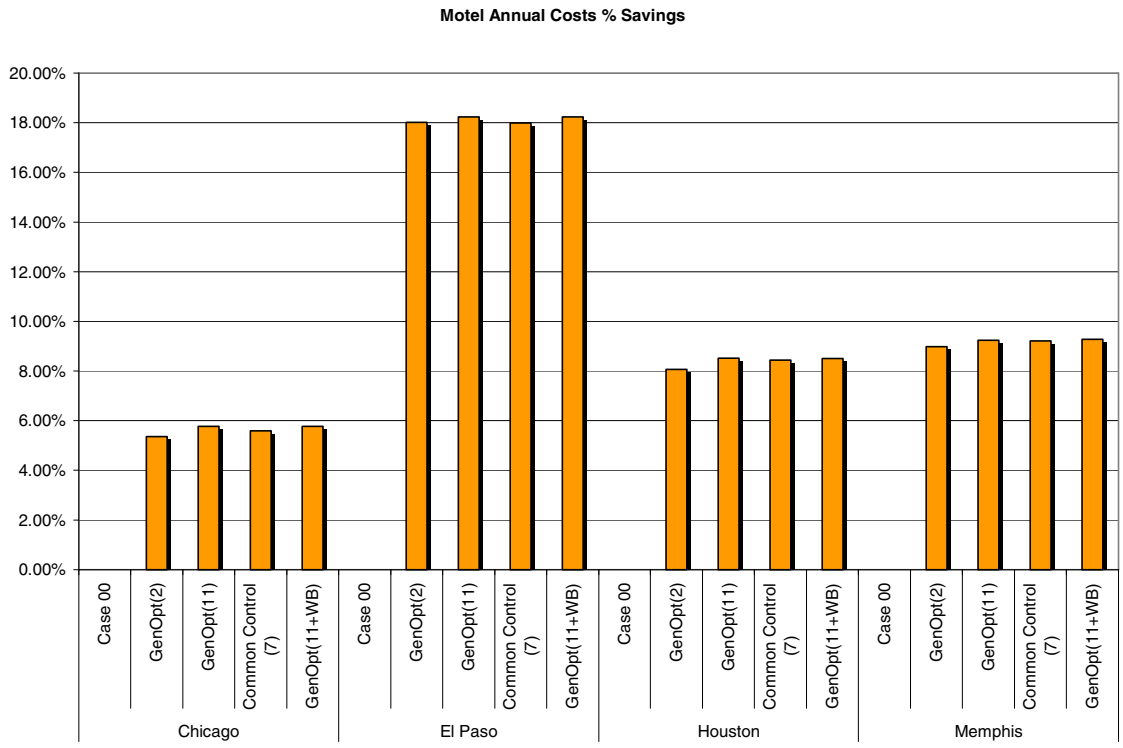

(a) *Motel.*

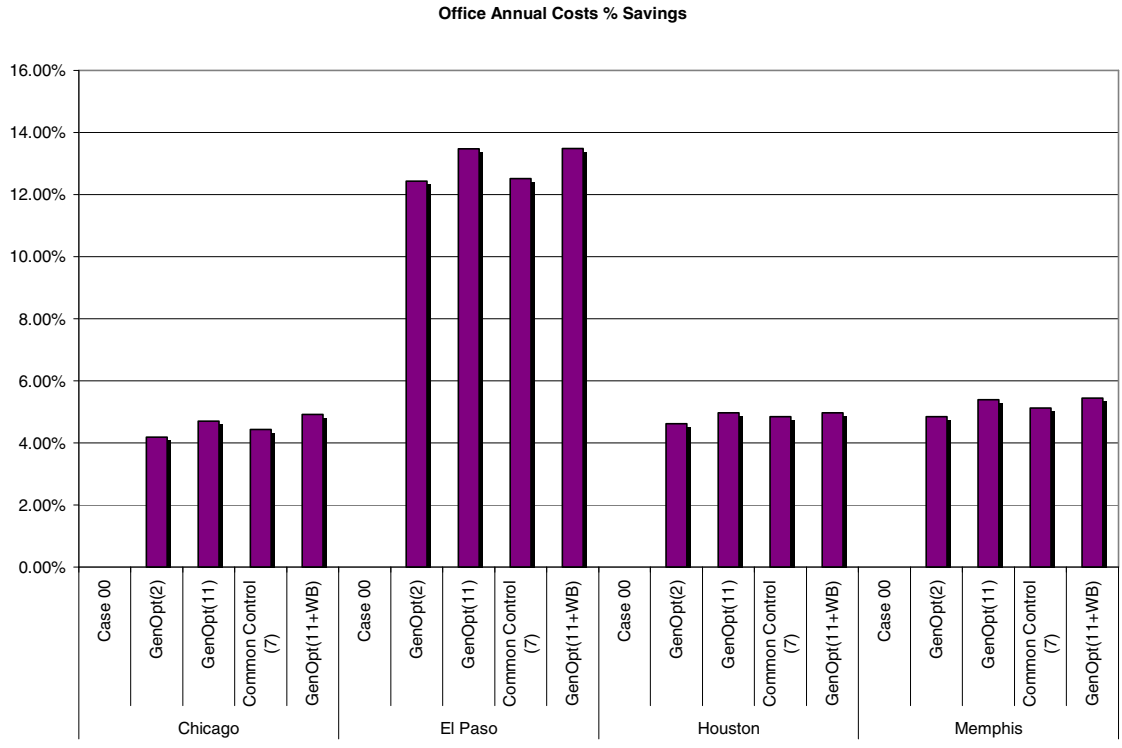

(b) *Office building.*

Figure 6.18 *Annual savings per control strategy (11-parameter with wet-bulb).*

As can be seen by the results above there is little savings potential by adding in the wet-bulb check to the control strategy. For each case, the savings from the optimized "GenOpt (11+WB)" are just a fraction higher, if not the same, as the optimized 11-parameter case. With the lack of savings potential found, this strategy was investigated no further.

6.4.6. 12-hour Forecasting and Thermal Mass Augmentation

The second exploratory control strategy investigates the use of forecasting future loads. As this strategy only makes sense if the system has significant thermal mass, the thermal mass has been augmented by adding a storage tank into the system. Four new parameters were needed for this control strategy and are shown in Figure 6.19 and listed below.

- Heating dominated ΔT, this is used in the strategy to determine if the heat pumps are running predominately in heating mode.
- Cooling dominated ΔT, this is used in the strategy to determine if the heat pumps are running predominately in cooling mode.
- Heating dominated offset, which is used to determine how much higher the setpoint will be if the system is heating dominated.
- Cooling dominated offset, which is used to determine how much lower the setpoint will be if the system is cooling dominated.

The general idea of the control strategy depends on the ability to predict the future loads of a building. For investigative purposes, the building loads obtained from DesignBuilder were used and the mean heat pump temperature difference was found for 12-hours in advance of each time step. From this mean ΔT, it could be determined if the operation of the system in the next 12-hours would be heating dominated or cooling dominated. Depending on the future operation the cooling tower setpoint can be increased or decreased.

The control strategy looks at whether or not the system is heating dominated, cooling dominated, or neutral. This is determined by the forecasted mean heat pump ΔT for the next 12-hours. If the mean heat pump ΔT is less than the cooling dominated ΔT parameter, then the system is cooling dominated, and the setpoint is shifted downward by the "cooling dominated offset" parameter. If the mean heat pump ΔT is greater than the heating dominated ΔT parameter, then the setpoint is shifted upward by the "heating dominated offset" parameter. If the system is between the cooling dominated ΔT parameter and the heating dominated ΔT parameter, the system is considered neutral, and the setpoint is not shifted.

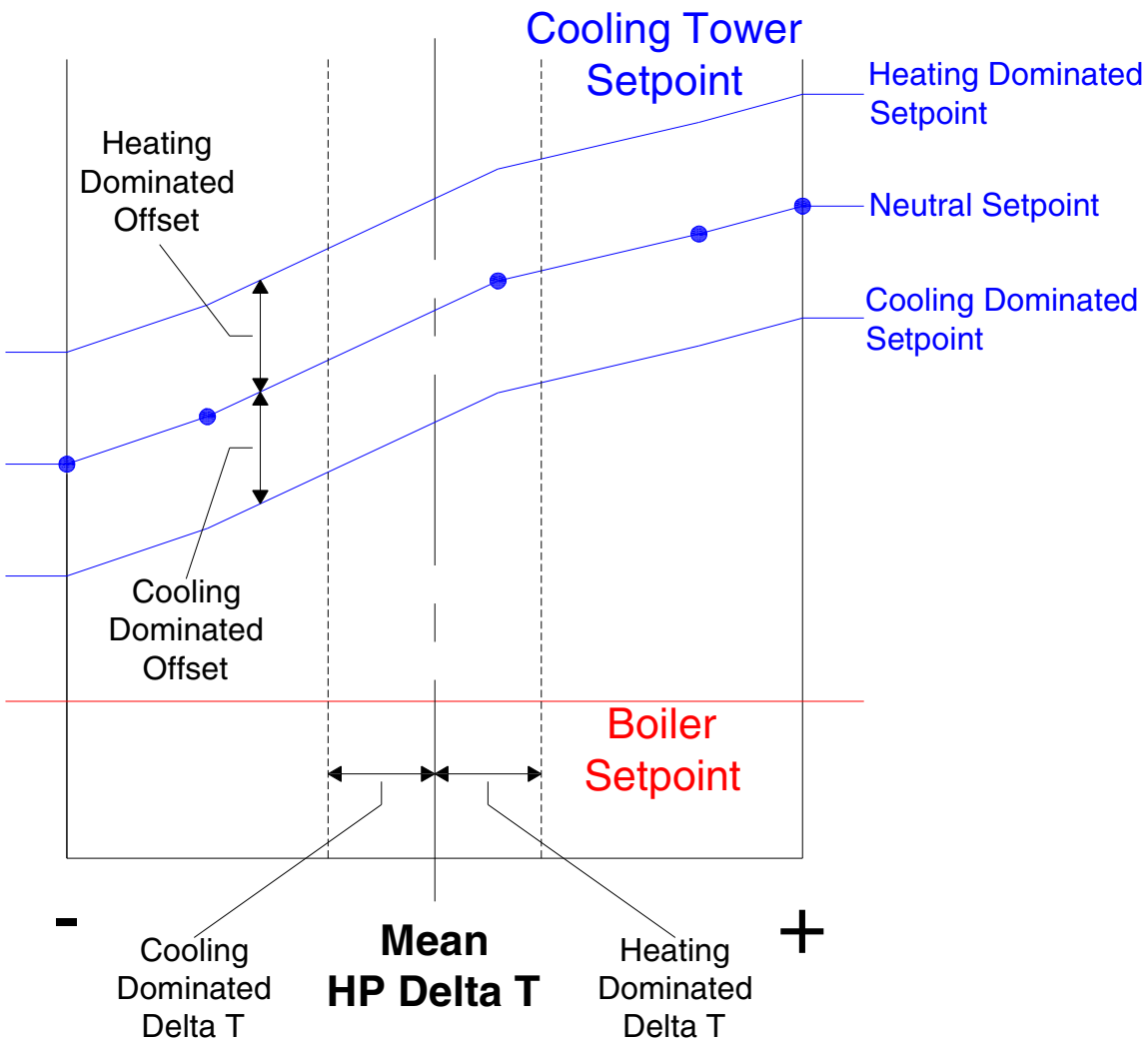

Figure 6.19 *Forecasting control strategy.*

The thermal storage tank added to the system was a well-mixed tank added inline before the "gang of heat pumps" as shown below in Figure 6.20. The thermal storage tank size was sized based on the peak load (heating or cooling) for each city and building. Pietsch (1990) suggests adequate storage to be 50 to100 gal/ton (50 to 100 L/kW). Pietsch's suggestion of 100 gal/ton was used as the basis of sizing the tanks for this work. Specifically, the peak load (heating or cooling) in tons was used to set the tank size, rather than nominal heat pump size. With the exception of Chicago, all locations were

sized on the peak cooling load. Thermal storage tank sizes used for this investigation can be seen below in Table 6.7. The thermal storage tank used for this work was a well-mixed tank, as a stratified tank model was not readily available. Presumably better performance or equivalent performance with a smaller stratified tank would be possible.

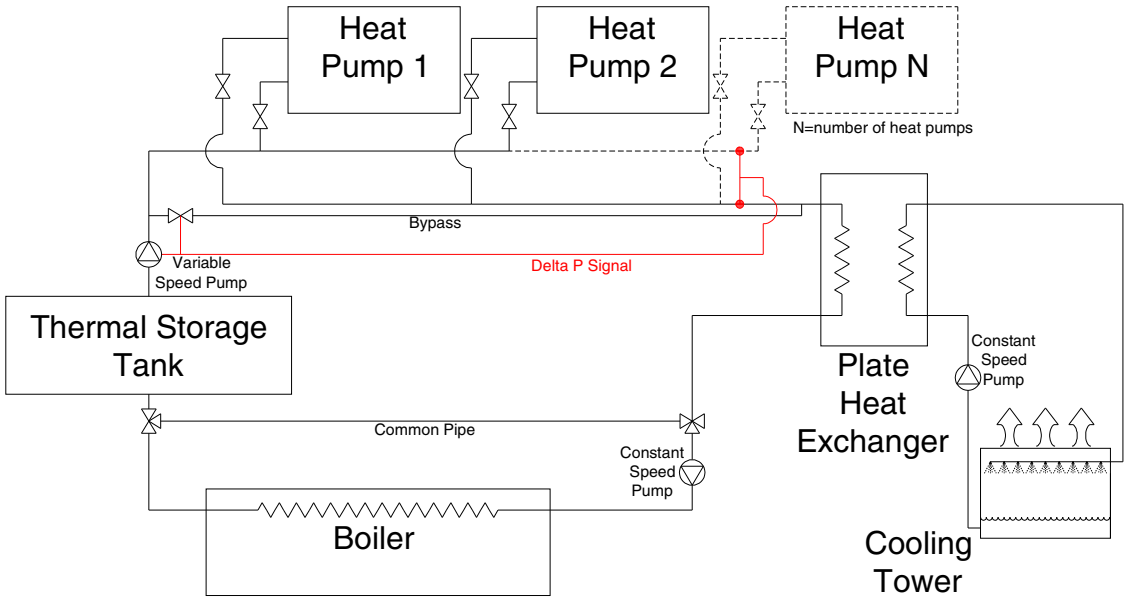

Figure 6.20 *WLHP system with thermal storage.*

Table 6.7 *Thermal storage tank sizes.*

Office Building		
	m^3	gallons
Chicago	99.6	26,312
El Paso	99.6	26,312
Houston	88.6	23,406
Memphis	101.8	26,893
Motel		
	m^3	gallons
Chicago	41.2	10,884
El Paso	35.2	9,299
Houston	39.8	10,514
Memphis	39.8	10,514

The annual HVAC savings for the 12-hour forecasting and thermal mass augmentation case is compared below to the optimized 2-parameter case, the optimized 11-parameter case, the 7-parameter common control with the boiler setpoint set to 10ºC (50ºF), and the optimized 11-parameter with wet-bulb case. The results are shown in Figure 6.21.

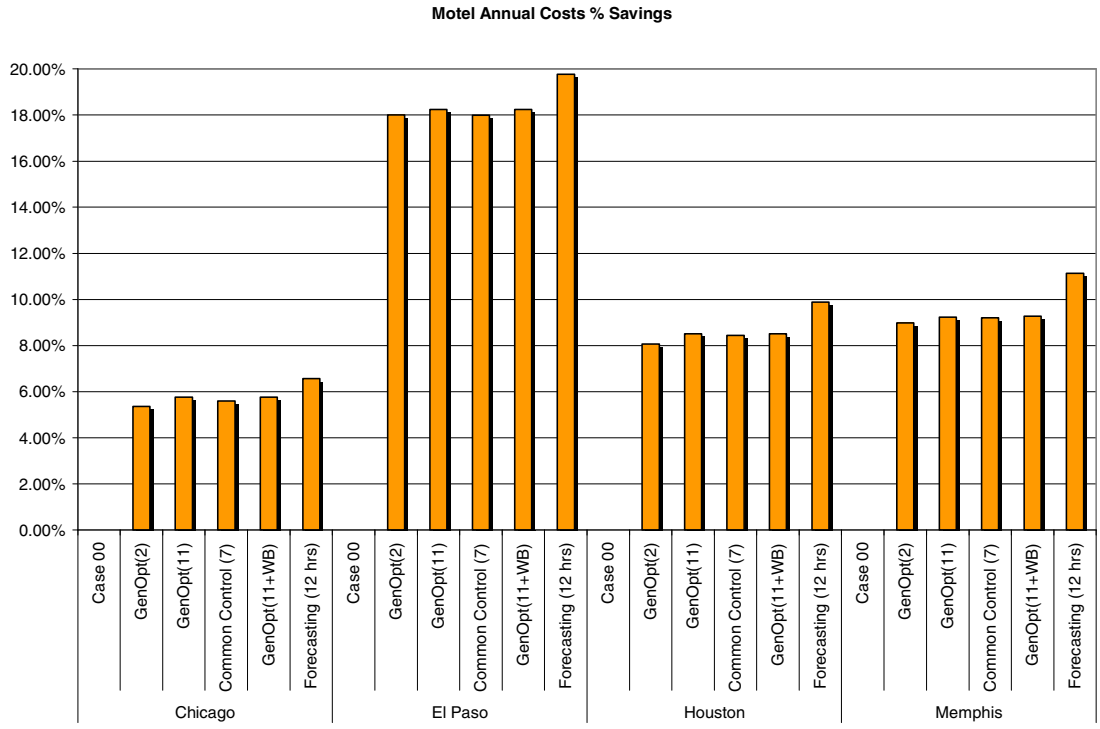

(a) *Motel.*

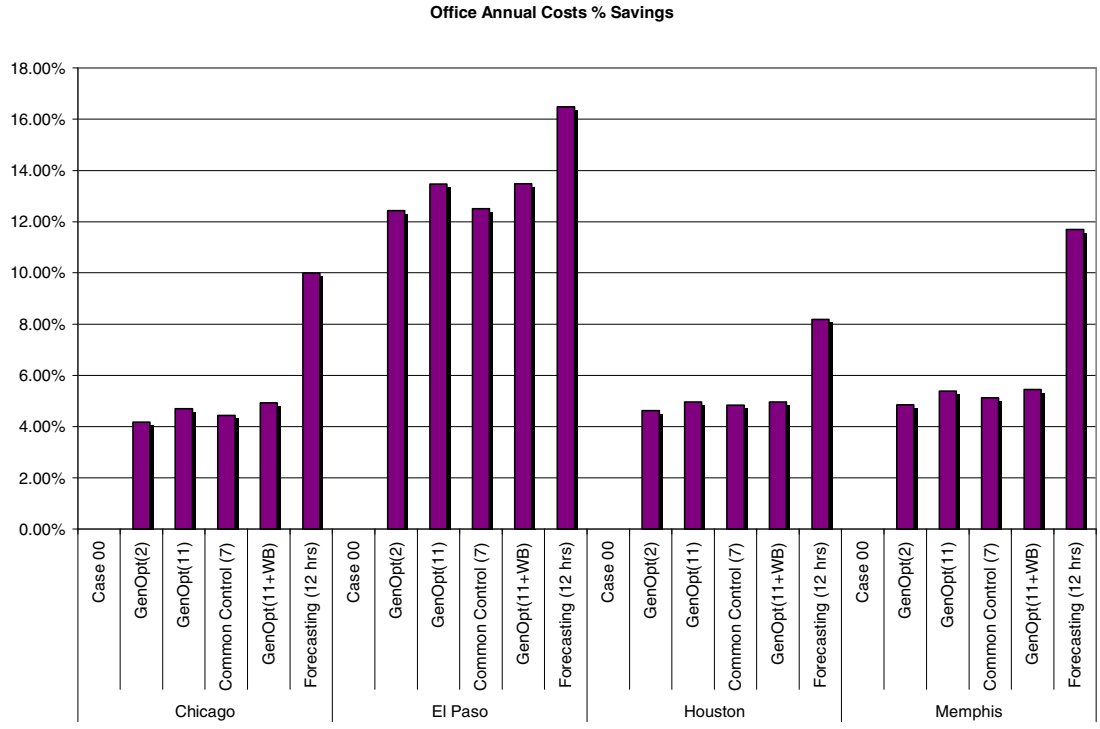

(b) *Office building.*

Figure 6.21 *Annual savings per control strategy (12-hour forecasting and augmented thermal mass).*

The results above show great potential for extra savings over the optimized 11-parameter case, especially with the office building. It should be noted that much of the savings is due to augmenting the thermal mass within the system and thereby taking advantage of shoulder season days were both heating and cooling are needed in a single day. A detailed look into the reasons for the savings is presented in the next section.

A tabulated list of parameters for the 12-hour forecasting and thermal mass augmentation case can be found below in Table 6.8. A more detailed table including the cooling tower parameters, boiler parameter, and the forecasting parameters can be found in Appendix E. It is interesting to note that the two building in Memphis are likely the only cases where the control strategy will actually utilize any significant forecasting. For the office building in Chicago, the threshold for forecasting cooling mode dominated operation, -8.2ºC, never occurs. For the other two office buildings in El Paso and Houston, all temperature offsets are zero, so forecasting a non-neutral mode of operation has no effect on performance.

For the motel buildings in Chicago, Houston, and El Paso, a forecast of cooling mode dominate operation will only change the setpoint less than 1ºC. This seems likely to have a small effect, but the actual impact on operation has not been checked.

Table 6.8 *Forecasting parameters.*

		Cooling ΔT	Heating ΔT	Cooling Offset	Heating Offset
Motel	Chicago	0	0	0.1	0
	El Paso	-0.1	0	0.6	0
	Houston	-0.1	4.1	0.5	0
	Memphis	-3.8	2.0	0.7	0.2
Office	Chicago	-8.2	0	8.3	0
	El Paso	0	0	0	0.04
	Houston	0	0.6	0	0
	Memphis	-3.2	1.3	2.2	0.6

More detailed results of the savings for each case with results by city and building type can be found in Appendix F. The table in Appendix F gives a breakdown of the HVAC energy consumption by component. It lists the total annual savings for each case, and the annual cost comparison for each case based on $0.08/kW-hr.

6.5. Results Verification

The results presented in the above sections only show annual performance. In an effort to verify these results, it seems useful to examine system operation over a few days (like the simulations reported in the last section, also simulated on four-minute time steps) so that the various control schemes can be compared in some detail. Two cases with significant additional savings are chosen for additional review:

- The office building in El Paso - the forecasting control strategy with augmented thermal mass gives an additional 3% in savings over the optimized 11-parameter control strategy. However, the optimized forecasting parameters are all essentially zero – the control strategy does not really rely on forecasting. This

case will show the effects of the augmented thermal mass, essentially independent of any forecasting.

- The office building in Memphis – the optimized 11-parameter strategy gives 5.4% in savings over the base case, but the optimized forecasting strategy gives 11.7% savings over the base case. The optimized forecasting parameters make a significant difference in the way the control strategy performs.

6.5.1. El Paso

A shoulder season day, January 31, and a summer day, June 19, were chosen for an in-depth review. Figure 6.22 shows the cooling tower control strategy for four cases including the base case, optimized 2-parameter case, optimized 11-parameter case, and the optimized 12-hour forecasting case. The extra four parameters for the 12-hour forecasting and thermal mass augmentation case are:

- Heating dominated ΔT: 0ºC
- Cooling dominated ΔT: 0ºC
- Heating dominated offset: 0.04ºC
- Cooling dominated offset: 0ºC

It may immediately be noted that the offset parameters are so small that it is dubious whether they have any effect at all. However the 10 parameters that form the cooling tower setpoint profile is noticeably different. The rest of this section looks at the effects of these four strategies on system operation and performance.

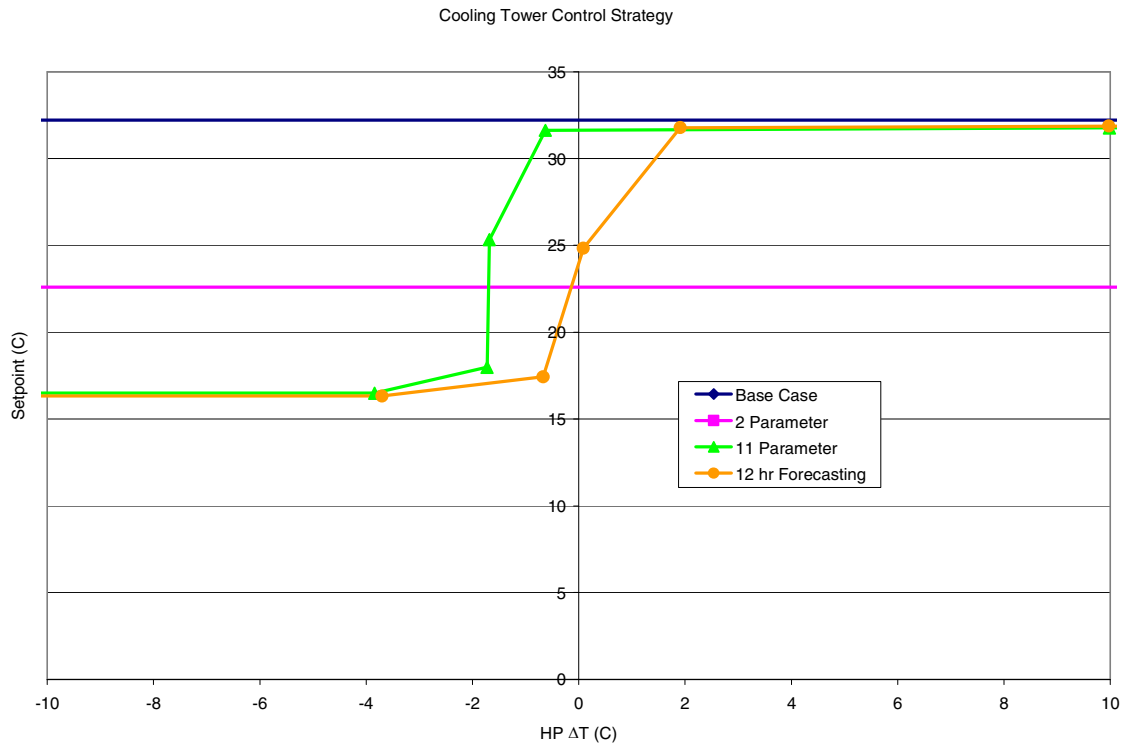

Figure 6.22 *Control profiles.*

Figure 6.23 shows the setpoints for each of the four cases for January 31. As discussed above, the cooling tower is operated to control the heat pump entering fluid temperature. Also plotted is the heating and cooling load for the day. As can be seen, the morning starts off with a short period of heating followed by a period of cooling. The effects of this can be seen by the varying cooling tower setpoints for the 11-parameter case and the 12-hour forecasting and thermal mass augmentation case. Of particular interest is the fact that, although the optimized forecasting strategy has all of the forecasting related parameters essentially zeroed out, it still behaves in some respects as if it were forecasting. During this day, when the building switches from heating to cooling, the heat pump ΔT will start out with a positive value around 3.5ºC, then drop. Based on the control profiles in Figure 6.22, the forecasting strategy will start to lower

the setpoint well before the 11-parameter control strategy. This is advantageous, coming as it does before the cooling load starts.

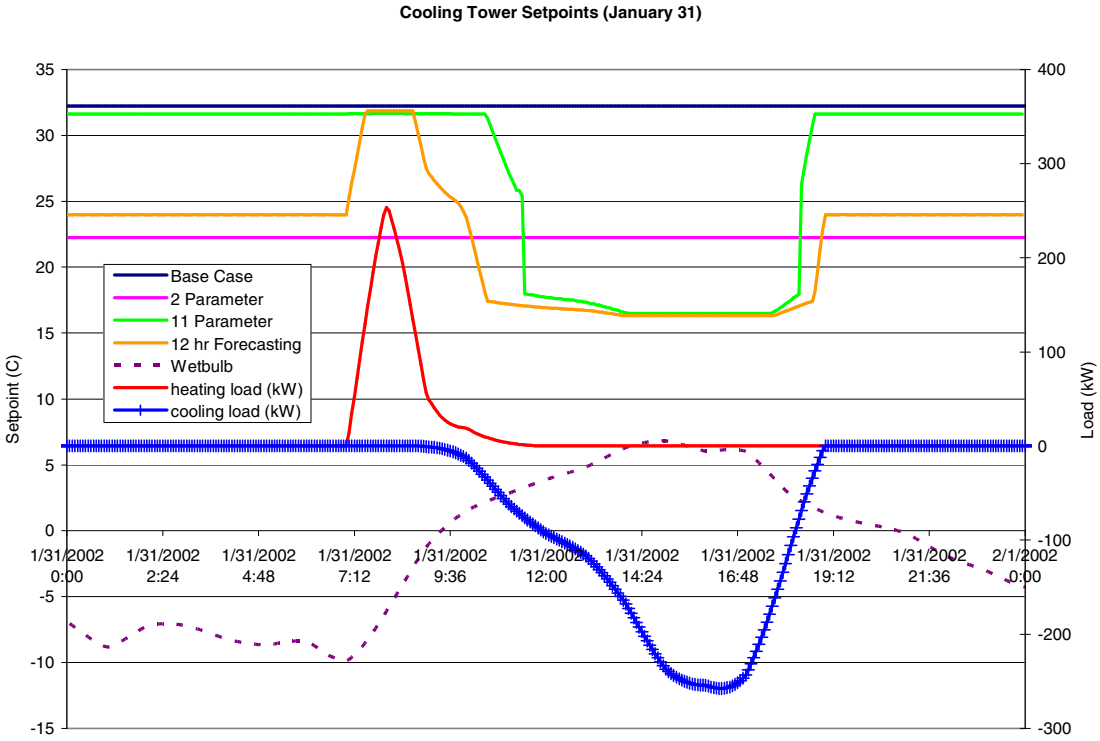

Figure 6.23 *Cooling tower setpoints (January 31).*

Figure 6.24 shows the heat pump entering fluid temperature for the four cases throughout the day. During the cooling period, it is shown that the 2-parameter case reduces the temperature compared to that of the base case, the 11-parameter reduces it even more, and the 12-hour forecasting with thermal mass case reduces it slightly more. With the reduction in heat pump entering fluid temperature, one would expect the COP of the heat pumps providing cooling to increase, which is what is shown in Figure 6.25. It should be noted that the augmented thermal storage within the loop allows the cooling tower to come on and stay on with the forecasting strategy, whereas the other strategies

show a saw-tooth temperature behavior caused by the cooling tower fan going on and off to meet the setpoints.

It should be noted that the heat pump entering fluid temperature, for the cases without augmented thermal mass, oscillates above and below the setpoint to a greater degree than would be expected in real-life. This is due to the structure of the simulation. As discussed in Section 4.3, the simulation was run with multiple superblocks within HVACSim+. Without multiple superblocks, the sudden transients due to the controllers switching the cooling tower on and off would cause problems with convergence of the simulation. Adding a superblock gives, in effect, a transit delay to the system and forces the control signal to be based on the previous time step's temperature values. The saw-tooth temperature response, shown in Figure 6.24, is partially due to the effects of having multiple superblocks. For example, when the heat pump entering fluid temperature for the base case rises above the setpoint of 32.2ºC (90ºF), the cooling tower is switched on. The actual heat pump entering fluid temperature may then quickly fall below the setpoint minus the deadband. But, the control signal for the cooling tower does not see this effect until the following time step, causing the cooling tower to be switched on/off every other time step. Although this is not ideal, it is difficult to overcome without running the simulation in one superblock. Oscillation of the heat pump entering fluid temperature around the setpoint will result in the COP also oscillating, as shown in Figure 6.25. However, as the COP is close to linear with respect to heat pump entering fluid temperature, small oscillation errors in the entering fluid temperature should have a very small effect in the computed energy consumption.

There are two minor points to note. First, at approximately 2:40 AM the heat pump entering fluid temperature falls very quickly. This is caused by the heat input from the variable speed pump, operating at 30% full flow, causing the loop temperature to slowly rise over time even without any equipment in operation. At that point shown in Figure 6.24, the loop temperature rises above 32.2ºC (90ºF), the cooling tower setpoint, and the cooling tower comes on for a short time causing the drastic change in loop temperature. Second is the fact that there appears to be several boiler on/off cycles between 7:40 AM and 9:40 AM for the 11-parameter case but not for the base case and 2-parameter case. The reason there is no on/off cycle for either is that they are both running the whole time the heating load is present. The reason there is an on/off cycle for the 11-parameter is because the boiler setpoint is much lower (2.8ºC) than the base case setpoint (15.6ºC) and the 2-parameter setpoint (16.8ºC).

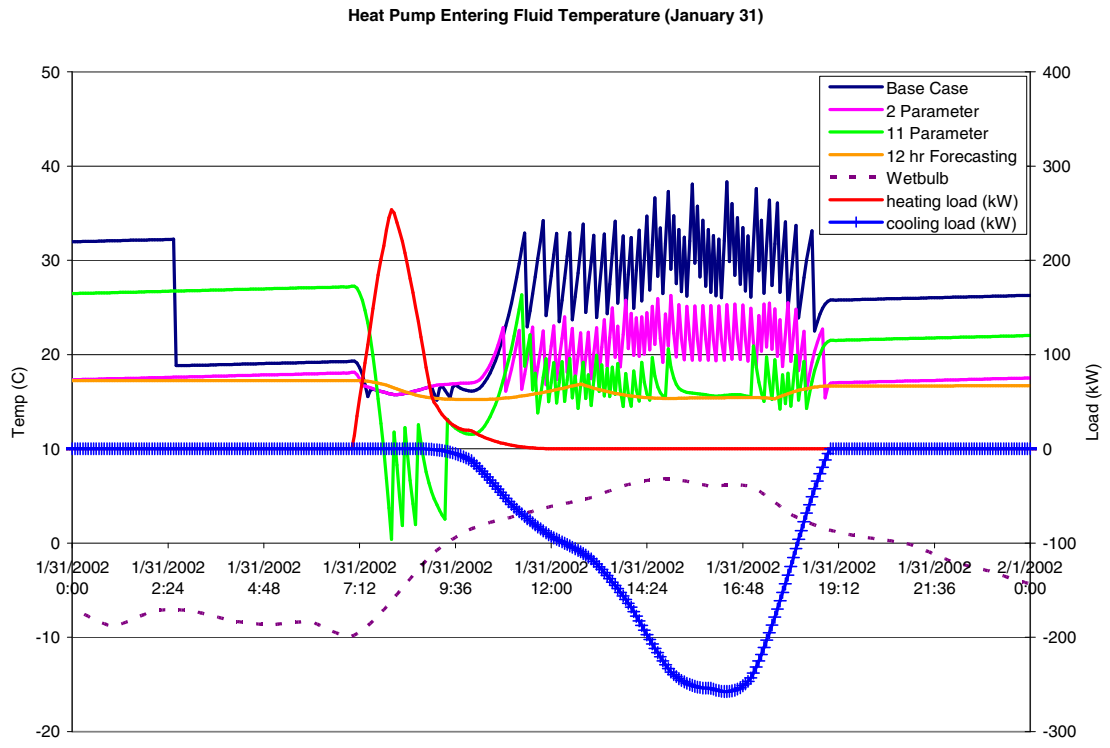

Figure 6.24 *Heat pump entering fluid temperature (January 31).*

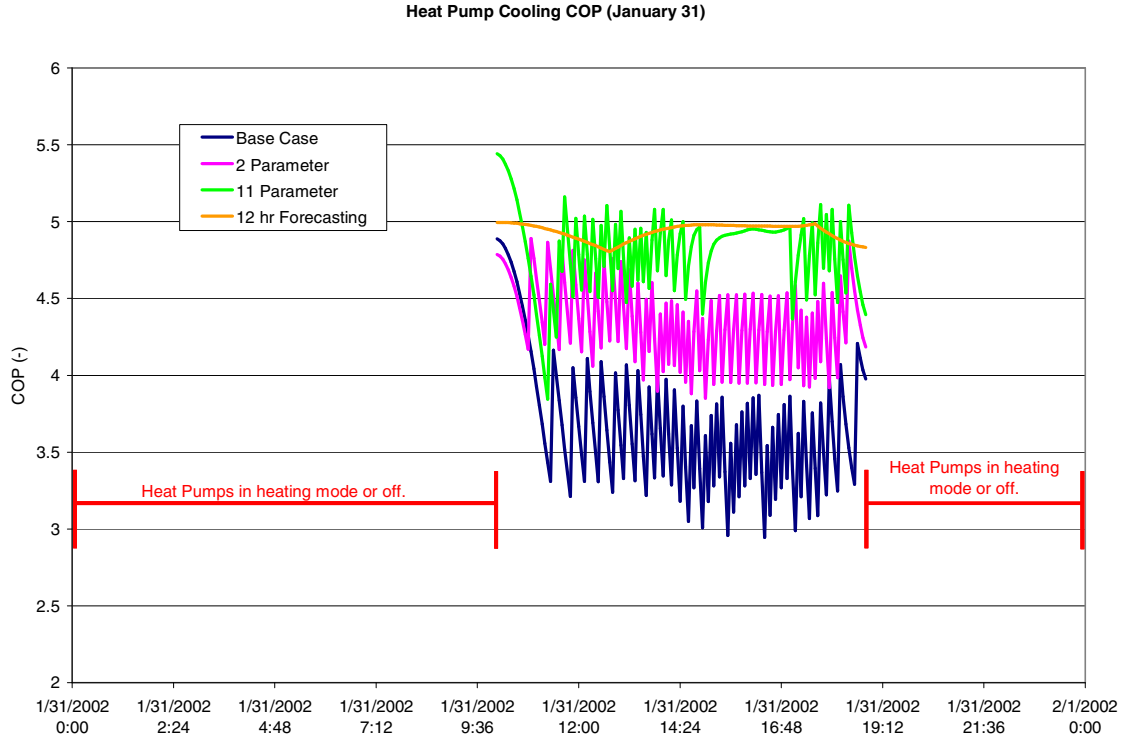

Figure 6.25 *Heat pump cooling COP (January 31).*

Figure 6.26 plots the heat pump energy consumption throughout the day. As can be seen the 11-parameter and 12-hour forecasting cases, both of which have higher COPs, consume significantly less energy than the base case which runs at lower COPs and higher entering fluid temperatures. Because of the different boiler setpoint temperatures, the 11-parameter strategy has lower heat pump entering fluid temperatures and therefore higher heat pump energy consumption than the 2-parameter case. However, this will be offset by the lower boiler energy consumption for the 11-parameter case.

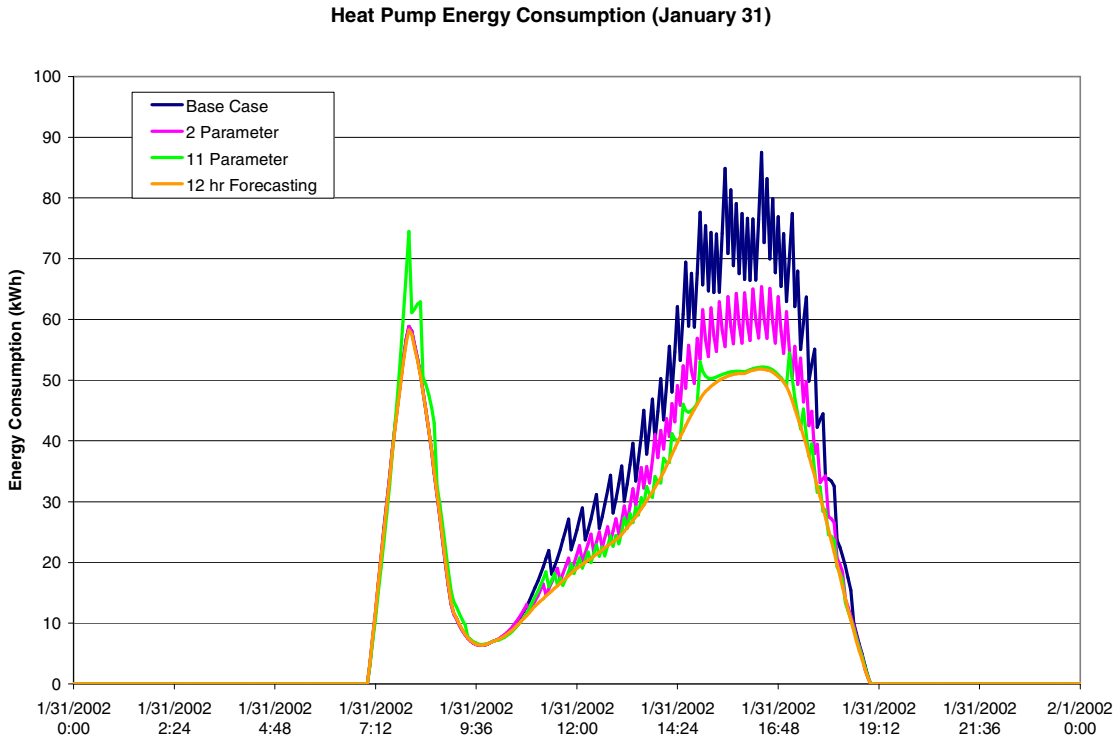

Figure 6.26 *Heat pump energy consumption (January 31).*

Table 6.9 lists the HVAC energy consumption by component and finally the total HVAC energy consumption for the day. As is shown, the 12-hour forecasting and thermal mass augmentation case uses 44.2% less energy for this day compared to the base case. The forecasting strategy saved heat pump energy, facilitated by an increase in cooling tower energy. But interestingly the majority of the savings come from the ability of the augmented thermal storage to store energy to be used for later, which in this case was used instead of the boiler operation. As is shown in Table 6.9, the forecasting strategy saved the most by not running the boiler at all on January 31.

Table 6.9 *HVAC energy consumption (January 31).*

Energy Consumption (kWh)	Base Case	2-parameter	11-parameter	12 hr Forecasting
Heat Pump	6,790	5,795	5,396	5,176
Main Circ Pump	136	136	136	136
Cooling Tower Fan	276	395	529	537
Cooling Tower Circ Pump	109	155	208	214
Boiler	3,531	3,694	2,762	0
Boiler Circ Pump	25	44	4	0
Total	**10,867**	**10,221**	**9,036**	**6,062**

June 19 is a typical summer cooling day; Figure 6.27 shows the setpoints for each of the four cases for this day. Also plotted are the cooling loads for the day. As can be seen at around 7:00 AM, a large cooling load is caused by the thermostats coming off of setback. This in turn causes the setpoints for the 11-parameter and 12-hour forecasting and thermal mass augmentation cases to hit their minimum point very quickly and stay at the minimum setpoint throughout the day.

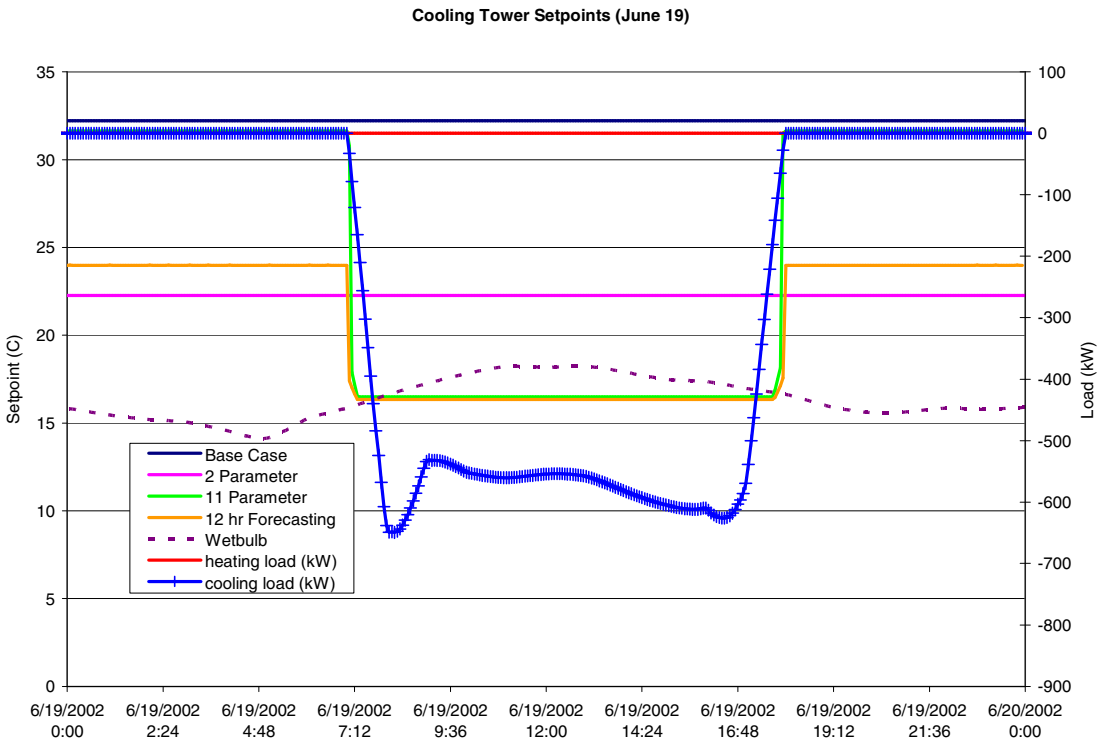

Figure 6.27 *Cooling tower setpoints (June 19).*

Figure 6.28 shows the heat pump entering fluid temperature for the four cases on June 19. This plot shows the effects of the thermal storage that is being used with the forecasting control strategy as the heat pump entering fluid temperature is slower to rise. It is interesting to note that the 2-parameter and the 11-parameter cases have identical heat pump entering fluid temperatures when the load is present, even though there is approximately 5ºC (9ºF) difference in their cooling tower setpoints. The reason the setpoints can be different and the heat pump entering fluid temperatures can be the same is that the cooling tower is running continuously for both cases and the setpoint for neither case is achieved. The cooling tower was sized based on standard conditions of 35ºC (95ºF) cooling tower entering fluid temperature, 29.4ºC (85ºF) cooling tower

exiting fluid temperature, and 23.9ºC (75ºF) outdoor wet-bulb temperature. While this works well for the base case, the cooling tower may be undersized for lower setpoints. To put this in perspective, the setpoints were optimized using this specific cooling tower size. It is likely that a larger cooling tower size would result in different setpoints. This is a topic for future investigation. The effects of this can also be seen in Figure 6.29 where the 2-parameter and 11-parameter heat pump cooling COPs are identical.

It is interesting to note the wet-bulb temperature profile for the summer day of June 19. The wet-bulb temperature increases approximately 4ºC during the day. Figure 4.27 shows that during this time the setpoints will never be achieved since they are lower then the wet-bulb. This appears to be the ideal situation for running the cooling tower more at night, when the wet-bulb temperature is lower, and pre-conditioning the loop for the daily cooling load is possible. However, the forecasting strategy investigation does not directly address this opportunity.

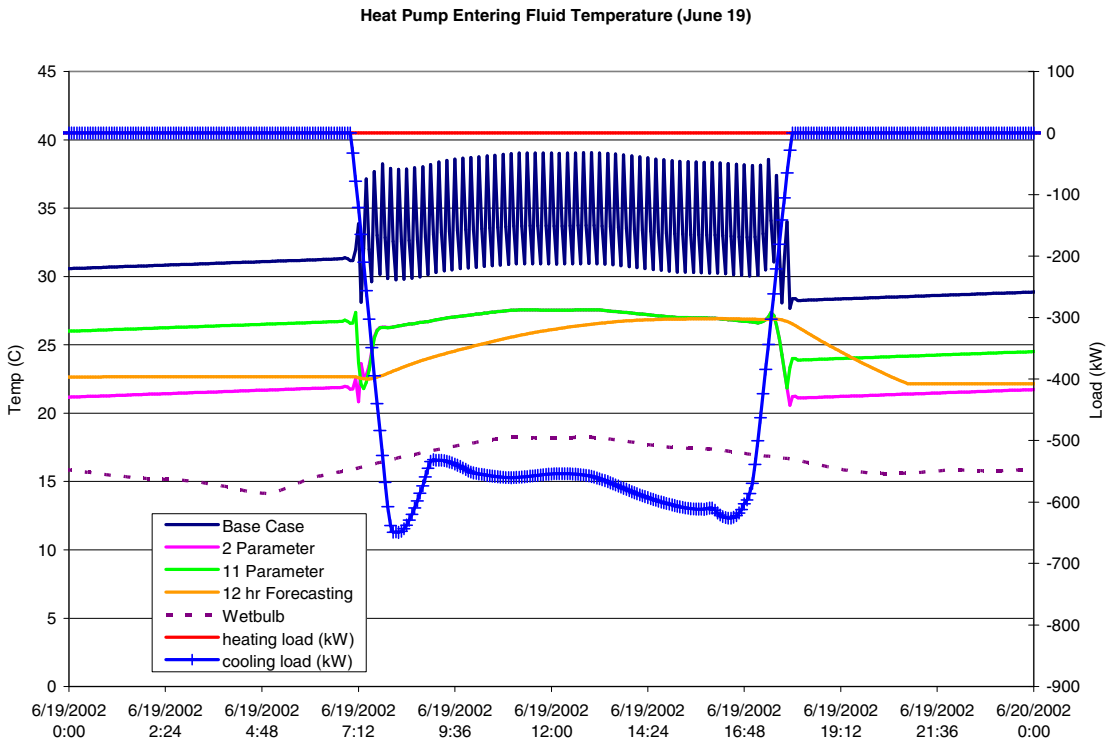

Figure 6.28 *Heat pump entering fluid temperature (June 19).*

As discussed previously, with lower entering fluid temperatures to the heat pump one can expect higher COPs for the heat pump. Figure 6.29 shows the cooling COP for June 19 when the heat pump is in operation.

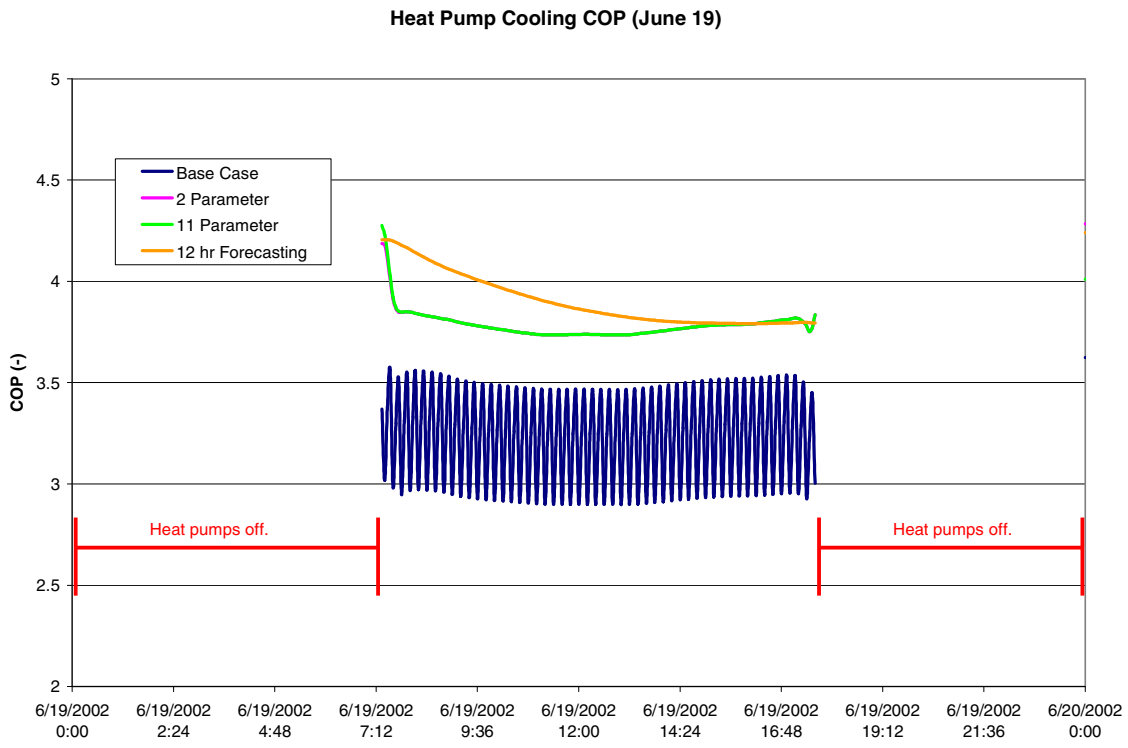

Figure 6.29 *Heat pump cooling COP (June 19).*

Figure 6.30 shows the heat pump energy consumption for June 19. Again, the effects of the thermal storage can be seen by the difference in energy consumption from the 12-hour forecasting to the 11-parameter case.

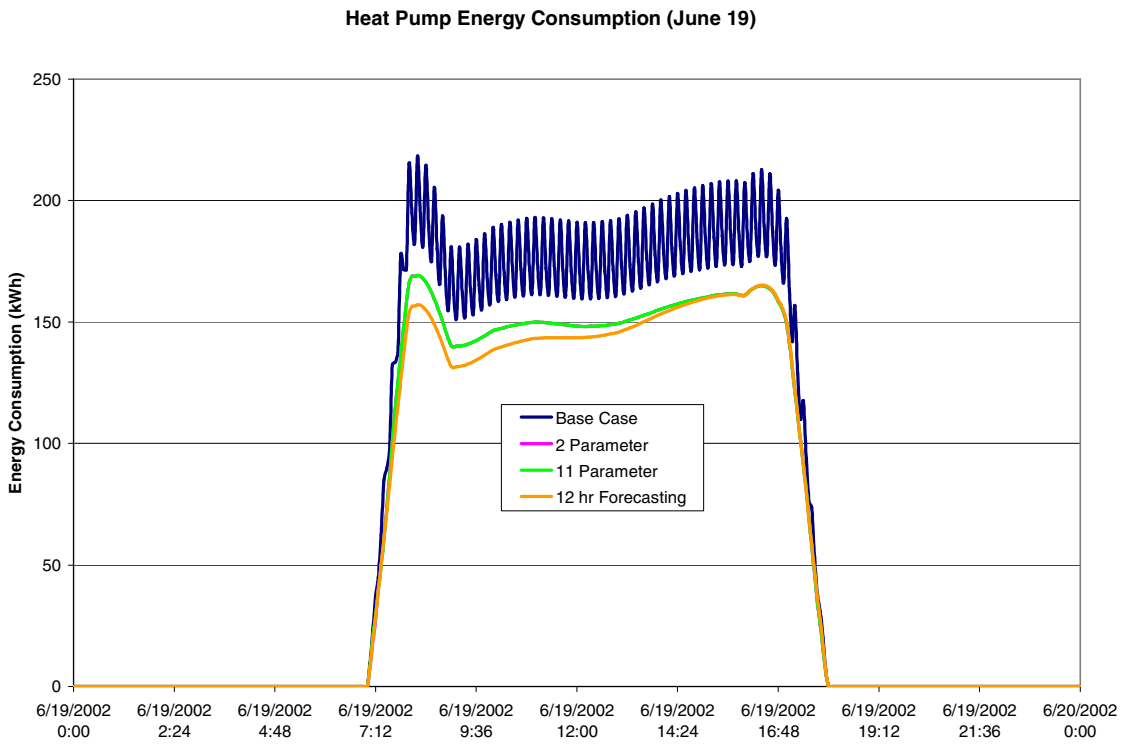

Figure 6.30 *Heat pump energy consumption (June 19).*

Table 6.10 lists the HVAC energy consumption by component and finally the total HVAC energy consumption for June 19. As is shown, the 12-hour forecasting and thermal mass augmentation case uses almost 13% less energy for this day compared to the base case with the savings coming from the cooling tower running more to cool the thermal mass, which in turn allows the heat pump to run with lower entering fluid temperatures. The extra cooling tower energy is exceeded by the reduction in heat pump energy consumption.

Table 6.10 *HVAC energy consumption (June 19).*

Energy Consumption (kWh)	Base Case	2-parameter	11-parameter	12 hr Forecasting
Heat Pump	27,093	23,050	23,050	22,384
Main Circ Pump	257	257	257	257
Cooling Tower Fan	790	1,201	1,201	1,536
Cooling Tower Circ Pump	311	472	472	604
Boiler	0	0	0	0
Boiler Circ Pump	0	0	0	0
Total	**28,451**	**24,980**	**24,980**	**24,782**

Finally, the monthly energy consumption was plotted, Figure 6.31, for each of the four cases. As is shown, the 12-hour forecasting saves more energy, over the other three cases, during the shoulder season than it does during the warmer months, where the savings potential over the 2-parameter and 11-parameter is not as high. It is interesting to note that significant savings come from the 12-hour forecasting and thermal mass augmentation case not requiring any boiler operation during the months of January, February, and December. The energy that is saved during those shoulder months (January, February and December) adds up to give the extra savings potential that is shown in Figure 6.21.

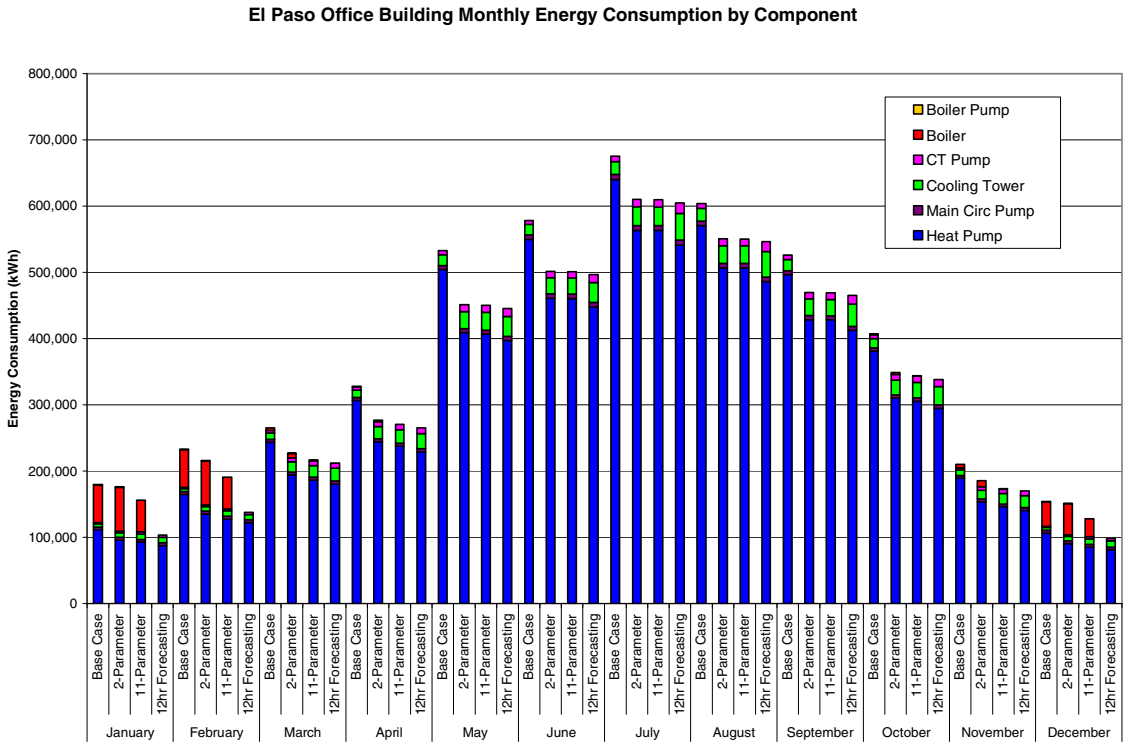

Figure 6.31 *Monthly HVAC energy consumption comparison for the office building in El Paso.*

6.5.2. Memphis

Since El Paso's extra savings potential from the 12-hour forecasting and thermal mass augmentation case was related more to the augmented thermal storage and not to the forecasting, a similarly detailed analysis was done for a case where the forecasting parameters have much more of an impact on the control strategy, the office building in Memphis. The forecasting parameters are:

- Heating dominated ΔT: 1.3ºC
- Cooling dominated ΔT: -3.2ºC

- Heating dominated offset: 0.6ºC
- Cooling dominated offset: 2.3ºC

As can be seen in Figure 6.32, this set of parameters causes a noticeable difference in the cooling setpoint whenever the average ΔT for the next 12 hours is less than -3.2°C. There is a smaller difference when significant heating is forecasted; the control profile is shifted upwards 0.6ºC. The rest of this section looks at the effects the different control strategies have on system operation and performance for a shoulder season day, March 11, and a summer day, July 18.

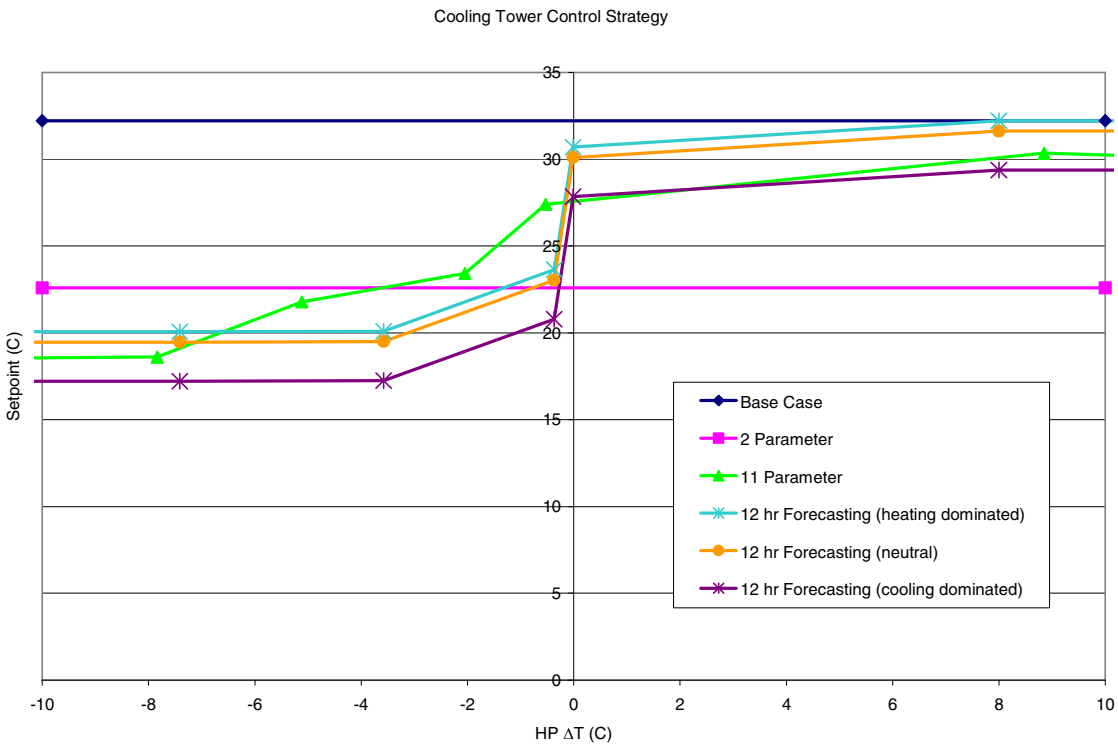

Figure 6.32 *Control profiles.*

Figure 6.33 shows the setpoints for each of the four cases for March 11. Also plotted is the heating and cooling load for the day, the forecasted mean heat pump ΔT, and the current heat pump ΔT. As can be seen, the morning starts off with a short period of heating followed by a period of cooling. As is shown, the forecasted mean ΔT never falls below the cooling dominated ΔT (-3.2ºC) and never rises above the heating dominated ΔT (1.3ºC) for the day. Therefore, the cooling tower will operate with the neutral setpoint profile throughout the day. During the shoulder season the cooling dominated ΔT will only be exceeded when the morning heating load is substantially smaller in magnitude and length compared to the afternoon cooling load.

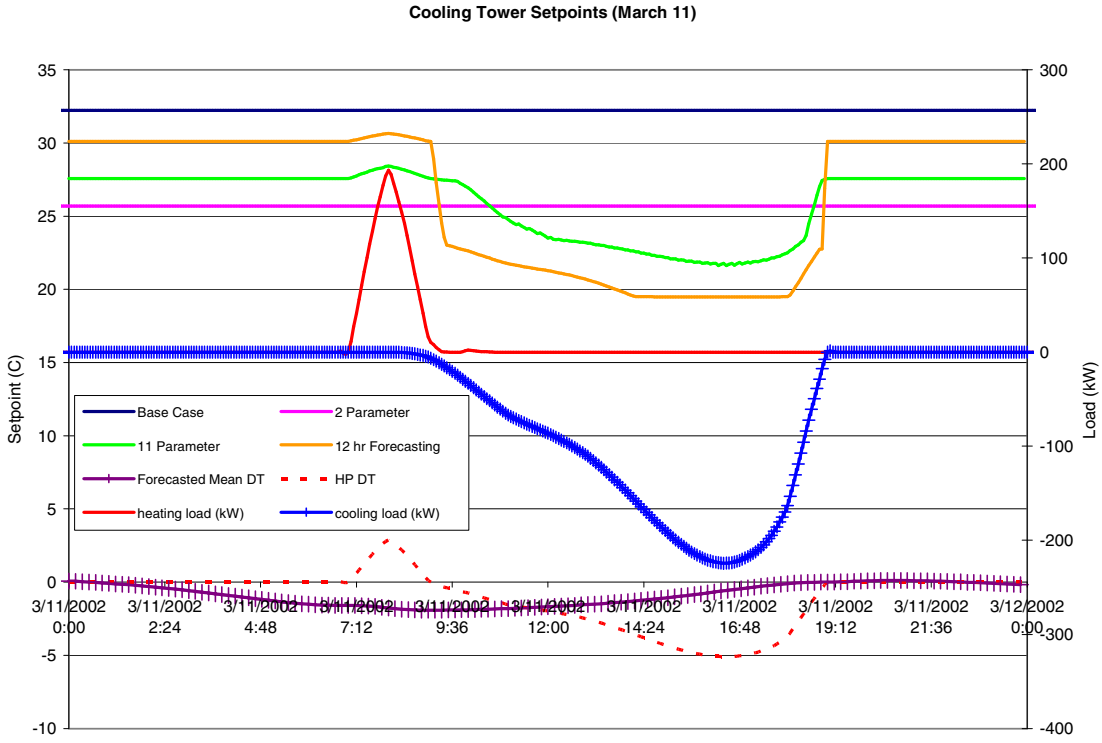

Figure 6.33 *Cooling tower setpoints (March 11).*

Figure 6.34 shows the heat pump entering fluid temperature for the four cases throughout the day. As the heating load increases the heat pump entering fluid temperature for each case begins to fall, with much more noticeable drop offs from the base case, 2-parameter case, and the 11-parameter case. The much more gradual fall in heat pump entering fluid temperature for the 12-hour forecasting case is largely due to the augmented thermal storage in the system. The heat pump entering fluid temperature for the base case falls until it reaches the boiler setpoint (15.6ºC (60ºF)), at which time the boiler begins operation until the temperature rises above 16.6ºC (61.9º F) (setpoint plus the dead band). There are two noticeable on/off cycles for the base case. With the boiler setpoints for the 2-parameter case (2.0ºC (35.6ºF)) and the 11-parameter case (6.6ºC (43.9ºF)) being much lower compared to the base case setpoint, the heat pump entering fluid temperature is allowed to fall much farther for these cases. It should be noted that the boiler was modeled to always give a desired set outlet temperature of 17ºC (62.6ºF). The boiler operation is quite sensitive to this setpoint. With the setpoints for the 2-parameter case and the 11-parameter case being so low compared to the set desired outlet temperature the boiler cycles on/off more, causing the saw-tooth pattern. The energy saved from the thermal storage allowing the 12-hour forecasting case to not run the boiler for this day adds up to substantial savings as is discussed below.

As with El Paso, the augmented thermal mass with the 12-hour forecasting and thermal mass augmentation case allows the WLHP system to run the cooling tower without cycling on and off continuously to meet the setpoint. Without augmentation of the thermal mass, the base case, 2-parameter case, and 11-parameter case all have the

cooling tower continuously cycling on and off causing the saw-tooth pattern. Contrarily, the 12-hour forecasting case has two short off cycles during the day, around 12:00 PM – 1:00 PM and 4:15 PM – 4:45 PM, when the heat pump entering fluid temperature has met the setpoint. The reduction in heat pump entering fluid temperature for the 12-hour forecasting and thermal mass augmentation case allows for higher COPs for the heat pumps that are operating in cooling and thereby better cooling performance. The effects that the lower heat pump entering fluid temperatures have on COP can be seen in Figure 6.35; with the most notable effect being the high COP of the 12-hour forecasting and thermal mass augmentation case.

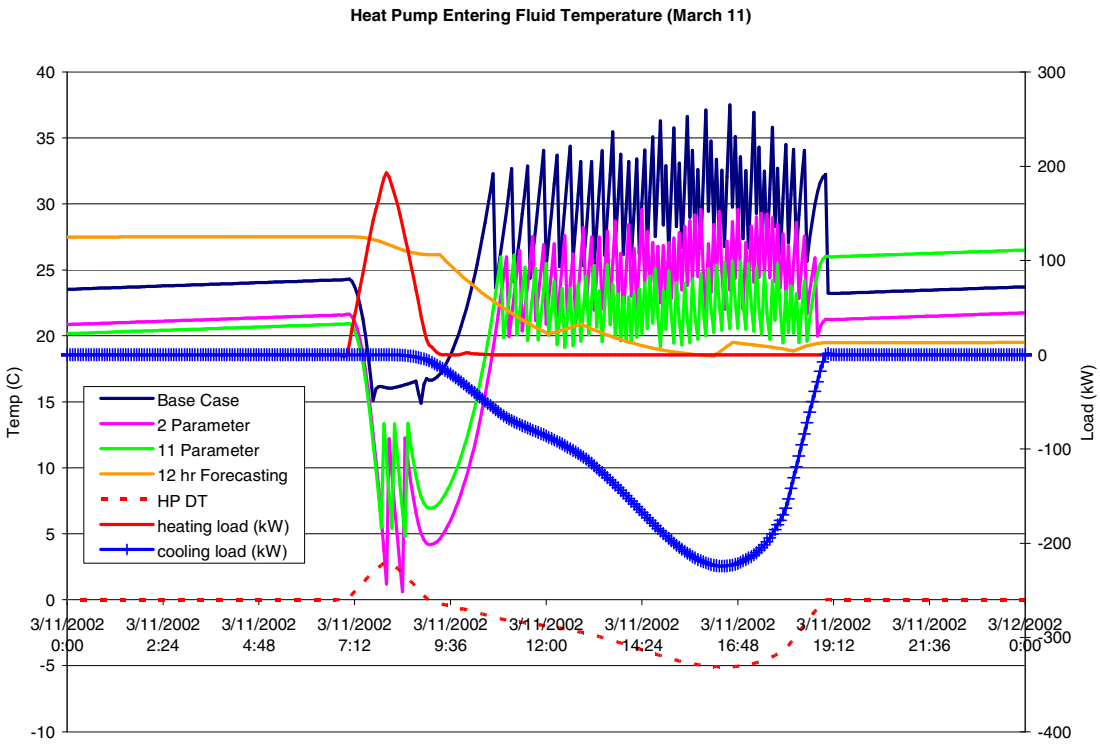

Figure 6.34 *Heat pump entering fluid temperature (March 11).*

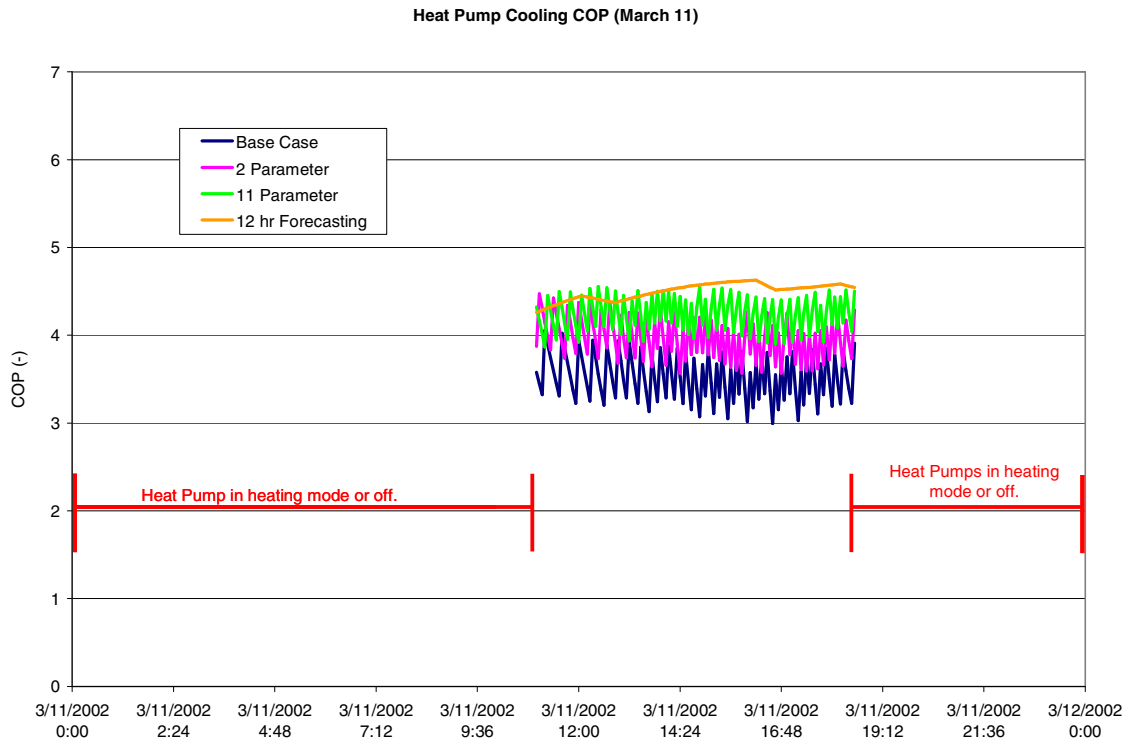

Figure 6.35 *Heat pump cooling COP (March 11).*

During the morning heating period, the lower boiler setpoints for the 2-parameter case and 11-parameter case allow for lower boiler energy consumption, but causes increased heat pump energy during that period to meet the load. This can be seen in Figure 6.36 below. During the afternoon cooling period the lower cooling tower setpoints for the 2-parameter, 11-parameter, and 12-hour forecasting cases allow for reduction in heat pump energy at the cost of running the cooling tower more. For this particular day the net effect is significant savings.

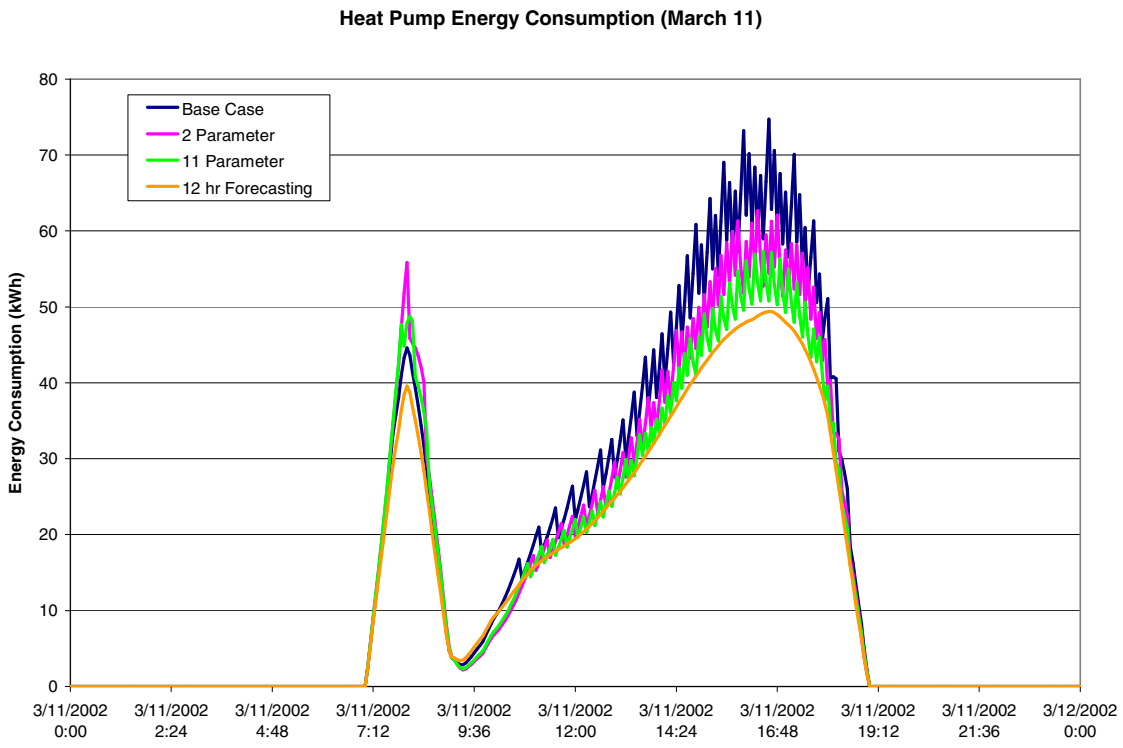

Figure 6.36 *Heat pump energy consumption (March 11).*

Table 6.11 lists the HVAC energy consumption by component and the final total HVAC energy consumption for the day. As is shown, the 12-hour forecasting and thermal mass augmentation case uses 29.4% less energy for this day as compared to the base case. As with the El Paso shoulder season day, the savings come primarily by using heat stored in the augmented thermal mass instead of the boiler, and secondarily from more efficient heat pump performance at the cost of operating the cooling tower fan and pump more.

Table 6.11 *HVAC energy consumption (March 11).*

Energy Consumption (kWh)	Base Case	2-Parameter	11-Parameter	12 hr Forecasting
Heat Pump	6,121	5,567	5,230	4,851
Main Circ Pump	136	136	136	136
Cooling Tower Fan	291	358	425	843
Cooling Tower Circ Pump	114	141	167	334
Boiler	2,048	1,443	1,653	0
Boiler Circ Pump	16	2	3	0
Total	**8,726**	**7,646**	**7,613**	**6,163**

Figure 6.37 shows the setpoints for each of the four cases, the cooling load, the forecasted mean ΔT, the heat pump ΔT, and the wet-bulb temperature for July 18. The effects of the forecasting strategy can be seen by the 12-hour forecasting setpoints. At approximately 1:30 AM, the 12-hour forecasting strategy switches from the neutral profile to the cooling dominated profile dropping the cooling tower setpoint well before there is a load present. The setpoint switches back to the neutral profile at approximately 11:30 AM when the forecasted mean ΔT is greater than -3.2ºC. The wet-bulb temperature shown in Figure 6.37 illustrates why it would be beneficial to run the cooling tower more at night and early morning. As is shown, the wet-bulb temperature changes almost 4ºC from early in the morning to the middle of the day.

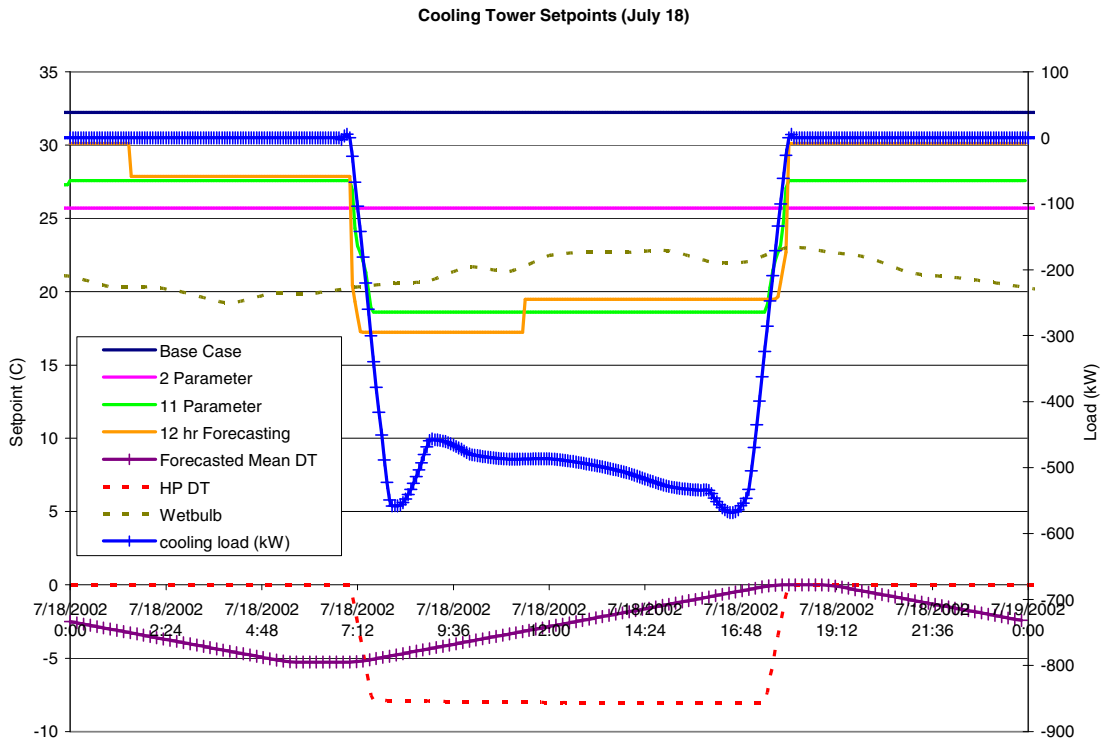

Figure 6.37 *Cooling tower setpoints (July 18).*

Figure 6.38 shows the heat pump entering fluid temperatures for the four cases, the cooling load, the forecasted mean ΔT, and the heat pump ΔT for July 18. This plot illustrates the effects of the forecasting as the cooling tower begins operation at approximately 1:30 AM. This corresponds to the time the cooling tower setpoint switches from the neutral profile to the cooling dominated profile in Figure 6.37. At this point, cooling tower operation begins lowering the heat pump entering fluid temperature before the load is present. This plot also shows the effects of the augmented thermal storage as the heat pump entering fluid temperature is slower to rise throughout the day for the 12-hour forecasting case. Even though the 12-hour forecasting case setpoint switches upward at 11:30 AM, it has no adverse effect on operation. The cooling tower

continues to operate and the heat pump entering fluid temperature continues to slowly drift upward.

As discussed in Section 6.5.1., for a brief time during the day the 2-parameter case and 11-parameter case have identical heat pump entering fluid temperatures. Again, this is a situation where the cooling tower is running continuously for the two cases and the setpoint is never met.

It should also be noted that the for the 12-hour forecasting case the cooling tower continues operation after the load disappears in order to meet the setpoint whereas the other three case operate during the cooling load period only. This may be a reason why, overall, the motel doesn't show as much potential for extra savings. The motel has no setback and more uniform heat gains, so there is little "downtime" compared to the office building.

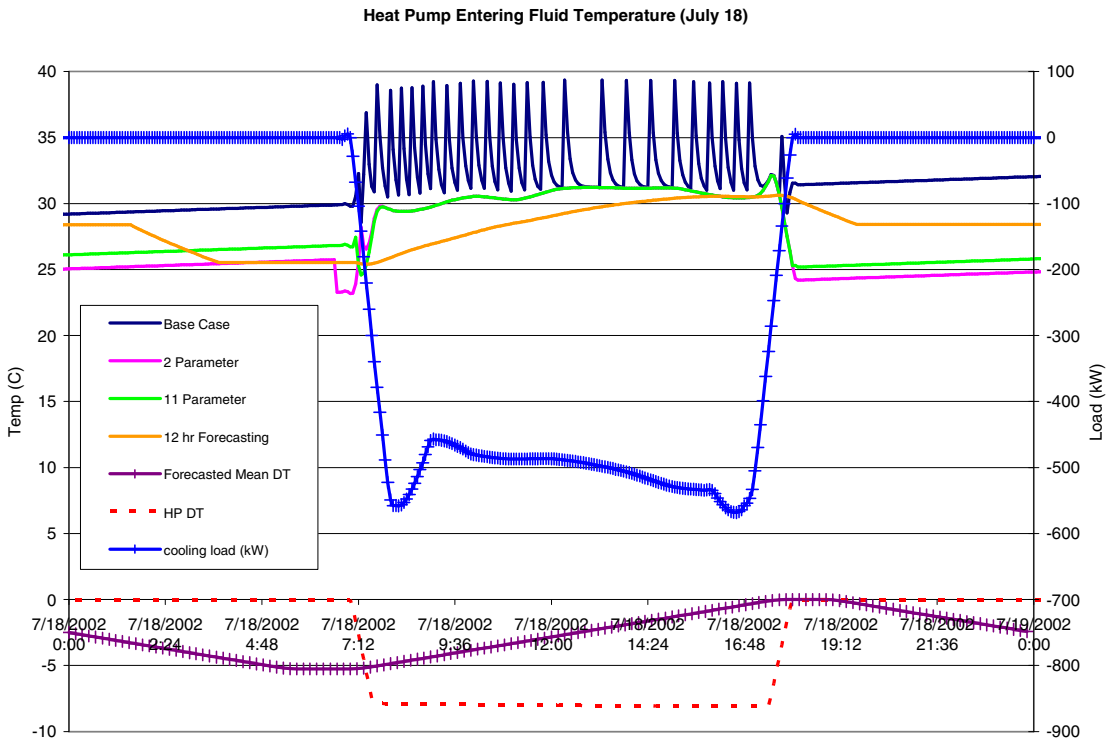

Figure 6.38 *Heat pump entering fluid temperature (July 18).*

As with the El Paso summer day, the lower heat pump entering fluid temperatures translate into higher COPs and higher cooling performance. This is shown in Figure 6.39 for the four cases on July 18. Again, the 12-hour forecasting strategy has higher COPs.

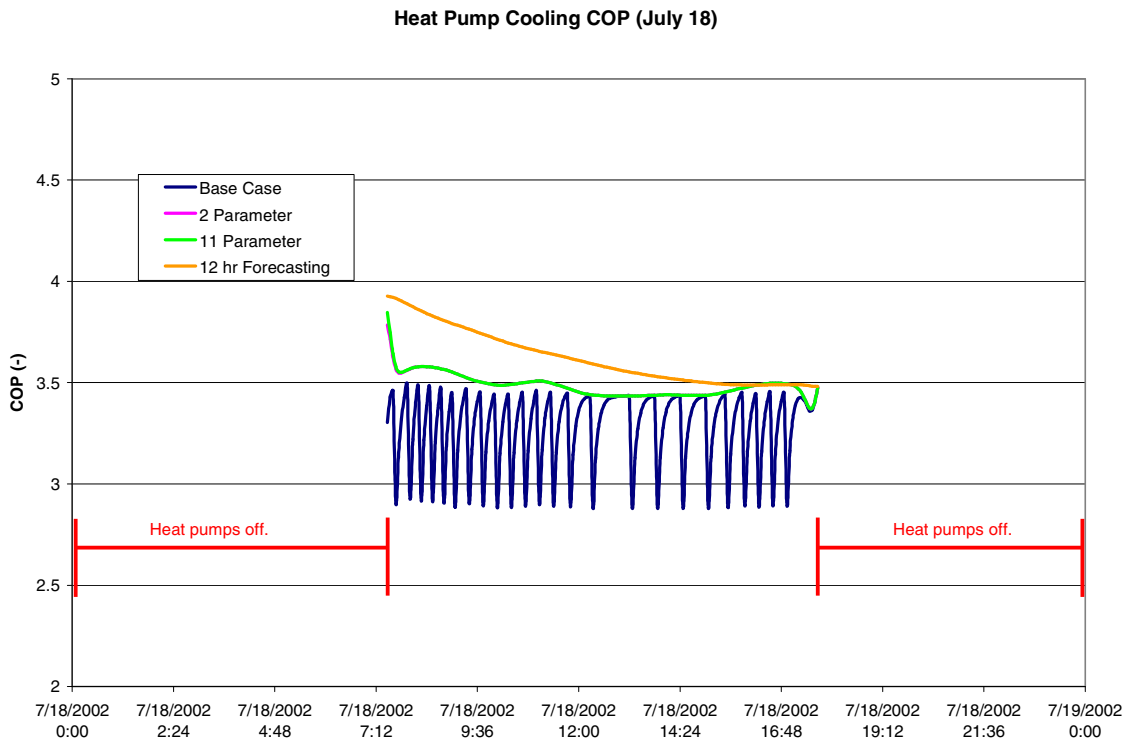

Figure 6.39 *Heat pump cooling COP (July 18).*

Figure 6.40 shows the heat pump energy consumption for July 18. Since the cooling tower operates continuously for the 2-parameter and 11-parameter cases there is no apparent difference in heat pump energy consumption for the day. Again, the potential for the forecasting and thermal mass augmentation strategy is shown by the lower heat pump energy consumption for the day.

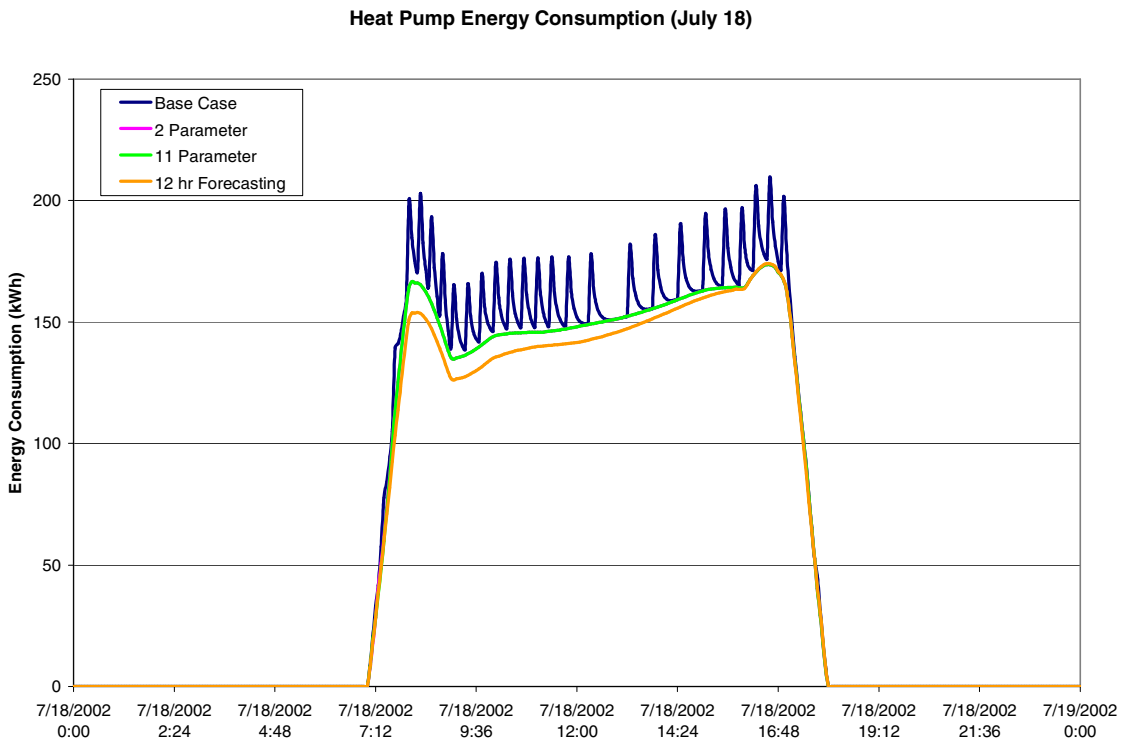

Figure 6.40 *Heat pump energy consumption (July 18).*

Table 6.12 lists the HVAC energy consumption by component and the final total HVAC energy consumption for the office building in Memphis on July 18. As is shown, the 12-hour forecasting and thermal mass augmentation case saves 5.6% of the energy used by the base case. As in El Paso, the 12-hour forecasting case continues cooling tower operation even with no load present which causes an increase in cooling tower fan and pump energy, but also allows for lowering the loop temperatures later.

Table 6.12 *HVAC energy consumption (July 18).*

Energy Consumption (kWh)	Base Case	2-Parameter	11-Parameter	12 hr Forecasting
Heat Pump	24,781	23,213	23,204	22,387
Main Circ Pump	228	228	228	228
Cooling Tower Fan	992	1,215	1,215	1,641
Cooling Tower Circ Pump	390	478	478	648
Boiler	0	0	0	0
Boiler Circ Pump	0	0	0	0
Total	**26,390**	**25,134**	**25,125**	**24,904**

Finally, the monthly energy consumption by component was plotted, Figure 6.41, for each of the four cases. As is shown, the 12-hour forecasting saves more energy over the other 3 cases during the shoulder season than it does during the warmer months, where the savings potential over the 2-parameter and 11-parameter is not as high. This is largely due to thermal storage and boiler operation. As can be seen the 12-hour forecasting case requires less than half the boiler operation required by the other 3 cases for the months of January and February and the boiler requires no operation during the month of December. This was also shown in the detailed results above with savings of over 29.4% during the shoulder season day of March 11, and only 5.6% during the summer day of July 18. The energy that is saved during those shoulder months adds up to give the extra savings potential that is shown in Figure 6.21.

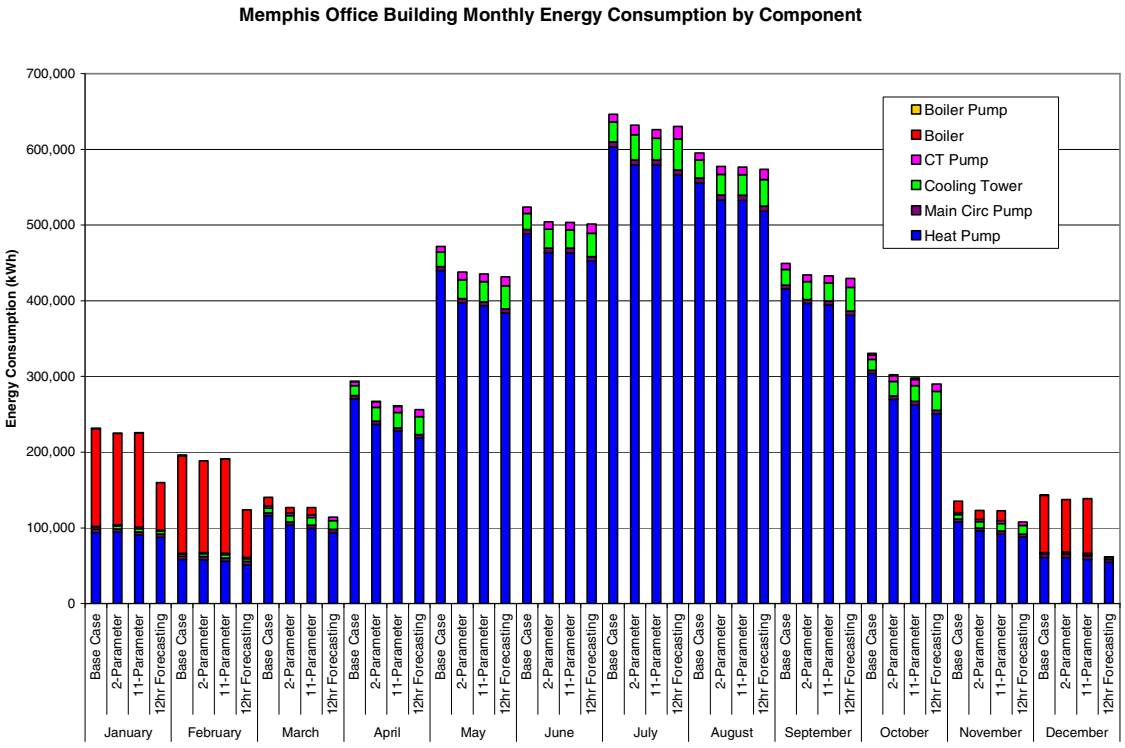

Figure 6.41 *Monthly HVAC energy consumption comparison for the office building in Memphis.*

6.6. Conclusions/Recommendations

This chapter described the optimization of controls for WLHP systems. It is shown that for all optimized cases investigated there is the potential for savings over the base case strategy. It should be noted that although the control strategies were optimized, that does not guarantee that the global minimum has been found in every case. In some cases, actual energy savings might be higher than those presented.

First, a 2-parameter control strategy (fixed boiler and cooling tower setpoints) was optimized for two buildings in 13 locations giving savings over the base case ranging from 1.0% to 18.2%.

Next, an 11-parameter control strategy (10 cooling tower parameters and 1 boiler parameter) was optimized for the two buildings and 13 locations giving savings from 1.1% to 18.3%.

A 2-parameter common control strategy was investigated next, but no entirely satisfactory recommendation can be made because of the sensitivity of the parameters to climate.

A 7-parameter common control strategy (6 cooling tower parameters and 1 boiler parameter) was investigated that dynamically changes the cooling tower setpoint based on a setpoint profile and the temperature difference of the heat pumps in the WLHP system. The results illustrated that while the common control strategies did not perform quite as well as the optimized strategies, they gave very good results and can be recommended for use.

Two exploratory control strategies were investigated. A control strategy that utilizes the outdoor wet-bulb temperature proved to have little additional savings potential to the already optimized 11-parameter control strategy. However, a control strategy utilizing forecasting and augmented thermal mass did prove to add savings

potential and should be investigated further. Savings range from 0.8% to 6.3% over the optimized 11-parameter case.

Recommendations for further research and development include the following:

1. The control strategies investigated in this work all used the ΔT across the heat pump as an indicator of the relative dominance of heating or cooling at any moment in time. An improvement that should be investigated would incorporate some measure of flow, perhaps the control signal to the variable speed drive for the pump, to make this a more accurate indicator.
2. Thermal storage was shown to have a significant impact on system performance, even when the forecasting control strategy did little forecasting. As real-world forecasting will introduce additional challenges, it would be worth investigating non-forecasting control strategies for WLHP systems with augmented thermal mass.
3. Likewise, it might be possible to use, as an alternative to forecasting, information from the previous day, with the assumption that the coming day will be similar.
4. Since the thermal storage was shown to have a significant impact, a range of thermal storage tank sizes and stratified thermal storage are worth investigating.
5. Only one forecasting period (12 hours) was investigated and all forecasted ΔT were averaged with uniform weight; different periods and different weightings should be investigated, and the relationship between

augmented thermal mass and the forecasting period should be investigated.

6. Only one action was investigated for the forecasting portion of the forecasting control strategy – adjusting the cooling tower setpoint up or down based on the forecast. However, other strategies could and should be investigated. For example, it would be possible, once having determined that a significant cooling load is forecast for the next day, to run the cooling tower to cool the storage tank. This could be controlled by running it until the rate of change of the tank temperature had fallen to a low level, indicating that the tank had been lowered to the minimum economically-feasible temperature. Or, with the same forecast, the cooling tower could be operated in the middle of the night to reduce the tank temperature for the next day.
7. This study had two building types, two system configurations (with and without augmented thermal mass), and thirteen locations. However, there are a number of aspects of the WLHP system that were kept fixed, and which may have an effect on the optimal setpoints and savings. Possible variations that should be investigated include heat pump type, design flow rate for each heat pump, minimum flow fraction for the main loop, part-load pump characteristics, variable airflow cooling towers, cooling tower size, etc.
8. Analyzing different electricity rate structures other than the $0.08/kW-hr used for every location for this study should be investigated.

7. SUMMARY, CONCLUSIONS & RECOMMENDATIONS

Chapters 1 through 3 described the simulation and experimental validation of a hybrid ground source heat pump (HGSHP) system that used a cooling tower as its supplemental heat rejecter. The validation of such systems is previously unreported in literature. Seven months of experimental data from OSU's HGSHP research facility was used for the validation. Validation of the system was considered from two perspectives, the design engineer's perspective and the researcher's perspective.

Chapters 4 through 6 described the simulation, validation, and controls optimization of water loop heat pump (WLHP) systems. Two types of validation were done; a short experimental validation and an intermodel validation between HVACSim+ and EnergyPlus. Four days of experimental data from OSU's HGSHP research facility were used for the experimental validation. Several different control strategies were investigated and optimized. A dynamic common control strategy was found that can be applied to various building types in different climate zones. A set of parameters was found for use in very cold climate regions and another set of parameters was found four use in mixed, warm, and hot climate regions. Exploratory investigations of two types of control strategies were investigated. The first added an outdoor wet-bulb temperature

parameter and the second added forecasting future loads, and had augmented thermal storage.

7.1. Conclusions (Chapters 1-3)

- The predicted HGSHP system simulation matched very well to experimental results when each component was calibrated.
- The system simulation had the advantage of perfect knowledge of the system loads and near-perfect knowledge of the weather. No designer will have these advantages!
- The goodness of the results for the uncalibrated model certainly relied on mitigating errors, with the largest problem occurring due to operating the heat pumps outside the range of catalog data provided by the manufacturer. Caution is warranted in applying equation-fit models outside the range of data used to fit the data. This is illustrated by the succession of "incremental improvements" to the system simulation, which improve the accuracy. The "best" simulation with all "improvements" gives total energy consumption 4.6% less than the experiment, where as the simulation with the improved heat pump model gives total energy consumption about 6% less than the experiment. Whereas the temperature response of the simulated results largely improved compared to the experimental results, the overall energy consumption also improved.

- From the designers' perspective, the performance of the system simulation with all models relying only on manufacturers' data was quite good and should be acceptable for design purposes.
- The system simulation here relies on experimental measurements for heat losses and gains in buried and exposed piping. Use of models for the piping losses/gains would introduce additional error.
- More manufacturer's data is needed for equipment such as cooling towers and plate heat exchangers to better model performance.

7.2. Recommendations (Chapters 1-3)

Recommendations for further research and development include the following:

1. For designers, an HGSHP design procedure that would optimally size the cooling tower and ground loop heat exchanger is needed.
2. As horizontally-buried piping is a common feature of GSHP and HGSHP systems, it would be useful to have a component model that covers this feature.
3. The equation-fit-based heat pump model used here performed poorly with catalog data. This was largely due to the fact that it was operated well outside the catalog data range. A parameter-estimation-based model and/or some checks on the input data to the model combined with some more intelligent extrapolation should be investigated.
4. The sensitivity of the cooling tower results to the uncertainty in wet-bulb temperature suggests caution by practitioners when using control based on the

wet-bulb temperature. Further research into control strategies that either does not depend on the wet-bulb temperature or that only partly depend on the wet-bulb temperature is warranted.

5. While it is almost certainly impossible to predict fouling in an accurate manner, research that investigates fouling scenarios and approximate approaches may make it possible to develop recommendations for designers. Also, fouling factors for the system with cooling towers should be investigated and tabulated for designers' use.

7.3. Conclusions (Chapters 4-6)

- The WLHP system simulation predicted HVAC energy consumption very well compared to experimental data when the components were calibrated.
- The WLHP system simulation in HVACSim+ matched the temperature response very well compared to system simulation in EnergyPlus with slight variation caused by slightly different loop mass for the two systems.
- A range of control strategies were investigated
    - 2-parameters, a fixed boiler and cooling tower setpoint, individually optimized gave a range of savings over the base case (15.6ºC (60ºF) – 32.2ºC (90ºF)) of 1.0% to 18.2%.
    - Several attempts were made to develop a common 2-parameter control strategy, but because the individually optimized 2-parameter setpoints varied widely all attempts proved unsuccessful.

- 11-parameters (10 cooling tower parameters and 1 boiler parameter) were used to develop a dynamic cooling tower control profile that varied the setpoint based on heat pump entering fluid temperature and the temperature difference across the heat pumps. The parameters were individually optimized for two building types in 13 locations and gave results ranging from 1.1% to 18.3% over the base case.
- A 7-parameter (6 cooling tower parameters and 1 boiler parameter) common control strategy was developed that was based on the individually optimized 11-parameter profiles. The control strategy did not give results as good as the optimized 11-parameter strategy, but gave results that were reasonably good for each building in every location, ranging between 0.9% and 18.1% compared to the base case and can be recommended for use.
- An exploratory investigation was performed by adding an outdoor wet-bulb temperature parameter, but showed very little additional savings over the optimized 11-parameter.
- An exploratory investigation of a control strategy that used forecasting with augmented thermal mass showed excellent potential. Savings ranged from 0.8% to 6.3% over the individually optimized 11-parameter case.

7.4. Recommendations (Chapters 4-6)

Recommendations for further research and development include the following:

1. It would be beneficial to have more experimental data and have experimental data available for both heating and cooling seasons to use for a longer term validation.
2. Further work to help predict fouling of the plate heat exchanger would be useful.
3. Since the control strategies investigated with this work all depended on the ΔT across the heat pumps for indicating the mode of operation (relative dominance of heat or cooling at any time), and this is not an accurate measure, different measures should be investigated such as using a flow sensor to more accurately indicate the variation between heating and cooling.
4. Only one forecasting period (12 hours) was investigated and all forecasted ΔT were averaged with uniform weight; different periods and different weightings should be investigated, and the relationship between augmented thermal mass and the forecasting period should be investigated.
5. As the prediction of future loads is problematic, it would be worth investigating the use of information from the previous day, with the assumption that the coming day would be similar.
6. Thermal storage should be investigated further to determine the feasibility and savings potential of adding a thermal storage tank to the loop without forecasting controls and investigations should be done into the optimal sizing of the tanks. As this work utilized a mixed tank, further investigation should be done into the use of stratified tanks.
7. Only one action was investigated for the forecasting portion of the forecasting control strategy – adjusting the cooling tower setpoint up or down based on the forecast. However, other strategies could and should be investigated. For

example, it would be possible, once having determined that a significant cooling load is forecast for the next day, to run the cooling tower to cool the storage tank. This could be controlled by running it until the rate of change of the tank temperature had fallen to a low level, indicating that the tank had been lowered to the minimum economically-feasible temperature. Or, with the same forecast, the cooling tower could be operated in the middle of the night to reduce the tank temperature for the next day.

8. Analyzing different electricity rate structures other than the $0.08/kW-hr used for every location for this study should be investigated.
9. As this study investigated two building types and 13 locations, more work should be done into different building types and more locations. The 3 U.S. climate zones that were not investigated with this work should definitely be investigated.
10. Many aspects of the WLHP system were kept fixed which may have an effect on the optimal setpoints and overall energy savings. Variations in design should be investigated. Possible areas of investigation are;
    1. heat pump type and design flow rate
    2. minimum flow fraction for the main loop
    3. part-load pump characteristics
    4. larger cooling tower sizes
    5. variable airflow cooling towers

REFERENCES

Amcot. 2005. The Amcot Silver Series Cooling Tower. Retrieved October 14, 2005. (http://www.amcot.com/temp/Fiberglass.pdf).

ASHRAE. 1995. Commercial/Institutional Ground-Source Heat Pumps Engineering Manual. Atlanta: American Society of Heating, Refrigerating and Air-Conditioning Engineers, Inc.

ASHRAE. 1999. 1999 ASHRAE Handbook—HVAC Applications, chapter 31. Atlanta. American Society of Heating, Refrigerating and Air-Conditioning Engineers, Inc.

ASHRAE. 2000. 2000 ASHRAE Handbook—Cooling Towers, chapter 36. Atlanta. American Society of Heating, Refrigerating and Air-Conditioning Engineers, Inc.

ASHRAE. 2004. ANSI/ASHRAE/IESNA Standard 90.1-2004, Energy Standard for Buildings Except Low-Rise Residential Buildings. Atlanta. American Society of Heating, Refrigerating and Air-Conditioning Engineers, Inc.

Austin, W., C. Yavuzturk, J.D. Spitler. 2000. Development Of An In-Situ System For Measuring Ground Thermal Properties. *ASHRAE Transactions* 106(1):365-379.

Briggs, R., R. Lucas, Z. Taylor. 2002. Climate Classification for Building Energy Codes and Standards. Pacific NW National Laboratory Technical Paper Final Review Draft. Richland , Washington.

California Energy Commission. 2005. 2005 Building Energy Efficiency Standards Nonresidential Compliance Manual. CEC-400-2005-006-CMF Revision 3. California.

Cane, R. L. D., Clemes, S. B., and Forgas D. A., 1993. Validation of Water-Loop Heat Pump System Modeling. ASHRAE Transactions, vol.99, Part 2, pp. 3-12.

Chen, X. 1996. Addition of Annual Building Energy Analysis Capability to a Design Load Calculation Program. M.S. thesis, Oklahoma State University, School of Mechanical and Aerospace Engineering. Available online at www.hvac.okstate.edu.

Chiasson, A. D., C. Yavuzturk. 2003. Assessment of the Viability of Hybrid Geothermal Heat Pump Systems with Solar Thermal Collectors. *ASHRAE Transactions* 109(2):487-500.

Clark, D. R. 1985. HVACSIM+ Building Systems and Equipment Simulation Program Reference Manual. NBSIR 84-2996. National Bureau of Standards.

Crawley, D.B., L.K. Lawrie, F.C. Winkelmann, W. F. Buhl, C.O. Pedersen, R.K. Strand, R.J. Liesen, D.E. Fisher, M.J. Witte, R.H. Henninger, J. Glazer, and D.B. Shirey., 2002. *EnergyPlus: New, Capable, and Linked*. Proceedings of the eSim 2002 conference, Montreal, Quebec, Canada, IBPSA-Canada.

Department of Energy. 2001. Assessment of Hybrid Geothermal Heat Pump Systems: Geothermal heat pumps offer attractive choice for space conditioning and water heating. DOE/EE-0258.

Department of Energy. 2003. Map of Proposed Climate Zones. Created March 24, 2003. Retrieved February 16, 2007. <http://www.energycodes.gov/implement/pdfs/color_map_climate_zones_Mar03.pdf>

DesignBuilder Software Ltd. 2006. DesignBuilder Software. Retrieved January 24, 2006 <http://www.designbuilder.co.uk/>.

Eskilson, P. 1987. *Thermal Analysis of Heat Extraction Boreholes*. Doctoral Thesis. University of Lund, Department of Mathematical Physics. Lund, Sweden.

Feng, Xue-Fei, 1999. Energy analysis of BOK Building. M.S. thesis, Oklahoma State University, School of Mechanical and Aerospace Engineering. Available online at www.hvac.okstate.edu.

Florida Heat Pump, 2005. Water to Water Domestic Water Heater Specification Data Sheet FHP Manufacturing Energy Wise HVAC Equipment. Page 7. Last updated April 2001. Retrieved December 1, 2005. (http://www.fhp-mfg.com/newpdfs/WP_WW/WP_Spec.pdf)

Gehlin, S., and B. Nordell. (2003). Determining undisturbed ground temperatures for thermal response test. *ASHRAE Transactions*. 109(1): 151-156.

Hensley, J.C., 1983. Cooling Tower Fundamentals. The Marley Cooling Tower Company, Kansas City, MO.

Hern, S. 2004. *Design of an Experimental Facility for Hybrid Ground Source Heat Pump Systems*. M.S. Thesis, Oklahoma State University, School of Mechanical and Aerospace Engineering. Available online at www.hvac.okstate.edu.

Howell, R. H., 1988. Energy Requirements For Closed Loop Storage Heat Pump Systems With Different Internal Loads For Various Geographic Locations. ASHRAE Transactions, vol.94, Part 1, pp. 1679-1690.

Howell, R. H., and Zaidi, J. H., 1990. Analysis of Heat Recovery in Water-Loop Heat Pump Systems. ASHRAE Transactions, vol.96, Part 1, pp. 1039-1047.

Howell, R. H., and Zaidi, J. H., 1991. Heat Recovery in Buildings Using Water-Loop Heat Pump Systems: Part 1-Energy Requirements and Savings. ASHRAE Transactions, vol.97, Part 2, pp. 736-749.

Hughes, P. J., 1990. Survey of Water-Source Heat Pump System Configurations in Current Practice. ASHRAE Transactions, vol.96, Part 1, pp.1021-1028.

Incropera, F.P., and DeWitt, D.P., 2002. *Fundamentals of Heat and Mass Transfer*. 5th ed. John Wiley & Sons, Hoboken, NJ.

Jin, H. and Spitler, J.D. 2003. Parameter Estimation Based Model of Water-to-Water Heat Pumps with Scroll Compressors and Water/Glycol Solutions. Building Services Engineering Research and Technology. 24(3):203-219.

Kavanaugh, S. P., and K. Rafferty. 1997. *Ground-source heat pumps: Design of geothermal systems for commercial and institutional buildings*. Atlanta: American Society of Heating, Refrigerating and Air-Conditioning Engineers, Inc.

Kavanaugh, S.P. 1998. A design method for hybrid groundsource heat pumps. *ASHRAE Transactions* 104(2):691- 698.

Khan, M.H., A. Varanasi, J.D. Spitler, D.E. Fisher, R.D. Delahoussaye. 2003. Hybrid Ground Source Heat Pump System Simulation Using Visual Modeling Tool For Hvacsim+. Proceedings of Building Simulation 2003 pp. 641-648. Eindhoven, Netherlands.

Khan, M. 2004. Modeling, Simulation and Optimization of Ground Source Heat Pump Systems. M.S. Thesis, Oklahoma State University, School of Mechanical and Aerospace Engineering. Available online at www.hvac.okstate.edu.

Kush, E.A., 1990. Detailed Field Study of a Water-Loop Heat Pump System. ASHRAE Transactions, vol.96, Part 1, pp. 1048-1063.

Kush, E.A., and Brunner, C. A., 1991. Field Test Results Applied to Optimizing Water-Loop Heat Pump Design and Performance. ASHRAE Transactions, vol.97, Part 2, pp. 727-735.

Lebrun, J., and Silva, C.A. 2002. Cooling tower – model and experimental validation. *ASHRAE Transactions* 108(1):751-759.

McLain, H.A., and M. Martin. 1999. A preliminary evaluation of the DOE-2.1E ground vertical well model using Maxey School measured data. *ASHRAE Transactions* 105(2): 1233-1244.

McQuiston, F.C., Parker, J.D., and Spitler, J.D., 2005. Heating, Ventilating, and Air Conditioning: Analysis and Design. 6th ed. John Wiley & Sons, Hoboken, NJ.

Palahanska-Mavrov, M., Wang, G., and Liu, M., 2006. Optimal Supply Water Temperature Control of Water Source Heat Pump. International Solar Energy Conference, Solar Engineering 2005 - Proceedings of the 2005 International Solar Energy Conference, pp. 317-323.

Phetteplace, G., and W. Sullivan. 1998. Performance of a hybrid ground-coupled heat pump system. *ASHRAE Transactions* 104(1):763-770.

Pietsch, J. A., 1990. Water-Loop Heat Pump Systems Assessment. ASHRAE Transactions, vol.96, Part 1, pp. 1029-1038.

Pietsch, J. A., 1991. Optimization of Loop Temperatures in Water-Loop Heat Pump Systems. ASHRAE Transactions, vol.97, Part 2, pp. 713-726.

Rabehl, R.J., J.W. Mitchell, and W.A. Beckman. 1999. Parameter Estimation and the Use of Catalog Data in Modeling Heat Exchangers and Coils. HVAC&R Research 5(1):3-17.

Ramamoorthy, M. H. Jin, A. Chiasson, J.D. Spitler. 2001. Optimal Sizing of Hybrid Ground-Source Heat Pump Systems that use a Cooling Pond as a Supplemental Heat Rejecter – A System Simulation Approach. *ASHRAE Transactions* 107(1):26-38.

Sanner, B., Hellström,G., Spitler, J.D. and Gehlin, S. 2005. Thermal Response Test – Current Status and World-Wide Application. Proceedings World Geothermal Congress 2005, Antalya, Turkey April 24-29.

Shonder, J.A., and J. Beck. 2000. Field Test of a New Method for Determining Soil Formation Thermal Conductivity and Borehole Resistance. *ASHRAE Transactions* 106(1): 843-850.

Singh, J.B., and G. Foster. 1998. Advantages of Using the Hybrid Geothermal Option. The Second Stockholm International Geothermal Conference. The Richard Stockton College of New Jersey.

Spitler, J.D., 2006. Personal Communication.

Tang, C.C. 2005. *Modeling Packaged Heat Pumps In A Quasi-Steady State Energy Simulation Program.* M.S. Thesis, Oklahoma State University, School of Mechanical and Aerospace Engineering. Available online at www.hvac.okstate.edu.

Thornton, J.W., T.P. McDowell, J.A. Shonder, P.J. Hughes, D. Pahud, and G. Hellstrom. 1997. Residential vertical geothermal heat pump system models: Calibration to data. *ASHRAE Transactions* 103 (2): 660-674.

Varanasi, A. 2002. Visual Modeling Tool for HVACSIM+. M.S. Thesis, Oklahoma State University, School of Mechanical and Aerospace Engineering. Available online at www.hvac.okstate.edu.

Wetter, M. 2000. GenOpt Generic Optimization Program. Lawrence Berkeley National Laboratory.

Wetter, M. 2004. Simulation-Based Building Energy Optimization. PhD Thesis, University of California, Berkeley.

Xu, X. 2006. Personal Communication.

Xu, X., J. D. Spitler. 2006. Modeling of Vertical Ground Loop Heat Exchangers with Variable Convective Resistance and Thermal Mass of the Fluid. Proceedings of the 10th International Conference on Thermal Energy Storage. Ecostock 2006, Pomona, NJ.

Yavuzturk, C., J.D. Spitler. 1999. A Short Time step Response Factor Model for Vertical Ground Loop Heat Exchangers. *ASHRAE Transactions* 105(2): 475-485.

Yavuzturk, C., J.D. Spitler. 2000. Comparative Study to Investigate Operating and control Strategies for Hybrid Ground Source Heat Pump Systems Using a Short Time step Simulation Model. *ASHRAE Transactions* 106(2):192-209.

Yavuzturk, C. and J.D. Spitler. 2001. Field Validation of a short time step model for vertical ground-loop heat exchangers. *ASHRAE Transactions* 107(1): 618-626.

Young, R. (2004). Development, Verification, and Design Analysis of the Borehole Fluid Thermal Mass Model for Approximating Short Term Borehole Thermal Response. M.S. Thesis, Oklahoma State University, School of Mechanical and Aerospace Engineering. Available online at www.hvac.okstate.edu.

APPENDIX A

Gang Heat Pump Model IDD

```
GANG HEAT PUMP:SIMPLE,
\memo This heat pump model is an adaptation of XIAOWEI \XU's Type555
HVACSim+ Model
   A1,  \field Heat Pump Name
        \required-field
   A2,  \field Source Side Inlet Node
        \required-field
   A3,  \field Source Side Outlet Node
        \required-field
   A4,  \field Heating Load Schedule
        \required-field
        \type object-list
        \object-list ScheduleNames
   A5,  \field Cooling Load Schedule
        \required-field
        \type object-list
        \object-list ScheduleNames
   N1,  \field Number of Heat Pumps in Gang
        \required-field
        \type real
        \minimum> 0.0
         \default 1
   N2,  \field Total System Mass Flow Rate
        \required-field
        \type real
        \minimum> 0.0
```

```
     \units m3/s
N3,  \field Heating COP Coefficient 1
     \required-field
     \type real
N4,  \field Heating COP Coefficient 2
     \required-field
     \type real
N5,  \field Heating COP Coefficient 3
     \required-field
     \type real
N6,  \field Heating COP Coefficient 4
     \required-field
     \type real
N7,  \field Heating COP Coefficient 5
     \required-field
     \type real
N8,  \field Heating COP Coefficient 6
     \required-field
     \type real
N9,  \field Cooling COP Coefficient 1
     \required-field
     \type real
N10, \field Cooling COP Coefficient 2
     \required-field
     \type real
N11, \field Cooling COP Coefficient 3
     \required-field
     \type real
N12, \field Cooling COP Coefficient 4
     \required-field
     \type real
N13, \field Cooling COP Coefficient 5
     \required-field
     \type real
N14, \field Cooling COP Coefficient 6
     \required-field
     \type real
```

```
N15, \field Heating System Mass Flow Rate
     \required-field
     \type real
     \minimum> 0.0
     \units m3/s
N16, \field Cooling System Mass Flow Rate
     \required-field
     \type real
     \minimum> 0.0
     \units m3/s
N17, \field Heating Capacity
     \required-field
     \type real
     \minimum> 0.0
     \units W
N18; \field Cooling Capacity
     \required-field
     \type real
     \minimum> 0.0
     \units W
```

WLHP Controller Model IDD

```
WLHP OPTIMAL SETPOINT BASED OPERATION,
   A1, \field Name
       \required-field
       \reference ControlSchemeList
   A2, \field Pietsch heat pump List
       \required-field
       \type object-list
       \object-list Pietschheatpumplist
   A3, \field Priority Control Loop
       \required-field
       \type alpha
   N1 ,\field Minimum X Boiler Set Point
       \required-field
       \type real
       \units C
       \minimum -100
       \maximum 100
   N2 ,\field Minimum Y Boiler Set Point
       \required-field
       \type real
       \units C
       \minimum 0
       \maximum 100
   N3 ,\field Middle X Boiler Set Point
       \required-field
       \type real
       \units C
       \minimum -100
       \maximum 100
   N4 ,\field Middle Y Boiler Set Point
       \required-field
       \type real
       \units C
       \minimum 0
```

```
    \maximum 100
N5 ,\field Maximum X Boiler Set Point
    \required-field
    \type real
    \units C
    \minimum 0
    \maximum 100
N6 ,\field Maximum Y Boiler Set Point
    \required-field
    \type real
    \units C
    \minimum 0
    \maximum 100
N7 ,\field Minimum X CT Set Point
    \required-field
    \type real
    \units C
    \minimum -100
    \maximum 100
N8 ,\field Minimum Y CT Set Point
    \required-field
    \type real
    \units C
    \minimum 0
    \maximum 100
N9 ,\field Middle X CT Set Point
    \required-field
    \type real
    \units C
    \minimum -100
    \maximum 100
N10 ,\field Middle Y CT Set Point
    \required-field
    \type real
    \units C
    \minimum 0
    \maximum 100
```

```
N11 ,\field Maximum X CT Set Point
    \required-field
    \type real
    \units C
    \minimum 0
    \maximum 100
N12 ;\field Maximum Y CT Set Point
    \required-field
    \type real
    \units C
    \minimum 0
    \maximum 100
```

APPENDIX B

Heat Pump Data and COP Coefficients – Motel

Heat pump used – ClimateMaster CCE07 at a design flow rate of 1.4 GPM (0.088 kg/s)

EWT (°F)	GPM	WPD		Cooling-EAT 80/67°F						Heating-EAT 70°F				
		PSI	FT	TC	SC	Sens/Tot Ratio	kW	HR	EER	HC	kW	HE	LAT	COP
20	1.9	3.7	8.5							5.5	0.5	3.8	91	3.22
30	1	1.4	3.2	9.7	6.9	0.71	0.36	10.9	26.7	6	0.51	4.3	93.1	3.44
	1.4	2.2	5.1	9.8	6.9	0.7	0.33	10.9	29.9	6.3	0.52	4.5	94.1	3.55
	1.9	3.3	7.6	9.9	6.9	0.7	0.31	10.9	31.7	6.4	0.52	4.7	94.8	3.62
40	1	1	2.3	9.4	6.8	0.72	0.41	10.8	22.9	6.9	0.53	5.1	96.5	3.79
	1.4	1.5	3.5	9.6	6.9	0.71	0.37	10.9	25.8	7.2	0.54	5.4	97.9	3.91
	1.9	2.1	4.9	9.7	6.9	0.71	0.36	10.9	27.4	7.4	0.55	5.6	98.6	3.97
50	1	0.9	2.1	9	6.7	0.74	0.46	10.6	19.6	7.8	0.56	5.9	100	4.1
	1.4	1.4	3.2	9.3	6.8	0.73	0.42	10.8	22.1	8.2	0.57	6.3	101.6	4.23
	1.9	2	4.6	9.5	6.8	0.72	0.4	10.8	23.4	8.4	0.57	6.5	102.4	4.3
60	1	0.8	1.8	8.6	6.5	0.76	0.52	10.4	16.6	8.7	0.58	6.7	103.6	4.39
	1.4	1.3	3	8.9	6.6	0.74	0.48	10.5	18.8	9.2	0.59	7.2	105.4	4.53
	1.9	1.9	4.4	9.1	6.7	0.74	0.46	10.6	20	9.4	0.6	7.4	106.3	4.61
70	1	0.7	1.6	8.1	6.3	0.78	0.58	10.1	14	9.6	0.61	7.6	107.1	4.67
	1.4	1.2	2.8	8.5	6.5	0.76	0.53	10.3	15.9	10.2	0.62	8.1	109.1	4.82
	1.9	1.8	4.2	8.6	6.5	0.76	0.51	10.4	16.9	10.5	0.63	8.3	110.2	4.9
80	1	0.7	1.6	7.6	6.1	0.79	0.65	9.8	11.8	10.6	0.63	8.4	110.7	4.93
	1.4	1.1	2.5	8	6.2	0.78	0.6	10	13.3	11.1	0.64	9	112.9	5.1
	1.9	1.6	3.7	8.1	6.3	0.78	0.57	10.1	14.2	11.5	0.65	9.3	114.1	5.19
85	1	0.6	1.4	7.4	5.9	0.8	0.68	9.7	10.8	11	0.64	8.9	112.5	5.06
	1.4	1	2.3	7.7	6.1	0.79	0.63	9.9	12.2	11.6	0.65	9.4	114.8	5.24
	1.9	1.5	3.5	7.9	6.2	0.78	0.61	10	13	12	0.66	9.7	116.1	5.33
90	1	0.6	1.4	7.2	5.8	0.81	0.72	9.6	9.9	11.5	0.65	9.3	114.2	5.19
	1.4	1	2.3	7.5	6	0.8	0.67	9.8	11.1	12.1	0.66	9.9	116.7	5.38
	1.9	1.4	3.2	7.6	6.1	0.79	0.64	9.8	11.9	12.5	0.67	10.2	118	5.48
100	1	0.5	1.2	6.7	5.5	0.81	0.81	9.5	8.3					
	1.4	0.9	2.1	7	5.7	0.81	0.75	9.6	9.3					
	1.9	1.3	3	7.2	5.8	0.81	0.72	9.6	9.9					
110	1	0.5	1.2	6.4	5.2	0.81	0.91	9.5	7					
	1.4	0.9	2.1	6.6	5.4	0.81	0.84	9.5	7.8					
	1.9	1.3	3	6.7	5.5	0.81	0.81	9.5	8.3					

COP Coefficients

Heating	C1	2.87548
	C2	0.05659
	C3	-0.00027
	C4	13.89410
	C5	-60.19299
	C6	0.06440
Cooling	C7	5.66454
	C8	-0.17731
	C9	0.00173
	C10	36.09242
	C11	-65.15757
	C12	-0.42544

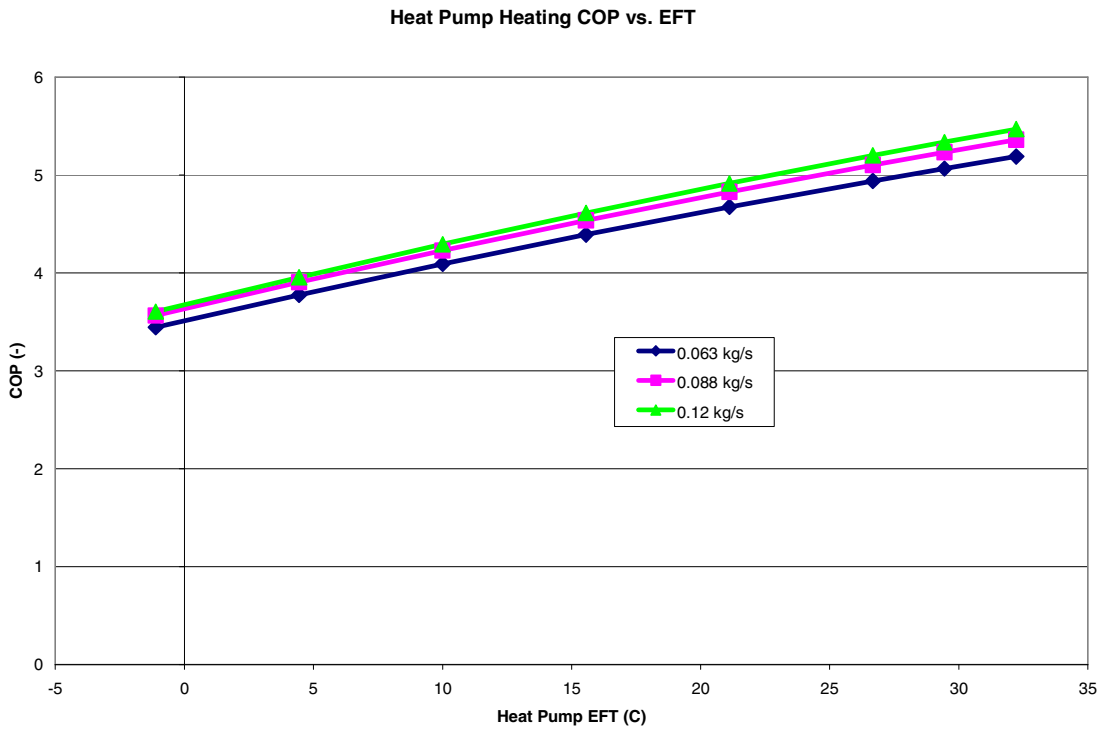

Heat pump heating COP vs. entering fluid temperature

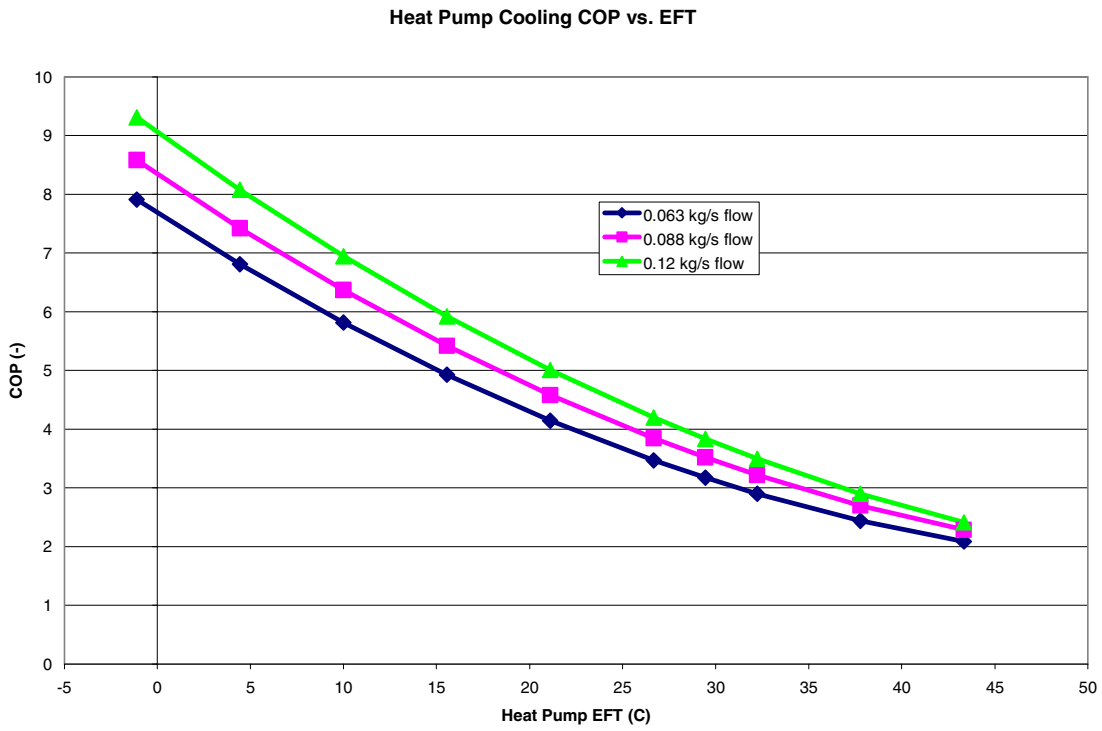

Heat pump cooling COP vs. entering fluid temperature

Heat Pump Data and COP Coefficients – Office Building

Heat pump used – ClimateMaster GS060 at a design flow rate of 11.3 GPM (0.71 kg/s)

EWT (°F)	GPM	WPD		Cooling-EAT 80/67°F						Heating-EAT 70°F				
		PSI	FT	TC	SC	Sens/Tot Ratio	kW	HR	EER	HC	kW	HE	LAT	COP
20	15	5.1	11.8							41.5	3.99	27.9	89.2	3.05
30	7.5	1.6	3.6	68	46.8	0.69	2.73	77.4	24.9	43.8	4.05	30	90.3	3.17
	11.3	3.1	7.1	68.2	46.4	0.68	2.68	77.4	25.5	46.1	4.09	32.2	91.4	3.31
	15	4.9	11.4	68.4	46.1	0.67	2.63	77.4	26	48.5	4.13	34.4	92.4	3.44
40	7.5	1.5	3.5	65.8	46.1	0.7	3.15	76.5	20.9	51.3	4.25	36.8	93.7	3.54
	11.3	3	6.9	66	45.8	0.69	3.07	76.5	21.5	53.3	4.28	38.7	94.7	3.65
	15	4.8	11.1	66.3	45.5	0.69	2.99	76.5	22.1	55.3	4.32	40.6	95.6	3.75
50	7.5	1.5	3.4	63.5	45.5	0.72	3.58	75.7	17.8	58.7	4.44	43.5	97.2	3.87
	11.3	2.9	6.7	63.8	45.2	0.71	3.47	75.6	18.4	60.4	4.48	45.2	98	3.96
	15	4.6	10.7	64.1	44.8	0.7	3.36	75.5	19.1	62.2	4.51	46.8	98.8	4.04
60	7.5	1.4	3.3	62.6	45.3	0.72	3.9	75.9	16	66.1	4.64	50.3	100.6	4.18
	11.3	2.8	6.5	62.9	44.9	0.71	3.74	75.7	16.8	68.5	4.67	52.6	101.7	4.3
	15	4.5	10.4	63.2	44.6	0.7	3.58	75.4	17.7	71	4.71	54.9	102.9	4.42
70	7.5	1.4	3.2	61.7	45	0.73	4.23	76.1	14.6	73.5	4.83	57	104	4.46
	11.3	2.7	6.3	62	44.7	0.72	4.02	75.7	15.4	76.6	4.87	60	105.5	4.61
	15	4.3	10	62.4	44.3	0.71	3.8	75.4	16.4	79.7	4.9	63	106.9	4.77
80	7.5	1.3	3.1	58.7	44.2	0.75	4.7	74.8	12.5	80.9	5.03	63.7	107.5	4.71
	11.3	2.6	6.1	59.2	43.8	0.74	4.46	74.4	13.3	83.8	5.05	66.6	108.8	4.86
	15	4.2	9.7	59.7	43.5	0.73	4.22	74.1	14.1	86.7	5.07	69.4	110.1	5.01
90	7.5	1.3	3	55.8	43.4	0.78	5.17	73.4	10.8	88.3	5.23	70.5	110.9	4.95
	11.3	2.5	5.9	56.4	43	0.76	4.9	73.1	11.5	91	5.24	73.1	112.1	5.09
	15	4.1	9.4	56.9	42.7	0.75	4.64	72.8	12.3	93.7	5.25	75.8	113.4	5.23
100	7.5	1.2	2.9	54.4	42.9	0.79	5.72	73.9	9.5					
	11.3	2.4	5.6	54.8	42.6	0.78	5.43	73.3	10.1					
	15	3.9	9	55.3	42.2	0.76	5.14	72.8	10.7					
110	7.5	1.2	2.8	52.9	42.5	0.8	6.28	74.4	8.4					
	11.3	2.4	5.4	53.3	42.1	0.79	5.96	73.6	8.9					
	15	3.8	8.7	53.6	41.8	0.78	5.64	72.8	9.5					

COP Coefficients

Heating	C1	3.04222
	C2	0.06170
	C3	-0.00033
	C4	0.44765
	C5	0.02310
	C6	0.00396
Cooling	C7	6.58176
	C8	-0.15719
	C9	0.00126
	C10	0.57600
	C11	0.19207
	C12	0.00056

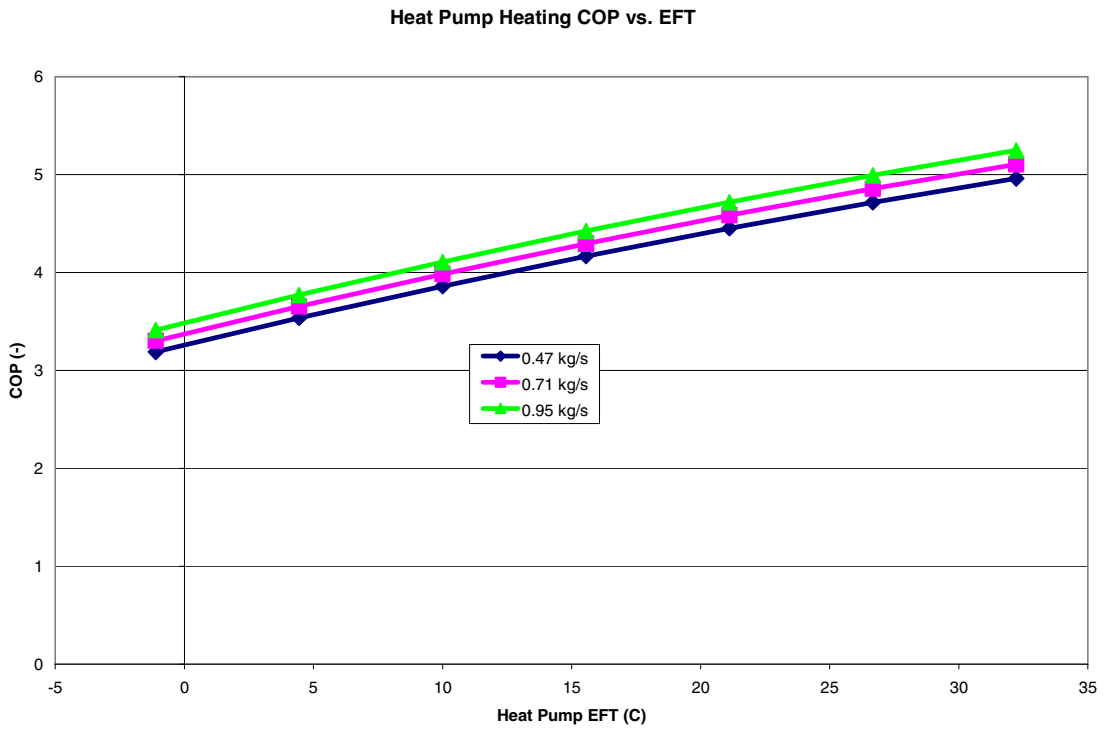

Heat pump heating COP vs. entering fluid temperature

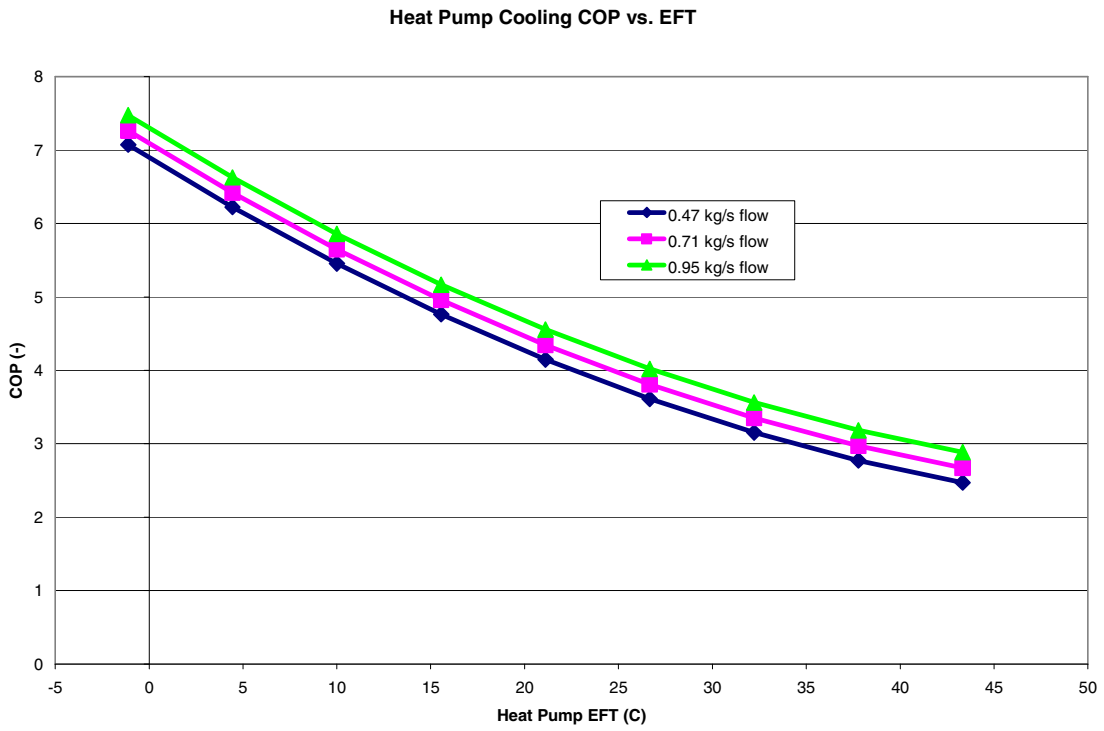

Heat pump cooling COP vs. entering fluid temperature

Variable Speed Pump Figures of FFF vs. FFP

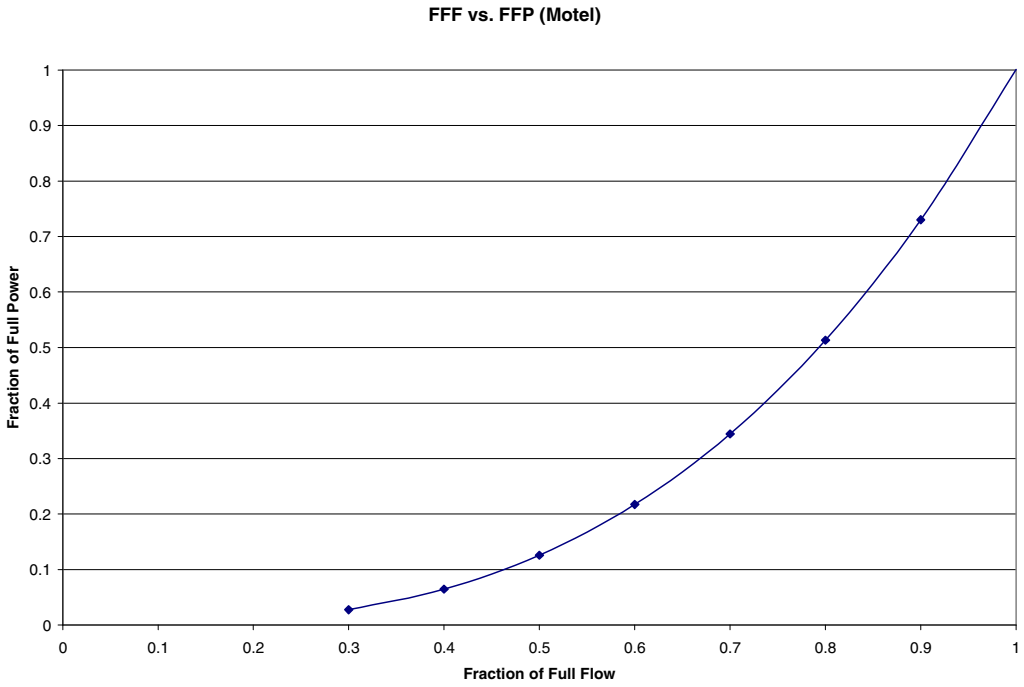

Fraction of Full Flow vs. Fraction of Full Power (Motel)

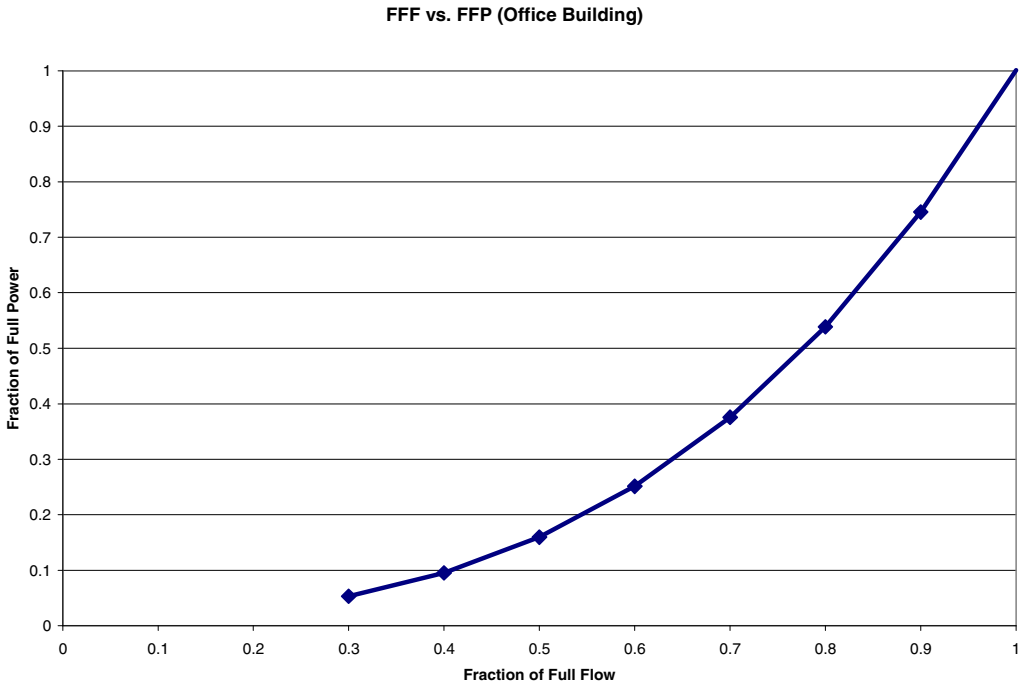

Fraction of Full Flow vs. Fraction of Full Power (Office Building)

Cooling Tower and Boiler Sizes used for WLHP Simulations

	City	Cooling Tower UA (W/K)	Cooling Tower Nominal Capacity (BTU/h)	Cooling Tower Nominal Capacity (kW)	Boiler Nominal Capacity (BTU/h)	Boiler Nominal Capacity (kW)
Motel	Albuquerque	15,685	1,500,000	439	747,125	219
	Baltimore	20,181	1,800,000	527	1,127,286	330
	Boise	15,685	1,500,000	439	1,049,297	307
	Burlington	20,181	1,800,000	527	1,351,718	396
	Chicago	15,685	1,500,000	439	1,305,797	382
	Duluth	15,685	1,500,000	439	1,415,339	414
	El Paso	15,685	1,500,000	439	408,876	120
	Fairbanks	15,685	1,500,000	439	1,527,333	447
	Houston	20,181	1,800,000	527	568,877	167
	Memphis	20,181	1,800,000	527	861,257	252
	Miami	20,181	1,800,000	527	6,050	2
	Phoenix	20,181	1,800,000	527	196,597	58
	Tulsa	20,181	1,800,000	527	1,138,167	333
Office Building	Albuquerque	39,214	3,000,000	878	2,069,455	606
	Baltimore	45,871	3,600,000	1,054	2,531,201	741
	Boise	39,214	3,000,000	878	2,844,510	833
	Burlington	34,024	2,400,000	703	3,247,351	951
	Chicago	39,214	3,000,000	878	3,161,349	926
	Duluth	39,214	3,000,000	878	3,227,136	945
	El Paso	45,871	3,600,000	1,054	1,477,526	433
	Fairbanks	34,024	2,400,000	703	3,430,616	1,005
	Houston	39,214	3,000,000	878	2,489,515	729
	Memphis	45,871	3,600,000	1,054	2,368,782	694
	Miami	39,214	3,000,000	878	428,796	126
	Phoenix	59,762	4,200,000	1,230	1,599,100	468
	Tulsa	45,871	3,600,000	1,054	2,604,180	763

APPENDIX C

Optimized 11-parameter Setpoints

		Cooling Tower Setpoints (°C)										Boiler Setpoint (°C)
		X-1	Y-1	X-2	Y-2	X-3	Y-3	X-4	Y-4	X-5	Y-5	
Motel	Albuquerque	-4.9	15.5	-1.8	17.6	0.4	30.9	5.1	31.8	5.5	32.1	12.5
	Baltimore	-7.0	17.1	-2.3	20.2	-2.0	23.0	-1.1	27.8	8.6	30.0	8.2
	Boise	-6.5	17.9	-1.5	18.8	-0.3	21.4	2.7	26.0	8.8	30.3	7.0
	Burlington	-7.1	18.3	-2.8	20.4	-0.9	22.9	1.7	26.8	8.8	30.0	5.9
	Chicago	-9.9	15.7	-2.4	16.3	-0.3	30.1	-0.1	31.7	9.4	31.9	10.8
	Duluth	-9.8	19.1	-6.7	19.3	-4.2	19.4	-2.0	19.8	9.8	32.5	2.0
	El Paso	-2.6	15.3	-1.9	15.6	-1.3	21.2	8.7	32.5	9.9	33.7	9.4
	Fairbanks	-5.3	17.7	1.3	19.1	9.5	19.3	9.5	19.4	9.5	20.6	2.0
	Houston	-6.6	17.9	-3.1	17.9	-2.4	21.0	-2.0	28.9	8.5	31.1	7.5
	Memphis	-7.3	17.5	-3.6	20.0	-2.4	22.7	0.0	26.7	8.6	30.3	8.4
	Miami	-8.8	16.8	-2.5	18.5	-2.5	27.4	-0.3	29.6	9.3	33.2	2.1
	Phoenix	-6.5	16.3	-2.4	16.9	-1.3	21.2	2.2	26.6	9.3	30.4	7.3
	Tulsa	-7.2	18.3	-3.2	20.2	-2.0	22.4	0.5	26.9	8.8	30.4	6.4
Office Building	Albuquerque	-9.7	19.7	-3.8	19.7	-1.4	19.7	-0.2	32.3	9.8	32.4	6.0
	Baltimore	-7.3	18.7	-4.0	21.6	-2.6	23.8	-0.8	27.3	8.6	30.3	6.6
	Boise	-6.1	19.0	-1.1	21.6	-1.1	25.4	-0.2	28.9	8.1	30.4	2.9
	Burlington	-7.2	18.6	-2.7	21.3	-1.2	22.8	-0.4	27.7	9.1	30.4	6.1
	Chicago	-7.5	18.5	-4.1	21.3	-2.6	23.8	-0.8	27.0	8.5	30.2	8.1
	Duluth	-7.4	20.4	-3.4	20.4	-1.2	20.7	-0.5	32.3	7.1	33.1	2.1
	El Paso	-3.8	16.5	-1.7	18.0	-1.7	25.3	-0.6	31.6	10.0	31.8	2.6
	Fairbanks	-6.5	19.1	-1.8	21.6	-1.1	24.2	-0.2	27.9	9.7	30.3	2.1
	Houston	-7.5	18.6	-4.3	21.5	-3.0	23.6	-1.0	27.1	8.3	30.2	7.9
	Memphis	-7.8	18.6	-5.1	21.8	-2.0	23.4	-0.5	27.4	8.8	30.3	6.6
	Miami	-5.6	17.8	-1.9	18.6	-1.6	23.0	-1.5	31.6	8.7	31.6	6.8
	Phoenix	-7.2	18.5	-3.2	20.8	-1.7	23.4	-0.6	27.2	8.8	30.4	6.4
	Tulsa	-7.4	19.0	-3.9	20.1	-2.4	23.1	-1.2	27.3	8.4	30.5	7.5

Note: The values given in the "X" columns (i.e. "X-1, X-2, etc.) are heat pump ΔT values. The values given in the "Y" columns are setpoint values.

APPENDIX D

Detailed Savings Comparison – Motel

		Energy Consumption (kW-hr)							Savings & Annual Costs	
		Heat Pump	Main Circ Pump	Cooling Tower	CT Pump	Boiler	Boiler Pump	Total	% Savings	Annual Operating Cost
Albuquerque	Case 00	175,568	2,510	4,508	2,270	29,133	81	214,070		$17,126
	GenOpt(2)	136,547	2,510	7,328	3,690	28,247	20	178,342	16.7%	$14,267
	Com. Cont. (2)a	138,550	2,510	6,813	3,431	28,325	22	179,652	16.1%	$14,372
	Com. Cont. (2)b	137,719	2,510	6,956	3,503	28,341	21	179,051	16.4%	$14,324
	Com. Cont. (2)c	137,257	2,510	6,958	3,504	28,909	34	179,174	16.3%	$14,334
	GenOpt(11)	135,571	2,510	7,306	3,679	28,952	46	178,064	16.8%	$14,245
	Com. Cont. (7)a	137,209	2,510	6,888	3,469	28,548	27	178,651	16.5%	$14,292
	Com. Cont. (7)b	137,006	2,510	6,889	3,469	28,780	34	178,688	16.5%	$14,295
Baltimore	Case 00	177,138	2,975	4,093	2,061	92,464	186	278,917		$22,313
	GenOpt(2)	155,850	2,975	6,160	3,102	89,784	65	257,936	7.5%	$20,635
	Com. Cont. (2)a	156,368	2,975	6,073	3,059	89,429	60	257,963	7.5%	$20,637
	Com. Cont. (2)b	156,104	2,975	6,289	3,168	89,369	60	257,964	7.5%	$20,637
	Com. Cont. (2)c	154,434	2,975	6,291	3,169	91,210	91	258,169	7.4%	$20,654
	GenOpt(11)	154,716	2,975	5,877	2,960	90,568	79	257,174	7.8%	$20,574
	Com. Cont. (7)a	155,298	2,975	5,816	2,929	90,189	72	257,279	7.8%	$20,582
	Com. Cont. (7)b	154,461	2,975	5,817	2,929	91,084	91	257,355	7.7%	$20,588
Boise	Case 00	152,669	2,279	3,299	1,662	102,415	214	262,539		$21,003
	GenOpt(2)	124,770	2,279	5,464	2,752	99,471	73	234,808	10.6%	$18,785
	Com. Cont. (2)a	126,766	2,279	5,059	2,548	99,021	67	235,741	10.2%	$18,859
	Com. Cont. (2)b	126,133	2,279	5,174	2,605	99,010	67	235,268	10.4%	$18,821
	Com. Cont. (2)c	124,289	2,279	5,175	2,606	100,973	102	235,424	10.3%	$18,834
	GenOpt(11)	124,369	2,279	5,377	2,708	100,003	82	234,818	10.6%	$18,785
	Com. Cont. (7)a	125,231	2,279	5,125	2,581	99,899	80	235,197	10.4%	$18,816
	Com. Cont. (7)b	124,287	2,279	5,126	2,581	100,884	102	235,259	10.4%	$18,821
Burlington	Case 00	154,057	2,337	2,500	1,259	210,053	376	370,583		$29,647
	GenOpt(2)	142,431	2,337	4,062	2,046	202,196	129	353,201	4.7%	$28,256
	Com. Cont. (2)a	142,694	2,337	3,897	1,962	202,331	131	353,352	4.6%	$28,268
	Com. Cont. (2)b	142,431	2,337	4,062	2,046	202,196	129	353,201	4.7%	$28,256
	Com. Cont. (2)c	138,176	2,337	4,063	2,047	206,692	195	353,511	4.6%	$28,281
	GenOpt(11)	140,464	2,337	3,971	2,000	204,008	150	352,930	4.8%	$28,234
	Com. Cont. (7)a	140,827	2,337	3,831	1,929	203,975	149	353,049	4.7%	$28,244
	Com. Cont. (7)b	138,307	2,337	3,831	1,929	206,628	195	353,228	4.7%	$28,258

		Energy Consumption (kW-hr)							Savings & Annual Costs	
		Heat Pump	Main Circ Pump	Cooling Tower	CT Pump	Boiler	Boiler Pump	Total	% Savings	Annual Operating Cost
Chicago	Case 00	167,688	2,629	3,431	1,728	160,560	305	336,342		$26,907
	GenOpt(2)	152,739	2,629	5,220	2,634	155,002	102	318,326	5.4%	$25,466
	Com. Cont. (2)a	152,739	2,629	5,220	2,634	155,002	102	318,326	5.4%	$25,466
	Com. Cont. (2)b	152,477	2,629	5,534	2,793	154,882	101	318,417	5.3%	$25,473
	Com. Cont. (2)c	149,462	2,629	5,535	2,793	158,112	153	318,685	5.2%	$25,495
	GenOpt(11)	148,501	2,629	4,909	2,472	158,278	162	316,952	5.8%	$25,356
	Com. Cont. (7)a	151,594	2,629	4,721	2,378	155,957	114	317,393	5.6%	$25,391
	Com. Cont. (7)b	149,608	2,629	4,721	2,378	158,030	153	317,519	5.6%	$25,402
Duluth	Case 00	146,632	2,194	1,848	930	284,117	488	436,209		$34,897
	GenOpt(2)	143,136	2,194	2,879	1,450	274,176	181	424,015	2.8%	$33,921
	Com. Cont. (2)a	143,640	2,194	2,760	1,390	274,015	179	424,177	2.8%	$33,934
	Com. Cont. (2)b	143,633	2,194	2,827	1,423	273,823	177	424,077	2.8%	$33,926
	Com. Cont. (2)c	137,839	2,194	2,828	1,424	279,995	266	424,547	2.7%	$33,964
	GenOpt(11)	141,512	2,194	2,716	1,368	276,207	203	424,200	2.8%	$33,936
	Com. Cont. (7)a	141,512	2,194	2,716	1,368	276,207	203	424,200	2.8%	$33,936
	Com. Cont. (7)b	137,962	2,194	2,717	1,368	279,889	266	424,396	2.7%	$33,952
El Paso	Case 00	238,755	3,350	6,318	3,182	1,732	9	253,345		$20,268
	GenOpt(2)	187,419	3,350	10,095	5,085	1,773	2	207,724	18.0%	$16,618
	Com. Cont. (2)a	189,925	3,350	9,320	4,693	1,710	2	209,000	17.5%	$16,720
	Com. Cont. (2)b	188,915	3,350	9,507	4,788	1,706	2	208,268	17.8%	$16,661
	Com. Cont. (2)c	188,888	3,350	9,508	4,788	1,767	3	208,304	17.8%	$16,664
	GenOpt(11)	187,090	3,350	9,960	5,016	1,738	3	207,155	18.2%	$16,572
	Com. Cont. (7)a	188,617	3,350	9,377	4,722	1,689	2	207,757	18.0%	$16,621
	Com. Cont. (7)b	188,604	3,350	9,377	4,722	1,701	3	207,756	18.0%	$16,620
Fairbanks	Case 00	218,952	3,092	1,288	649	582,545	836	807,361		$64,589
	GenOpt(2)	229,480	3,092	2,245	1,131	559,163	335	795,445	1.5%	$63,636
	Com. Cont. (2)a	227,640	3,092	2,025	1,020	562,216	361	796,354	1.4%	$63,708
	Com. Cont. (2)b	227,681	3,092	2,093	1,054	561,702	357	795,979	1.4%	$63,678
	Com. Cont. (2)c	214,025	3,092	2,094	1,054	576,138	542	796,944	1.3%	$63,756
	GenOpt(11)	229,418	3,092	2,238	1,127	559,212	335	795,422	1.5%	$63,634
	Com. Cont. (7)a	222,532	3,092	2,036	1,025	567,316	410	796,410	1.4%	$63,713
	Com. Cont. (7)b	214,130	3,092	2,036	1,025	576,101	542	796,925	1.3%	$63,754
Houston	Case 00	280,203	4,814	8,147	4,103	4,113	14	301,393		$24,111
	GenOpt(2)	251,770	4,814	10,951	5,516	4,015	3	277,069	8.1%	$22,165
	Com. Cont. (2)a	251,475	4,814	11,338	5,711	4,018	3	277,359	8.0%	$22,189
	Com. Cont. (2)b	252,638	4,814	10,510	5,293	4,028	3	277,285	8.0%	$22,183
	Com. Cont. (2)c	252,584	4,814	10,510	5,293	4,113	5	277,320	8.0%	$22,186
	GenOpt(11)	251,319	4,814	10,346	5,210	4,036	4	275,730	8.5%	$22,058
	Com. Cont. (7)a	251,261	4,814	10,503	5,289	4,063	4	275,935	8.4%	$22,075
	Com. Cont. (7)b	251,230	4,814	10,503	5,290	4,099	5	275,942	8.4%	$22,075

		Energy Consumption (kW-hr)							Savings & Annual Costs	
		Heat Pump	Main Circ Pump	Cooling Tower	CT Pump	Boiler	Boiler Pump	Total	% Savings	Annual Operating Cost
Memphis	Case 00	235,113	4,161	6,234	3,140	25,033	64	273,746		$21,900
	GenOpt(2)	207,783	4,161	8,514	4,288	24,408	20	249,174	9.0%	$19,934
	Com. Cont. (2)a	207,691	4,161	8,654	4,358	24,294	18	249,177	9.0%	$19,934
	Com. Cont. (2)b	209,061	4,161	8,149	4,104	24,333	19	249,827	8.7%	$19,986
	Com. Cont. (2)c	208,710	4,161	8,150	4,104	24,720	28	249,874	8.7%	$19,990
	GenOpt(11)	207,092	4,161	8,380	4,220	24,582	25	248,461	9.2%	$19,877
	Com. Cont. (7)a	207,391	4,161	8,275	4,168	24,500	22	248,517	9.2%	$19,881
	Com. Cont. (7)b	207,205	4,161	8,276	4,168	24,713	28	248,551	9.2%	$19,884
Miami	Case 00	396,034	6,480	11,353	5,718	0	0	419,585		$33,567
	GenOpt(2)	358,055	6,480	14,558	7,332	0	0	386,425	7.9%	$30,914
	Com. Cont. (2)a	357,331	6,480	15,428	7,772	0	0	387,011	7.8%	$30,961
	Com. Cont. (2)b	358,388	6,480	14,388	7,246	0	0	386,503	7.9%	$30,920
	Com. Cont. (2)c	358,388	6,480	14,388	7,246	0	0	386,503	7.9%	$30,920
	GenOpt(11)	357,437	6,480	14,052	7,077	0	0	385,046	8.2%	$30,804
	Com. Cont. (7)a	357,205	6,480	14,313	7,208	0	0	385,207	8.2%	$30,817
	Com. Cont. (7)b	357,205	6,480	14,313	7,208	0	0	385,207	8.2%	$30,817
Phoenix	Case 00	346,849	5,476	7,743	3,899	391	2	364,361		$29,149
	GenOpt(2)	273,564	5,476	12,331	6,210	372	0	297,954	18.2%	$23,836
	Com. Cont. (2)a	276,403	5,476	11,659	5,872	392	0	299,803	17.7%	$23,984
	Com. Cont. (2)b	275,155	5,476	11,845	5,965	381	0	298,823	18.0%	$23,906
	Com. Cont. (2)c	275,149	5,476	11,845	5,965	398	1	298,835	18.0%	$23,907
	GenOpt(11)	273,599	5,476	12,205	6,147	374	0	297,801	18.3%	$23,824
	Com. Cont. (7)a	274,652	5,476	11,807	5,946	375	0	298,257	18.1%	$23,861
	Com. Cont. (7)b	274,649	5,476	11,807	5,946	386	1	298,265	18.1%	$23,861
Tulsa	Case 00	230,804	3,920	5,833	2,938	56,929	116	300,540		$24,043
	GenOpt(2)	204,507	3,920	8,058	4,058	55,389	42	275,974	8.2%	$22,078
	Com. Cont. (2)a	205,108	3,920	7,947	4,002	55,080	37	276,094	8.1%	$22,088
	Com. Cont. (2)b	206,674	3,920	7,575	3,815	55,112	38	277,133	7.8%	$22,171
	Com. Cont. (2)c	205,753	3,920	7,575	3,815	56,102	56	277,221	7.8%	$22,178
	GenOpt(11)	203,999	3,920	7,896	3,977	55,444	43	275,279	8.4%	$22,022
	Com. Cont. (7)a	204,111	3,920	7,783	3,920	55,516	45	275,294	8.4%	$22,024
	Com. Cont. (7)b	203,612	3,920	7,784	3,920	56,097	56	275,388	8.4%	$22,031

Detailed Savings Comparison – Office

		Energy Consumption (kW-hr)							Savings & Annual Costs	
		Heat Pump	Main Circ Pump	Cooling Tower	CT Pump	Boiler	Boiler Pump	Total	% Savings	Annual Operating Cost
Albuquerque	Case 00	225,736	3,839	6,143	2,701	26,075	186	264,680		$21,174
	GenOpt(2)	190,763	3,839	9,524	4,189	24,937	31	233,282	11.9%	$18,663
	Com. Cont. (2)a	191,872	3,839	9,217	4,053	24,966	33	233,981	11.6%	$18,718
	Com. Cont. (2)b	191,011	3,839	9,421	4,143	25,402	34	233,850	11.6%	$18,708
	Com. Cont. (2)c	190,472	3,839	9,445	4,154	27,568	60	235,537	11.0%	$18,843
	GenOpt(11)	189,889	3,839	9,518	4,186	22,870	35	230,338	13.0%	$18,427
	Com. Cont. (7)a	191,057	3,839	9,263	4,074	24,722	40	232,996	12.0%	$18,640
	Com. Cont. (7)b	190,823	3,839	9,271	4,077	25,604	55	233,669	11.7%	$18,694
Baltimore	Case 00	183,656	3,637	7,764	3,053	59,209	396	257,715		$20,617
	GenOpt(2)	171,262	3,637	10,407	4,095	55,453	66	244,922	5.0%	$19,594
	Com. Cont. (2)a	169,296	3,637	13,689	5,394	56,891	73	248,980	3.4%	$19,918
	Com. Cont. (2)b	168,996	3,637	14,975	5,909	57,360	73	250,950	2.6%	$20,076
	Com. Cont. (2)c	167,629	3,637	15,008	5,922	60,134	125	252,455	2.0%	$20,196
	GenOpt(11)	168,820	3,637	10,420	4,098	56,836	89	243,901	5.4%	$19,512
	Com. Cont. (7)a	168,670	3,637	10,473	4,119	57,014	90	244,003	5.3%	$19,520
	Com. Cont. (7)b	168,064	3,637	10,483	4,123	58,318	121	244,746	5.0%	$19,580
Boise	Case 00	172,072	3,660	4,281	1,883	78,361	545	260,802		$20,864
	GenOpt(2)	150,706	3,660	6,757	2,972	74,779	90	238,964	8.4%	$19,117
	Com. Cont. (2)a	150,992	3,660	6,568	2,888	75,513	99	239,720	8.1%	$19,178
	Com. Cont. (2)b	150,429	3,660	6,743	2,965	75,612	98	239,506	8.2%	$19,161
	Com. Cont. (2)c	148,641	3,660	6,771	2,978	79,006	167	241,223	7.5%	$19,298
	GenOpt(11)	150,190	3,660	6,733	2,961	73,441	92	237,076	9.1%	$18,966
	Com. Cont. (7)a	149,920	3,660	6,557	2,884	75,823	122	238,966	8.4%	$19,117
	Com. Cont. (7)b	149,105	3,660	6,564	2,887	77,189	163	239,567	8.1%	$19,165
Burlington	Case 00	164,021	3,477	2,812	1,520	181,693	1,145	354,668		$28,373
	GenOpt(2)	161,460	3,477	3,898	2,107	173,486	203	344,631	2.8%	$27,570
	Com. Cont. (2)a	160,069	3,477	4,176	2,260	175,121	222	345,325	2.6%	$27,626
	Com. Cont. (2)b	159,914	3,477	4,602	2,492	174,977	219	345,681	2.5%	$27,654
	Com. Cont. (2)c	155,491	3,477	4,613	2,498	180,254	365	346,697	2.2%	$27,736
	GenOpt(11)	158,129	3,477	3,916	2,116	176,003	260	343,901	3.0%	$27,512
	Com. Cont. (7)a	158,703	3,477	3,814	2,061	176,248	257	344,560	2.8%	$27,565
	Com. Cont. (7)b	156,026	3,477	3,817	2,063	179,384	363	345,129	2.7%	$27,610

		Energy Consumption (kW-hr)							Savings & Annual Costs	
		Heat Pump	Main Circ Pump	Cooling Tower	CT Pump	Boiler	Boiler Pump	Total	% Savings	Annual Operating Cost
Chicago	Case 00	176,090	3,572	4,950	2,177	120,388	826	308,003		$24,640
	GenOpt(2)	166,475	3,572	7,043	3,103	114,789	138	295,120	4.2%	$23,610
	Com. Cont. (2)a	164,889	3,572	8,145	3,596	116,097	151	296,450	3.8%	$23,716
	Com. Cont. (2)b	164,526	3,572	9,203	4,073	116,084	149	297,607	3.4%	$23,809
	Com. Cont. (2)c	161,681	3,572	9,227	4,084	120,209	253	299,026	2.9%	$23,922
	GenOpt(11)	163,729	3,572	6,675	2,936	116,439	175	293,524	4.7%	$23,482
	Com. Cont. (7)a	163,729	3,572	6,675	2,936	116,439	175	293,524	4.7%	$23,482
	Com. Cont. (7)b	162,010	3,572	6,684	2,940	118,877	250	294,332	4.4%	$23,547
Duluth	Case 00	167,628	3,449	2,802	1,232	290,429	1,744	467,285		$37,383
	GenOpt(2)	171,887	3,449	3,875	1,704	277,205	321	458,441	1.9%	$36,675
	Com. Cont. (2)a	169,037	3,449	4,315	1,898	279,901	353	458,954	1.8%	$36,716
	Com. Cont. (2)b	168,948	3,449	4,604	2,025	279,818	348	459,194	1.7%	$36,735
	Com. Cont. (2)c	161,798	3,449	4,620	2,032	287,995	575	460,469	1.5%	$36,838
	GenOpt(11)	170,109	3,449	4,335	1,907	276,094	321	456,214	2.4%	$36,497
	Com. Cont. (7)a	166,536	3,449	4,149	1,825	281,747	408	458,114	2.0%	$36,649
	Com. Cont. (7)b	162,271	3,449	4,155	1,827	286,664	571	458,939	1.8%	$36,715
El Paso	Case 00	284,413	4,210	9,780	3,846	8,503	68	310,820		$24,866
	GenOpt(2)	239,087	4,210	15,233	5,992	7,643	10	272,175	12.4%	$21,774
	Com. Cont. (2)a	239,736	4,210	14,939	5,875	8,218	11	272,991	12.2%	$21,839
	Com. Cont. (2)b	238,703	4,210	15,678	6,167	8,303	11	273,072	12.1%	$21,846
	Com. Cont. (2)c	238,540	4,210	15,700	6,176	9,491	22	274,139	11.8%	$21,931
	GenOpt(11)	236,523	4,210	15,812	6,218	6,183	8	268,954	13.5%	$21,516
	Com. Cont. (7)a	238,607	4,210	15,007	5,902	7,868	14	271,608	12.6%	$21,729
	Com. Cont. (7)b	238,541	4,210	15,012	5,904	8,246	19	271,932	12.5%	$21,755
Fairbanks	Case 00	283,661	3,600	1,322	714	723,973	3,022	1,016,293		$81,303
	GenOpt(2)	307,638	3,600	2,205	1,192	691,033	746	1,006,413	1.0%	$80,513
	Com. Cont. (2)a	304,086	3,600	2,067	1,117	696,017	812	1,007,700	0.8%	$80,616
	Com. Cont. (2)b	304,421	3,600	2,148	1,161	695,206	801	1,007,337	0.9%	$80,587
	Com. Cont. (2)c	286,207	3,600	2,160	1,167	714,866	1,255	1,009,255	0.7%	$80,740
	GenOpt(11)	307,843	3,600	2,112	1,141	690,082	744	1,005,522	1.1%	$80,442
	Com. Cont. (7)a	297,209	3,600	2,029	1,097	702,543	932	1,007,411	0.9%	$80,593
	Com. Cont. (7)b	286,661	3,600	2,034	1,099	713,868	1,253	1,008,516	0.8%	$80,681
Houston	Case 00	283,500	4,030	10,603	4,663	8,377	59	311,232		$24,899
	GenOpt(2)	267,963	4,030	12,236	5,382	7,238	9	296,858	4.6%	$23,749
	Com. Cont. (2)a	265,657	4,030	22,220	9,842	8,142	11	309,903	0.4%	$24,792
	Com. Cont. (2)b	266,508	4,030	15,338	6,761	7,856	11	300,503	3.4%	$24,040
	Com. Cont. (2)c	266,373	4,030	15,348	6,765	8,659	19	301,196	3.2%	$24,096
	GenOpt(11)	265,247	4,030	12,897	5,672	7,874	13	295,733	5.0%	$23,659
	Com. Cont. (7)a	265,683	4,030	12,648	5,562	7,811	13	295,747	5.0%	$23,660
	Com. Cont. (7)b	265,616	4,030	12,655	5,565	8,291	18	296,175	4.8%	$23,694

		Energy Consumption (kW-hr)							Savings & Annual Costs	
		Heat Pump	Main Circ Pump	Cooling Tower	CT Pump	Boiler	Boiler Pump	Total	% Savings	Annual Operating Cost
Memphis	Case 00	234,255	3,978	10,419	4,097	20,041	145	272,935		$21,835
	GenOpt(2)	219,320	3,978	13,067	5,140	18,168	22	259,696	4.9%	$20,776
	Com. Cont. (2)a	216,705	3,978	20,985	8,293	19,495	26	269,481	1.3%	$21,558
	Com. Cont. (2)b	218,108	3,978	14,214	5,594	19,130	26	261,051	4.4%	$20,884
	Com. Cont. (2)c	217,747	3,978	14,230	5,601	20,292	44	261,892	4.0%	$20,951
	GenOpt(11)	216,704	3,978	13,356	5,253	18,897	31	258,218	5.4%	$20,657
	Com. Cont. (7)a	216,573	3,978	13,411	5,274	19,162	31	258,429	5.3%	$20,674
	Com. Cont. (7)b	216,389	3,978	13,422	5,278	19,830	43	258,940	5.1%	$20,715
Miami	Case 00	370,556	4,425	13,307	5,852	156	2	394,298		$31,544
	GenOpt(2)	351,600	4,425	15,072	6,629	103	0	377,829	4.2%	$30,226
	Com. Cont. (2)a	350,489	4,425	29,919	13,271	120	0	398,224	-1.0%	$31,858
	Com. Cont. (2)b	350,934	4,425	18,786	8,292	116	0	382,552	3.0%	$30,604
	Com. Cont. (2)c	350,933	4,425	18,786	8,293	159	0	382,597	3.0%	$30,608
	GenOpt(11)	350,508	4,425	15,195	6,683	95	0	376,906	4.4%	$30,153
	Com. Cont. (7)a	350,567	4,425	15,289	6,724	127	0	377,132	4.4%	$30,171
	Com. Cont. (7)b	350,565	4,425	15,289	6,724	139	0	377,143	4.4%	$30,171
Phoenix	Case 00	374,953	5,291	11,157	5,265	3,231	27	399,924		$31,994
	GenOpt(2)	320,257	5,291	17,720	8,364	2,640	3	354,275	11.4%	$28,342
	Com. Cont. (2)a	318,852	5,291	18,887	8,917	3,057	4	355,008	11.2%	$28,401
	Com. Cont. (2)b	317,762	5,291	21,295	10,066	3,067	4	357,485	10.6%	$28,599
	Com. Cont. (2)c	317,709	5,291	21,311	10,073	3,818	9	358,212	10.4%	$28,657
	GenOpt(11)	317,342	5,291	17,450	8,235	2,601	4	350,924	12.3%	$28,074
	Com. Cont. (7)a	317,690	5,291	17,333	8,180	2,862	5	351,360	12.1%	$28,109
	Com. Cont. (7)b	317,679	5,291	17,338	8,182	3,201	7	351,698	12.1%	$28,136
Tulsa	Case 00	202,013	3,784	8,953	3,521	44,583	362	263,216		$21,057
	GenOpt(2)	191,879	3,784	10,780	4,240	41,941	54	252,678	4.0%	$20,214
	Com. Cont. (2)a	189,412	3,784	17,858	7,037	43,128	59	261,277	0.7%	$20,902
	Com. Cont. (2)b	190,501	3,784	12,272	4,828	42,812	61	254,258	3.4%	$20,341
	Com. Cont. (2)c	189,648	3,784	12,289	4,835	44,545	101	255,201	3.0%	$20,416
	GenOpt(11)	188,922	3,784	11,462	4,508	43,138	77	251,892	4.3%	$20,151
	Com. Cont. (7)a	189,131	3,784	11,421	4,491	43,211	73	252,111	4.2%	$20,169
	Com. Cont. (7)b	188,663	3,784	11,427	4,494	44,002	99	252,470	4.1%	$20,198

APPENDIX E

Optimized 11-parameter with Wet-bulb Parameters

		Cooling Tower Setpoints (°C)										WB ΔT (°C)	Boiler Setpoint (°C)
		X-1	Y-1	X-2	Y-2	X-3	Y-3	X-4	Y-4	X-5	Y-5		
Motel	Chicago	-9.8	15.6	-2.5	16.2	-0.4	30.5	0.0	31.8	9.5	32.0	2.2	10.8
	El Paso	-2.8	15.3	-2.4	15.8	-2.0	21.7	8.7	33.0	9.9	33.9	0	9.6
	Houston	-6.6	17.8	-3.1	17.9	-2.4	21.1	-2.0	28.8	8.5	31.1	0	7.5
	Memphis	-7.0	17.7	-3.1	19.8	-2.3	23.1	-0.1	27.4	8.8	30.5	4.5	6.7
Office	Chicago	-7.3	18.5	-2.3	21.3	-0.8	24.4	0.0	28.7	8.7	30.7	0.1	5.7
	El Paso	-3.8	16.5	-1.7	18.0	-1.7	25.4	-0.6	32.0	10.0	32.0	0	2.5
	Houston	-7.5	18.7	-4.3	21.6	-2.9	23.6	-0.3	27.5	8.3	30.2	1.9	7.9
	Memphis	-7.8	18.7	-5.1	22.1	-2.2	23.8	-1.1	27.7	9.0	30.4	2.4	6.7

Note: The values given in the "X" columns (i.e. "X-1, X-2, etc.) are heat pump ΔT values. The values given in the "Y" columns are setpoint values.

Optimized 12-hour Forecasting and Thermal Mass Augmentation Parameters

		Cooling Tower Setpoints (°C)										Boiler Setpoint (°C)
		X-1	Y-1	X-2	Y-2	X-3	Y-3	X-4	Y-4	X-5	Y-5	
		Cooling tower and boiler parameters (**underlined**).										
		Cooling ΔT (°C)	Heating ΔT (°C)	Cooling Offset (°C)	Heating Offset (°C)							
		Forecasting parameter (*italics*).										
Motel	Chicago	**-9.6**	**15.6**	**-1.0**	**15.6**	**1.5**	**29.6**	**1.9**	**31.6**	**9.7**	**31.8**	**10.4**
		0.0	*0.0*	*0.1*	*0.0*							
	El Paso	**-2.5**	**15.3**	**-2.1**	**15.3**	**5.4**	**18.7**	**5.4**	**32.2**	**9.8**	**33.7**	**7.9**
		-0.1	*0.0*	*0.6*	*0.0*							
	Houston	**-6.3**	**17.8**	**-2.1**	**17.8**	**-0.7**	**20.6**	**0.5**	**28.3**	**8.8**	**31.1**	**7.2**
		-0.1	*4.1*	*0.5*	*0.0*							
	Memphis	**-6.2**	**15.0**	**-4.3**	**18.1**	**4.0**	**25.3**	**7.2**	**25.9**	**9.0**	**30.2**	**2.5**
		-3.8	*2.0*	*0.7*	*0.2*							
Office	Chicago	**-5.7**	**20.0**	**-0.2**	**20.0**	**-0.1**	**20.5**	**0.0**	**27.6**	**9.8**	**28.8**	**2.2**
		-8.2	*0.0*	*8.3*	*0.0*							
	El Paso	**-3.7**	**16.4**	**-0.7**	**17.3**	**0.1**	**24.8**	**1.9**	**31.8**	**10.0**	**31.9**	**2.4**
		0.0	*0.0*	*0.0*	*0.0*							
	Houston	**-7.1**	**19.1**	**-1.6**	**21.8**	**-0.9**	**24.2**	**0.0**	**29.1**	**8.2**	**30.9**	**3.8**
		0.0	*0.6*	*0.0*	*0.0*							
	Memphis	**-7.4**	**19.5**	**-3.6**	**19.5**	**-0.4**	**23.0**	**0.0**	**30.1**	**8.0**	**31.6**	**2.2**
		-3.2	*1.3*	*2.2*	*0.6*							

Note: The values given in the "X" columns (i.e. "X-1, X-2, etc.) are heat pump ΔT values. The values given in the "Y" columns are setpoint values.

APPENDIX F

Detailed Savings Comparison – Motel (Exploratory Results)

		Energy Consumption (kW-hr)							Savings & Annual Costs	
		Heat Pump	Main Circ Pump	Cooling Tower	CT Pump	Boiler	Boiler Pump	Total	% Savings	Annual Operating Cost
Chicago	Case 00	167,688	2,629	3,431	1,728	160,560	305	336,342		$26,907
	GenOpt(2)	152,739	2,629	5,220	2,634	155,002	102	318,326	5.4%	$25,466
	GenOpt(11)	148,501	2,629	4,909	2,472	158,278	162	316,952	5.8%	$25,356
	Com. Cont. (7)	149,608	2,629	4,721	2,378	158,030	153	317,519	5.6%	$25,402
	GenOpt(11+WB)	148,568	2,629	4,884	2,460	158,246	161	316,947	5.8%	$25,356
	Forecasting (12 hrs)	144,920	2,629	6,716	3,383	156,444	184	314,275	6.6%	$25,142
El Paso	Case 00	238,755	3,350	6,318	3,182	1,732	9	253,345		$20,268
	GenOpt(2)	187,419	3,350	10,095	5,085	1,773	2	207,724	18.0%	$16,618
	GenOpt(11)	187,090	3,350	9,960	5,016	1,738	3	207,155	18.2%	$16,572
	Com. Cont. (7)	188,604	3,350	9,377	4,722	1,701	3	207,756	18.0%	$16,620
	GenOpt(11+WB)	187,274	3,350	9,835	4,953	1,737	3	207,151	18.2%	$16,572
	Forecasting (12 hrs)	182,222	3,350	11,271	5,676	752	1	203,272	19.8%	$16,262
Houston	Case 00	280,203	4,814	8,147	4,103	4,113	14	301,393		$24,111
	GenOpt(2)	251,770	4,814	10,951	5,516	4,015	6	277,071	8.1%	$22,166
	GenOpt(11)	251,319	4,814	10,346	5,213	4,036	4	275,733	8.5%	$22,059
	Com. Cont. (7)	251,230	4,814	10,503	5,290	4,099	4	275,940	8.4%	$22,075
	GenOpt(11+WB)	251,316	4,814	10,350	5,212	4,048	4	275,744	8.5%	$22,059
	Forecasting (12 hrs)	246,403	4,814	12,038	6,062	2,276	3	271,597	9.9%	$21,728
Memphis	Case 00	235,113	4,161	6,234	3,140	25,033	64	273,746		$21,900
	GenOpt(2)	207,783	4,161	8,514	4,288	24,408	20	249,174	9.0%	$19,934
	GenOpt(11)	207,092	4,161	8,380	4,220	24,582	25	248,461	9.2%	$19,877
	Com. Cont. (7)	207,205	4,161	8,276	4,168	24,713	28	248,551	9.2%	$19,884
	GenOpt(11+WB)	207,234	4,161	8,294	4,177	24,460	22	248,349	9.3%	$19,868
	Forecasting (12 hrs)	203,380	4,161	9,857	4,964	20,860	18	243,240	11.1%	$19,459

Detailed Savings Comparison – Office (Exploratory Results)

[redacted]	[redacted]	Energy Consumption (kW-hr)							Savings & Annual Costs	
		Heat Pump	Main Circ Pump	Cooling Tower	CT Pump	Boiler	Boiler Pump	Total	% Savings	Annual Operating Cost
Chicago	Case 00	176,090	3,572	4,950	2,177	120,388	826	308,003		$24,640
	GenOpt(2)	166,475	3,572	7,043	3,103	114,789	138	295,120	4.2%	$23,610
	GenOpt(11)	163,729	3,572	6,675	2,936	116,439	175	293,524	4.7%	$23,482
	Com. Cont. (7)	162,010	3,572	6,684	2,940	118,877	250	294,332	4.4%	$23,547
	GenOpt(11+WB)	163,219	3,572	6,806	2,993	116,097	171	292,858	4.9%	$23,429
	Forecasting (12 hrs)	160,691	3,572	8,831	3,885	100,109	139	277,227	10.0%	$22,178
El Paso	Case 00	284,413	4,210	9,780	3,846	8,503	68	310,820		$24,866
	GenOpt(2)	239,087	4,210	15,233	5,992	7,643	10	272,175	12.4%	$21,774
	GenOpt(11)	236,523	4,210	15,812	6,218	6,183	8	268,954	13.5%	$21,516
	Com. Cont. (7)	238,541	4,210	15,012	5,904	8,246	19	271,932	12.5%	$21,755
	GenOpt(11+WB)	236,533	4,210	15,805	6,216	6,147	8	268,918	13.5%	$21,513
	Forecasting (12 hrs)	228,128	4,210	19,554	7,695	0	0	259,588	16.5%	$20,767
Houston	Case 00	283,500	4,030	10,603	4,663	8,377	59	311,232		$24,899
	GenOpt(2)	267,963	4,030	12,236	5,382	7,238	9	296,858	4.6%	$23,749
	GenOpt(11)	265,247	4,030	12,897	5,672	7,914	15	295,775	5.0%	$23,662
	Com. Cont. (7)	265,616	4,030	12,655	5,565	8,291	18	296,175	4.8%	$23,694
	GenOpt(11+WB)	265,762	4,030	12,598	5,540	7,823	14	295,767	5.0%	$23,661
	Forecasting (12 hrs)	259,238	4,030	15,358	6,761	358	1	285,745	8.2%	$22,860
Memphis	Case 00	234,255	3,978	10,419	4,097	20,041	145	272,935		$21,835
	GenOpt(2)	219,320	3,978	13,067	5,140	18,168	22	259,696	4.9%	$20,776
	GenOpt(11)	216,704	3,978	13,356	5,253	18,897	31	258,218	5.4%	$20,657
	Com. Cont. (7)	216,389	3,978	13,422	5,278	19,830	43	258,940	5.1%	$20,715
	GenOpt(11+WB)	216,933	3,978	13,232	5,204	18,698	30	258,075	5.4%	$20,646
	Forecasting (12 hrs)	209,784	3,978	16,545	6,519	4,179	6	241,010	11.7%	$19,281

VITA

JASON EARL GENTRY

Candidate for the Degree of

Master of Science

Thesis: SIMULATION AND VALIDATION OF HYBRID GROUND SOURCE AND WATER-LOOP HEAT PUMP SYSTEMS

Major Field: Mechanical Engineering

Biographical:

Personal Data: Born in Huntingdon Tennessee on December 1, 1980, the son of Randy and Kathy Gentry. Married Clarissa F. Carroll on July 26, 2003.

Education: Graduated from Huntingdon High School in May 1999. Received a Bachelor of Science degree in Engineering from the University of Tennessee at Martin in May 2005. Completed the requirements for the Master of Science degree with a major in Mechanical Engineering in May 2007.

Experience: Employed as an undergraduate research assistant for the University of Tennessee at Martin Center for Energy Management from February 2004 to June 2005. Employed as a contract editor for the International Ground Source Heat Pump Association from October 2005 to August 2006. Employed as a graduate research assistant for the Oklahoma State University Building and Environmental Thermal Systems Research Group from July 2005 to March 2007. Employed by Mid-State Construction Company in Livingston, Tennessee from April 2007 to present as project manager of their geothermal division.

Professional Memberships: American Society of Heating Refrigerating and Air Conditioning Engineers (ASHRAE), International Ground Source Heat Pump Association (IGSHPA), Society of Manufacturing Engineers (SME), Society of Automotive Engineers (SAE).

ABSTRACT

Name: Jason Earl Gentry Date of Degree: May, 2007

Institution: Oklahoma State University Location: Stillwater, Oklahoma

Title of Study: SIMULATION AND VALIDATION OF HYBRID GROUND SOURCE AND WATER-LOOP HEAT PUMP SYSTEMS

Pages in Study: 275 Candidate for the Degree of Master of Science

Major Field: Mechanical Engineering

Scope and Method of Study: This study focused first on the simulation and validation of hybrid ground source heat pump (HGSHP) systems. Validation of such systems is previously unreported in literature. The simulation was done using HVACSim+. Validation was done using seven months (March to September 2005) of five-minutely experimental data from an HGSHP research facility located on the campus of Oklahoma State University (OSU). The validation results were considered from the perspective of both researchers and designers with regards to accuracy of HVAC energy consumption prediction.

The second part of this study focused on the simulation, validation, and control optimization of water-loop heat pump (WLHP) systems. The WLHP simulation was also done using HVACSim+. Four days (September 22-25, 2006) of five-minutely data from the OSU HGSHP research facility were used for experimental validation purposes. Intermodel validation was done between HVACSim+ and EnergyPlus to further validate the model. Control optimization was done on two building types in 13 U.S. cities. Single setpoint controls, dynamic controls, controls based on outdoor wet-bulb temperature, and controls utilizing forecasting with thermal mass augmentation were considered.

Findings and Conclusions: The predicted HGSHP system simulation matched very well to experimental results when each component was calibrated. From the designers' perspective, the performance of the system simulation with all models relying only on manufacturers' data was quite good and should be acceptable for design purposes.

Likewise, the WLHP system predicted HVAC energy consumption very well compared to experimental data when the components were calibrated. A common control strategy was developed that was based on the individually optimized setpoint profiles of the dynamic controller. Results were reasonably good for each building in every location and can be recommended for use. An exploratory investigation of the control strategy that used forecasting with augmented thermal mass showed excellent savings potential and should be investigated further.

ADVISER'S APPROVAL: Dr. Jeffrey D. Spitler